The Development of Late Transition Metal Catalysis for Hydrocarbon C–H Activation: Studies of Ru, Pd, Rh and Cu

Xiaofan Jia

Beijing, China

B.S. Chemistry, Beijing University of Chemical Engineering, 2014

M.A. Chemistry, University of Virginia, 2015

A Dissertation presented to the Graduate Faculty

of the University of Virginia in Candidacy for the degree of

Doctor of Philosophy

Department of Chemistry

University of Virginia

December 2020

ABSTRACT

JIA, XIAOFAN The Development of Late Transition Metal Catalysis for Hydrocarbon C–H Activation: Studies of Ru, Pd, Rh and Cu. (Under the direction of Professor T. Brent Gunnoe).

Olefin hydroarylation, also called arene alkylation, via late transition metal mediated C–H activation provides a pathway for the production of alkyl arenes that are produced on large scale from arenes and olefins. Late transition metal catalyzed arene alkyl-/alkenylation offers opportunities to overcome drawbacks of commercial acid-catalyzed arene alkylation including polyalkylation, an inability to generate anti-Markovnikov addition products for reactions with α-olefins, and substrate controlled regioselectivity for reactions with substituted arenes.

Olefin hydroarylation catalysts based on TpRu(II) (Tp = trispyrazolylborate) complexes have been shown to generate ethylbenzene from benzene and ethylene. Previous studies have shown that TpRu(II) catalysts with lower electron density can achieve higher catalytic turnovers. In this thesis, four new TpRu complexes and derivatives are reported. TpRu(NO)Ph_2 exhibited low stability due to the facile reductive elimination of the phenyl group. (Tp^{Br3})Ru(NCMe)(Ph)(P(OCH_2)$_3$CEt) showed no catalytic activity due to the steric bulk introduced by the bromine substituents. (TTz)Ru(NCMe)(Ph) (P(OCH_2)$_3$CEt) (TTz = hydrotris(1,2,4-triazol-1-yl)borate) gave ~150 turnover numbers (TONs) of ethylbenzene. Ru catalysts supported by tris-triazyl ligands, L_nRu(P(OCH_2)$_3$CEt)(NCMe)Ph {L_n = CH_3OTMM (4,4',4"-ethoxyethanetriyl)tris(1-benzyl-1H-1,2,3-triazole), PhTTM (tris(1-phenyl-1H-1,2,3-triazol-4-yl)methanol), is demonstrated to be selective toward styrene production. The selectivity of styrene versus ethylbenzene varies as a function of ethylene pressure, and replacing the MeOTTM ligand with PhTTM reduces the selectivity toward styrene. Our studies show that ethylene serves as the hydrogen acceptor (oxidant) in this Ru catalyzed arene alkenylation reaction.

$Pd(OAc)_2$ has been reported to catalyze the conversion of arenes and olefins to vinyl arenes, although generally with low selectivity. Commonly observed side products include vinyl carboxylates and stilbene. The selectivity for styrene formation by $Pd(OAc)_2$ is studied as a function of reaction temperature, ethylene pressure, Brønsted acid additive, Cu(II) oxidant amount, and oxygen pressure. Under optimized conditions, at high temperatures (180 °C) and low olefin pressure (20 psig), nearly quantitative yield (> 95%) of styrene is produced based on the limiting reagent copper(II) pivalate. We propose the selectivity for styrene versus vinyl pivalate at 180 °C is due to a newly elucidated palladium-catalyzed conversion of benzene and *in situ* formed vinyl pivalate to styrene.

A systematic investigation of the differences in Pd and Rh catalyzed arene alkenylation reactions is described in this thesis. The selectivity for vinyl ester vs. alkenyl arene is probed by using the ethylene hydrophenylation reaction as a model. The regioselectivity for α-olefin hydrophenylation is examined using propylene. Four alkenylated products are observed: allylbenzene, β-trans-methylstyrene, β-cis-methylstyrene and α-methylstyrene. There are two primary differences for Pd vs. Rh catalysis. First, the L:B ratio (linear = anti-Markovnikov products; branched = Markovnikov products) for Rh catalyzed reactions is greater than the Pd catalyzed processes. Second, the ratio of allylbenzene to β-trans-methylstyrene varies greatly between Rh (1.2) and Pd (0.06). We also compared the regioselectivity between Rh and Pd catalysis in reactions with mono-substituted arenes and found that Rh catalysis has better higher selectivity for *meta* functionalization, and Rh is better able to tolerate the presence of halogen groups.

A single step synthetic method for stilbene and its derivatives is described here based on our well-studied Rh-catalyzed arene alkenylation chemistry. The synthesis involves direct C–H activation, eliminating the need for additional steps to install leaving or directing groups, thereby reducing stoichiometric waste. A substoichiometric amount of copper(II) salt is used as a direct oxidant, which is regenerated by dioxygen from air *in situ*, making dioxygen the terminal oxidant. Also, we have investigated the scope of the catalysis using a wide range of arenes with different functional groups. This catalysis has shown a great tolerance to functionalities including fluoro, chloro, trifluoromethyl, ester, nitro, acetoxy, cyano and ether groups. The unique tolerance to halogen groups, especially of bromo and iodo groups, allows for facile further functionalization of the substrates. Two compounds of pharmacological interest, Resveratrol and DMU-212 {(*E*)-1,2,3-trimethoxy-5-(4-methoxystyryl)benzene}, were synthesized from this single-step approach, and it has been demonstrated that this synthetic method can be used in gram-scale synthesis using a very simple reaction setup.

Additionally, water oxidation using multinuclear $[(DAM)Cu_3(\mu^3\text{-}O)][Cl_4]$ (DAM = dodecaaza macrotetracycle) complexes is reported. Turnover frequencies (TOFs) of 14.0 s^{-1} at pH 7 and 17.7 s^{-1} at pH 8.2 are observed. We have discovered that the $[DAMCu_3(\mu^3\text{-}O)][Cl_4]$ remains active for water oxidation under acidic conditions. $[DAMCu_3(\mu^3\text{-}O)][Cl_4]$ also shows activity as an light alkane oxidation catalyst. Under optimized conditions, partial oxidation of methane to methanol with hydrogen peroxide was observed with 179% yield relative to copper catalyst under 30 bars of methane after 12 hours reaction at room temperature

AKNOWLEDGEMENTS

First and foremost, I would like to thank my Ph.D. advisor, Prof. Brent Gunnoe. There is no way for me to complete my Ph.D. without your guidance and help. I appreciate everything you taught me in your class, during our group meetings, and in our discussions. Your optimism and enthusiasm in science motivated me to solve problems and make me a better mentor and scientist. Thank you for being so supportive during the past few years. You made this journey unforgettable and enjoyable.

To the Gunnoe lab members, it is such a great honor to work with you in the past six years. The lab became a very important part of my life. I enjoy every single day of work with all of you. To Mike and Shaojin, thank you for teaching me how to use and operate gloveboxes, high-pressure reactors, and instruments. You help me adapted to the lab fast and smoothly. To Junqi, thank you for being a friend and mentor. You are such a smart and hardworking guy, the way you think and interpret data so inspiring. Thank you for teaching me your synthetic skill as well as the NMR technique. I learned a lot from you! To Nichole, thank you for being an amazon friend and colleague. It is my pleasure and honor to share the office with you. Thank you for being so patient reading my terrible-wrote drafts and manuscripts and providing helpful comments, that means a lot to me! To Shunyan and Weihao, thank you for being valuable friends of mine and being so helpful when I need help. Thank you, Kathleen, Ben, Brad, Bala, Ke, Kaeleigh, Fanji, Ana, Ryan, Nathan, as well as our excellent undergrad researchers, for helping me become a good scientist and teaching me a variety of chemistry technique and knowledge.

I would also like to thank my committee members, Dr. Dean Harman, Dr. Lin Pu, Dr. Ian Harrison, and Dr. Joshua Choi. Thank you for taking some time out to help me to polish my chemistry. The advice and suggestions you provided in my candidacy exam, annual reports, and thesis defense are constructive and enlightened.

Special thanks to prof. Lin Pu for allowing me to research in your lab in my first year as a MA student. I feel fortunate to be a part of your lab, and I learned a lot from you during this one-year research experience. I appreciate all the help from the student and visiting scholar in the Pu lab. To Jun Ying, my first mentor in Pu's lab, thank you for being so patient and helpful when you trained me. As a student with zero organic synthesis experiment, you taught me all the air-free, moister free synthesis techniques as well as separation/purification and characterization methods. To Chao, Xuedan and Shifeng, thank you for all of the help you gave me in the lab, and outside the lab, you made my first year studying aboard memorable and comfortable. To the visiting scholars, Dr. Wencai Huang, Dr. Shanyong Chen, Dr. Shuangxi Gu, and Dr. Xuepeng Zhang, the way you do research and the stories you share with me motivated me to be a good scientist. To Gengyu, you are a great friend and scientist with passion and enthusiasm in both life and science, and I believe you are strong, and there is nothing you could not overcome.

To Prof. Sen Zhang, thank you for being a valuable friend and teacher and for all the advice and discussions about science. Your lab becomes one of the most productive labs in the department in a short time, which is very impressive. I know you will be a fantastic PI and do more exciting science. Also, the collaboration with your lab has been very successful and I have learnt a lot from you and your students. To Chang, thank you for being a great friend and collaborator. I enjoy discussing 2D material with you and the food you made.

To Prof. Robert Gilliard, it was a great honor to be your lab neighbor. You are a great scientist and team leader. It is my pleasure to see your group grow in the past four years and I am pretty sure with you and your great team, your lab will make a tremendous contribution to the main group and organometallics community. To Luke, Jacob, Kelsie, and Dr. Wilson, I missed our time

sharing office, and we had a lot of great discussions, I hope you enjoy your Ph.D. life and looking forward to reading your new chemistry.

To my friend outside the lab, Xiaolin, Zhonghua and Xianran, our trip to the Yellowstone was unforgettable. I am looking forward to exploring more places with you in the future. To Weicheng, we've been through many interesting times, and thank you for being so supportive. I hope you could find the next stop quickly. To Haoyi and Qi, both of you set extraordinary examples of scientist for me to follow since college. Good luck with your postdoc in the US, and I hope we could get together soon!

Finally, to my family, although most of you are on the other side of the planet, I still could feel your support during the past six years. Thank you for everything you gave me in the past 28 years. I could have done nothing without your support. You play such an important role in every important moment of my life. Thank you for your scarifications when you raise me up and create such a warm, secure and free environment for me. To my wonderful wife, Nanxi, thank you for giving me support and help, discussing ideas, and preventing several wrong turns. Thank you for bringing our daughter Ellie to the world and taking care of both of us when trying hard to synthesize stilbenes.

Table of Content

List of Figures

List of Schemes

List of Tables

1 Introduction

1.1 Organometallic Complexes and Applications in Catalysis

1.1.1 Organometallics Chemistry

Organometallic chemistry lies at the interface of organic chemistry and inorganic chemistry. The goal of organometallic chemistry is to study the structure, properties and reactions of organometallic compounds, which are defined as compound containing one or more chemical bonds between a carbon atom of an organic group and a metal including alkaline, alkaline earth, transition metal and, sometimes, metalloids such as boron, silicon and tin. A related category of molecules is “metal-organic," which refers to metal containing compounds lacking direct metal-carbon bonds, but which contain organic ligands such as metal β-diketonates, alkoxides, dialkylamides, and phosphines. Metal-organic compounds are also of interest.[1]

A large number of organometallic molecules have been discovered/synthesized and used to investigate reactivity as well as to develop new synthetic methods for organic and polymer chemistry.[1] Figure 1.1 shows two examples of classic organometallic complexes (i.e., the Pt and Fe complexes) and one example of a metal-organic complex (i.e., the Rh complex).

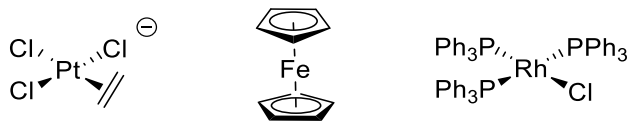

Zeise's salt **Ferrocene** **Wilkinson's catalyst**

Figure 1.1. Examples of organometallic and metal-organic complexes: Zeise's salt (Pt), ferrocene (Fe) and Wilkinson's catalyst (Rh).

Zeise's salt, potassium trichloro(η^2-ethylene)platinate(II), is an air stable, yellow compound with an formula of $K[PtCl_3(C_2H_4)]\cdot H_2O$. It was discovered by William Christopher Zeise, at the University of Copenhagen, through the addition of K_2PtCl_4 salt into boiling ethanol. As one of the first organometallics compounds reported,[2] Zeise's salt has receives attention in the field of organometallics chemistry. The coordination of ethylene to a transition metal was unique at that time, and it stimulated much interest in organometallic chemistry.[3]

Ferrocene was discovered by T.J. Kealy and P.L.Paulson in 1951 at University in Pittsburgh.[4] Cyclopentadienyl magnesium bromide (CpMgBr) was reacted with iron(II) chloride in attempt to create a fulvalene. When an orange complex formed, the chemists hypothesized that the iron was bound to one carbon in each ring. A year later, in 1952, G. Wilkinson and R. B. Woodward deduced the sandwich structure: two anionic cyclopentadienyl (Cp) rings each donating 6 π electrons to the Fe^{2+} cation.[5] The stability of ferrocene and structure defied conventional bonding descriptions of the time, and the discovery significantly increased interest in organometallic chemistry. In fact, Wilkinson shared the Nobel Prize in 1973 for his work on ferrocene.

Wilkinson's catalyst is the common name for chloridotris(triphenylphosphine)rhodium(I), a coordination complex of rhodium with the formula $RhCl(PPh_3)_3$ (Ph = phenyl).[6] This reddish brown solid has been widely used as a catalyst for the hydrogenation of olefins.[7] The discovery and exploration of this compound have led to several advancements in the field of organometallics as well as homogeneous catalysis.

1.1.2 Application of Organometallic Complexes in Catalysis

In 1836, the term “catalysis” was introduced by Berzelius and was defined by Ostwald in 1894. In Ostwald's definition, the catalyst is a substance that increases the rate of a chemical reaction without being consumed.[7] In an organometallic complex catalyzed process, the catalyst will undergo a series of transformations to yield the product. The regeneration of the starting complex is required to close the catalytic cycle and because of this, catalyst can be used in a sub-stoichiometric amount relative to limiting reagent.[8] An example of a rhodium catalyzed olefin (using ethylene as the example) hydrogenation is shown in Scheme 1.1.

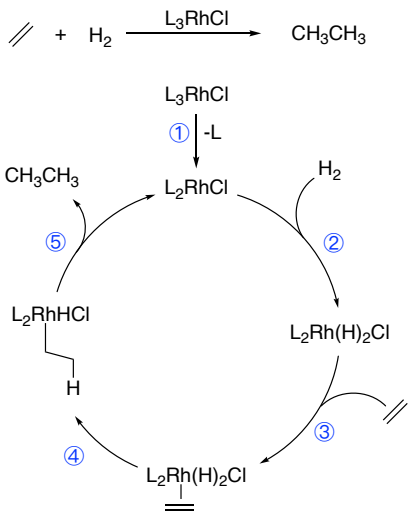

Scheme 1.1. Catalytic cycle of Rh(I) catalyzed ethylene hydrogenation to produce ethane (L = triphenylphosphines).

The catalytic cycle, which is the combination of steps comprising an overall catalytic process, of ethylene hydrogenation is shown in Scheme 1.1. The overall reaction is shown at the top, which is the conversion of ethylene and dihydrogen to ethane. In this example, there are five steps in this catalytic cycle: ① Dissociation of the ligand L (L triphenylphosphine) to create a vacant site for dihydrogen coordination; ② Oxidative addition of dihydrogen to the rhodium center to form a rhodium dihydride intermediate; ③ ethylene coordination to Rh; ④ ethylene insertion into one of the rhodium-hydride bonds; ⑤ reductive elimination of ethane and regeneration of the starting Rh catalyst.

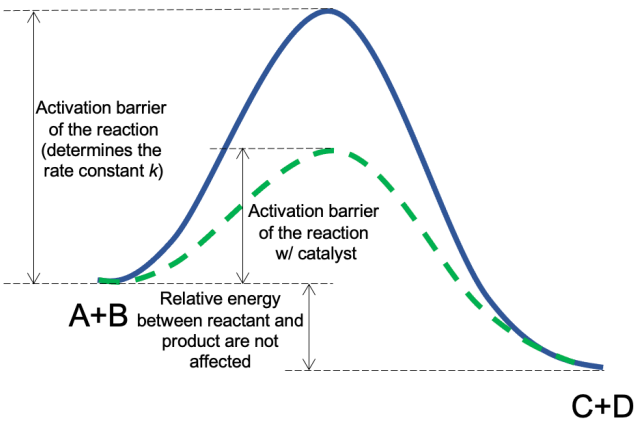

Figure 1.2. A simplified reaction diagram for an uncatalyzed and a catalyzed reaction A=B → C+D.

Catalysts work by providing an alternative mechanism involving a different transition state with a lower overall activation barrier than the reaction without the catalyst. Hence, catalysts can enable reactions that would otherwise be slow due to a high kinetic barrier. In many cases, the addition of a catalyst allows for a reaction to occur under milder conditions. A simplified depiction of the energy change upon inclusion of a catalyst is shown in Figure 1.2. In this example, for the generic reaction representation from A+B to C+D, the presence of the catalyst lowers the activation energy of the reaction and thereby increases the rate of the reaction. Only energy if the transition state is affected (kinetic parameter), the energies of the starting material and the product (thermodynamic parameter) remain the same.

1.1.3 Examples of Transition Metal Catalysts

There are several examples of homogeneous transition metal catalysts that have been implemented on an industrial scale, including use in the Wacker process, olefin hydroformylation, the Monsanto acetic acid process and the related Cativa process, and

cross-coupling reactions.[1, 9-11] The Wacker process (Scheme 1.2) uses $PdCl_2$ salts to oxidize ethylene to acetaldehye on a scale of ~4 million tons per year.[1] This served as the world's major source of acetaldehyde until 1980 due to the low cost of ethylene feedstock at the time.[12] A general catalytic cycle of the Wacker's process is shown below (Scheme 1.2).

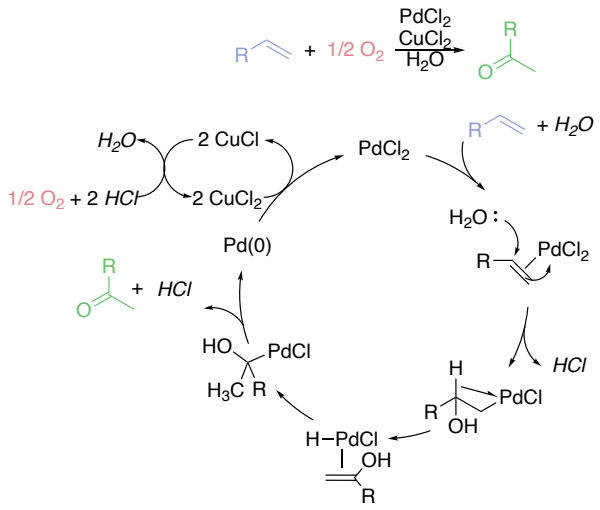

Scheme 1.2. Catalytic cycle for the Wacker process.

A proposed catalytic cycle of the Wacker process involves nucleophilic addition of water to coordinated ethylene to yield a Pd–alkyl–OH intermediate followed by a β-hydride elimination to form an enol–Pd–H species. The enol insert to the palladium hydride bond to form a (α-OH)alkyl–Pd and then release acetaldehyde followed by formation of Pd(0). To recycle palladium, the resulting Pd(0) is oxidized by two equivalents of $CuCl_2$, and the reduced CuCl in turn is re-oxidized to $CuCl_2$ by dioxygen in the presence of HCl. Two processes are commercialized for the production of acetaldehyde: a one-stage process and a two-stage process.[13] In the one stage process, ethylene and purified dioxygen are passed concurrently in a reaction tower at ~130 °C and 400 kPa.[13] An aqueous solution of

$PdCl_2$ and $CuCl_2$ serves as catalyst mixture, and $CuCl_2$ is regenerated *in situ*. In the contrast, in the two stage process, the Pd catalyzed reaction and copper reoxidation are carried out separately in tubular reactors. This allows the use of unpurified air instead of purified dioxygen. Both processes allow the use of atmospheric dioxygen as the ultimate oxidant and enable the Wacker process to be viable for use in industries and laboratories.

Rhodium-catalyzed carbonylation of methanol to form acetic acid, the Monsanto acetic acid process, is another example of successful industrial application of homogeneous catalysis. Fourteen billion pounds of acetic acid manufacturing capacity is produced by this process (80% of global acetic acid capacity). The Monsanto acetic acid process uses $[RhI_2(CO)_2]^-$ to convert methanol and CO to acetic acid at 180 °C and 30 atm. The catalytic cycle of the Monsanto acetic acid process is shown in Scheme 1.3. This process involves the oxidative addition of MeI to the Rh catalyst; migratory insertion of CO to Rh-Me bond and reductive elimination of Me(CO)I and formation of the product via hydrolysis. Similar process catalyzed by iridium catalyst $[IrI_2(CO)_2]^-$ (as known as the Cativa process)was developed by BP.[10] Studies have suggested that the performance of this iridium catalyst could be promoted by ruthenium, and this combination leads to a superior catalyst comparing to Rh.

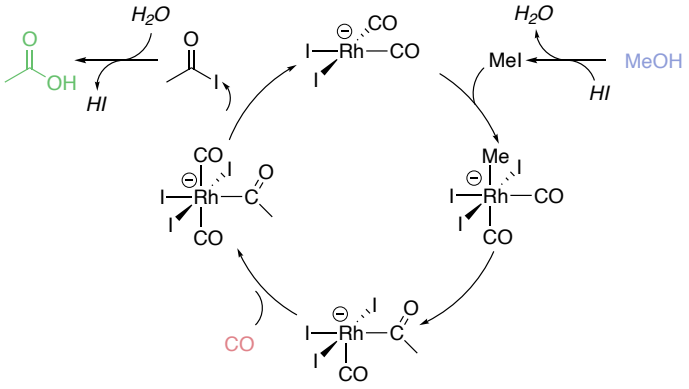

Scheme 1.3. Catalytic cycle for the Monsanto acetic acid process.

There are many variations of C–C coupling reactions, two of which, the Stille reaction of organostannanes and the Suzuki-Miyaura cross-coupling of organoboron compounds, are important cross coupling reactions that have been widely used and studied by synthetic organic chemists[14-16] A general catalytic cycle for Pd catalyzed C–C cross coupling reactions is shown in Scheme 1.4. Generally, the catalytic reaction involves oxidative addition of a halogenated arene to a Pd(0) catalyst with subsequent metathesis of the coupling partner to yield a Pd(II) di-hydrocarbyl species. Finally, the coupling product reductively eliminates from Pd(II) and the active Pd(0) catalyst is regenerated.

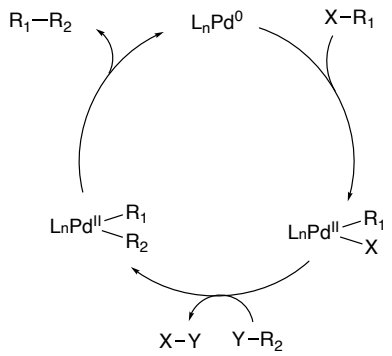

Scheme 1.4. General catalytic cycle for Pd mediated C–C cross coupling reactions.

1.2 Hydrocarbons and Chemical Processing

1.2.1 Overview: Hydrocarbons as Chemical Feedstocks

Hydrocarbons such as benzene, toluene, xylenes, methane, ethane and propane and their derivatives including ethylene, propylene, methanol, ethanol, isopropanol, ethylene glycol and propylene glycol, serve as importance resources for the chemical industry. The majority of hydrocarbons used by the chemical industry are derived from natural gas and petroleum.[17] Two major hydrocarbon feedstocks for petrochemicals are light alkanes, which are derived from natural gas, and arenes, which are generally derived from petroleum or naphtha.[18] Currently, in the United States, a major source for aromatic chemicals, including benzene, toluene, and xylenes (also known as the BTX series), is catalytic reforming of naphtha, the C5-C9 aliphatic and cycloaliphatic fraction of fossil sources.

Despite the mature technologies for chemical production based on hydrocarbons, the functionalization of hydrocarbons can be challenging because hydrocarbon C–H bonds are typically chemically inert (C–H bond dissociation energies (BDEs) are often 95-110

kcal/mol). For hydrocarbon functionalization, once a C–H bond is replaced with a carbon–functional group bond, the products tend to be more reactive than the starting material. As a result, it can be difficult to achieve the high selectivity for desired products.

1.2.2 Transition Metal Mediated C–H Activation

Over the past century, there has been an increase in the development of transition metal mediated C–H functionalization of hydrocarbons. This has expanded knowledge of hydrocarbon functionalizations and has allowed scientists to develop new methods to synthesize valuable products, such as alcohols, ketones, acids, and peroxides from hydrocarbons.[19-21] Often, the result of "functionalization" of a C–H bond is the replacement of a C–H bond with C–O, C–N, or C–X (X = halogen) bonds. Generallyk, the activation of saturated hydrocarbons (alkanes) is more challenging compared to the activation of an unsaturated olefin or arene, which is partly due to challenges associated with alkane coordination to active metal catalyst sites.

Several pathways of C–H activation have been proposed for transition metal (Scheme 1.5).[22-24] C–H activation via σ-bond metathesis is often observed from the alkyl or hydride complexes of early transition metals with a d^0 electronic configuration.[25, 26] The outcome of the reaction is usually the interchange of hydrocarbyl groups between a hydrocarbon and a metal aryl or alkyl complex. For electron-rich and low valent middle or late transition metals, oxidative addition is often observed.[27] In one form of oxidative addition, a low(er)-valent complex, LnM^n, reacts to add one molecule of "A–B" to form $LnM^{n+2}(A)(B)$. For C–H activation, A–B = a C–H bond. The metal is formally oxidized by two electrons as a

result of the oxidative addition. Reductive elimination reaction is the reverse of oxidative addition. The electrophilic subsitiution C–H activation is typically observed with electron-deficient late transition metals, and involves activation of a coordinated C–H bond toward intermolecular deprotation (often by an uncoordinated counter-anion).[20]

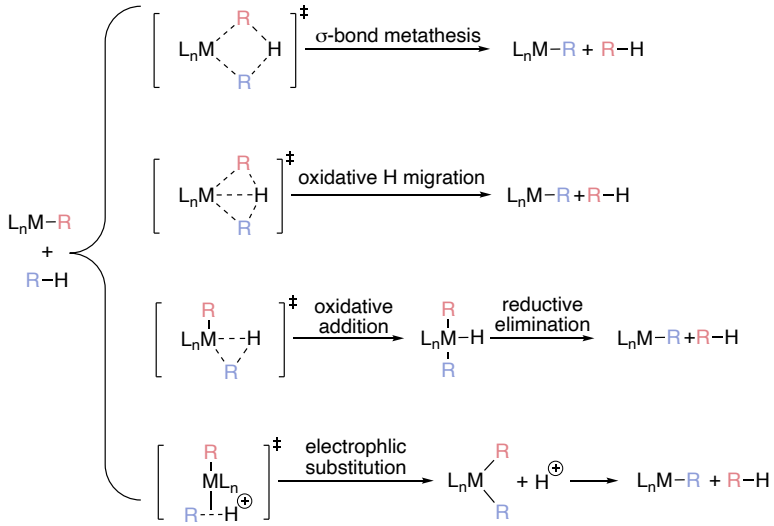

Scheme 1.5.Four different pathway for transition metal mediated C–H activation.

1.2.3 Carboxylate Assisted C–H Bond Activation (Concerted Metalation Deprotonation)

Concerted metalation deprotonation (CMD), the cleavage of aromatic C–H bonds promoted by a metal and a basic ligand, has been studied extensively.[28] Utilization of carboxylate ligands, in particular, has been proven to be an effective strategy for C–H activation. A key aspect of the CMD process using carboxylate ligands it the formation of the six membered transition state (Figure 1.3).

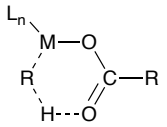

Figure 1.3. Six-membered transition state in carboxylate assisted C–H bond activation during a CMD process.

Previous studies by Catellani and co-workers on Mizoroki-Heck catalytic reactions have suggested that the use of KOAc with K_2CO_3 can enhance the palladium catalyzed arylation processes.[29-36] Larlock, Chen and co-workers[37, 38] discovered that a stoichiometric amount of carboxylate base additives can facilitate the palladium catalyzed C–H bond functionalization. In their studies of direct arylation of imidazolineones with aryl iodoes as arylating agent, Larlock and Chen observe that the addition of NaOAc is beneficial.[39, 40] Mechanistic studies, including isotopically labeling, have been used to suggest an carboxylate assisted C–H activation pathway. Taking advantage of carboxylate base, site selective C-2 arylation of indoles was achieved under mild conditions with aryl iodates as arylating reagent and Ag_2O as the base in the present of o-nitrobenzoic acid.[41, 42] In catalysis not using palladium, Sames and coworkers found the addition of cesium carboxylate enables rhodium catalyzed direct C-2 arylation of pyrroles and indoles.[41, 43] Under similar conditions, other bases, including carbonates and phosphates of alkali metals were found to be ineffective (Scheme 1.6).[41]

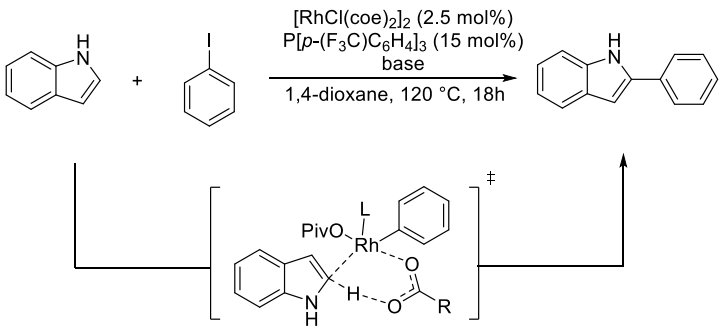

Scheme 1.6. Rh catalyzed direct C-2 arylation of indoles using iodobenzene as arylating reagent in the presence of CsOPiv (OPiv = pivalate). The reaction is proposed to proceed via a carboxylate assisted C–H activation.

The oxidative crossing-coupling between an olefin C–H bond and an arene C–H bond, known as the Fujiwara-Moritani reaction,[44-46] is a $Pd(OAc)_2$ catalyzed reaction that is used to synthesize alkenyl arenes. [47] In 2000, the mechanism of the C–H bond activation step was probed using a computational study by Sakaki and co-workers.[48] In this study, Sakaki and co-workers found that benzene C–H bond activation is more facile for palladium carboxylate compared to the traditional Pd(0) active species for cross-coupling reactions. Based their calculations, the benzene C–H activation mediated by $Pd(\kappa^2\text{-}O_2CH)_2$ is thermodynamically favored with a ΔG of -16.5 kcal/mol whereas benzene C–H activation mediated by Pd(0) is thermodynamically uphill. The thermodynamically favorable carboxylate assisted C–H activation is attributed to the a strong O–H bond is formed through the coordination of formate ligand (Scheme 1.7).

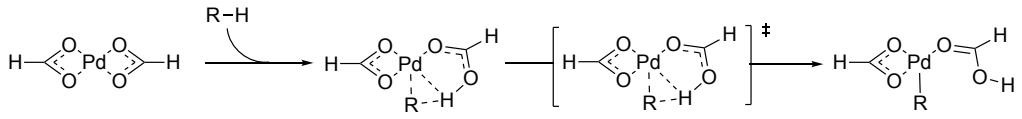

Scheme 1.7. Carboxylate assisted C–H activation in Fujiwara-Moritani reaction.

Traditional C–C coupling reactions require the use of pre-functionalized (often aryl halide or pseudo-halide) substrates and/or a stoichiometric trans-metallating reagent such as tin or boron-based compounds. This results in stoichiometric quantities of halogenated waste and often a second metal-containing waste product. These substrate requirements limit use of Pd C–C coupling reactions in large-scale processes. Thus, there is motivation for the development of new catalytic processes that achieve C–C coupling using unfunctionalized organic substrates.[49] Transition metal catalyzed arylation via C–H activation provide a potentially atom economiuc pathway for C–C bond forming processes (Scheme 1.8).[50] The reaction directly functionalizes the arene C–H bond to form metal–carbon bond and then coupling with the coupling partner yields the product.

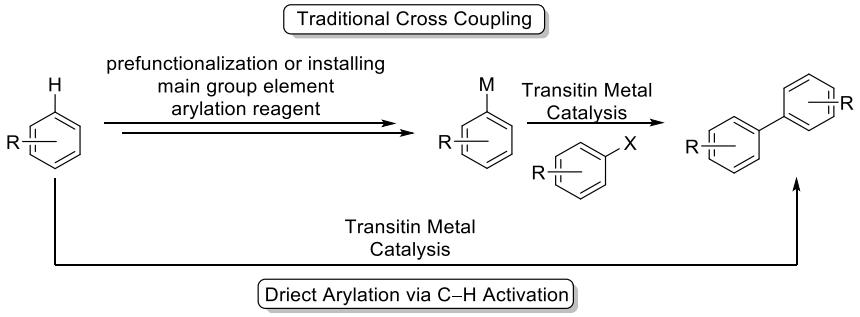

Scheme 1.8. Comparison between traditional transition metal mediated cross-coupling vs transition metal mediated direct arylation via C–H activation.

In 1982, Tajima[51] and Ames[52-54] reported a palladium catalzyed direct arylation of arenes with iodo or bromo arene as coupling partner. Recent mechanistc studies have

shown that base-assisted metalations are of relevance in an increasing number of transformations.[55-60] The influence of the carboxylic acid is investigated by Fagnou, Lafrance and co-workers. [61] They have found that the yield of intramoleculer direct arylation is significantly improved by addition of a catalytic amount of pivalic acid. The authors attribute this enhancment by suggesting the KOPiv is acting as proton shuttle during a concerted metalation deprotonatoin pathway (Scheme 1.9).

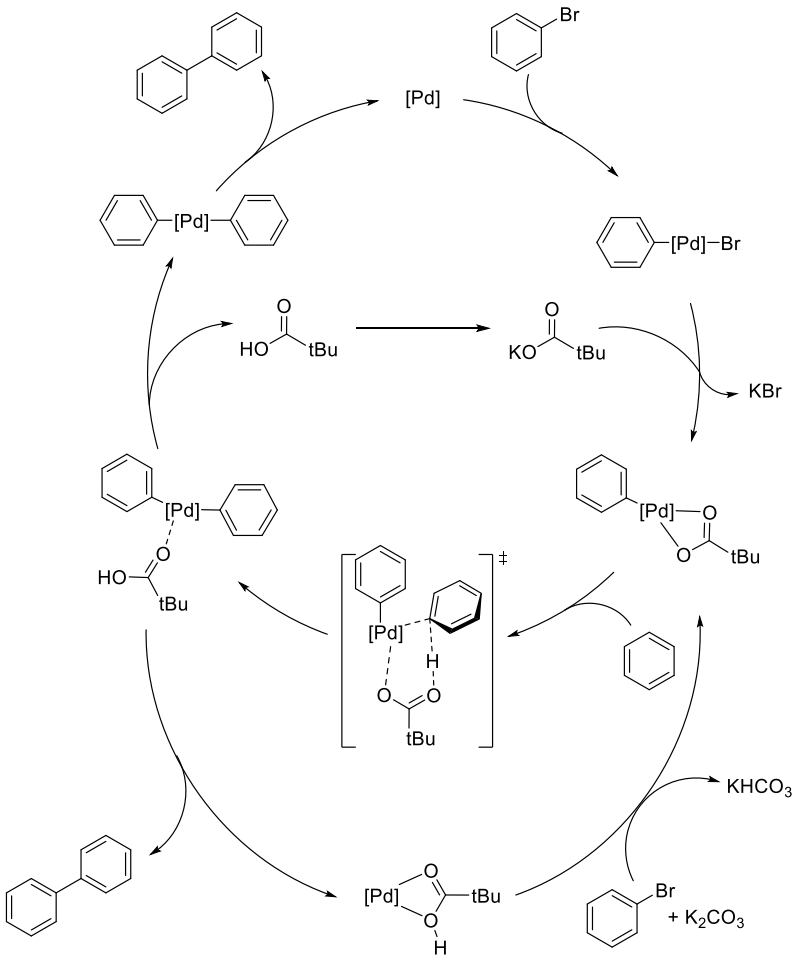

Scheme 1.9. Catalytic cycle for a Pd catalyzed arene-arene coupling reaction via CMD arene C–H activation. Pivalate is acting as proton shuttle.

1.3 Alkyl and Alkenyl Arenes

1.3.1 Overview

Benzene and alkyl benzenes (toluene and xylenes) from fossil resources have served as important building blocks for many industrial products such as plastics, elastomers, detergent, pharmaceuticals and other materials that derived from simple aromatic precursors.[18] Figure 1.4 shows the global benzene consumption breakdown in 2014 during which 71.6 million tons of benzene were consumed. Most benzene (~57%) is used to

produced ethylbenzene via a benzene alkylation using ethylene, and over 90% of ethylbenzene is converted to styrene via an energy intensive dehydrogenation process.[62, 63] The second largest produced alkyl benzene is cumene, which is made via benzene alkylation using propylene. Nearly 100% of cumene undergoes an oxidation process to cumene hydroperoxide, which serves as a precursor for the other important industrial products such as acetone and phenol.[64] Linear alkylbenzenes (LABs) and branched alkylbenzenes (BABs) account for ~5% of global benzene demand. [65] LABs are important due to applications in the manufacturing of detergents, surfactants, and fine chemicals.[66] The term linear alkylbenzene in commercial processes refers to *m*-aryl alkanes in which *m* is ≥ 2, which are synthesized from acid catalyzed processes using benzene and α-olefins. Acid catalyzed benzene alkylation reaction using α-olefins are incapable of producing 1-aryl alkane products.[67]

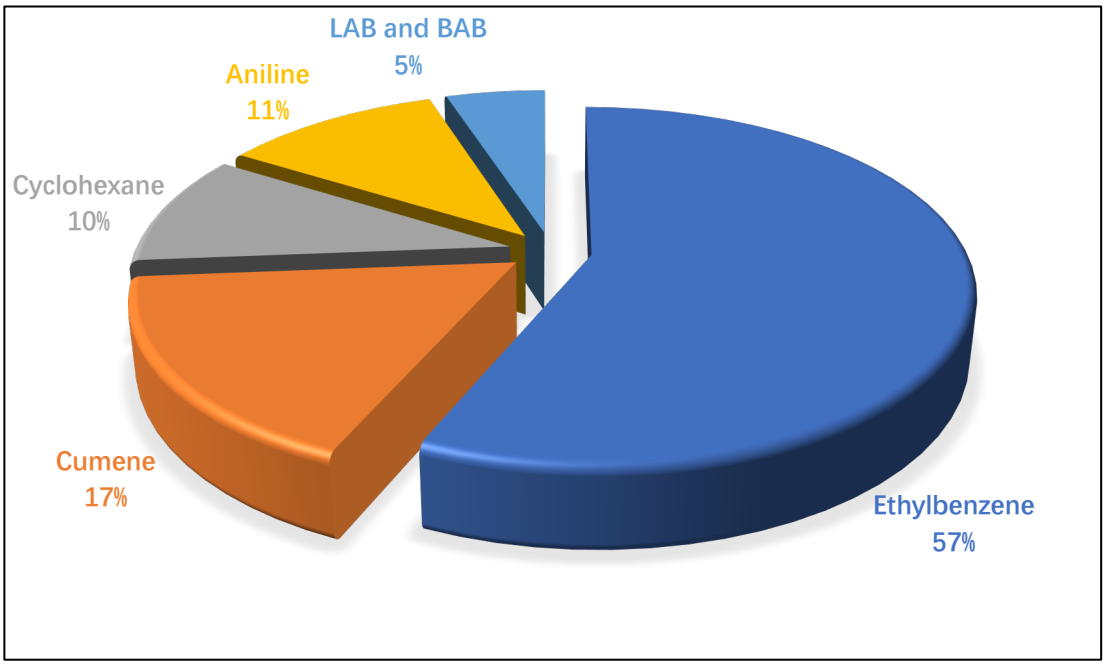

Figure 1.4. Global benzene consumption breakdown 2014 (LAB = linear alkylbenzene, BAB = branched alkylbenzene).

1.3.2 Current Synthetic Methods for Alkyl Arene Synthesis

Friedel-Crafts alkylation, discovered in late 1870s by Charles Friedel and James M. Crafts, has provided a way to covert alkenes (e.g., ethylene, propylene, isobutene, etc.) and arene to alkyl areens in the presence of a Lewis acid (often in combination with Brønsted acid). The generally accepted mechanism of Friedel-Crafts arene alkylation is an electrophilic arene substitution reaction (Scheme 1.10). The initial protonation of the alkene by the Brønsted acid and Lewis acid produces a carbocationic intermediate, which is followed by an electrophilic attack by the alkyl carbocation on the aromatic to form a Wheland intermediate. Deprotonation of the Wheland intermediate generates the alkyl arene.

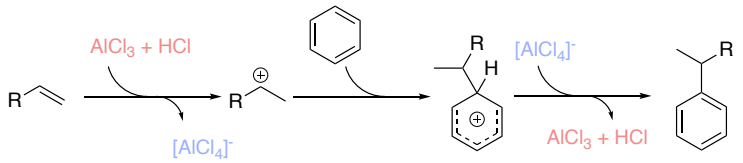

Scheme 1.10. Catalytic cycle for $AlCl_3$/HCl catalyzed Friedel-Crafts alkylation.

Friedel-Crafts alkylation under mild conditions dominated the industrial ethylbenzene production from benzene and ethylene for a long time.[62, 63] However, the nature of the electrophilic arene substitution reaction presents limitations that are based on the reaction mechanism. For example, electrophilic attack by the carbocation favors electron-rich arenes, which generally results in the alkylated benzene product being more reactive than the benzene starting material (e.g., ethylbenzene is typically 2 to 5 times more reactive than benzene in acid catalyzed ethylation reactions using ethylene). Thus, the production of di/tri-ethylbenzenes is problematic.[62] Also, for conversion of arenes and α-olefins, the formation of 1-aryl alkanes is not viable, which is a result of carbocationic intermediates. For example, when using propylene and benzene to make propyl benzenes, branched cumene is produced exclusively.

1.3.3 Zeolite-based Catalysts

The development of zeolite-based catalysts for arene alkylation addressed the issue of catalyst recyclability.[66, 68, 69] In general, zeolite catalysts can be easily isolated from the reaction mixture and subsequently reused. ZSM families, such as ZSM-5 and ZSM-22, are often used because of their selectivity and low toxicity. Another reason for ZSM-5 zeolite catalyst being used for benzene alkylation with ethylene is that its pore size can facilitate ethylbenzene diffusion, while it limits the formation of polyethylbenzenes (PEBs).

However, when comparing it to the traditional homogeneous Friedel-Crafts alkylation catalyst, the acidity in the zeolite catalyst is reduced, which can lead to lower catalyst reactivity and require higher temperatures for arene alkylation reactions.[66] Importantly, zeolite catalyzed arene alkylation still undergoes an acid-based mechanism, which means most of the limitations discussed in the previous section are relevant when using zeolite catalysts.

1.3.4 Arene Alkylation/Alkenylation Catalyzed by Late-Transition Metal

An alternative pathway to the traditional acid-based Friedel-Crafts alkylation is transition metal mediated arene alkylation and alkenylation via C–H activation, which defined as the addition of an arene C–H bond across an olefin C=C bond to produce alkyl/alkenyl benzene. In comparison to traditional Friedel-Crafts alkylation, it has many advantages. First, the catalysis undergoes a different pathway and there is no significant difference between the product and the starting arene (e.g. ethylbenzene and benzene) so thus that the polyalkylation is avoided. Second, different from acid-based catalyzed alkylation in which a carbocations is involved in the catalysis, transition metal catalyzed hydroarylation involves an olefin insertion step which offers the opportunity for selectivity of linear products. The regioselectivity is controlled by the olefin insertion step (*i.e.*, 1,2- vs 2,1-insertion) and it is possible to selectively produce 1-phenyl alkanes or their unsaturated alkenyl variants over the branched product. Third, transition metal mediated arene alkyl-/alkenylation has made it possible to functionalize electron deficient arenes

such as nitrobenzene and it has provided a pathway to selectively functionalize the position that cannot be synthesized by traditional acid-based catalysis where the electronic property dominates the selectivity.

The following sections describe a brief summary of the field of transition metal catalyzed arene alkyl- and alkenylation chemistry.

1.3.4.1 Olefin Hydroarylation Catalyzed by Ir(III) complexes

In 2000, Periana and coworkers reported that the dinuclear iridium complex, Ir(μ-acac-O,O,C^3)(acac-O,O)(acac-C^3)]$_2$ (Figure 1.5)could serves as a catalyst for the olefin hydroarylation reaction to convert benzene and ethylene to ethylbenzene.[70-72]

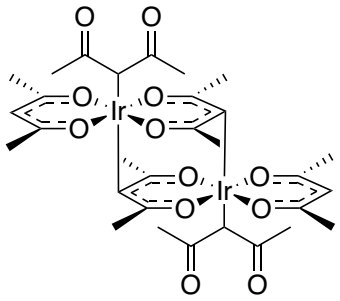

Figure 1.5. Structure of Ir(μ-acac-O,O,C^3)(acac-O,O)(acac-C^3)]$_2$ (acac = acetylacetonato or 2,4-pentanedione).

Heating a benzene/acetic acid solution of complex Ir(μ-acac-O,O,C^3)(acac-O,O)(acac-C^3)]$_2$ under 1.96 MPa for 3 hours at 180 °C resulted in 455 catalytic turnovers of ethylene benzene production with a turnover frequency (TOF) of 0.0421 s^{-1}. Under similar conditions, the propylene hydroarylation reaction gave a turnover number (TON) of 13 after 20 minutes with a TOF of 0.011 s^{-1}. In this reaction, a 61:39 ratio of linear n-propyl

benzene to cumene is observed, indicating the reaction proceeds in a different route than the Friedel–Crafts alkylation reaction where only the Markovnikov product, cumene, is produced.[72]

In 2003, Periana, Goddard and co-workers reported an Ir(III) complex, trans-(κ^2-O,O-acac)$_2$Ir(Ph)(L) [acac = acetylacetonate; L = H_2O, py, olefin; (acac)$_2$Ir], which could also catalyze ethylene hydrophenylation.[71, 73, 74] The detailed mechanistic study using computational methods has illustrated the catalytic cycle of this reaction.[74] For catalysis using trans-(κ^2-O,O-acac)$_2$Ir(Ph)(L) [acac = acetylacetonate; L = H_2O, py, olefin; (acac)$_2$Ir] it has been proposed that the initial steps in the catalytic process are: 1) replacement of L by olefin; 2) *trans* to *cis* isomerization of the Ph and coordinated olefin. The rate limiting step of olefin migratory insertion then takes place producing the Ir(III)-phenethyl species. A concerted C–H bond activation occurs afterwards, of which the authors describe as an oxidative hydrogen migration. The character of the transition state structure is a seven-coordinate Ir(V), with a full bond formed between the migrating hydrogen and iridium (Scheme 1.11)

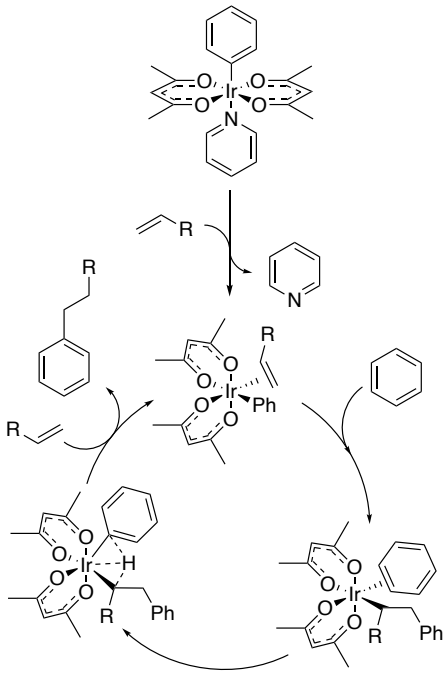

Scheme 1.11. Catalytic cycle of trans-(κ^2-O,O-acac)$_2$Ir(Ph)(py) catalyzed olefin hydroarylation.

We have recently discovered that iridium catalyst precursor, $IrCl_3$, could catalyze oxidative arene alkenylation in the presence of oxidant (copper salt, oxygen, etc.) to produce respectable yields of styrene. Interestingly, the reaction using α-olefin produces up to 15:1 linear to branched ratio (L:B). This is higher than what we had found from Pd catalysis (6:1 L:B) and Rh catalysis (10:1 L:B). Detailed mechanistic studies are undergoing to investigate the origin of this selectivity.

1.3.4.2 Olefin hydroarylation using Ru(II) complexes supported by Tp and Related Ligands

The Gunnoe groups have been studying a series of neutral ruthenium(II) catalysts with the general formula TpRu(L)(NCMe)Ph (Tp = hydridotris(pyrazolyl)borate; L = CO, PMe_3, $P(pyr)_3$, $P(OCH_2)_3CEt$; pyr = *N*-pyrrolyl) for catalytic ethylene hydrophenylation.[75-82]

The catalytic cycle of the TpRu(L)(NCMe)Ph catalyzed ethylene hydrophenylation is shown in Scheme 1.12 which involves 1) NCMe dissociation and ethylene coordination; 2) olefin insertion of olefin into the Pt–Ph bond; 3) coordination of benzene, and 4)aromatic C–H activation via σ-bond metathesis by TpRu-phenethyl fragment to yield the product, ethylbenzene ,and recover the catalyst precursor.

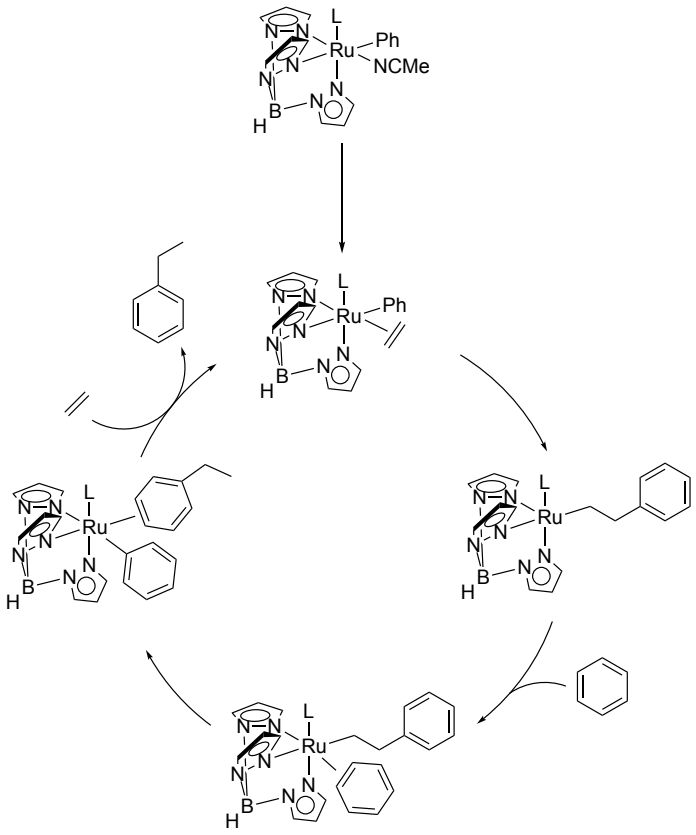

Scheme 1.12. Catalytic cycle of TpRu(L)(NCMe)Ph ethyelene hydrophenylation.

In those studies, we demonstrated that less electron donating ligands (or a strong π acid) "L" result in a decrease in the activation barrier for ethylene insertion into Ru–Ph bonds,[75, 77, 80] and, as a result, the more electron-deficient TpRu(L)(NCMe)Ph complexes are relatively better catalysts for olefin hydroarylation.

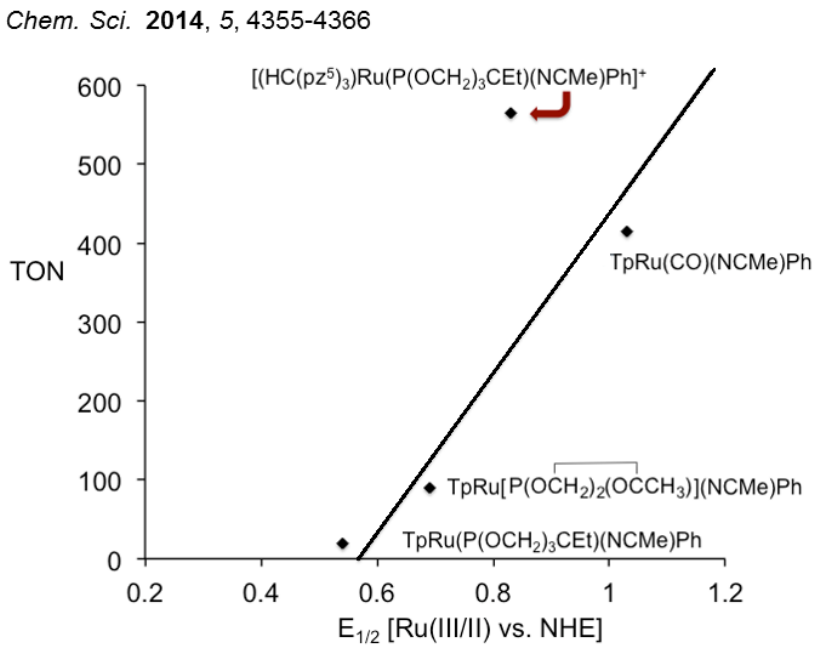

Figure 1.6. Ru(III/II) potential vs. TON of ethylene hydrophenylation reaction.

Figure 1.6 shows the relationship between Ru(II/III) redox potential and catalytic turnover numbers from TpRu(L)(NCMe)Ph catalyzed ethylene hydrophenylation. Based on these result, we anticipate that catalyst with higher Ru(III/II) potential, indicating a more electron deficient Ru center, will produce more ethylene benzene.

Detailed studies have revealed why TpRu(L)(NCMe)Ph bearing a strong donating ligand L cannot be an effective catalyst. The slowed olefin insertion allows for ethylene C–H activation to take place over ethylene insertion, ultimately forming the thermally stable and catalytically inactive η^3-methylallyl complex[75, 77, 79, 80] competes with ethylene insertion. (Scheme 1.13)

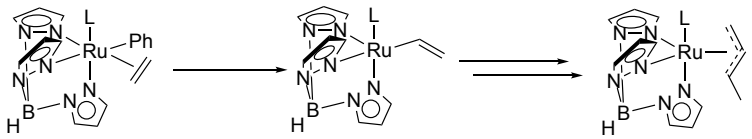

Scheme 1.13. Olefinic C–H activation and the formation of TpRu(L)(h3-allyl) resting state when using TpRu(L)(NCMe)Ph with a strong donating L.

Hence, the most electron-poor complex among the series TpRu(L)(NCMe)Ph, with L = CO, proved to be the longest-lived catalyst. Accordingly, more electron-poor Ru(II) complexes have been pursued in efforts to further improve catalytic activity.

1.3.4.3 Olefin Hydroarylation Catalyzed by Square Planer Pt(II) Complexes

Benefitting from the strong covalent bonding between platinum and carbon/hydrogen, many platinum complexes have been reported to mediate arene C–H activation and olefin insertion. Platinum catalyzed olefin hydroarylation, the combination of those two steps, has been studied extensively by many research groups.[83-88]

In 2008, Goldberg and co-workers synthesized the unsymmetrical (pyridyl)pyrrolide ligand supported Pt(II) complex. The hydroarylation of ethylene using this neutral Pt(II) complex resulted in 26 TON of ethylbenzene at 100 °C.[89, 90] The catalytic cycle of this reaction is shown in Scheme 1.14.

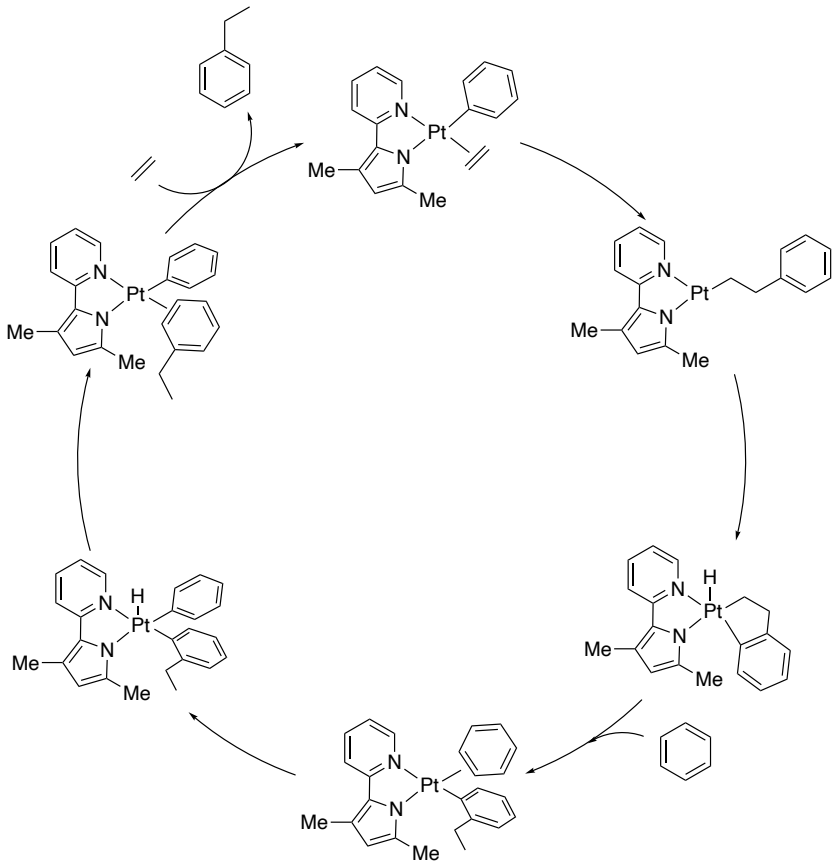

Scheme 1.14. Catalytic cycle of Pt(II) catalyzed ethylene hydrophenylation reported by Goldberg et al.

Tilly and co-workers reported that Pt(II) complexes supported by 2,2′-pyridyl-indolate ligands catalyze hydroarylation of ethylene, propylene and norbornene with highest reported TO of ethylbenzene product at ~25 TOs.[91]

In the Gunnoe lab, we have published a series of Pt(II) catalysts for olefin hydroarylation.[76, 92-95] We have reported a cationic complex [(tbpy)Pt(Ph)(THF)][BAr'$_4$] (tbpy = 4,4′-di-tert-butyl-2,2′-bipyridine, Ar' = 3,5-bis(trifluoromethyl)phenyl) that could produce ~66 TOs of ethylbenzene and ~35 TOs of diethylbenzene after 16 hours of reaction at 100 °C under 15 psig of ethylene pressure. The reaction temperature and higher ethylene pressure (120 °C and 0.03 MPa) resulted in the production of ~119 TOs of ethylbenzene,

diethylbenzenes, and styrene, corresponding to an 89% yield. A TOF of 7.1×10^{-3} s^{-1} for ethylbenzene production is reached with 0.1 MPa of ethylene pressure at 120 °C after 4 hours.

Detailed mechanistic studies have revealed that the Pt(II) catalyzed olefin hydroarylation proceeds via the following pathway: 1) THF dissociation and ethylene coordination; 2) olefin insertion into the Pt–Ph bond; 3) coordination of benzene; and 4) aromatic C–H activation via σ-bond metathesis by Pt–phenethyl fragment to yield the product, ethylbenzene, and recover the catalyst precursor.

Two different C–H activation pathways were proposed for the platinum catalysis. The first is a single step concerted pathway where the H atom is transferred from the arene via a metathesis reaction. The second possibility is a two-step pathway involving an oxidative addition (O.A.) of the arene and reductive elimination (R.E.) of the product. DFT calculations (Scheme 1.15) have suggested that for the [(bpy)Pt(Ph)(THF)][BAr'$_4$] catalytic system, the activation barrier of the two step O.A./R.E. pathway is 2.3 kcal/mol lower than single step metathesis pathway.

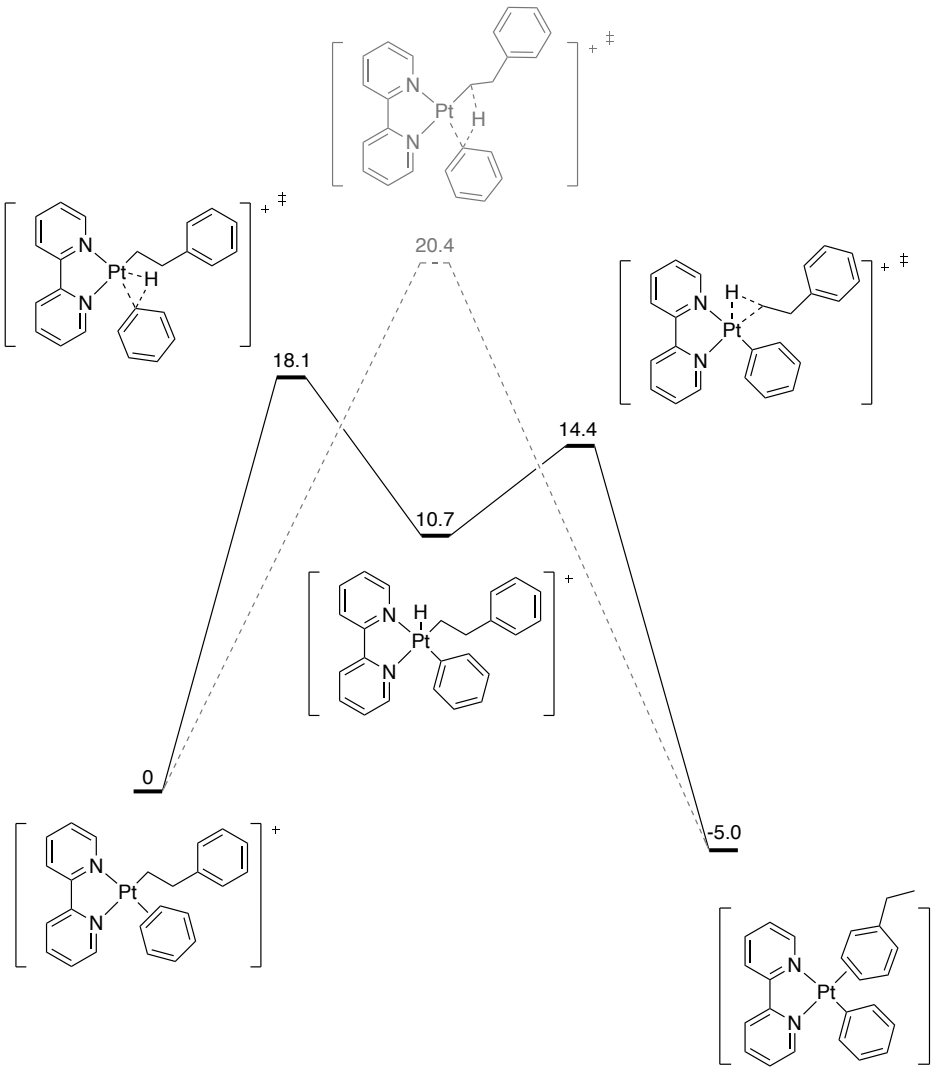

Scheme 1.15. Computational energy profile diagram of two [(bpy)Pt(Ph)(THF)][BAr'$_4$] mediated C–H activation. Comparison of oxidative addition (black) and σ-bond metathesis pathway (grey).

Modification of the bpy ligands has allowed us to investigate the influence of electronic and steric properties of the ligand on catalysis. We have reported that the change on catalyst activity and Markovnikov selectivity is observed when the 4 and 4′ position on the ligand are modified. Changing the substituents from electron donating methoxy or tert-butyl substituents to electron withdrawing nitro group the selectivity shifts toward the anti-Markovnikov product. A slight trend toward linear-selective catalysis was observed with

more electron-withdrawing substituents. These ligand modifications resulted in slight changes in the alkylation (ethylbenzene)/alkenylation (styrene) product selectivity (Table 1.1)

Table 1.1. The influence of ligand modification on alkylation/alkenylation selectivity in the Pt catalyzed ethylene hydrophenylation reaction.

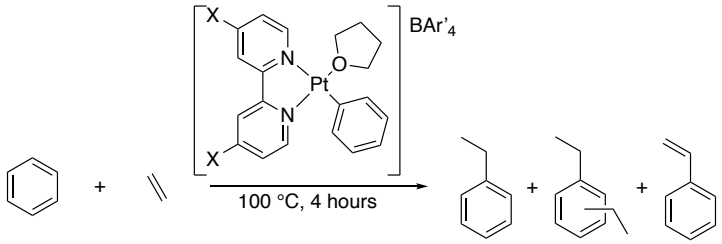

X	Ethylbenzene (TON)	Diethylbenzenes (TON)	Styrene (TON)	Ethylbenzenes:Styrene Ratio
OMe	3.3	0.7	0.4	8.3
tBu	4.0	0.9	0.5	8.0
H	5.5	1.4	0.7	7.9
Br	0.2	0	1.3	0.2
CO_2Et	1.9	0.5	1.2	1.6
NO_2	0	0	1	/

Conditions: 0.01 mol% catalyst loading relative to benzene, 0.3 MPa ethylene, 100 ºC for 4 h.

For [(Brbpy)Pt(Ph)(THF)][BAr'$_4$] and [(EtOCObpy)Pt(Ph)(THF)][BAr'$_4$] catalyzed ethylene hydrophenylation reactions, styrene is the major product, although the catalyst activity is bad where the total TON is 1.5 and 3.6, respectively.

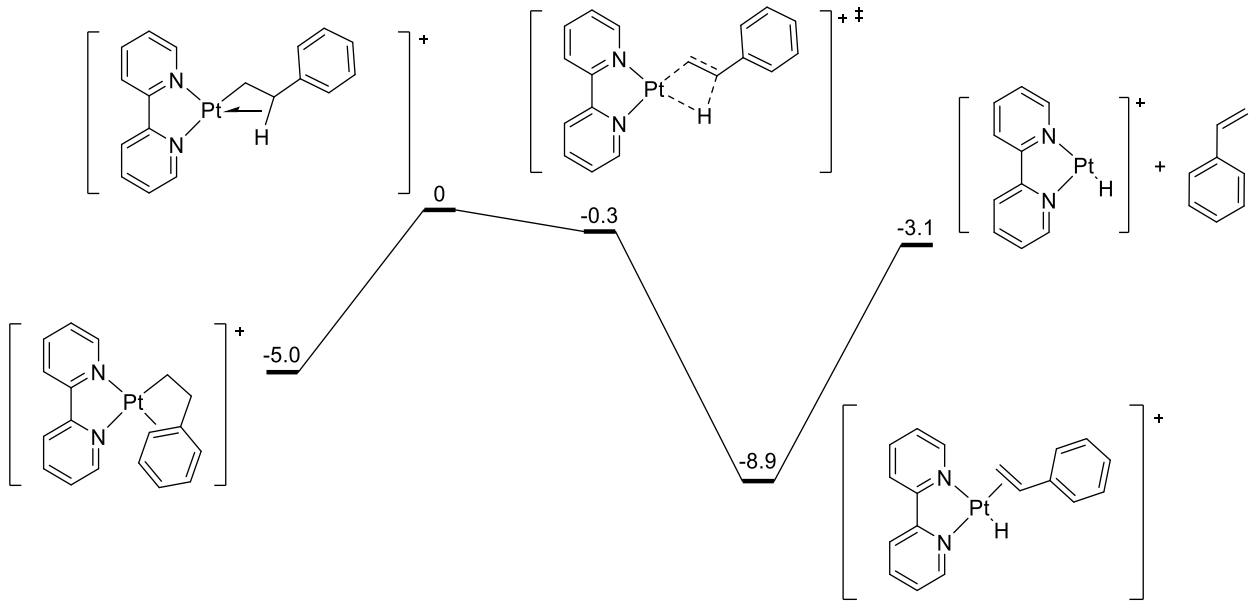

Scheme 1.16. DFT energy profile diagram of [(bpy)Pt(Ph)(THF)][BAr'4] catalyzed styrene production.

The formation of the unsaturated product styrene suggested an alteration needed to be made to the hypothesized mechanism. It was proposed that styrene is produced by β-hydride elimination from (bpy)Pt(CH_2CH_2Ph)$^+$. The β-hydride elimination is reversible and styrene dissociation carries an activation barrier of 7.6 kcal/mol so it is unfavorable, and more importantly under catalytic conditions, the resulting Pt-hydride decomposes. (Scheme 1.16)

1.3.4.4 Arene Alkenylation Catalyzed by Rhodium Complexes

Although in our Pt(II) studies, the production of styrene was also coupled with the formation of platinum hydride which leads to the irreversible reduction to form platinum black, this selectivity shift from alkylation to alkenylation is very promising due to the possibility of direct synthesis of styrene in a single step.

In 2015, our group reported that catalyst precursor (^{Fl}DAB)Rh(TFA)(η^2-C_2H_4) (^{Fl}DAB = *N*,*N'*-bis(pentafluorophenyl)-2,3-dimethyl-1,4-diaza-1,3-butadiene; TFA = trifluoroacetate) catalyzed benzene alkenylation using ethylene in the presence of $Cu(OAc)_2$ as oxidant.

In this reaction, benzene first coordinates to the Rh center followed by a C–H activation step to release HX (X= OAc or TFA) forming a M–Ph intermediate. The coordinated ethylene then inserts into the M–C bond to form M–CH_2CH_2Ph intermediate, and β-hydride elimination then generates coordinated styrene and a metal-hydride complex. This provides a strategy for the direct, single-step production of styrene. Cu(II) salts were used as *in situ* oxidants to regenerate the catalyst and complete the cycle. Utilization of Cu(II) salts is attractive to be used in situ because the reduced Cu(I) complexes can be reoxidized to Cu(II) with dioxygen, which is demonstrated by the Wacker-Hoechst process for ethylene oxidation. Under optimized conditions, over 800 TOs can be reached after 96 hours and neither ethylbenzene nor vinyl acetate production was detected.

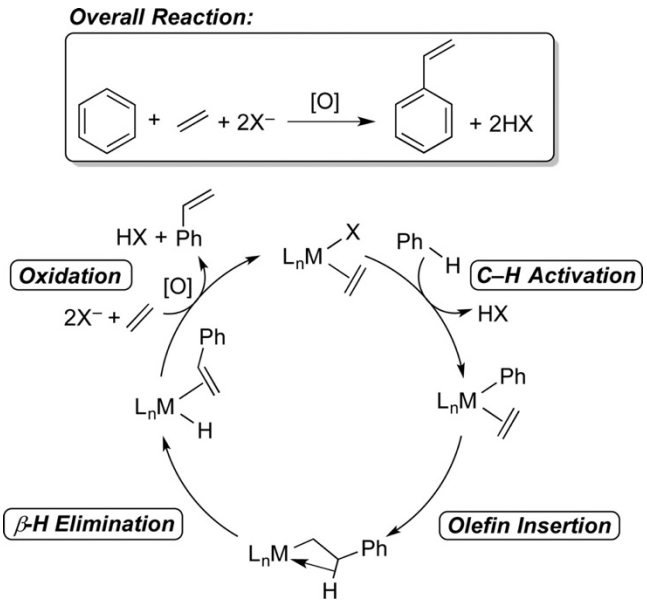

Scheme 1.17. Proposed cycle for transition metal–catalyzed styrene production from benzene and ethylene using CuX2 as an oxidant.

Another advantage of transition metal catalyzed hydroarylation is its access to non-acidic conditions, which gives the opportunity for selective production of linear alkylbenzenes. Traditional Friedel-Crafts alkylation leads to generation of a carbocation intermediate, which will rearrange to form the most stable carbocation. The stability follows the order of primary < secondary < tertiary carbon. Recently, our group reported the Rh complex, $[Rh(\mu\text{-}OAc)(\eta^2\text{-}C_2H_4)]_2$, is a catalyst precursor for the conversion of α-olefins and arenes to alkenyl arenes with high anti-Markovnikov selectivity (up to a 10:1 L:B ratio) using Cu(II) as oxidant.[96] The catalytic results with different olefins and arenes are summarized in Table 1.2

Table 1.2. Comparison of arene alkylation using $AlCl_3$ as the primary catalyst versus $[Rh(\mu\text{-}OAc)(\eta^2\text{-}C_2H_4)_2]_2$.

	Arene	Coupling Partner	*o*:*m*:*p*	L:B	TON	Product
$AlCl_3$	toluene	propylene	3:1:2.6	>98% B	n.r.	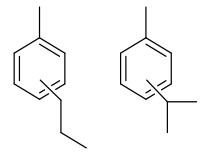
Rh	toluene	propylene	1:8.9:9.3	9.4:1	86(17)	
$AlCl_3$	chlorobenzene	2-chloropropane	6.4:1:5.1	100% B	n.r.	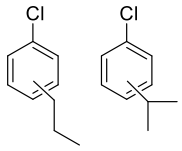
Rh	chlorobenzene	propylene	1:11:7	10:1	116(3)	
$AlCl_3$	anisole	2-chloropropane	62:4:34	100% B	n.r.	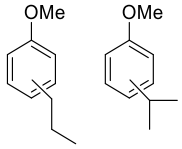
Rh	anisole	propylene	1:2.4:6.4	7.8:1	92(7)	
$AlCl_3$	benzene	propylene	n/a	100% B	95	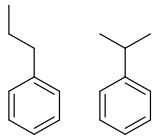
Rh	benzene	propylene	n/a	8:1	80(4)	
$AlCl_3$	benzene	1-hexene	n/a	100% B	67	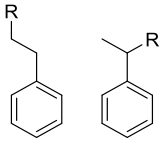 R = propyl
Rh	benzene	1-pentene[§]	n/a	8:1	122(10)	
Rh	benzene	neohexene[§]	n/a	100% L	30(8)	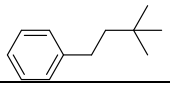
Rh	benzene	isobutylene[§]	n/a	100% L	100(2)	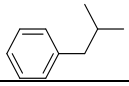
$AlCl_3$	benzene	isobutylene	n/a	100% B	n.r.	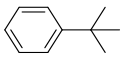

* The $AlCl_3$ results are from references. **Rh** = $[Rh(\mu\text{-}OAc)(\eta^2\text{-}C_2H_4)_2]_2$. Unsaturated products are produced from Rh catalyzed reaction and all the products results shown in the table are after hydrogenation.

1.3.4.5 Arene Alkenylation (Oxidative olefin hydrorylation) Catalyzed by Palladium Complexes

Palladium complexes, either Pd(II) or Pd(0), have been reported as exceptional catalysts for a variety of C–C coupling reactions. However, the application of palladium catalysts in oxidative olefin hydroarylation has been limited due to the low selectivity and/or low yield. Pioneering work performed by Fujiwara and co-workers reported styrene production using $Pd(OAc)_2$ and an AgOAc oxidant, but yields (relative to oxidant) were low (~12%), and also observed were the undesired production of stilbene and biphenyl.[97] Periana and co-workers reported styrene production using $Pd(OAc)_2$ with $Cu(OAc)_2/O_2$ as the oxidant system, but they observed significant vinyl acetate production (~2.5 times the amount of styrene produced) as a byproduct.[70] Ishii and co-workers reported that (DBM)$Pd(OAc)_2$ (DBM = dibenzoylmethane) affords 58% selectivity for styrene production (stilbene and vinyl propionate, a product of reaction with solvent, are also produced) using a polyoxometalate oxidant, but their yields were low (2%).[98] Sanford and co-workers reported that (3,5-dichloropyridyl)$Pd(OAc)_2$ affords styrene with 100% selectivity.[99] However, their process suffers from low yields (~33%) and uses an expensive oxidant ($PhCO_3tBu$) that cannot be aerobically regenerated. The Gunnoe lab has been working on the optimization of Pd catalyzed oxidative olefin hydroarylation. Efforts have been made by Dr. Bradley McKeown and Dr. Benjamin Vaughan to design and synthesize ligated Pd(II) catalysts including the cationic bipyridine supported Pd(II) complex [(tbpy)Pd(Me)(NCMe)][BArF4] (tbpy = 4,4'-di-*t*butyl-2,2'-bipyridyl). Comparing to

similar Pt(II) catalyst, this Pd catalyzed ethylene hydrophenylation reaction showed a significant selectivity change to favor styrene over ethylbenzene. With the second Pd(II) complex, diazabutadiene-ligated (DAB)$Pd(OAc)_2$, we have found the formation of biphenyl and stilbene to be suppressed.

However, under most anaerobic conditions and aerobic conditions where O_2 is used as the terminal oxidant, vinyl acetate production is significant. The reaction still needs further optimization to compete with Rh catalysis.

1.4 Reference

1. Crabtree, R. H., *The organometallic chemistry of the transition metals*. John Wiley & Sons: 2009.
2. Zeise, W., Von der Wirkung zwischen Platinchlorid und Alkohol, und von den dabei entstehenden neuen Substanzen. *Annalen der Physik* **1831,** *97* (4), 497-541.
3. Mingos, D. M. P., A historical perspective on Dewar's landmark contribution to organometallic chemistry. *J. Organomet. Chem.* **2001,** *635* (1), 1-8.
4. Kealy, T. J.; Pauson, P. L., A New Type of Organo-Iron Compound. *Nature* **1951,** *168* (4285), 1039-1040.
5. Wilkinson, R., Whiting, and Woodward. *J. Am. Chem. Soc* **1952,** *74*, 2125.
6. Tris(triphenylphosphine)halorhodium(I). In *Inorg. Synth.*, 1967; pp 67-71.
7. Meakin, P.; Jesson, J. P.; Tolman, C. A., Nature of chlorotris(triphenylphosphine)rhodium in solution and its reaction with hydrogen. *J. Am. Chem. Soc.* **1972,** *94* (9), 3240-3242.
8. Hartwig, J. F., *Organotransition metal chemistry: from bonding to catalysis*. Univ Science Books: 2010.
9. Pospech, J.; Fleischer, I.; Franke, R.; Buchholz, S.; Beller, M., Alternative Metals for Homogeneous Catalyzed Hydroformylation Reactions. *Angew. Chem. Int. Ed.* **2013,** *52* (10), 2852-2872.

10. Sunley, G. J.; Watson, D. J., High productivity methanol carbonylation catalysis using iridium: The Cativa™ process for the manufacture of acetic acid. *Catal. Today* **2000,** *58* (4), 293-307.

11. Jira, R., Acetaldehyde from ethylene--a retrospective on the discovery of the Wacker process. *Angew. Chem. Int. Ed. Engl.* **2009,** *48* (48), 9034-9037.

12. Wittcoff, H. A.; Reuben, B. G.; Plotkin, J. S., Chemicals and Polymers from Ethylene. In *Industrial Organic Chemicals*, Wiley: Hoboken, NJ, 2012; pp 139-209.

13. Acetaldehyde. In *Ullmann's Encyclopedia of Industrial Chemistry*.

14. Stille, J. K., The Palladium-Catalyzed Cross-Coupling Reactions of Organotin Reagents with Organic Electrophiles [New Synthetic Methods (58)]. *Angew. Chem. Int. Ed.* **1986,** *25* (6), 508-524.

15. Hassan, J.; Sévignon, M.; Gozzi, C.; Schulz, E.; Lemaire, M., Aryl−Aryl Bond Formation One Century after the Discovery of the Ullmann Reaction. *Chem. Rev.* **2002,** *102* (5), 1359-1470.

16. Miyaura, N.; Suzuki, A., Palladium-Catalyzed Cross-Coupling Reactions of Organoboron Compounds. *Chem. Rev.* **1995,** *95* (7), 2457-2483.

17. Hashiguchi, B. G.; Konnick, M. M.; Bischof, S. M.; Gustafson, S. J.; Devarajan, D.; Gunsalus, N.; Ess, D. H.; Periana, R. A., Main-Group Compounds Selectively Oxidize Mixtures of Methane, Ethane, and Propane to Alcohol Esters. *Science* **2014,** *343* (6176), 1232-1237.

18. Chemicals from Natural Gas and Petroleum. In *Industrial Organic Chemicals*, 2004; pp 57-99.

19. Introduction: CH Activation. *Chem. Rev.* **2017,** *117* (13), 8481-8482.

20. Balcells, D.; Clot, E.; Eisenstein, O., C—H Bond Activation in Transition Metal Species from a Computational Perspective. *Chem. Rev.* **2010,** *110* (2), 749-823.

21. Shilov, A. E.; Shul'pin, G. B., Activation of C−H Bonds by Metal Complexes. *Chem. Rev.* **1997,** *97* (8), 2879-2932.

22. C-H Transformation at Arenes. In *Handbook of C–H Transformations*, 2005; pp 99-256.

23. Smith, M. R., Review of C−H Activation. Topics in Current Chemistry, 292. *J. Am. Chem. Soc.* **2011,** *133* (10), 3684-3684.

24. Labinger, J. A.; Bercaw, J. E., Understanding and exploiting C-H bond activation. *Nature* **2002,** *417* (6888), 507-514.

25. Watson, P. L., Methane exchange reactions of lanthanide and early-transition-metal methyl complexes. *J. Am. Chem. Soc.* **1983,** *105* (21), 6491-6493.

26. Thompson, M. E.; Baxter, S. M.; Bulls, A. R.; Burger, B. J.; Nolan, M. C.; Santarsiero, B. D.; Schaefer, W. P.; Bercaw, J. E., .sigma.-Bond metathesis for carbon-hydrogen bonds of hydrocarbons and Sc-R (R = H, alkyl, aryl) bonds of permethylscandocene derivatives. Evidence for noninvolvement of the .pi. system in electrophilic activation of aromatic and vinylic C-H bonds. *J. Am. Chem. Soc.* **1987,** *109* (1), 203-219.

27. Janowicz, A. H.; Bergman, R. G., Carbon-hydrogen activation in completely saturated hydrocarbons: direct observation of M + R-H .fwdarw. M(R)(H). *J. Am. Chem. Soc.* **1982,** *104* (1), 352-354.

28. David, L.; Keith, F., Overview of the Mechanistic Work on the Concerted Metallation–Deprotonation Pathway. *Chem. Lett.* **2010,** *39* (11), 1118-1126.

29. Bressy, C.; Alberico, D.; Lautens, M., A Route to Annulated Indoles via a Palladium-Catalyzed Tandem Alkylation/Direct Arylation Reaction. *J. Am. Chem. Soc.* **2005,** *127* (38), 13148-13149.

30. Martins, A.; Lautens, M., Aromatic ortho-Benzylation Reveals an Unexpected Reductant. *Org. Lett.* **2008,** *10* (21), 5095-5097.

31. Thansandote, P.; Lautens, M., Construction of Nitrogen-Containing Heterocycles by C□H Bond Functionalization. *Chem. Eur. J* **2009,** *15* (24), 5874-5883.

32. Lautens, M.; Piguel, S., A New Route to Fused Aromatic Compounds by Using a Palladium-Catalyzed Alkylation – Alkenylation Sequence. *Angew. Chem. Int. Ed.* **2000,** *39* (6), 1045-1046.

33. Catellani, M., Novel Methods of Aromatic Functionalization Using Palladium and Norbornene as a Unique Catalytic System. In *Palladium in Organic Synthesis: -/-*, Tsuji, J., Ed. Springer Berlin Heidelberg: Berlin, Heidelberg, 2005; pp 21-53.

34. Catellani, M., Catalytic multistep reactions via palladacycles. *Synlett* **2003,** *2003* (03), 0298-0313.

35. Catellani, M.; Motti, E.; Della Ca', N., Catalytic Sequential Reactions Involving Palladacycle-Directed Aryl Coupling Steps. *Acc. Chem. Res.* **2008,** *41* (11), 1512-1522.

36. Catellani, M.; Frignani, F.; Rangoni, A., A Complex Catalytic Cycle Leading to a Regioselective Synthesis of o,o′-Disubstituted Vinylarenes. *Angewandte Chemie International Edition in English* **1997,** *36* (1-2), 119-122.

37. Shi, F.; Larock, R. C., Remote C–H Activation via Through-Space Palladium and Rhodium Migrations. In *C-H Activation*, Yu, J.-Q.; Shi, Z., Eds. Springer Berlin Heidelberg: Berlin, Heidelberg, 2010; pp 123-164.

38. Lu, J.; Tan, X.; Chen, C., Palladium-Catalyzed Direct Functionalization of Imidazolinone: Synthesis of Dibromophakellstatin. *J. Am. Chem. Soc.* **2007,** *129* (25), 7768-7769.

39. Lebrasseur, N.; Larrosa, I., Room Temperature and Phosphine Free Palladium Catalyzed Direct C-2 Arylation of Indoles. *J. Am. Chem. Soc.* **2008,** *130* (10), 2926-2927.

40. Ruiz-Rodríguez, J.; Albericio, F.; Lavilla, R., Postsynthetic Modification of Peptides: Chemoselective C-Arylation of Tryptophan Residues. *Chem. Eur. J* **2010,** *16* (4), 1124-1127.

41. Wang, X.; Lane, B. S.; Sames, D., Direct C-Arylation of Free (NH)-Indoles and Pyrroles Catalyzed by Ar−Rh(III) Complexes Assembled In Situ. *J. Am. Chem. Soc.* **2005,** *127* (14), 4996-4997.

42. Potavathri, S.; Pereira, K. C.; Gorelsky, S. I.; Pike, A.; LeBris, A. P.; DeBoef, B., Regioselective oxidative arylation of indoles bearing N-alkyl protecting groups: dual C-H functionalization via a concerted metalation-deprotonation mechanism. *J. Am. Chem. Soc.* **2010,** *132* (41), 14676-14681.

43. DeBoef, B.; Pastine, S. J.; Sames, D., Cross-coupling of sp(3) C-H bonds and alkenes: catalytic cyclization of alkene-amide substrates. *J. Am. Chem. Soc.* **2004,** *126* (21), 6556-6557.

44. Fujiwara, Y.; Moritani, I.; Danno, S.; Asano, R.; Teranishi, S., Aromatic substitution of olefins. VI. Arylation of olefins with palladium(II) acetate. *J. Am. Chem. Soc.* **1969,** *91* (25), 7166-7169.

45. Fujiwara, Y.; Moritani, I.; Matsuda, M.; Teranishi, S., Aromatic substitution of styrene-palladium chloride complex. II effect of metal acetate. *Tetrahedron Lett.* **1968,** *9* (5), 633-636.

46. Moritanl, I.; Fujiwara, Y., Aromatic substitution of styrene-palladium chloride complex. *Tetrahedron Lett.* **1967,** *8* (12), 1119-1122.

47. Oxidative Heck-Type Reactions (Fujiwara–Moritani Reactions). In *The Mizoroki–Heck Reaction*, 2009; pp 345-382.

48. Biswas, B.; Sugimoto, M.; Sakaki, S., C−H Bond Activation of Benzene and Methane by M(η2-O2CH)2 (M = Pd or Pt). A Theoretical Study. *Organometallics* **2000,** *19* (19), 3895-3908.

49. Farina, V., High-Turnover Palladium Catalysts in Cross-Coupling and Heck Chemistry: A Critical Overview. *Adv. Synth. Catal.* **2004,** *346* (13‐15), 1553-1582.

50. Ackermann, L.; Vicente, R.; Kapdi, A. R., Transition-Metal-Catalyzed Direct Arylation of (Hetero)Arenes by C-H Bond Cleavage. *Angew. Chem. Int. Ed.* **2009,** *48* (52), 9792-9826.

51. Nakamura, N., DIRECT PHENYLATION OF ISOXAZOLES USING PALLADIUM CATALYSTS: SYNTHESIS OF 4-PHENYLMUSCIMOL. **1982**.

52. Ames, D.; DE, A., Synthesis of dibenzofurans by palladium-catalysed intramolecular dehydrobromination of 2-bromophenyl phenyl ethers. **1983**.

53. Ames, D. E.; Opalko, A., Palladium-catalysed cyclisation of 2-substituted halogenoarenes by dehydrohalogenation. *Tetrahedron* **1984,** *40* (10), 1919-1925.

54. Ames, D. E.; Bull, D., Some reactions of 3-halogenocinnolines catalysed by palladium compounds. *Tetrahedron* **1982,** *38* (3), 383-387.

55. Lafrance, M.; Blaquiere, N.; Fagnou, K., Aporphine Alkaloid Synthesis and Diversification via Direct Arylation. *Eur. J. Org. Chem.* **2007,** *2007* (5), 811-825.

56. Lafrance, M.; Lapointe, D.; Fagnou, K., Mild and efficient palladium-catalyzed intramolecular direct arylation reactions. *Tetrahedron* **2008,** *64* (26), 6015-6020.

57. Campeau, L.-C.; Fagnou, K., Palladium-catalyzed direct arylation of simple arenes in synthesis of biaryl molecules. *Chem. Commun.* **2006,** (12), 1253-1264.

58. Lafrance, M.; Blaquière, N.; Fagnou, K., Direct intramolecular arylation of unactivated arenes: application to the synthesis of aporphine alkaloids. *Chem. Commun.* **2004,** (24), 2874-2875.

59. Campeau, L.-C.; Thansandote, P.; Fagnou, K., High-Yielding Intramolecular Direct Arylation Reactions with Aryl Chlorides. *Org. Lett.* **2005,** *7* (9), 1857-1860.

60. Campeau, L.-C.; Parisien, M.; Leblanc, M.; Fagnou, K., Biaryl Synthesis via Direct Arylation: Establishment of an Efficient Catalyst for Intramolecular Processes. *J. Am. Chem. Soc.* **2004,** *126* (30), 9186-9187.

61. Lafrance, M.; Fagnou, K., Palladium-Catalyzed Benzene Arylation: Incorporation of Catalytic Pivalic Acid as a Proton Shuttle and a Key Element in Catalyst Design. *J. Am. Chem. Soc.* **2006,** *128* (51), 16496-16497.

62. Styrene. In *Ullmann's Encyclopedia of Industrial Chemistry*.

63. Polystyrene and Styrene Copolymers. In *Ullmann's Encyclopedia of Industrial Chemistry*.

64. Phenol. In *Ullmann's Encyclopedia of Industrial Chemistry*, pp 1-20.

65. Size, G. M., Share & Trends Analysis Report By Application (Electronics, Composites, Energy), By Product (Graphene Nanoplatelets, Graphene Oxide), By Region, And Segment Forecasts, 2020–2027. **2020,** *28*.

66. Kocal, J. A.; Vora, B. V.; Imai, T., Production of linear alkylbenzenes. *Applied Catalysis A: General* **2001,** *221* (1), 295-301.

67. De Almeida, J.; Dufaux, M.; Taarit, Y. B.; Naccache, C., Linear alkylbenzene. *Journal of the American Oil Chemists' Society* **1994,** *71* (7), 675-694.

68. Čejka, J.; Wichterlová, B., Acid-Catalyzed Synthesis of Mono- and Dialkyl Benzenes over Zeolites: Active Sites, Zeolite Topology, and Reaction Mechanisms. *Catalysis Reviews* **2002,** *44* (3), 375-421.

69. Perego, C.; Ingallina, P., Combining alkylation and transalkylation for alkylaromatic production. *Green Chem.* **2004,** *6* (6), 274-279.

70. Taube, D.; Periana, R.; Matsumoto, T., Oxidative coupling of olefins and aromatics using a rhodium catalyst and a copper (II) redox agent. Google Patents: 2000.

71. Periana, R. A.; Liu, X. Y.; Bhalla, G., Novel bis-acac-O,O-Ir(III) catalyst for anti-Markovnikov, hydroarylation of olefins operates by arene CH activation. *Chem. Commun.* **2002,** (24), 3000-3001.

72. Matsumoto, T.; Periana, R. A.; Taube, D. J.; Yoshida, H., Regioselective hydrophenylation of olefins catalyzed by an Ir(III) complex. *J. Mol. Catal. A: Chem.* **2002,** *180* (1), 1-18.

73. Bhalla, G.; Oxgaard, J.; Goddard, W. A.; Periana, R. A., Anti-Markovnikov Hydroarylation of Unactivated Olefins Catalyzed by a Bis-tropolonato Iridium(III) Organometallic Complex. *Organometallics* **2005,** *24* (13), 3229-3232.

74. Oxgaard, J.; Muller, R. P.; Goddard, W. A., 3rd; Periana, R. A., Mechanism of homogeneous Ir(III) catalyzed regioselective arylation of olefins. *J. Am. Chem. Soc.* **2004,** *126* (1), 352-363.

75. Joslin, E. E.; McMullin, C. L.; Gunnoe, T. B.; Cundari, T. R.; Sabat, M.; Myers, W. H., Catalytic Hydroarylation of Ethylene Using TpRu(L)(NCMe)Ph (L = 2,6,7-Trioxa-1-phosphabicyclo[2,2,1]heptane): Comparison to TpRu(L′)(NCMe)Ph Systems (L′ = CO, PMe3, P(pyr)3, or P(OCH2)3CEt). *Organometallics* **2012,** *31* (19), 6851-6860.

76. McKeown, B. A.; Foley, N. A.; Lee, J. P.; Gunnoe, T. B., Hydroarylation of Unactivated Olefins Catalyzed by Platinum(II) Complexes. *Organometallics* **2008,** *27* (16), 4031-4033.

77. Foley, N. A.; Ke, Z.; Gunnoe, T. B.; Cundari, T. R.; Petersen, J. L., Aromatic C−H Activation and Catalytic Hydrophenylation of Ethylene by TpRu{P(OCH2)3CEt}(NCMe)Ph. *Organometallics* **2008,** *27* (13), 3007-3017.

78. Foley, N. A.; Lail, M.; Gunnoe, T. B.; Cundari, T. R.; Boyle, P. D.; Petersen, J. L., Combined Experimental and Computational Study of TpRu{P(pyr)3}(NCMe)Me (pyr =N-pyrrolyl): Inter- and Intramolecular Activation of C−H Bonds and the Impact of Sterics on Catalytic Hydroarylation of Olefins. *Organometallics* **2007,** *26* (23), 5507-5516.

79. Foley, N. A.; Lee, J. P.; Ke, Z.; Gunnoe, T. B.; Cundari, T. R., Ru(II) catalysts supported by hydridotris(pyrazolyl)borate for the hydroarylation of olefins: reaction scope, mechanistic studies, and guides for the development of improved catalysts. *Acc. Chem. Res.* **2009,** *42* (5), 585-597.

80. Foley, N. A.; Lail, M.; Lee, J. P.; Gunnoe, T. B.; Cundari, T. R.; Petersen, J. L., Comparative reactivity of TpRu(L)(NCMe)Ph (L = CO or PMe3): impact of ancillary

ligand l on activation of carbon-hydrogen bonds including catalytic hydroarylation and hydrovinylation/oligomerization of ethylene. *J. Am. Chem. Soc.* **2007,** *129* (21), 6765-6781.

81. Lail, M.; Bell, C. M.; Conner, D.; Cundari, T. R.; Gunnoe, T. B.; Petersen, J. L., Experimental and Computational Studies of Ruthenium(II)-Catalyzed Addition of Arene C−H Bonds to Olefins. *Organometallics* **2004,** *23* (21), 5007-5020.
82. Lail, M.; Arrowood, B. N.; Gunnoe, T. B., Addition of arenes to ethylene and propene catalyzed by ruthenium. *J. Am. Chem. Soc.* **2003,** *125* (25), 7506-7507.
83. Luinstra, G. A.; Wang, L.; Stahl, S. S.; Labinger, J. A.; Bercaw, J. E., C H activation by aqueous platinum complexes: A mechanistic study. *J. Organomet. Chem.* **1995,** *504* (1), 75-91.
84. Holtcamp, M. W.; Labinger, J. A.; Bercaw, J. E., C−H Activation at Cationic Platinum(II) Centers. *J. Am. Chem. Soc.* **1997,** *119* (4), 848-849.
85. Johansson, L.; Tilset, M.; Labinger, J. A.; Bercaw, J. E., Mechanistic Investigation of Benzene C−H Activation at a Cationic Platinum(II) Center: Direct Observation of a Platinum(II) Benzene Adduct. *J. Am. Chem. Soc.* **2000,** *122* (44), 10846-10855.
86. Vedernikov, A. N., Recent advances in the platinum-mediated CH bond functionalization. *Curr. Org. Chem.* **2007,** *11* (16), 1401-1416.
87. Holtcamp, M. W.; Henling, L. M.; Day, M. W.; Labinger, J. A.; Bercaw, J. E., Intramolecular and intermolecular C-H activation at a cationic PtII center. *Inorg. Chim. Acta* **1998,** *270* (1), 467-478.

88. Labinger, J. A., Platinum-Catalyzed C–H Functionalization. *Chem. Rev.* **2017,** *117* (13), 8483-8496.

89. Clement, M. L.; Grice, K. A.; Luedtke, A. T.; Kaminsky, W.; Goldberg, K. I., Platinum(II) olefin hydroarylation catalysts: tuning selectivity for the anti-Markovnikov product. *Chem. Eur. J* **2014,** *20* (52), 17287-17291.

90. Luedtke, A. T.; Goldberg, K. I., Intermolecular hydroarylation of unactivated olefins catalyzed by homogeneous platinum complexes. *Angew. Chem. Int. Ed. Engl.* **2008,** *47* (40), 7694-7696.

91. Karshtedt, D.; Bell, A. T.; Tilley, T. D., Pt−Ag Catalyst System for Hydroarylations with Unactivated Arenes and Olefins. *Organometallics* **2004,** *23* (18), 4169-4171.

92. McKeown, B. A.; Gonzalez, H. E.; Friedfeld, M. R.; Brosnahan, A. M.; Gunnoe, T. B.; Cundari, T. R.; Sabat, M., Platinum(II)-Catalyzed Ethylene Hydrophenylation: Switching Selectivity between Alkyl- and Vinylbenzene Production. *Organometallics* **2013,** *32* (9), 2857-2865.

93. McKeown, B. A.; Gonzalez, H. E.; Friedfeld, M. R.; Gunnoe, T. B.; Cundari, T. R.; Sabat, M., Mechanistic studies of ethylene hydrophenylation catalyzed by bipyridyl Pt(II) complexes. *J. Am. Chem. Soc.* **2011,** *133* (47), 19131-19152.

94. McKeown, B. A.; Gonzalez, H. E.; Gunnoe, T. B.; Cundari, T. R.; Sabat, M., PtII-Catalyzed Ethylene Hydrophenylation: Influence of Dipyridyl Chelate Ring Size on Catalyst Activity and Longevity. *ACS Catal.* **2013,** *3* (6), 1165-1171.

95. McKeown, B. A.; Gonzalez, H. E.; Michaelos, T.; Gunnoe, T. B.; Cundari, T. R.; Crabtree, R. H.; Sabat, M., Control of Olefin Hydroarylation Catalysis via a Sterically and Electronically Flexible Platinum(II) Catalyst Scaffold. *Organometallics* **2013,** *32* (14), 3903-3913.

96. Webster-Gardiner, M. S.; Chen, J.; Vaughan, B. A.; McKeown, B. A.; Schinski, W.; Gunnoe, T. B., Catalytic Synthesis of "Super" Linear Alkenyl Arenes Using an Easily Prepared Rh(I) Catalyst. *J. Am. Chem. Soc.* **2017,** *139* (15), 5474-5480.

97. Fujiwara, Y.; Moritani, I.; Danno, S.; Asano, R.; Teranishi, S., Aromatic substitution of olefins. VI. Arylation of olefins with palladium(II) acetate. *J. Am. Chem. Soc.* **1969,** *91* (25), 7166-7169.

98. Hatamoto, Y.; Sakaguchi, S.; Ishii, Y., Oxidative cross-coupling of acrylates with vinyl carboxylates catalyzed by a Pd(OAc)2/HPMoV/O2 system. *Org. Lett.* **2004,** *6* (24), 4623-4625.

99. Kalyani, D.; Deprez, N. R.; Desai, L. V.; Sanford, M. S., Oxidative C−H Activation/C−C Bond Forming Reactions: Synthetic Scope and Mechanistic Insights. *J. Am. Chem. Soc.* **2005,** *127* (20), 7330-7331.

2 Study of Ruthenium Catalysts for the Alkylation of Benzene

Portions of this chapter are adapted from Jia, X., Gary, J. B., Gu, S., Cundari, T. R., & Gunnoe, T. B. Oxidation Hydrophenylation of Ethylene Using a Cationic Ru(II) Catalyst: Styrene Production With Ethylene as the Oxidant. Isr. J. Chem. **2017***, 57, 1037-1046. Copyright 2017 Wiley-VCH Verlag GmbH & Co. KGaA, Weinheim.*

2.1 Introduction

A brief introduction of the Gunnoe lab's TpRu(II) chemistry applied to olefin hydroarylation is given in Chapter 1. We have discovered that the electron density of the Ru center has a significant influence on the catalyst performance.[1] We have demonstrated that more strongly donating ligands "L" (e.g., L: = PMe_3) for catalyst precursors of the type TpRu(L)(NCMe)Ph (L = CO, PMe_3, $P(OCH_2)_3CEt$, $P(pyr)_3$ or $P(O\overline{CH_2)_2(O)}CCH_3$; Tp = hydridotris(pyrazolyl)borate) result in an increase in the activation barrier for ethylene insertion into the Ru–Ph bonds of TpRu(L)(η^2-C_2H_4)Ph complexes and, as a result, ethylene C–H activation, ultimately to form thermally stable and catalytically inactive η^3-methylallyl complexes, competes with ethylene insertion. Accordingly, more electron-poor Ru(II) complexes have been pursued in efforts to further improve catalytic activity.

One strategy to reduce the electron density on Ru(II) is to use L ligands with less donor ability. Previously, our group determined and compared the electron density of the Ru(II) center using Ru(III/II) redox potentials from cyclic voltammetry.[1-3] A variety of ligands, including carbon monoxide, phosphines (PMe_3, $PPyr_3$ where Pyr = *N*-pyrrolyl) and phosphites ($P(OCH_2)_3CEt$, $P(O\overline{CH_2)_2(O)}CCH_3$) with varying steric and electronic

structures were installed onto the catalyst as the L ligand.[4] The most electron-poor complex among the series, TpRu(L)(NCMe)Ph with L = CO, proved to be the longest-lived catalyst. [5] An analog of CO is the isoelectronic linear nitrosyl NO^+ ligand, which is a 2-electron donor ligand. With a positive charge, NO^+ is generally considered to be a stronger π-acceptor than CO. We considered that a cationic complex $[TpRu(NO)(NCMe)Ph]^+$ complex would have a more electron deficient Ru center than TpRu(CO)(NCMe)Ph and may potentially lead to a better catalytic performance (Figure 2.1).

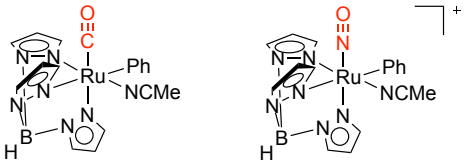

Figure 2.1. TpRu(NCMe)(Ph)(CO) complex and its more electron deficient analog $[TpRu(NO)(NCMe)Ph]^+$.

Another strategy to access more electron-deficient Ru(II) catalyst precursors has been to prepare Ru complexes using the charge neutral variants of the anionic Tp ligand by replacing boron with carbon (Scheme 2.1), which ultimately leads to a cationic Ru(II) complex.[6] Previous work in the Gunnoe lab has shown that the replacement of Tp with a tetra(pyrazolyl)alkane ligand resulted in an intramolecular C–H activation of the pyrazolyl ring.[7] Thus, the cationic Ru(II) complex was synthesized using $HC(pz^5)_3$ ($HC(pz^5)_3$ = tris(5-methyl-pyrazolyl)methane) in which the pyrazolyl 5-positions are protected by incorporation of methyl substituents.[6] Under optimized conditions, the cationic Ru(II) complex $[(HC(pz^5)_3)Ru(P(OCH_2)_3CEt)(NCMe)Ph][BAr'_4]$ successfully increased the

TONs (turnover numbers) of the ethylene hydrophenylation reaction by over 30-fold compared to TpRu(P(OCH$_2$)$_3$Et)(NCMe)Ph (Scheme 2.1).[4, 6]

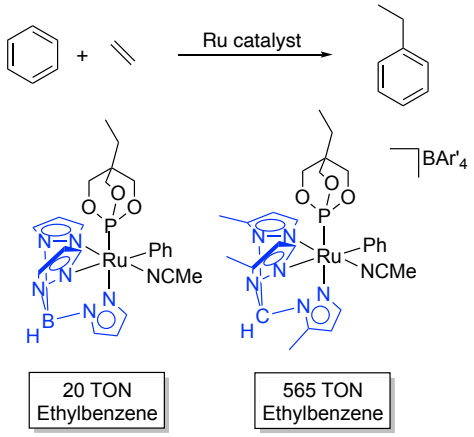

Scheme 2.1. Comparison of olefin hydroarylation activities using TpRu(P(OCH$_2$)$_3$CEt)(NCMe)Ph and [(HC(pz^5)$_3$)Ru(P(OCH$_2$)$_3$CEt)(NCMe)Ph][BAr'$_4$]

With the success of [(HC(pz^5)$_3$)Ru(P(OCH$_2$)$_3$CEt)(NCMe)Ph][BAr'$_4$] for catalytic hydrophenylation of ethylene, we sought to explore related motifs that provide reduced electron density at Ru. For example, tris(triazolyl)methanol ligands have a similar coordination mode as Tp and HC(pz^5)$_3$.[8-10] But, comparing with the trispyrazolyl borate/methane ligands, the more electronegative nitrogen on the triazole ring may decrease the donor ability of the ligand and lead to a more electron-deficient Ru(II) complex. Moreover, installation of electronic-withdrawing groups (e.g., Br) on the pyrazole ring provides another way to obtain electron-deficient Ru complexes.

2.2 Attempted Synthesis and Catalytic Olefin Hydroarylation using [TpRu(NO)(NCMe)Ph]$^+$

Compared to the TpRu(CO) complexes, the synthesis of [TpRu(NO)]$^+$ is a more challenging due to the instability of Ru nitrosyl complexes (see below). Here, a proposed synthetic route to TpRu(NO)(OTf)Ph (OTf = triflate acetate) is shown in Scheme 2.2.

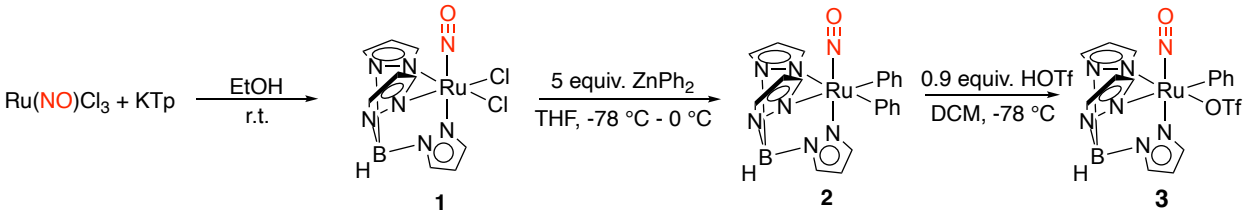

Scheme 2.2. Proposed synthetic route for TpRu(NO)(OTf)Ph.

TpRu(NO)Cl_2 (**1**) was synthesized followed by a literature reported procedure with slight modification (see Experimental section).[11, 12] The dichloride complex **1** was characterized by IR and NMR spectroscopy. The IR spectrum of **1** exhibited an intense absorption at 1898 cm^{-1}, which is due to NO stretching, and in the ^{1}H NMR spectrum of **1** resonances corresponding to the three Tp-pyrazolyl groups in **1** appear to be two sets of signals with a 1:2 intensity ratio (Figure 2.2).

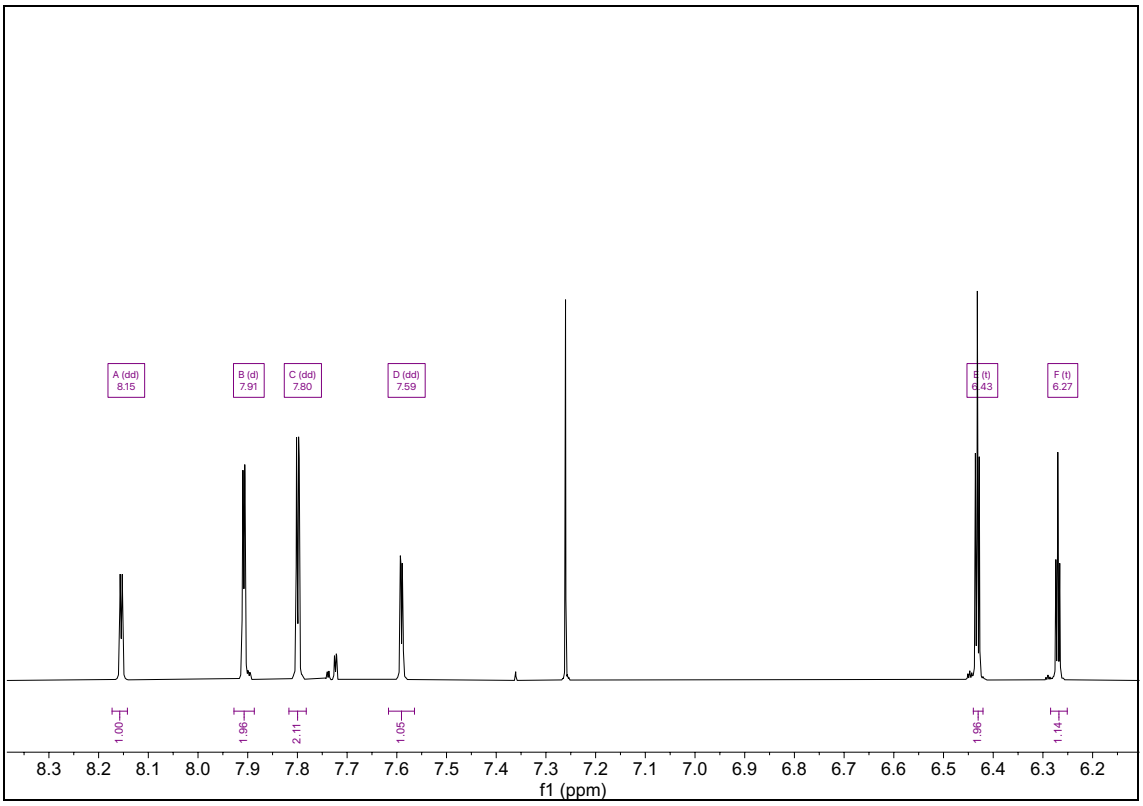

Figure 2.2. ^{1}H NMR spectrum of TpRu(NO)Cl$_2$ (1) in CDCl$_3$.

Several phenylating agents were tested for phenylation of **1** including PhMgX, Ph$_2$Mg, LiPh, Ph$_3$Al and Ph$_2$Zn. Dimethyl zinc proved to be the best phenylating reagent for **1**. The complex TpRu(NO)Ph$_2$ (**2**) was isolated in 54% yield.[11] The diphenyl complex **2** was characterized by IR and NMR spectroscopy. The IR spectrum of **2** exhibited an intense band at 1826 cm^{-1} indicating the retention of terminal and likely linear nitrosyl ligand. The ν_{NO} of **2** is higher energy than that of Cp*Ru(Ph)$_2$(NO) (Cp* = pentamethylcyclopentadiene; 1755 cm^{-1}),[13] demonstrating a smaller degree of π-back donation from Ru d orbital to π* orbital on NO supported with Tp. In the ^{1}H NMR spectrum of **2**, the resonances of the three Tp-pyrazolyl groups show two sets of signals with an intensity ratio of 1:2 (Figure 2.3).

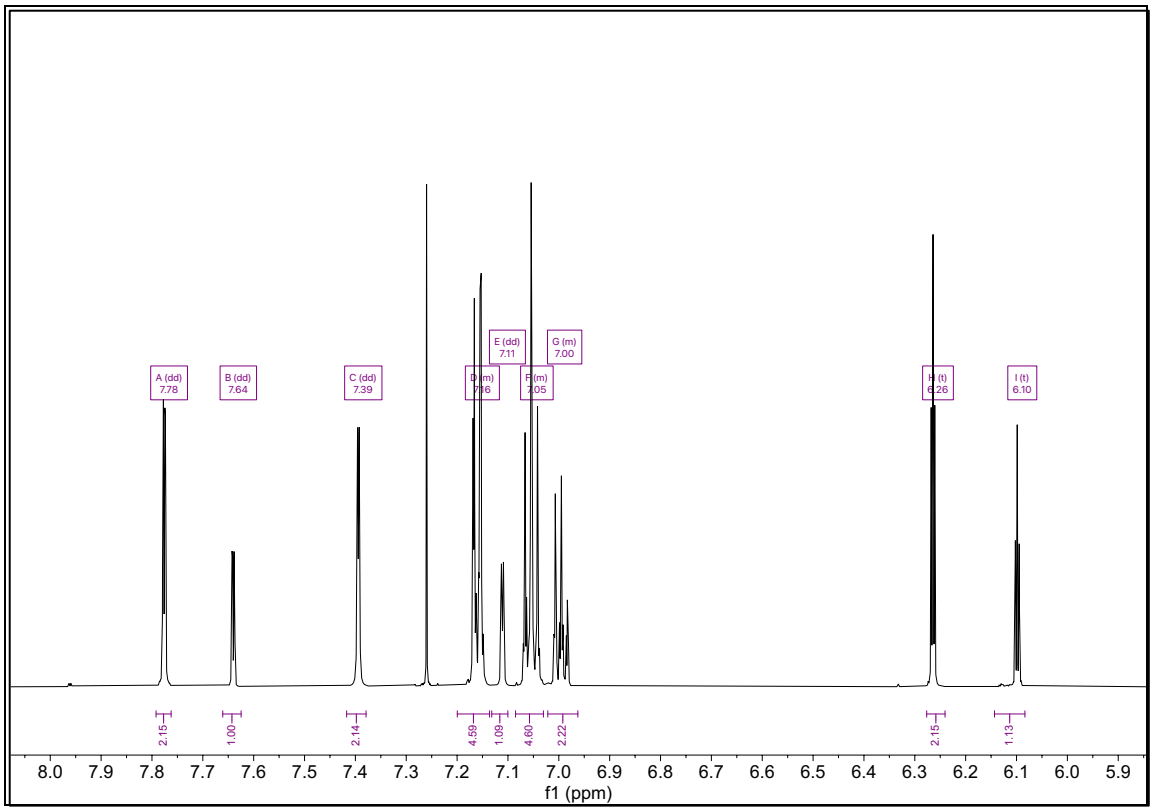

Figure 2.3. ^{1}H NMR spectrum of TpRu(NO)Ph$_2$ (2) in DCM-d_2.

Crystals obtained by slow diffusion of hexanes into a DCM (DCM = methylene chloride) solution of **2** were suitable for single crystal X-ray diffraction, and the resulting solid-state structure of the complex is shown in Figure 2.4. However, at room temperature, both solid **2** and the DCM solution of **2** decompose to form a black solid, and biphenyl is observed as a decomposition product by ^{1}H NMR spectroscopy (Figure 2.5). Although the detailed pathway and final Ru product from the conversion of **2** to form biphenyl was not characterized, it is likely that a straightforward reductive elimination of two phenyl groups initiates the decomposition of the Ru complex **2** (Scheme 2.3). It has been reported by Bercaw and coworkers that heating Cp*Ru(NO)Ph$_2$ in benzene produces biphenyl and dimers [Cp*Ru(μ-NO)]$_2$ and [Cp*Ru(μ-NO)(Ph)]$_2$ (Scheme 2.4).[13] With a structurally

similar but electronically less donating Tp ligand, complex **2** might be more likely to undergo the reductive elimination reaction than Cp*Ru(NO)Ph_2 under similar conditions.

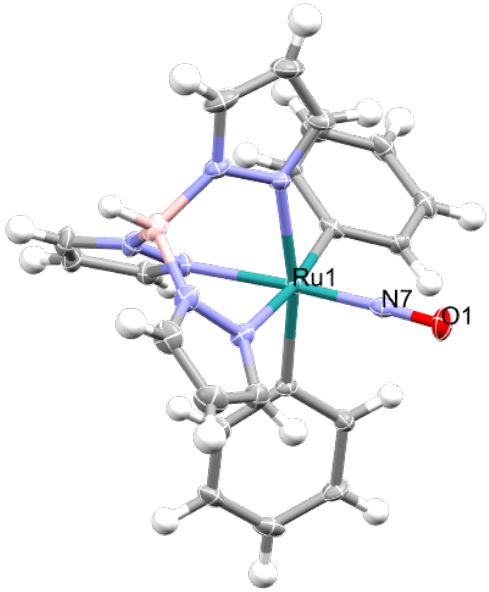

Figure 2.4. ORTEP diagram of TpRu(NO)Ph_2 (**2**) at 50% probability. Counterions and most hydrogen atoms are omitted for clarity.

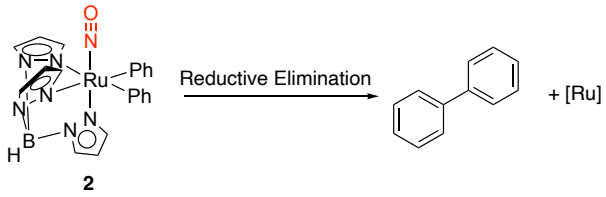

2

Scheme 2.3. Observed decomposition of TpRu(NO)Ph_2 (**2**) to form biphenyl. Ru products have not been characterized.

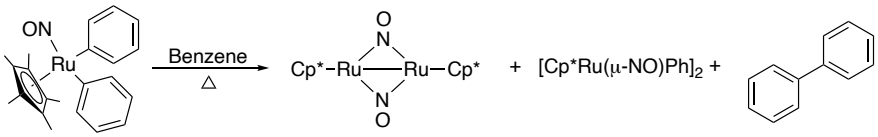

Scheme 2.4. Reported reductive elimination of Cp*Ru(NO)Ph_2.

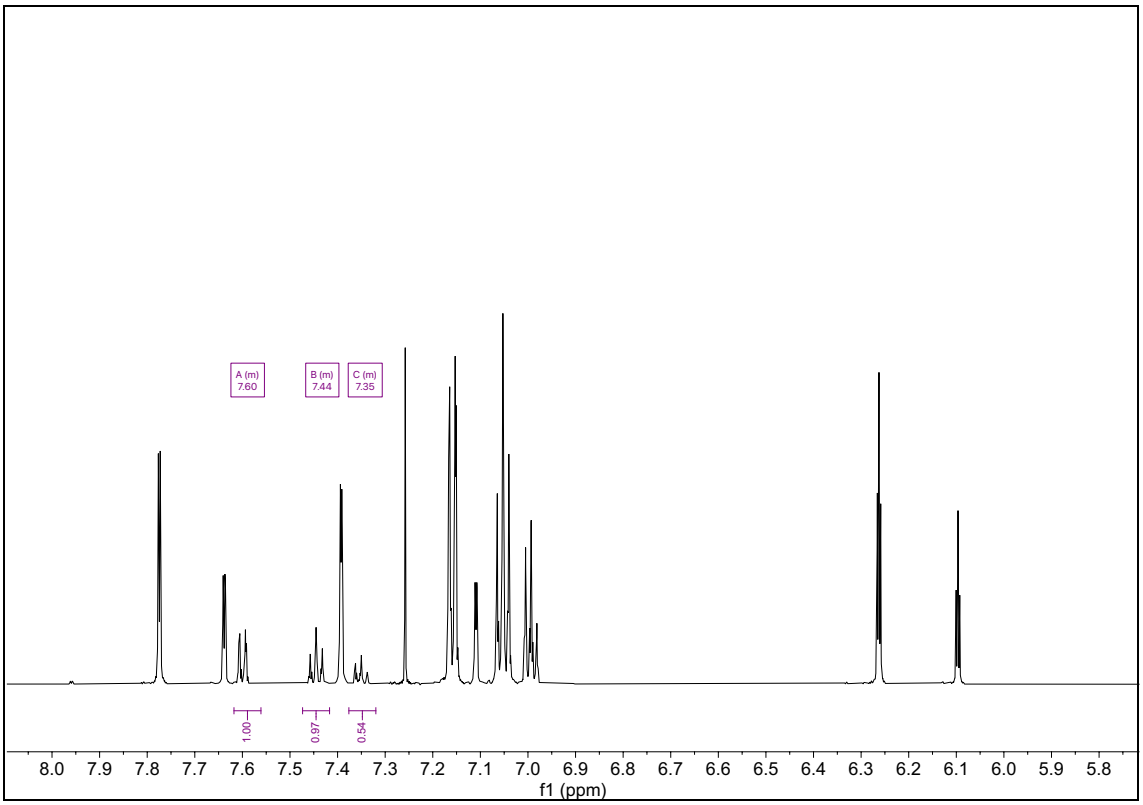

Figure 2.5. ^{1}H NMR spectrum of TpRu(NO)Ph_2 (**2**) in $CDCl_3$ after 24 hours at room temperature, the production of biphenyl is observed.

Although at room temperature complex **2** is not stable, it can be store at −40 ºC with no biphenyl formation after 2 days. Adding a cold DCM solution of 0.9 equivalents of HOTf into a DCM solution of **2** at –78 ºC under inert atmosphere results in the protonation of one of the phenyl groups. TpRu(NO)(OTf)Ph (**3**) was isolated with an 80% yield. The ^{1}H NMR spectrum of **3** is shown in Figure 2.6, due to the loss of symmetry, the resonances of the three Tp-pyrazolyl groups appear as 9 signals total in a 1:1 ratio.

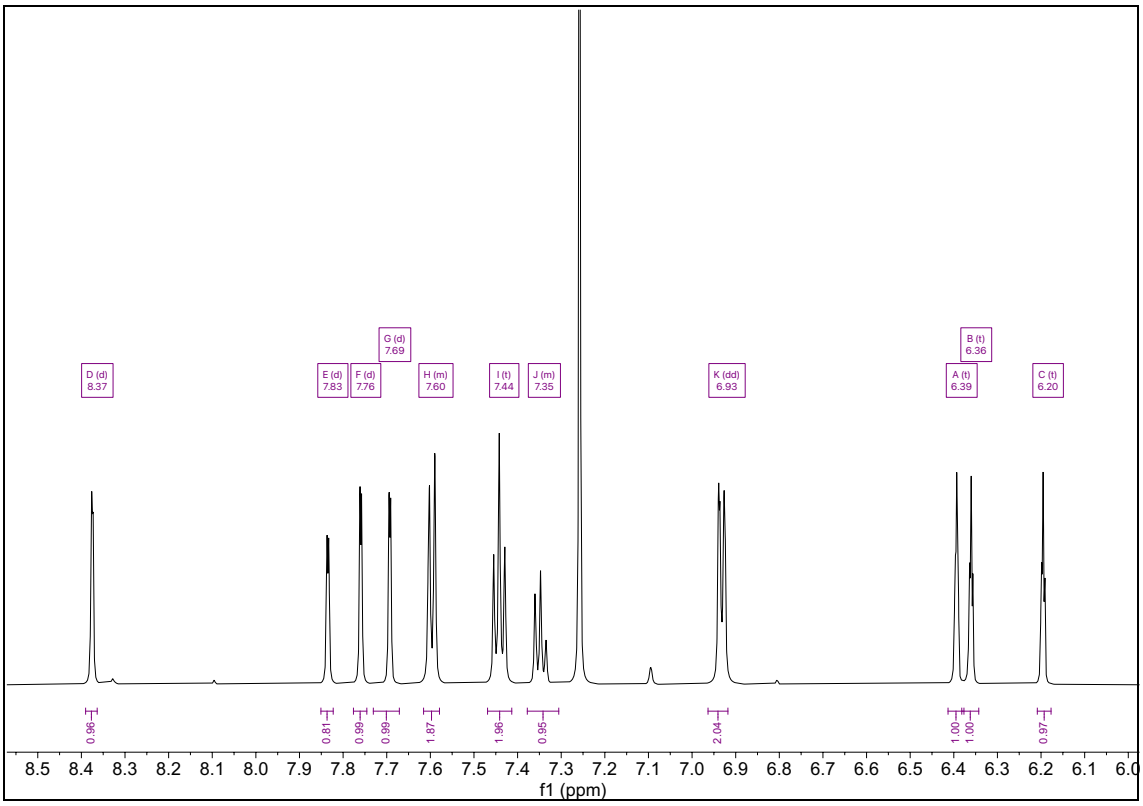

Figure 2.6. ^{1}H NMR spectrum of TpRu(NO)(OTf)Ph (**3**) in $CDCl_3$

Unfortunately, the replacement of a phenyl group with OTf decreased the stability of the Ru complex. The conversion of **3** is faster than **2**, after just a few minutes at room temperature, the pink $CDCl_3$ solution of **3** turns dark brown indicating reaction likely occurred.

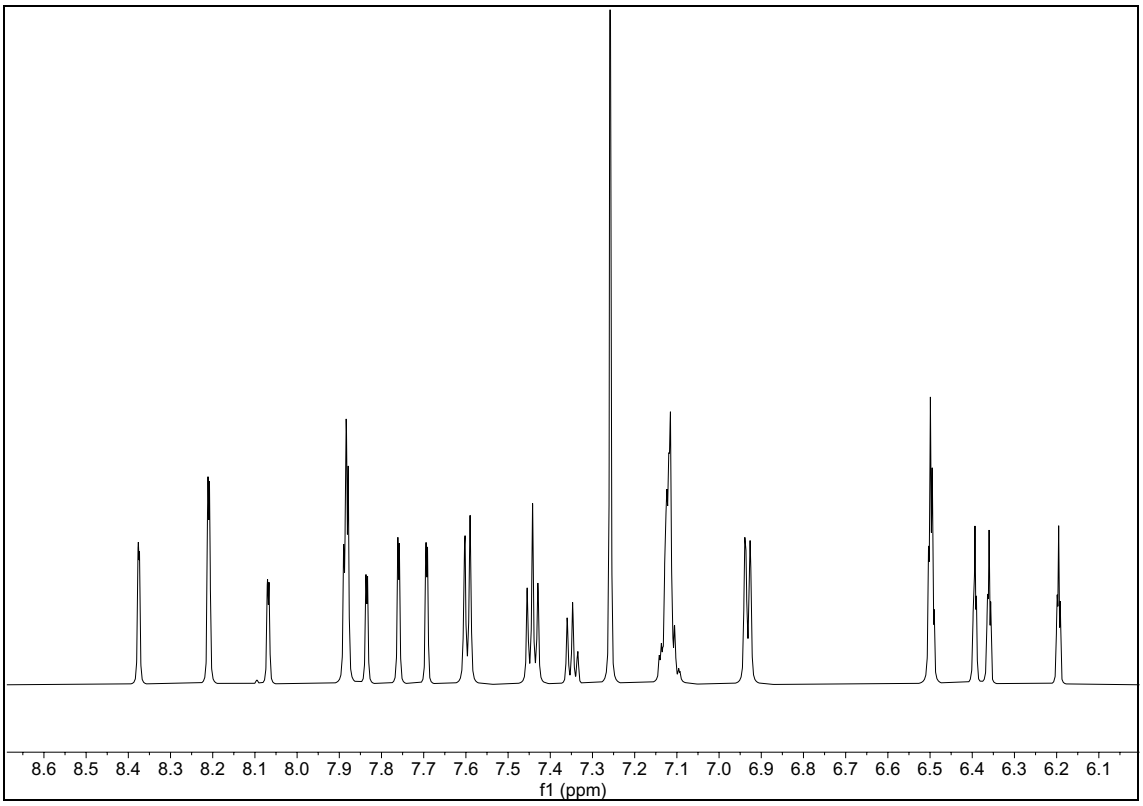

Figure 2.7. ^{1}H NMR spectrum of TpRu(NO)(OTf)Ph (**3**) in $CDCl_3$ after 10 minutes at room temperature.

After 10 min under room temperature, ^{1}HNMR was taken of the $CDCl_3$ solution of **3**, and new resonances were observed in the ^{1}H NMR spectrum (Figure 2.7). Several new peaks can be observed in the spectrum.

As we expected, the replacement of CO by NO^{+} triggered the reductive elimination of the complex **2** and resulted in the decomposition of the complex. The olefin hydroarylation was not attempted with **2** or **3** since the typical catalysis temperature for TpRu(L)(NCMe)Ph complexes are 90 ºC.

The complex $TpRu(NO)Me_2$, which can be synthesized from the reaction between **1** and $ZnMe_2$, is stable at room temperature and might be a good candidate for studying olefin hydroarylation. ^1H NMR spectrum of $TpRu(NO)Me_2$ is shown in Figure 2.8.

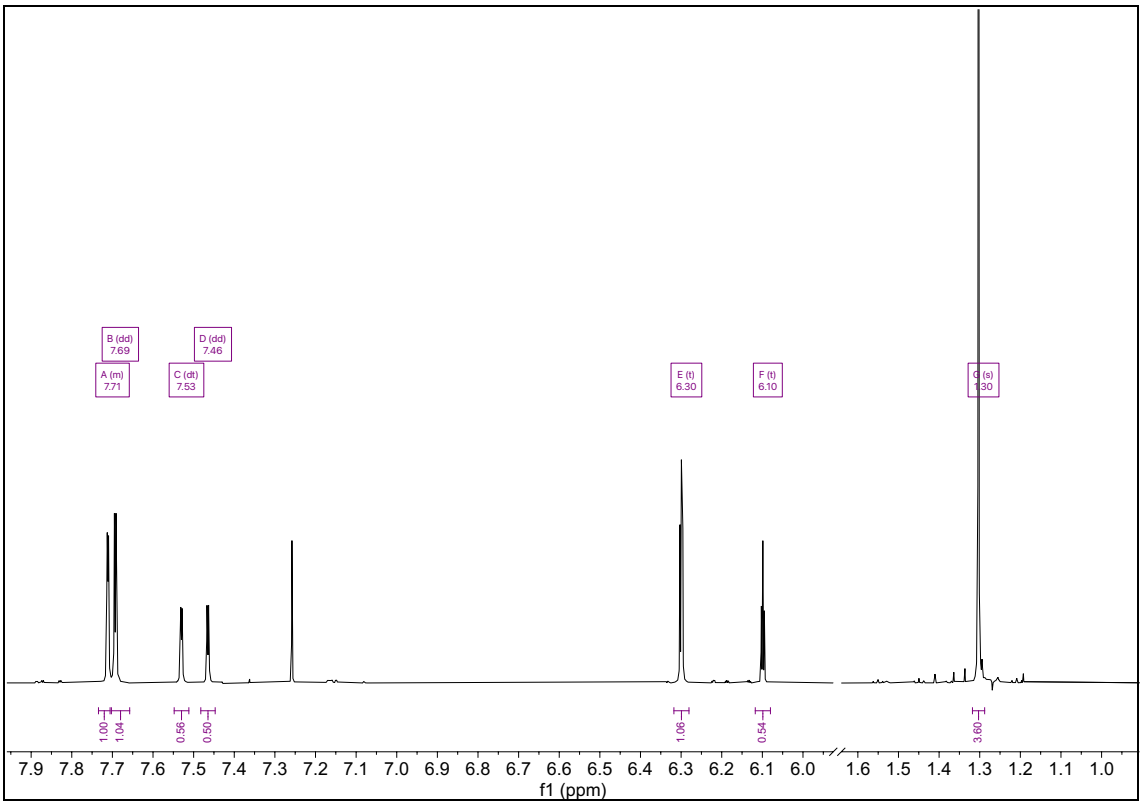

Figure 2.8. ^1H NMR spectrum of $TpRu(NO)Me_2$ in $CDCl_3$.

2.3 Ruthenium (II) Complex Supported by Tp^{Br3} Ligand

Bromoarenes are considered to be an electron deficient arenes due to the electronegative of bromine. We considered that replacing the hydrogens on the pyrazole rings of Tp by bromines would reduce the donor ability and allow access to less electron rich Ru(II) complexes than TpRu(L)(NCMe)Ph.

The ligand salt, $TlTp^{Br3}$, (Tp^{Br3} = hydrotris(3,4,5-tribromo)pyrazolylborate)[14, 15] was received from our collaborator. The ruthenium precursor (η^6-*p*-

cymene)Ru(P(OCH$_2$)$_3$CEt)(Ph)Br was prepared according to literature procedures.[4, 6, 8] An acetonitrile solution of complex (η^6-*p*-cymene)Ru(P(OCH$_2$)$_3$CEt)(Ph)Br was heated for 3.5 hours at 70 °C to yield the putative complex (NCMe)$_3$Ru(P(OCH$_2$)$_3$CEt)(Ph)Br (Scheme 2.5).[6] Then, this complex was reacted with TlTpBr$_3$ in a 1:1 ratio of NCMe/DCM to produce (Tp^{Br3})Ru P(OCH$_2$)$_3$CEt (NCMe)Ph (**4**) in 54% isolated yield as a pale yellow solid.

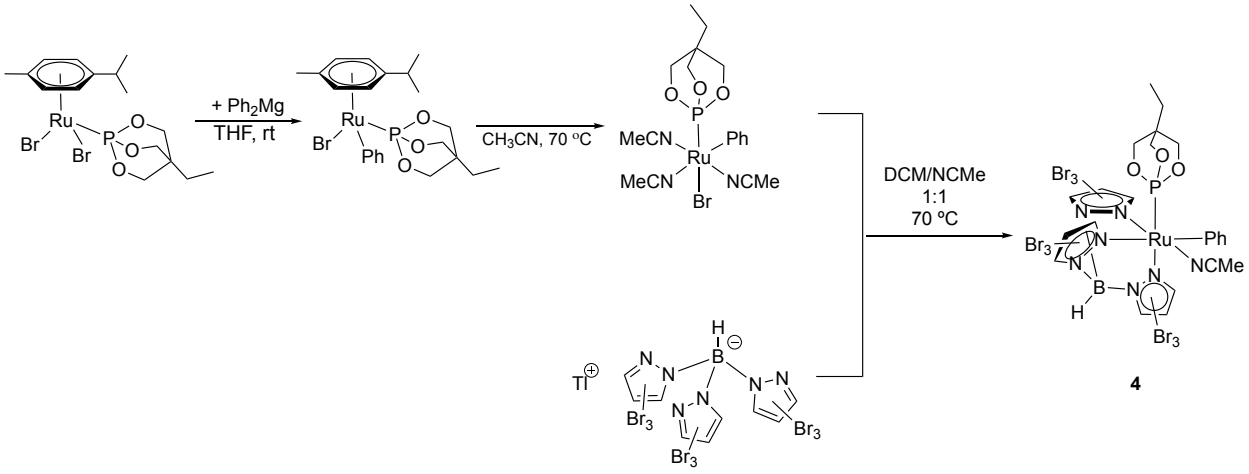

Scheme 2.5. Synthetic route for (Tp^{Br3})Ru(P(OCH$_2$)$_3$CEt)(NCMe)Ph (4).

The ^{1}H NMR spectrum of **4** is shown in Figure 2.9. The purification of **4** is challenging due to the poor solubility. Notably, in the ^{1}H NMR spectrum of **4**, five resonances due to the phenyl ligand are observed. This is different from TpRh(L)(NCMe)Ph complexes where the phenyl groups show three sets of proton resonances with an intensity ratio of 1:2:2 (ortho:meta:para phenyl C–*H*)

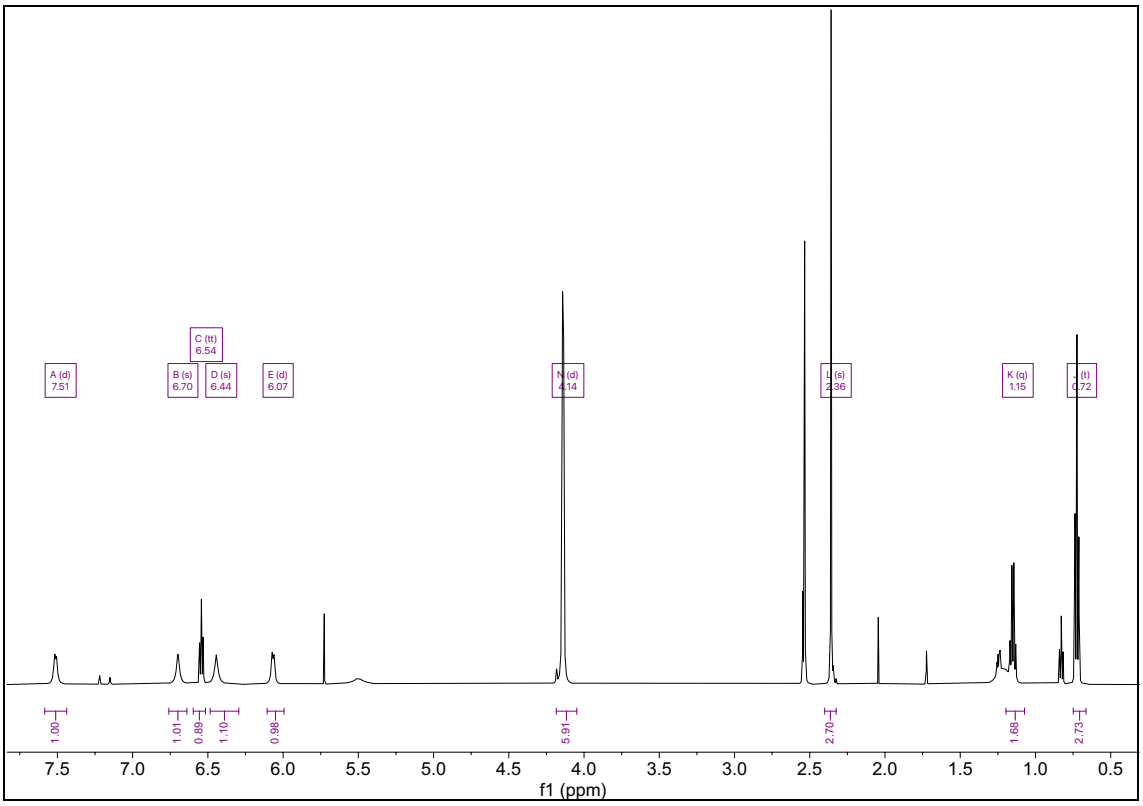

Figure 2.9. ^{1}H NMR spectrum of (Tp^{Br3})Ru(P(OCH_2)$_3$CEt)(NCMe)Ph (**4**) in DMSO-d_6.

In order to confirm the successful installation of the phenyl ligand, reaction of **4** with a Brønsted acid was performed based on the assumption that phenyl group could be protonated to form free benzene (Scheme 2.6). Adding 1 equivalent of trifluoroacetic acid to a $CDCl_3$ solution of **4** resulted in the disappearance of all five phenyl resonances (Figure 2.10), at the same time, a resonance consistent with the formation fo free benzene at 7.35 ppm was observed, which provided further confirmation of the identity of complex **4**.

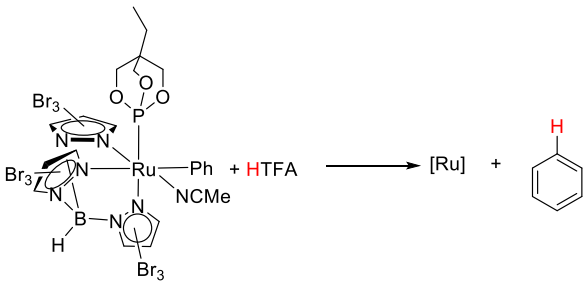

Scheme 2.6. Protonation of (Tp^{Br3})Ru $P(OCH_2)_3CEt$ (NCMe)Ph (**4**) by HTFA (trifluroracetic acid).

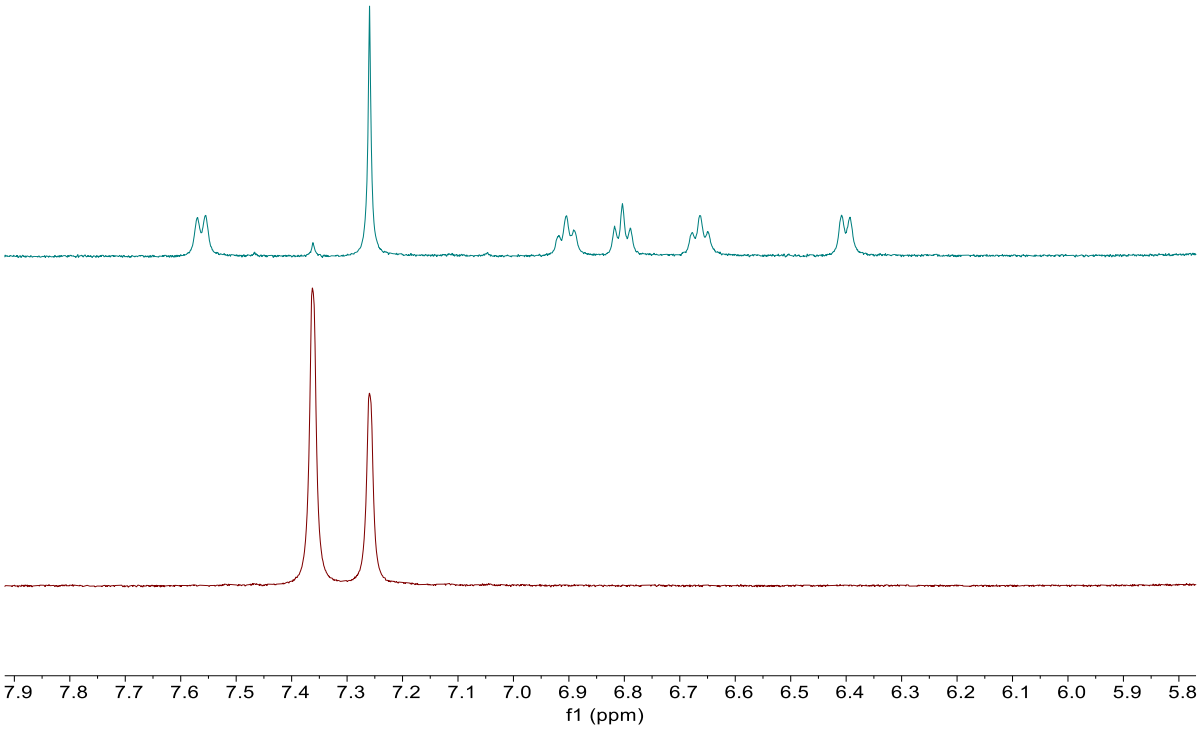

Figure 2.10. ^1H NMR spectra of protonation of (Tp^{Br3})Ru($P(OCH_2)_3CEt$)(NCMe)Ph (**4**) using HTFA. (Top: ^1H NMR of **4** prior to acid addition; Bottom: ^1H NMR after acid addtion).

In our previous TpRu(L)(NCMe)Ph complexes, the Ru–Ph bond undergoes rapid rotation on the NMR timescale at room temperature, as evidenced by the observation of three resonances due to the phenyl ligand in the NMR spectra. In contrast, the ^1H NMR

spectrum of complex **4** shows restricted rotation around the Ru–Ph bond. Variable temperature NMR was used to probe the rotation of the Ru–Ph bond in **4**.

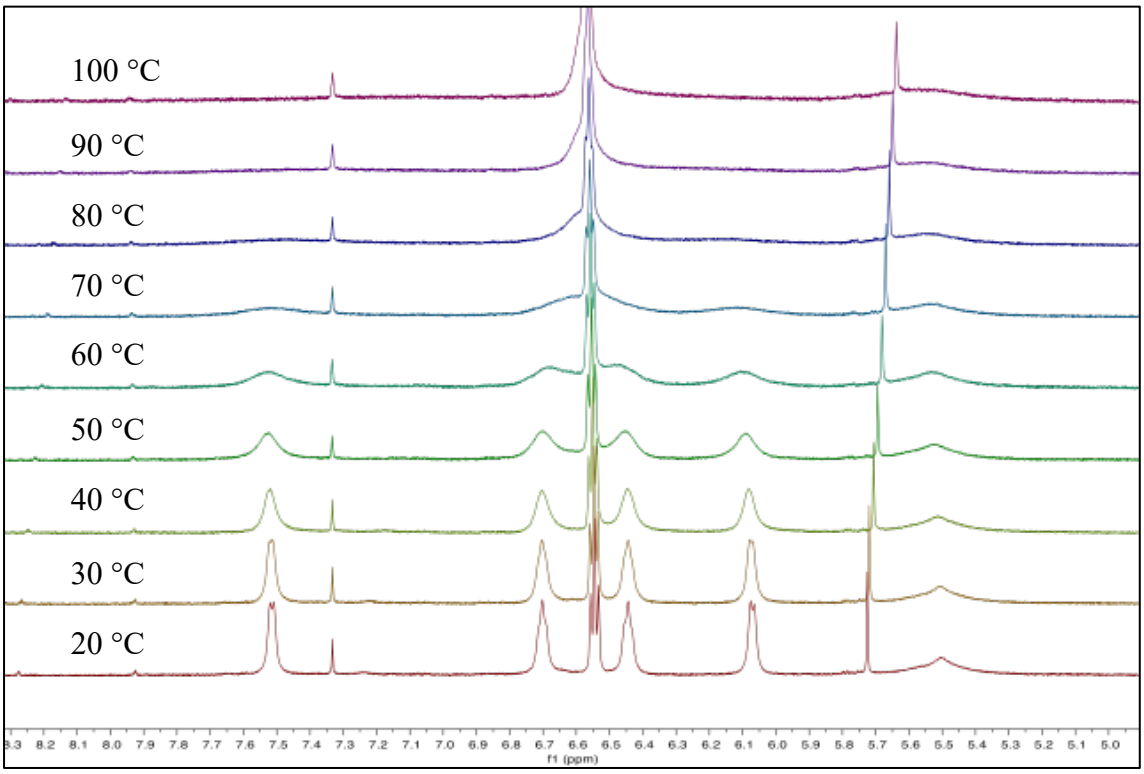

Figure 2.11. Variable temperature NMR spectra of $(Tp^{Br3})Ru(P(OCH_2)_3CEt)(NCMe)Ph$ (**4**) from 20 °C (bottom) to 100 °C (top) in DMSO-*d*$_6$.

Figure 2.11 shows stacked NMR spectra of **4** in DMSO from 20 °C (bottom) to 100 °C. Four of the phenyl-H resonances, which correspond to the ortho and meta H broadened are observed at low temperature, but these resonances broaden upon heating, indicating rotation of the Ru–Ph bond. Unfortunately, due to the limitation of the temperature of , the coalescence of the peaks was not observed.

Olefin hydroarylation reactions were attempted using **4** as the catalyst under different ethylene pressures and reaction temperatures. Under all conditions in Table 1.1, no

evidence of catalytic activity was observed. The lack of reactivity is likely due to the large sterically bulky bromine substituents on the Tp ligand, which might prevent olefin coordination.

Table 2.1. Olefin hydroarylation catalyzed by (Tp^{Br3})Ru(P(OCH_2)$_3$CEt)(NCMe)Ph (**4**) under different reaction temperature and ethylene pressures.

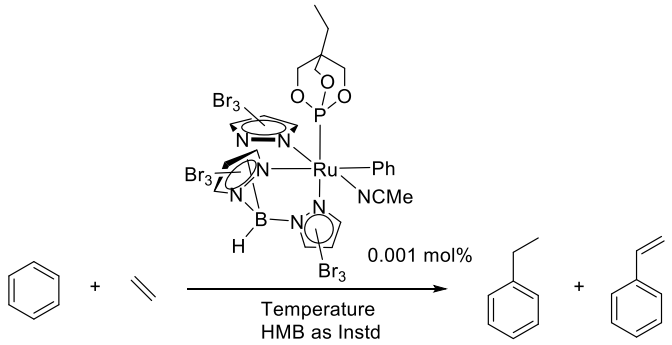

Entry	Ethylene Pressure (psig)	Temperature (°C)	Styrene (TOs)	Ethylbenzene (TOs)
1	15	90	–	–
2	45	90	–	–
3	15	120	–	–
4	45	120	–	–
5	25	150	–	–
6	45	150	–	–

2.4 1,2,3-Tristriazylborate (Ttz) Ligand

The salt KTtz was received from Prof. Harman's lab. The synthetic route of TtzRu(P(OCH_2)$_3$CEt)(NCMe)Ph (**5**) is shown in Scheme 2.7. The ruthenium precursor (η^6-*p*-cymene)Ru(P(OCH_2)$_3$CEt)(Ph)Br was prepared according to a literature procedure.[4, 6, 8] An acetonitrile solution of (η^6-*p*-cymene)Ru(P(OCH_2)$_3$CEt)(Ph)Br was heated for 3.5

hours at 70 °C to yield the putative complex $(NCMe)_3Ru(P(OCH_2)_3CEt)(Ph)Br$.[6] Then, $(NCMe)_3Ru(P(OCH_2)_3CEt)(Ph)Br$ was reacted with KTtz to produce $TtzRu(P(OCH_2)_3CEt)(NCMe)Ph$ (**5**) as a white solid in a 44% isolated yield. The ^1H NMR spectrum of **5** is shown in Figure 2.12, and the proton resonances of three Ttz-triazolyl groups show 6 resonances total. Cyclic voltammetry of complex **5** shows a reversible Ru(III/II) oxidation at 0.80 V (vs. NHE), which is a +0.25 V shift compared to the previously reported complex $TpRu(P(OCH_2)_3CEt)(NCMe)Ph$, indicating the extra N atom on the nitrogen heterocycle ring decreases the donor ability of the poly(triazolyl) ligand compared to Tp and results in a less electron rich Ru center. The Ru(III/II) redox potential of 0.80 V for **5** is also 0.02 V more negative than for the cationic Ru(II) complex $[(HC(pz^5)_3Ru(P(OCH_2)_3)CEt)(NCMe)Ph][BAr'_4]$,[6] which is reported to be a good catalyst for ethylene hydrophenylation.[6]

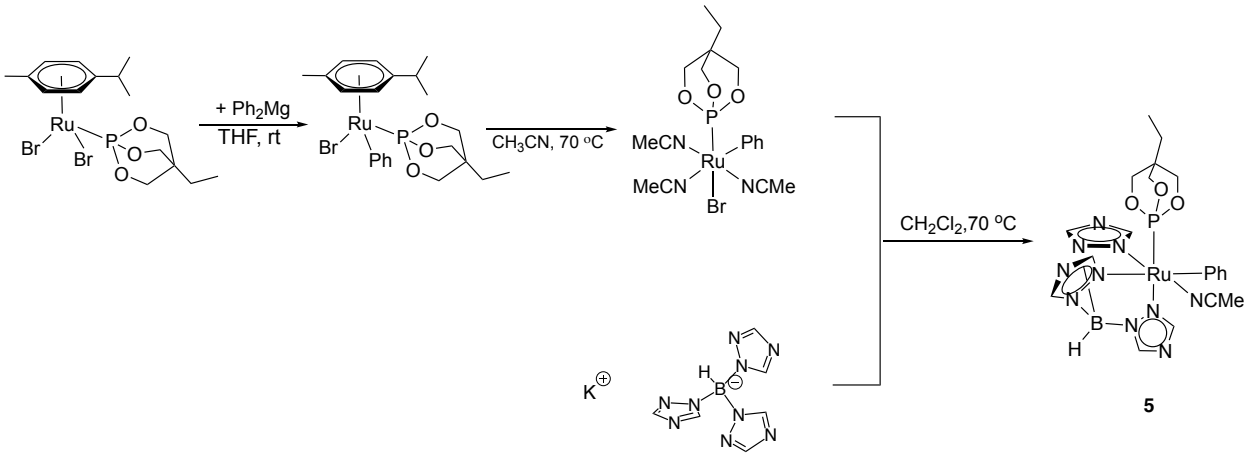

Scheme 2.7. Synthetic route for TtzRu(P(OCH$_2$)$_3$CEt)(NCMe)Ph (5)

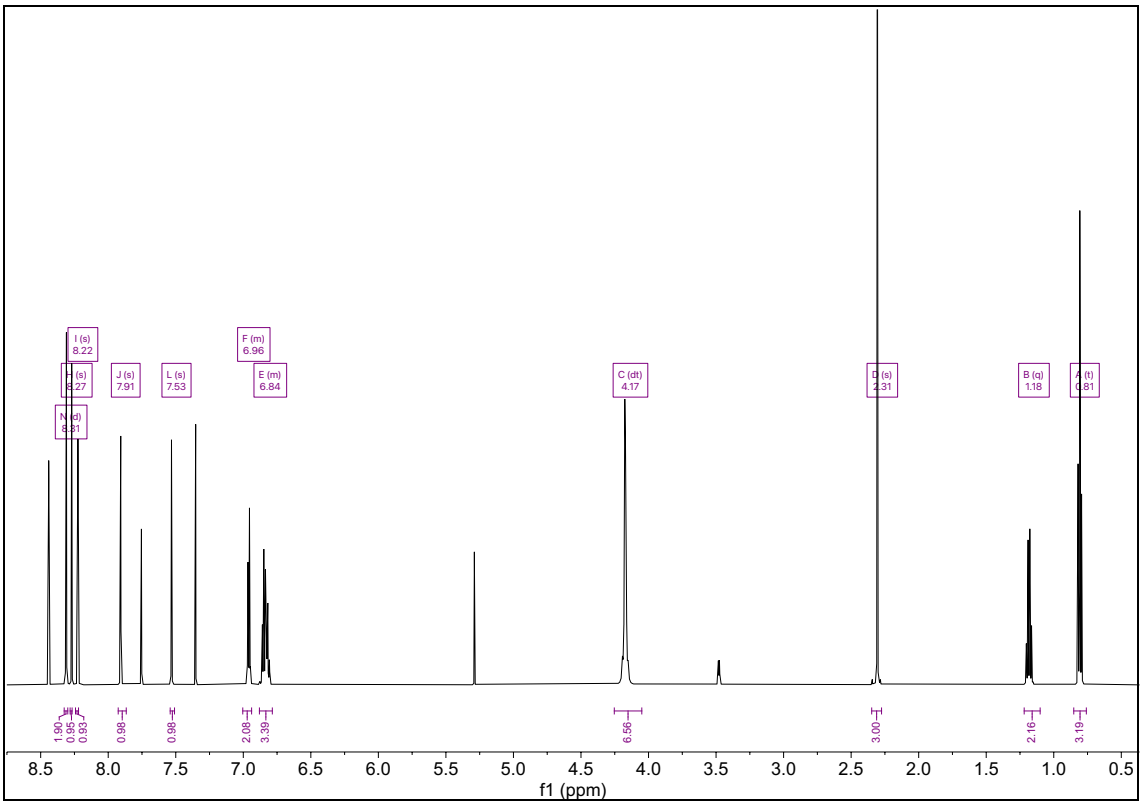

Figure 2.12. ^{1}H NMR spectrum of TtzRu(P(OCH$_2$)$_3$CEt)(NCMe)Ph (5) in CDCl$_3$.

Complex **5** was tested as the catalyst for ethylene hydrophenylation reactions. Due to the poor solubility of complex **5** in benzene, catalysis was performed under low catalyst loading where we assumed the complex was fully dissolved under catalytic conditions. The

results of catalysis under different temperatures are shown in Figure 2.13. At 75 °C, the rate of the reaction is slow, and the catalytic turnovers reached ~8 after 44 hours and then catalysis ceased, indicating likely deactivation of complex **5**. The catalytic performance of **5** increased as the temperature was increased above 90 °C and the initial TOFs (average for the first 10 hours) of the reaction at 90 °C, 105 °C and 120 °C were 0.00044, 0.00075 and 0.0013 hr^{-1}, respectively. However, the high reaction temperature also led to rapid catalyst deactivation, leading to shortened longevity of 44 hours for the reaction at 90 °C, 31 hours for the reaction at 105 °C and 15 hours at 120 °C reaction.

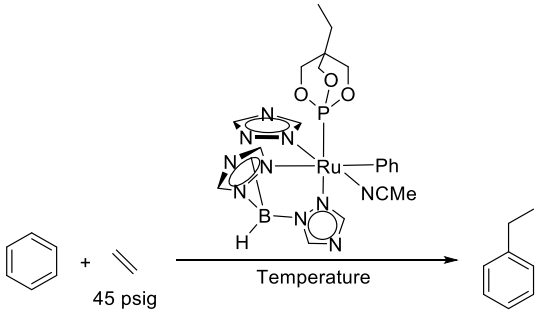

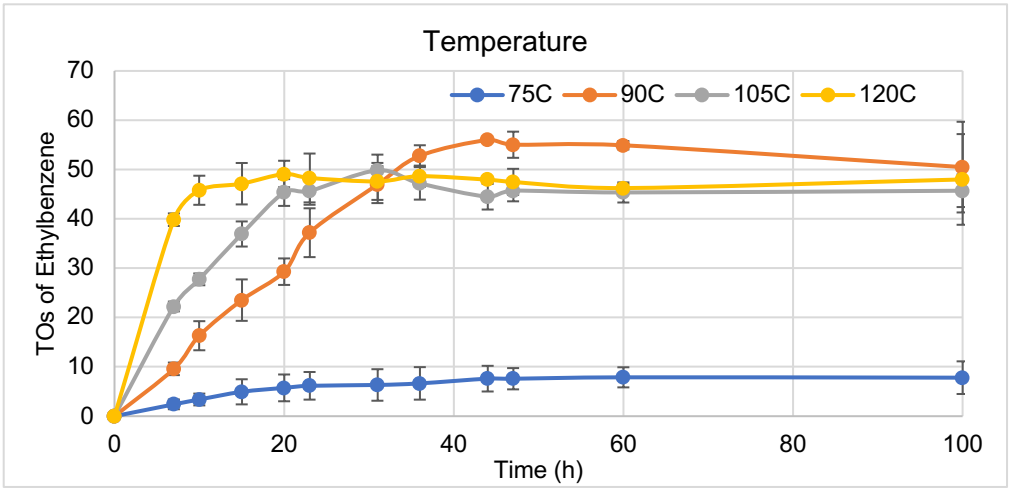

Figure 2.13. Catalytic ethylene hydrophenyaltion catalyzed by TtzRu(P(OCH$_2$)$_3$CEt)(NCMe)Ph (**5**) under different temperatures

The catalytic performance of TtzRu(P(OCH$_2$)$_3$CEt)(NCMe)Ph did not meet our expectations due poor catalyst longevity. Also, the replacement of Tp by the Ttz ligand led to worse solubility of the complex.

Some recent studies have explored the modulation of the σ-donor properties of Ttz via chemical interactions of the exo-nitrogen (4-N). Work by Papish and co-workers found that ligand protonation of Ttz complexes of first-row metals can have a significant effect on the electron density at the metal center,[16-21] and that these properties can be used to influence catalytic behavior. Thus, the influence of acid on the catalytic performance of **5** was investigated.

Table 2.2. Ethylene hydrophenylation catalyzed by TtzRu(P(OCH$_2$)$_3$CEt)(NCMe)Ph (**5**), with the addition of acid additives.

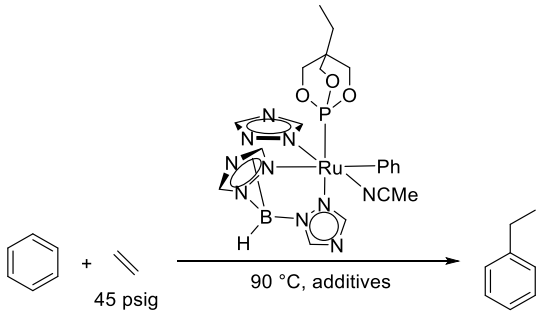

entry	Additives (3 equiv.)	Longevity (hours)	Reactivity (TOs of EB)
1	$HNTf_2$	Decomposition	–
2	HBArF	Decomposition	–
3	$LiNTf_2$	60	120(6)
4	$NaNTf_2$	48	91(3)
5	$KNTf_2$	48	54(9)
6	LiBArF	72	147(12)
7	$AlMe_3$	Decompose	–

Table 2.2 shows the result of catalytic ethylene hydrophenylation using **5** with the presence of different additives. The addition of a strong organic Brønsted acid (entries 1 and 2) led to decomposition of the catalyst, and no catalytic turnovers were observed. Lewis acids such as $LiNTf_2$, $NaNTf_2$ and $KNTf_2$ (entry 3-5) have shown to positively influence the catalysis with $LiNTf_2$ showing an approximate 100% increase compared to catalysis with no additive (TON = 60). This might be explained by the weak coordination of Li^+ with the exo-nitrogen (4-N) on the triazole. After 6 hours of reaction, 147 TOs of ethylbenzene were produced from reaction of **5** and LiBArF indicating Li^+ is responsible for the catalytic performance enhancement.

2.5 1,2,4-Tristriazoyl Methanol as Ligand

Tris(triazolyl)methanol ligands have a similar coordination mode as Tp and $HC(pz^5)_3$.[8-10] It was anticipated that tris(triazolyl)methanol ligand would have reduced donor ability compared to Tp and $HC(pz^5)_3$ since it possess one more electron negative nitrogen atom . Thus, we sought to prepare a Ru(II) catalyst precursor supported by a tris(triazolyl)methanol ligand to test for ethylene hydrophenylation.

The ruthenium precursor (η^6-*p*-cymene)Ru($P(OCH_2)_3CEt$)(Ph)Br and the pro-ligand CH_3OTMM {4,4',4"-(methoxymethanetriyl)tris(1-benzyl-1H-1,2,3-triazole)} were prepared according to literature procedures.[4, 6, 8] An acetonitrile solution of complex (η^6-*p*-cymene)Ru($P(OCH_2)_3CEt$)(Ph)Br was heated for 3.5 hours at 70 °C to yield the putative complex $(NCMe)_3Ru(P(OCH_2)_3CEt)(Ph)Br$.[6] Complex $(NCMe)_3Ru(P(OCH_2)_3CEt)(Ph)Br$ was then reacted with CH_3OTTM to produce

[(CH_3OTTM)Ru(P(OCH_2)$_3$CEt)(NCMe)Ph]Br (**6**) in 76% isolated yield. A metathesis reaction of **6** with NaBAr'$_4$ in THF gives the Ru(II) complex [(CH_3OTTM)Ru(P(OCH_2)$_3$CEt)(Ph)(NCMe)][BAr'$_4$] (**7**) in 95% isolated yield (Scheme 2.8).

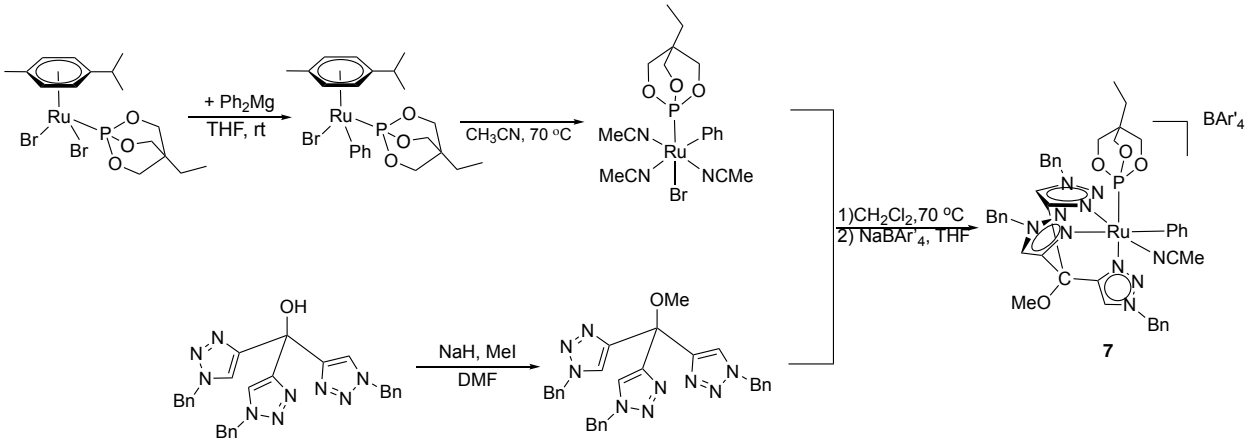

Scheme 2.8. Synthesis of [(CH_3OTTM)Ru(P(OCH_2)$_3$CEt)(NCMe)Ph][BAr'$_4$] (**7**) (CH_3OTMM = 4,4',4''-(methoxymethanetriyl)-tris(1-benzyl-1H-1,2,3-triazole), Bn = benzyl)

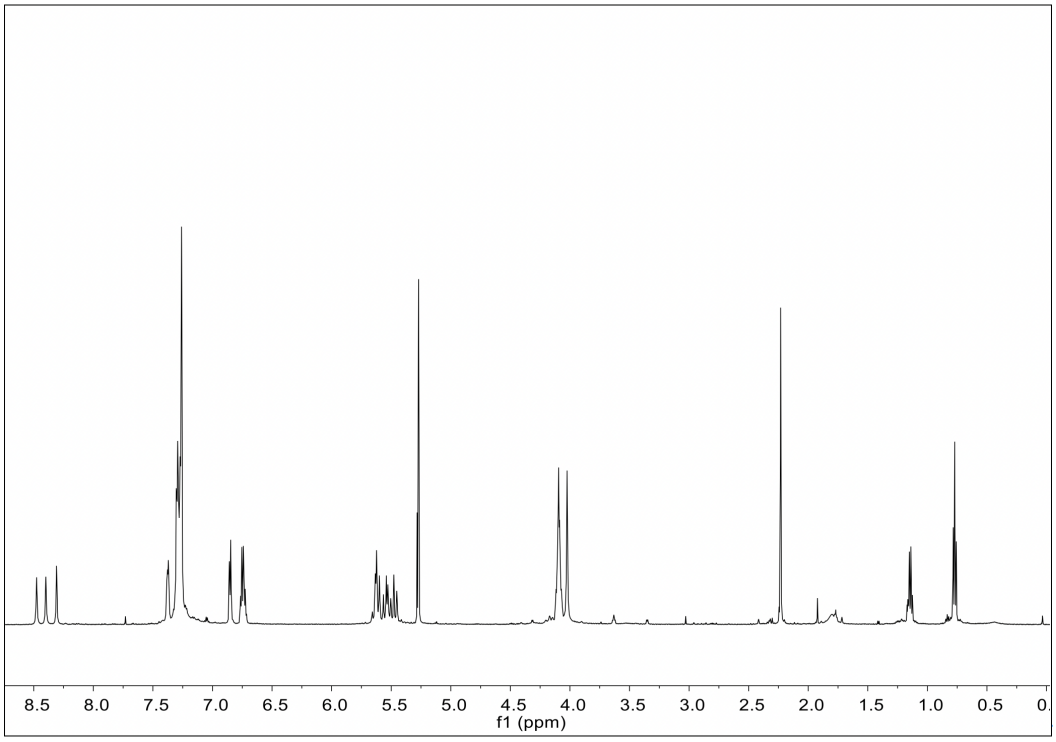

Figure 2.14. ^{1}H NMR spectrum of [(CH_3OTTM)Ru(P(OCH_2)$_3$CEt)(NCMe)Ph]Br (**6**) in $CDCl_3$.

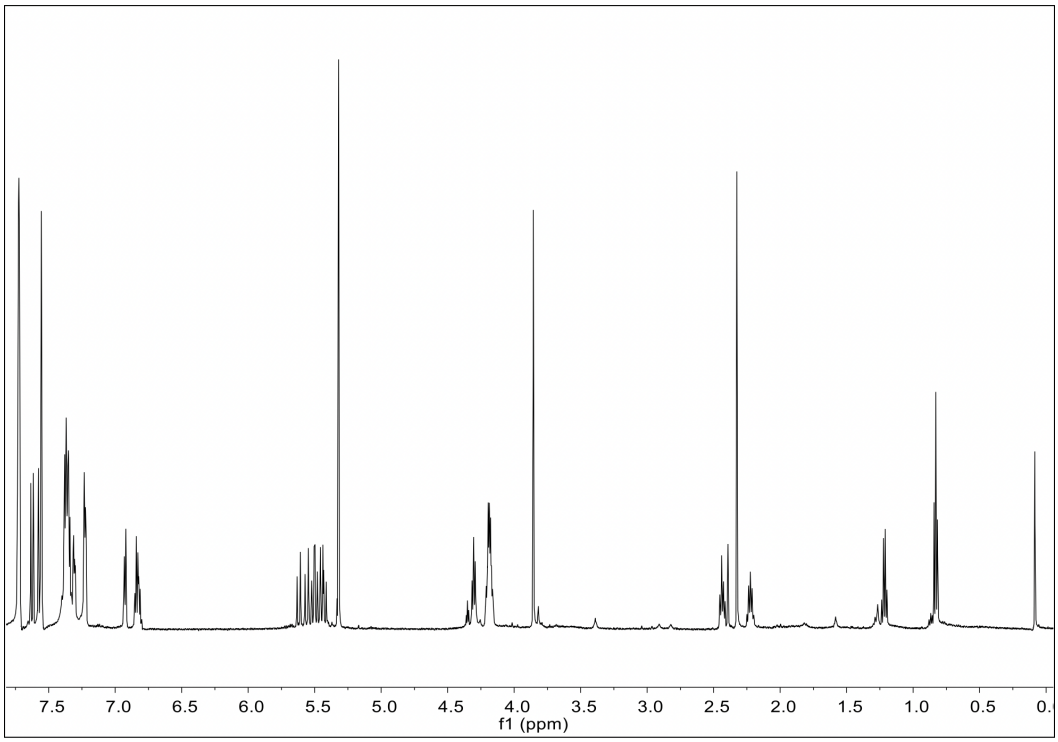

Figure 2.15. ^{1}H NMR spectrum of [(MeOTTM)Ru(P(OCH_2)$_3$CEt)(NCMe)Ph][BAr'$_4$] (**7**) in CD_2Cl_2.

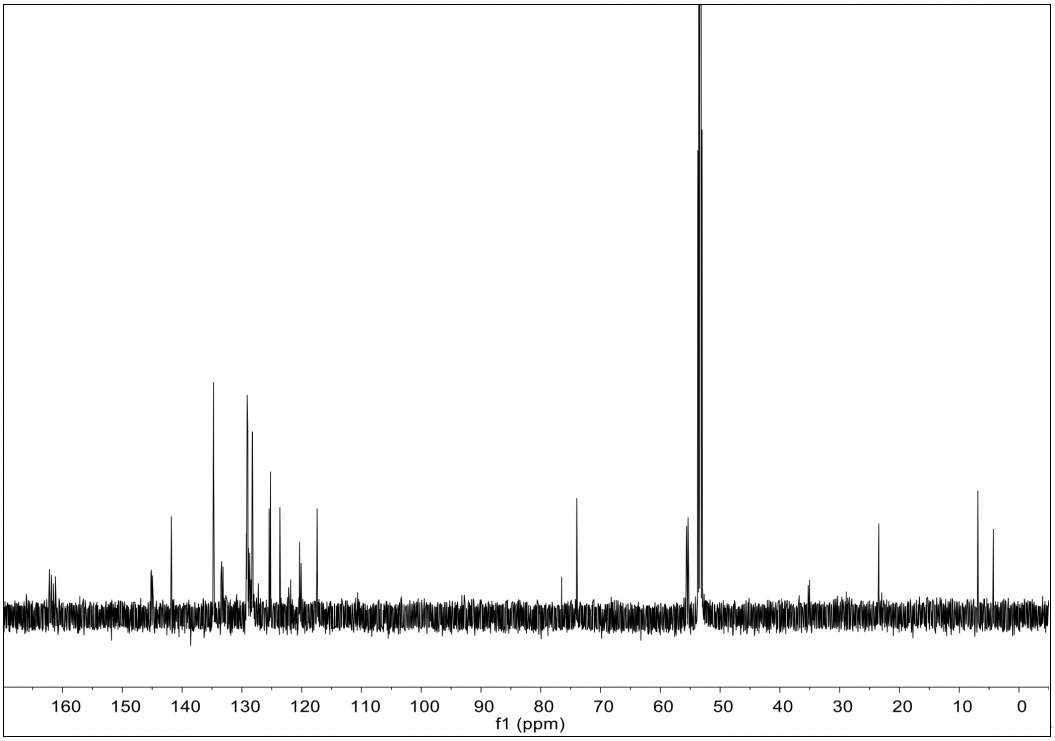

Figure 2.16. ^{13}C NMR spectrum of [(MeOTTM)Ru(P(OCH$_2$)$_3$CEt)(NCMe)Ph][BAr'$_4$] (**7**) in CD_2Cl_2.

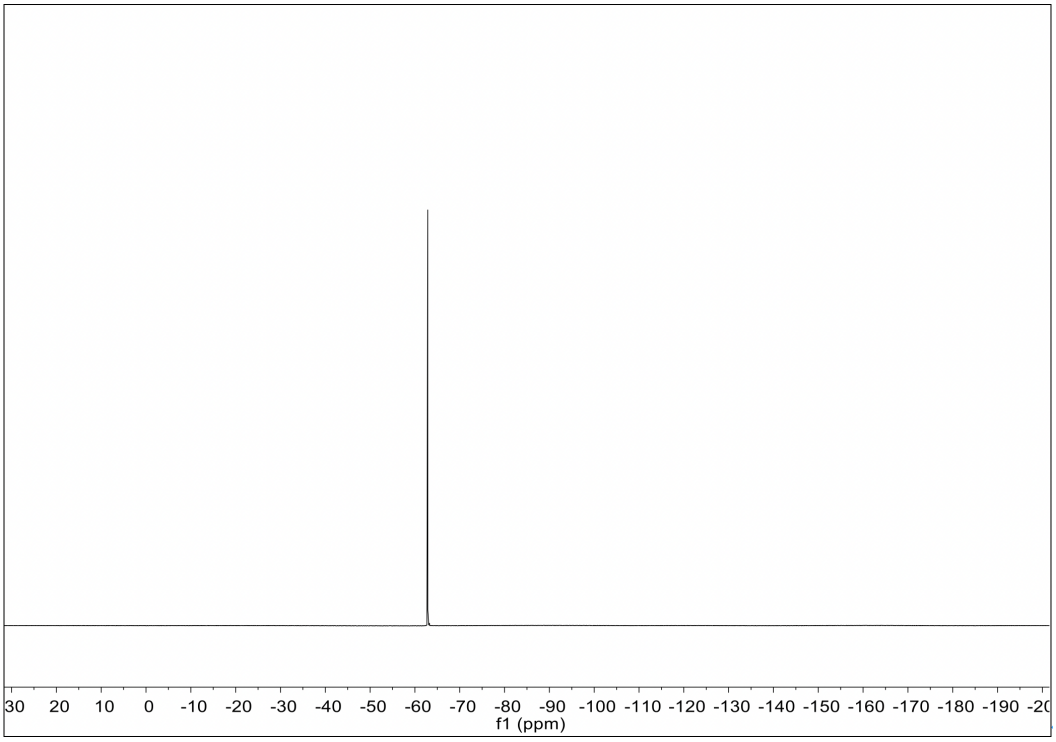

Figure 2.17. ^{19}F NMR spectrum of [(MeOTTM)Ru(P(OCH$_2$)$_3$CEt)(NCMe)Ph][BAr'$_4$] (**7**) in CD_2Cl_2.

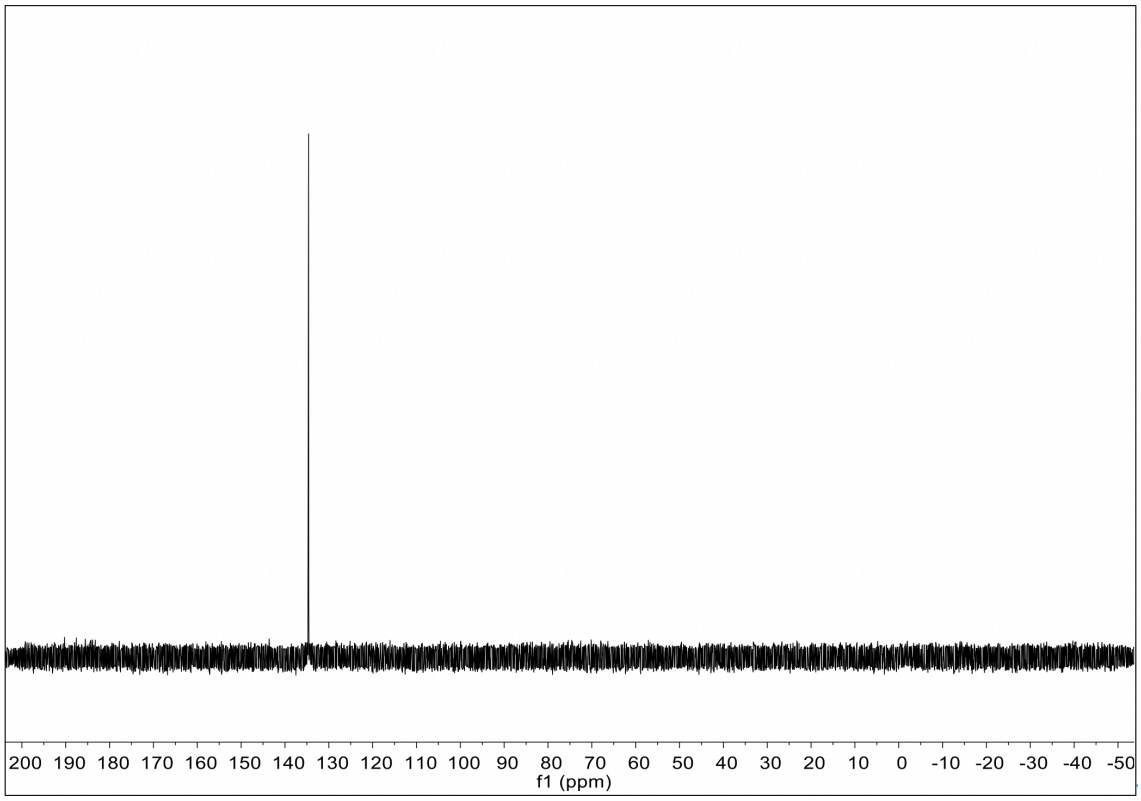

Figure 2.18. ^{31}P NMR spectrum of [(MeOTTM)Ru(P(OCH$_2$)$_3$CEt)(NCMe)Ph][BAr'$_4$] (**7**) in CD_2Cl_2.

Cyclic voltammetry of complex **7** shows a reversible Ru(III/II) oxidation at 0.86 V (vs. NHE), which is a +0.04 V shift compared to the previously reported complex [(HC(pz^5)$_3$Ru(P(OCH$_2$)$_3$)CEt)(NCMe)Ph][BAr'$_4$].[6] Thus, the exchange of HC(pz^5)$_3$ with CH$_3$OTTM has negligible impact on the Ru(III/II) redox potential. Therefore, we anticipated that complex **7** might display catalytic activity and selectivity for ethylene hydrophenylation similar to [(HC(pz^5)$_3$Ru(P(OCH$_2$)$_3$)CEt)(NCMe)Ph][BAr'$_4$].[6]

The use of complex **7** as a catalyst for ethylene hydrophenylation was investigated at different temperatures (Table 2.4). The catalytic reactions produce substantial quantities of both ethylbenzene and styrene. Heating 10 mL benzene solutions of complex **7** (0.001 mol %

relative to benzene) at different temperatures (90 °C, 120 °C, 150 °C and 180 °C) affords up to 57 TONs with a mixture of styrene and ethylbenzene after 4 hours (three experiments were performed at each temperature). The data show that higher temperatures facilitate the catalytic reaction. However, catalyst decomposition is also accelerated at elevated temperatures. The optimal temperature was determined to be 150 °C, which provided a styrene TON of 53. At all temperatures, styrene is favored over ethylbenzene with styrene/ethylbenzene ratios ranging from 6.9 to 70. At 150 °C, we explored ethylene hydrophenylation under different ethylene pressures (Table 2.4). The results indicate that the selectivity for styrene increases with increasing ethylene pressure, and quantitative selectivity toward styrene was observed under 75 psig of ethylene.

Table 2.3. TOs for catalytic hydrophenylation of ethylene using [(MeOTTM)Ru(P(OCH$_2$)$_3$CEt)(NCMe)Ph][BAr'$_4$] (**7**).

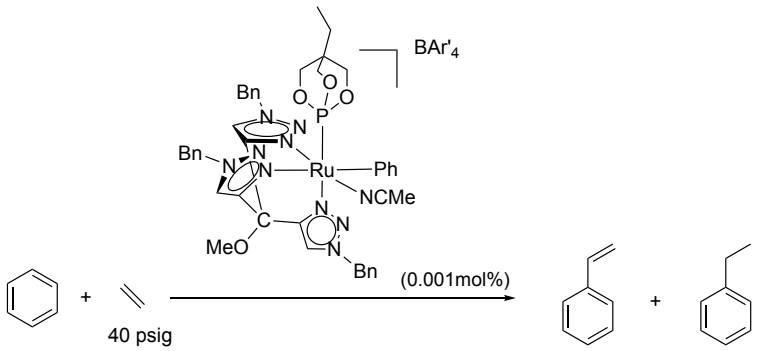

Entry[a]	Temperature (°C)	Styrene (TOs)	Ethylbenzene (TOs)	Selectivity (% Styrene)	Total TON
1	90	3.0(5)	0.41(4)	88	3.4
2	120	14(2)	0.20(2)	99	14
3	150	53(2)	4.3(1)	92	57
3	180	42(4)	6.1(7)	87	48

[a] Conditions: 0.001 mol % of complex **7** dissolved in 10 mL of benzene with decane as an internal standard and 40 psig of ethylene. [b] TOs were determined by GC-FID after 4 hours

and are the average of at least three separate experiments. Standard deviations are given in parentheses.

Table 2.4. TON of styrene and ethylbenzene and % styrene under different ethylene pressures using [(MeOTTM)Ru(P(OCH$_2$)$_3$CEt)(NCMe)Ph][BAr'$_4$] (**7**) as catalyst.[a]

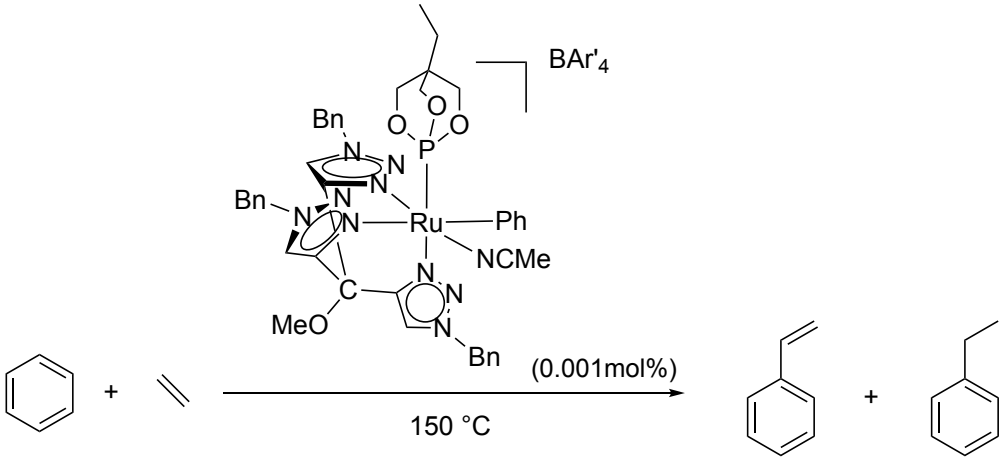

Entry[a]	Ethylene Pressure (psig)	Styrene (TOs)	Ethylbenzene (TOs)	Selectivity (% Styrene)
1	15	5.6(2)	7.2(4)	44
2	25	39(6)	7.5(7)	84
3	40	53(2)	4.3(1)	93
4	75	9.4(7)	0	100

[a] Conditions: 0.001 mol % of complex **7** dissolved in 10 mL benzene with decane as an internal standard at 150 °C. [b] TOs were determined by GC-FID after 4 hours and are the average of at least three separate experiments. Standard deviations are given in parentheses.

Since the cationic Ru(II) complex [(HC(pz^5)$_3$)Ru(P(OCH$_2$)$_3$CEt)(NCMe)Ph][BAr'$_4$] is selective for ethylbenzene production and is electronically similar to complex **7** (*i.e.*, similar Ru(III/II) potentials),[6] we considered that the formation of styrene using **7** might be a result of the steric influence of the benzyl groups at the triazolyl 4-position.[8] Thus, we sought to change the identity of the 4-position substituent to determine the influence of ancillary ligand sterics on selectivity. We prepared the complex

[(PhTTM)Ru(P(OCH$_2$)$_3$CEt)(NCMe)Ph]Br (**8**) (PhTTM = tris(1-phenyl-1H-1,2,3-triazol-4-yl)methanol) as shown in Scheme 2.9. Cyclic voltammetry data show that the electron densities for complex **7** (0.86 V vs NHE) and complex **8** (0.85 V vs NHE) are nearly identical, which suggests negligible differences in the electron donor ability of the MeOTTM and PhTTM ligands coordinated to Ru(P(OCH$_2$)$_3$CEt)(NCMe)Ph.

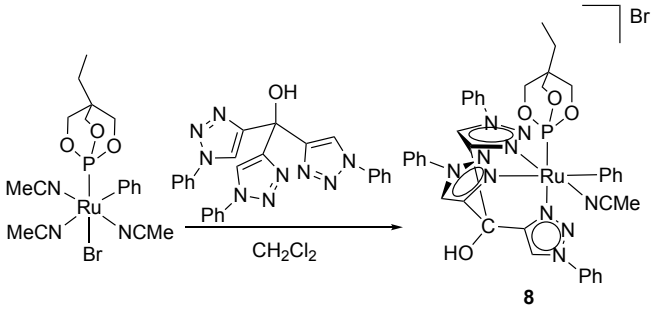

Scheme 2.9. Synthesis of [(PhTMM)Ru(P(OCH$_2$)$_3$CEt)(NCMe)Ph]Br (8).

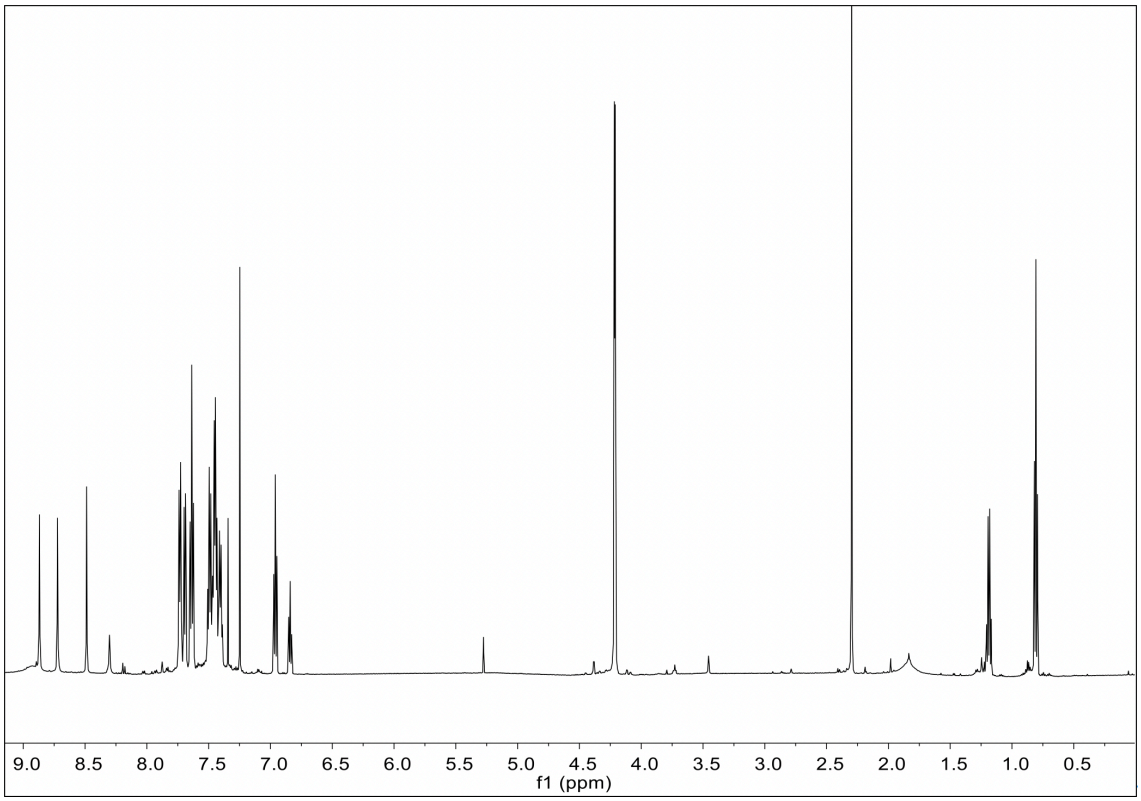

Figure 2.19. ^{1}H NMR spectrum of [(PhTTM)Ru(P(OCH_2)$_3$CEt)(NCMe)Ph]Br (**8**) in $CDCl_3$.

We probed ethylene hydrophenylation with **8** as a catalyst precursor at variable ethylene pressures. The results show that the cationic Ru catalyst **8** is less selective for styrene production than complex **7**. Although the steric A values, which are indicative of the steric bulk of the substituent based on impact on substituted cyclohexane confirmations,[22] show that the steric bulk of a phenyl group (A = 3) is larger than that of a benzyl group (A = 1.81),[23] the differences in the two-dimensional phenyl versus three-dimensional benzyl render any evaluation of relative steric influence challenging. At a minimum, the selectivity difference for ethylbenzene versus styrene production using complexes **6** and **8** indicate that the steric profile of the triazole substituent plays a role.

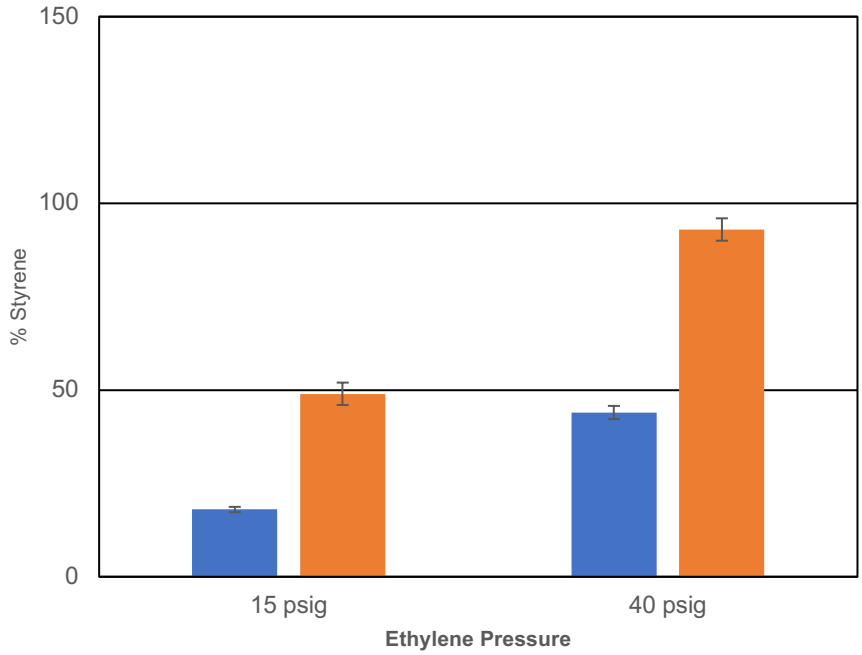

Figure 2.20. Percent styrene formation as a function of ethylene pressure using catalyst precursors [(MeOTTM)Ru(P(OCH$_2$)$_3$CEt)(NCMe)Ph]Br (**6**, orange) and [(PhTTM)Ru(P(OCH$_2$)$_3$CEt)(NCMe)Ph]Br (**8**, blue). Conditions: 0.001 mol % of complex **6** or **8** dissolved in 10 mL benzene with decane as an internal standard at 150 °C.

We recently reported that Rh catalyst precursors efficiently catalyze oxidative olefin hydroarylation with Cu(II) oxidants to form alkenyl arene.[24-26] Thus, we attempted to improve catalysis using complex **7** by adding external oxidants. However, when O_2 or Cu(II) salts were added to catalytic reaction using **7** , no improvement in catalysis was observed (Table 2.5).

Table 2.5. The effect of external oxidants on the oxidative ethylene hydrophenylation catalyzed using [(CH_3OTTM)Ru(P(OCH_2)$_3$CEt)(NCMe)Ph][BAr'$_4$] (**7**).

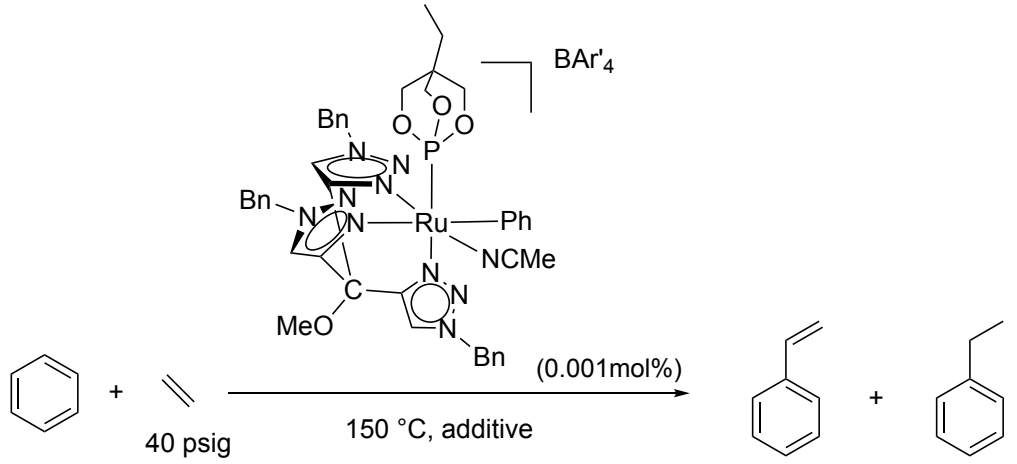

Entry[a]	Additive[b]	Styrene[c] (TOs)
1	–	53(2)
2	$Cu(OAc)_2$	< 15
3	$Cu(OPiv)_2$	< 15
4	O_2 (Air)	49(5)

[a] Reactions were performed with 0.001 mol % complex [(CH_3OTTM)Ru(P(OCH_2)$_3$CEt)(Ph)(NCMe)][BAr'$_4$] (**7**) dissolved in 10 mL benzene with decane as an internal standard at 150 °C with 40 psig of ethylene. [b] 10 equivalents of copper(II) salt relative to complex **7** were used for entries 2 and 3, 15 psig of air was used in entry 4. [c] TON were determined by GC-FID after 4 hours and are the average of three experiments. Standard deviations are given in parenthesis.

When using complex **7** as a catalyst under anaerobic conditions and in the absence of an external oxidant {e.g., Cu(II)}, we assume that ethylene serves as the oxidant for styrene production with the formation of one equivalent of ethane per equivalent of styrene. The production of ethane was confirmed by heating a C_6D_6 solution of complex **7** with 25 psig ethylene pressure at 70 °C for 40 hours. Monitoring by ^{1}H NMR spectroscopy revealed styrene-d_5 production as well as a singlet at 0.88 ppm, which is consistent with ethane-d_1. Additionally, ethane-d_1 was detected in the head space of the reactor by GC-MS. Thus, the

overall reaction for styrene formation is likely conversion of benzene and two equivalents of ethylene to styrene and ethane.

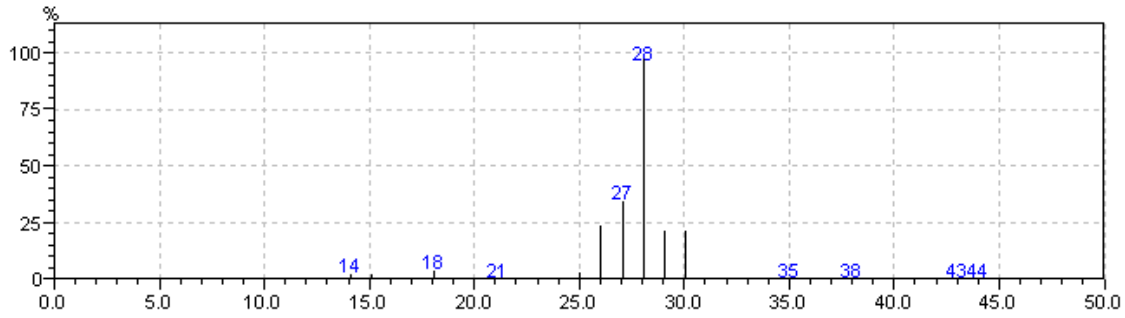

Figure 2.21. Mass fragmentation pattern for reactor headspace gas after 4-hour reaction, consistent with ethane (peak at m/z = 30 is corresponding to $C_2H_6^+$; peak at m/z = 29 corresponding to $C_2H_5^+$; peak at m/z = 28 corresponding to $C_2H_4^+$; peak at m/z = 27 corresponding to $C_2H_3^+$ the distribution of the peaks match the standard ethane spectrum 96%)

A proposed catalytic cycle for ethylene hydrophenylation is shown in Scheme 2.10. Initial exchange of coordinated NCMe with ethylene forms [(MeOTTM)Ru(P(OCH$_2$)$_3$)CEt)(η^2-C$_2$H$_4$)Ph][BAr'$_4$]. Then, ethylene inserts into the Ru–Ph bond to form a phenethyl intermediate.[27] The complex [(MeOTTM)Ru(P(OCH$_2$)$_3$CEt)(η^2-styrene)(H)]$^+$ can be formed *via* β-hydride elimination from [(MeOTTM)Ru(P(OCH$_2$)$_3$CEt)(CH$_2$CH$_2$Ph)]$^+$. Net ligand exchange of styrene and ethylene completes the process for styrene formation. Ethylene then inserts into the Ru–H bond of [(MeOTTM)Ru(P(OCH$_2$)$_3$CEt)(η^2-C$_2$H$_4$)(H)]$^+$ to form a Ru-ethyl complex. Finally, the coordination and C–H activation of benzene liberates ethane and regenerates the Ru−Ph starting catalyst.

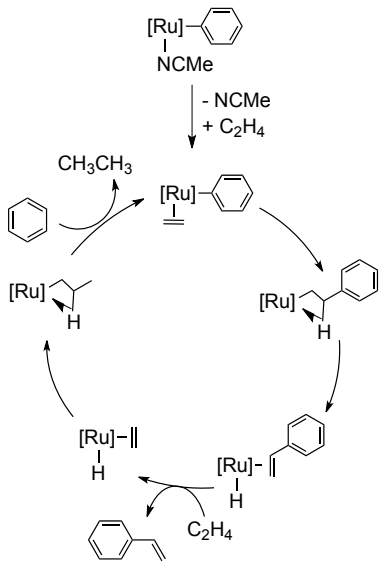

Scheme 2.10. Proposed catalytic cycle for oxidative ethylene hydrophenylation using [(MeOTTM)Ru(P(OCH$_2$)$_3$CEt)(Ph)(NCMe)][BAr'$_4$] (**7**) ([Ru] = [(MeOTTM)Ru(P(OCH$_2$)$_3$CEt)]$^+$).

One likely key step in olefin hydroarylation catalyzed by **7** and **8** is the dissociation of the coordinated acetonitrile to create a coordination site for ethylene. We expected that the cationic nature of complexes **7** and **8** might slow the rate of NCMe dissociation compared to the charge neutral complex TpRu(P(OCH$_2$)$_3$CEt)(NCMe)Ph. The rate of exchange between coordinated NCMe and free NCMe-d_3 was determined using ^{1}H NMR spectroscopy by heating acetonitrile-d_3 solutions of complex **7** at 70, 75, 90, and 105 °C (Scheme 2.11). Values for k_{obs} of 1.53(2) × 10^{-5} s^{-1} (70 °C), 2.8(3) × 10^{-5} s^{-1} (75 °C), 2.1(2) × 10^{-4} s^{-1} (90 °C) and 1.0(1) × 10^{-3} s^{-1} (105 °C), were determined by monitoring the reactions using ^{1}H NMR spectroscopy. As anticipated, at 70 °C the exchange rate for **7** is slower by ~2 fold compared to the charge neutral complex TpRu(P(OCH$_2$)$_3$)CEt)(NCMe)Ph (k_{obs} = 3.2(2) × 10^{-5} s^{-1} at 70 °C).[28]

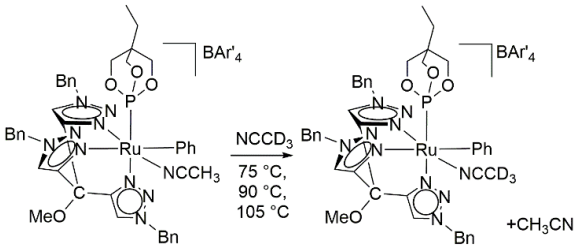

Scheme 2.11. Degenerate NCMe/NCMe-d_3 exchange for [(MeOTTM)Ru(P(OCH$_2$)$_3$CEt)(NCMe)Ph][BAr'$_4$] (**7**).

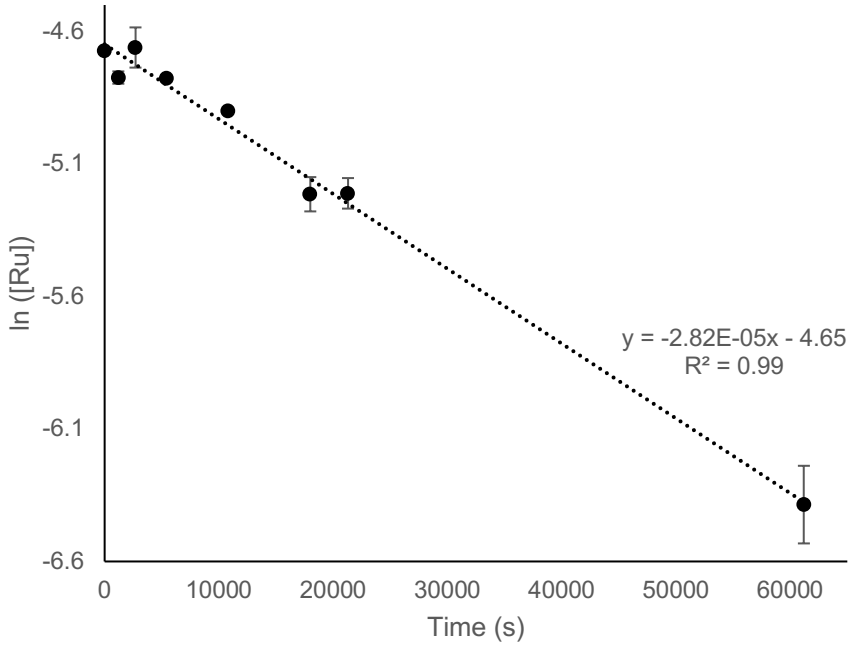

Figure 2.22. Sample ln[Ru] versus time plot of [(MeOTTM)Ru(P(OCH$_2$)$_3$CEt)(NCMe)Ph][BAr'$_4$] (7) for NCMe/NCMe-d_3 exchange at 75 °C (slope = −0.0000282, R^2 = 0.99); k_{obs} = 2.82 x 10^{-5} s^{-1}

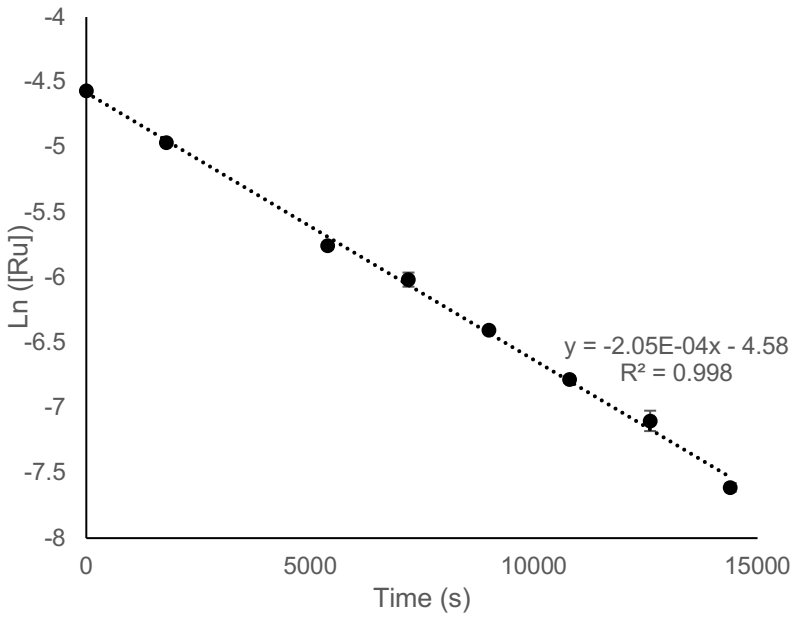

Figure 2.23. Sample ln([Ru])/T plot of [(MeOTTM)Ru(P(OCH$_2$)$_3$CEt)(NCMe)Ph][BAr'$_4$] (7) for NCMe/NCMe-d_3 exchange at 90 °C (slope = –0.000205, R^2 = 0.998); k_{obs} = 2.05 x 10^{-4} s^{-1}

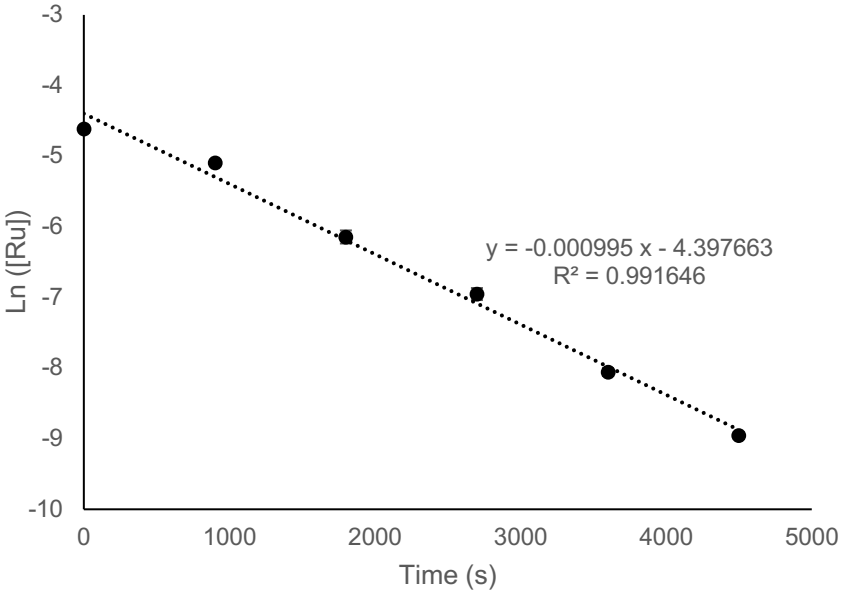

Figure 2.24. Sample ln([Ru])/T plot of [(MeOTTM)Ru(P(OCH$_2$)$_3$CEt)(NCMe)Ph][BAr'$_4$] (7) for NCMe/NCMe-d_3 exchange at 105 °C (slope = −0.000995, R^2 = 0.99); k_{obs} = 9.95 x 10^{-4} s^{-1}

We probed for a possible kinetic isotope effect (KIE) comparing the rates of catalysis using C_6H_6 and C_6D_6 (Scheme 2.12). For hydrophenylation of ethylene using C_6H_6 and C_6D_6, the previously reported complexes TpRu(CO)(NCMe)Ph and $[(HC(pz^5)_3)Ru(P(OCH_2)_3CEt)(NCMe)Ph][BAr'_4]$ exhibit KIEs of 2.1(1) and 2.11(5), respectively.[6, 28] We probed catalysis (0.001 mol% of **7** in benzene at 150 °C and 40 psig ethylene) in a 1:1 molar ratio of C_6H_6 to C_6D_6. Presumably, this leads to the formation of both $[(MeOTTM)Ru(P(OCH_2)_3CEt)(CH_2CH_2C_6H_5)][BAr'_4]$ and $[(MeOTTM)Ru(P(OCH_2)_3CEt)(CH_2CH_2C_6D_5)][BAr'_4]$ as intermediates, which would result in the production of per-protio styrene and styrene-d_5.[24] The ratio of styrene and styrene-d_5 provides a determination of the KIE for catalytic styrene formation. After 1 hour of catalysis, a k_H/k_D of 3.2(6) was determined by examining the ratio of perprotio-styrene (m/z = 104) to styrene-d_5 (m/z = 109) (Scheme 2.12. In addition, benzene H/D exchange is observed when heating up **7** in benzene-d_6 solution, indicating that reversible stoichiometric C_6D_6 activation by Ru likely occurs. This observation supports the possibility that the cleavage of the C–H bond of benzene precedes or is the rate-determining step in the catalytic cycle.

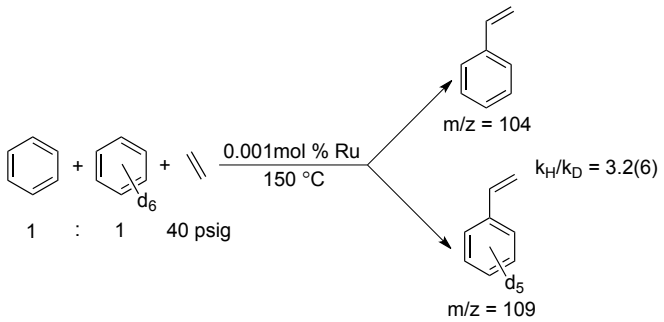

Scheme 2.12. KIE study using [(MeOTTM)Ru(P(OCH$_2$)$_3$CEt)(NCMe)Ph][BAr'$_4$] (7)

In an effort to gain more insight into the proposed mechanism of this Ru catalyzed arene alkenylation reaction, density functional theory (DFT) calculations were employed by Dr. Brannon Gary from University of North Texas. Complex **8** was employed as the model system as it eliminates the multiple possible confirmations associated with the benzyl substituents of the MeOTMM analog in complex [(MeOTTM)Ru(P(OCH$_2$)$_3$CEt)(Ph)(NCMe)][BAr'$_4$] (**7**). Examining the proposed mechanism given in Scheme 2.10, the species were optimized using the Gaussian09 software package[29] in the gas phase using the B3LYP functional[30, 31] and LANL2dz basis set for Ru and 6-31G(d,p) basis set on all other atoms. Single point energies of the optimized geometries were performed using LANL2DZ/6-311G(d,p) basis sets in benzene solvent using the SMD solvation model[32] with GD3BJ empirical dispersion,[33] and thermal frequency corrections at 423.15 K were employed to calculate Gibbs energy values.

Calculations were referenced to the starting precatalyst **8** as the zero point in Gibbs energy (Scheme 2.13). Loss of acetonitrile is calculated to be moderately endergonic by 12.1 kcal/mol, and binding of ethylene is slightly stabilizing compared to the 5-coordinate intermediate at 10.6 kcal/mol. The transition state for ethylene insertion into the Ph ligand

is calculated to be 31.6 kcal/mol, about 21 kcal/mol above the precursor [(PhTTM)Ru(P(OCH$_2$)$_3$)CEt](η^2–C$_2$H$_4$)Ph][BAr'$_4$]. This insertion results in an phenethyl ligand that possesses an agostic C–H bond interaction that is calculated to be 17.0 kcal/mol relative to the precatalyst **8**. A β-hydride elimination step is calculated to have a very low barrier at only 0.8 kcal/mol above the phenethyl intermediate with an overall free energy of 17.8 kcal/mol above **8**. The resulting Ru-styrene/hydride intermediate is calculated to be endergonic from the precatalyst **8** by 9.0 kcal/mol. Loss of styrene to yield the coordinatively unsaturated hydride species is 9.7 kcal/mol or approximately energetically equivalent to the styrene hydride. Ethylene binding to the hydride is calculated to be slightly more favorable, having an energy of 6.6 kcal/mol relative to the precatalyst. The transition state for ethylene insertion into the hydride is also quite low with a free energy of 15.0 kcal/mol, which results in an agostic stabilized ethyl intermediate with an energy of 12.3 kcal/mol. The largest calculated barrier in the system is the transition state for a σ-bond metathesis C–H activation in which benzene is exchanged for the ethyl ligand and has an energy of 37.0 kcal/mol relative to the precatalyst. An off-cycle intermediate is the binding of NCMe to the 5-coordinate hydride, which is calculated to be a possible resting state of the catalytic process with an energy of –4.5 kcal/mol relative the starting precatalyst.

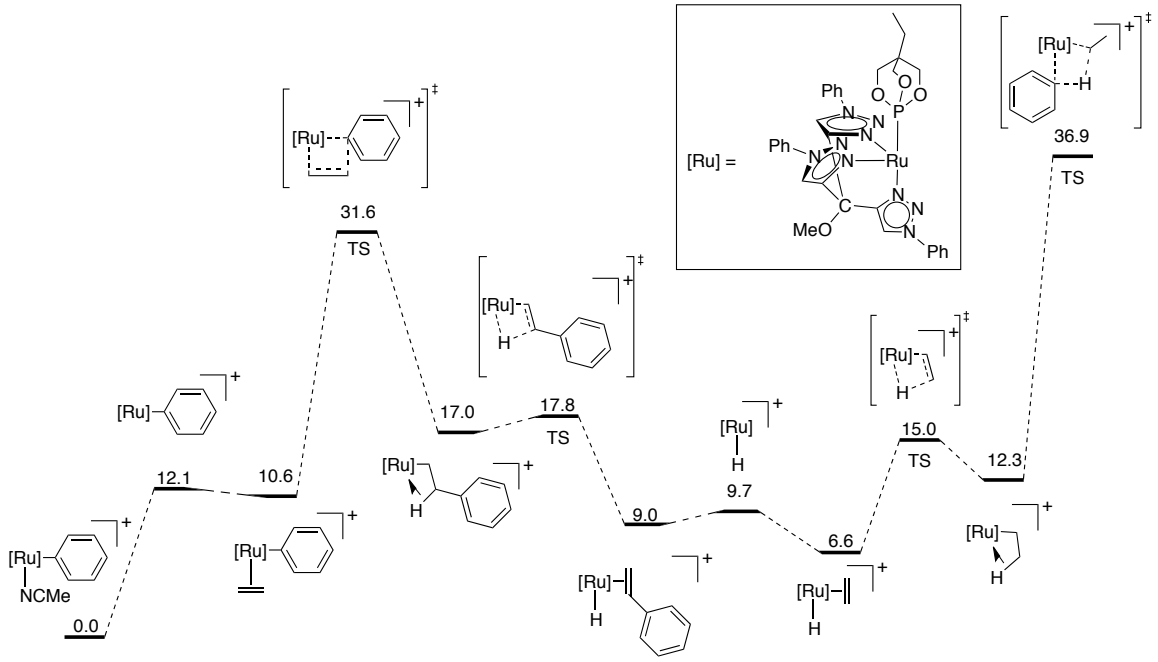

Scheme 2.13. Calculated free energies (in kcal/mol) for oxidative ethylene hydrophenylation to form styrene using **7** {[Ru] = (PhTMM)Ru(P(OCH$_2$)$_3$CEt)}.

The calculations indicate that the proposed mechanism shown in **Scheme 2.13** is plausible with the highest barrier resulting from C–H activation of benzene to release ethane, which is consistent with the observed kinetic isotope effect (k_H/k_D) of 3.2(6) (see above). Two possible explanations for the styrene selectivity (versus ethylbenzene) arise from the calculations. First, the σ-bond metathesis C–H activation of benzene with the phenethyl unit (the transition state that would likely be responsible for ethylbenzene formation) is calculated to be 3.6 kcal/mol higher in energy (40.5 kcal/mol) than the same benzene C–H activation by the Ru-ethyl fragment (36.9 kcal/mol). If one envisions a Curtin-Hammett scenario, then all of the olefin insertion steps are reversible and the product selectivity would be controlled by the relative energy barriers for benzene C–H activation (Scheme 2.14). That is, the overall calculated free energy of activation (using **8**

as the benchmark) for ethylbenzene formation is 40.5 kcal/mol while that for styrene formation is 36.9 kcal/mol. Another possible product controlling feature could be relative binding of styrene versus ethylene to the 5-coordinate hydride intermediate $[(PhTMM)Ru(P(OCH_2)_3CEt)(H)]^+$. Calculations predict the ethylene binding is favored over styrene coordination by 3.4 kcal/mol, again indicating a preference for styrene formation. In this explanation, it is the rapid equilibrium between $[(PhTMM)Ru(P(OCH_2)_3CEt)(H)(\eta^2\text{-styrene})]^+$ and $[(PhTMM)Ru(P(OCH_2)_3CEt)(H)(\eta^2\text{-}C_2H_4)]^+$, which the calculations predict favors the ethylene complex, and the relative rates of ethylbenzene formation from the styrene complex and styrene and ethane formation from ethylene complex that dictates the ethylbenzene/styrene ratio. The calculated free energy of activation from $[(PhTMM)Ru(P(OCH_2)_3CEt)(H)(\eta^2\text{-styrene})]^+$ to the benzene C–H activation transition state that produces ethylbenzene is 31.5 kcal/mol, while the calculated free energy of activation from $[(PhTMM)Ru(P(OCH_2)_3CEt)(H)(\eta^2\text{-}C_2H_4)]^+$ to the benzene C–H activation transition state that produces styrene/ethane is 30.3 kcal/mol. It is this more complete assessment that provides a rationalization for increased styrene production at higher ethylene pressures since these conditions should increase the ratio of $[(PhTMM)Ru(P(OCH_2)_3CEt)(H)(\eta^2\text{-}C_2H_4)]^+$ to $[(PhTMM)Ru(P(OCH_2)_3CEt)(H)(\eta^2\text{-styrene})]^+$.

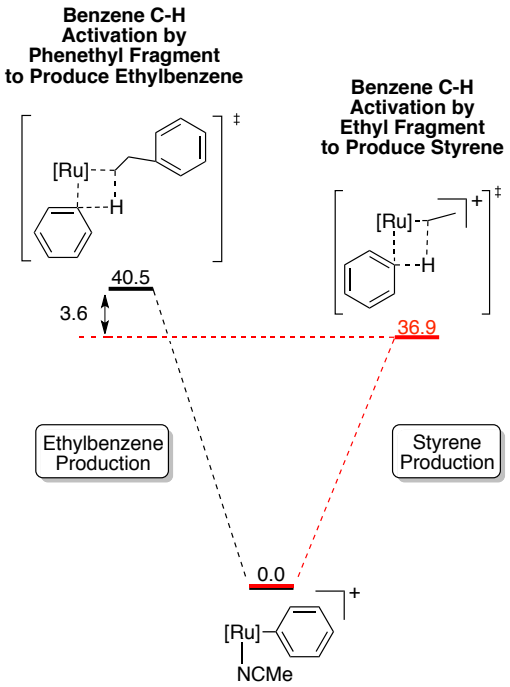

Scheme 2.14. The lower free energy of the transition state for benzene C–H activation by the [Ru]–ethyl complex (right) than that of the Ru-phenethyl complex (left) favors styrene production over ethylbenzene {[Ru] = (PhTTM)Ru(P(OCH$_2$)$_3$CEt)}.

2.6 Summary

In this chapter, effort has been made to synthesize electron-deficient Ru(II) pre-catalysts for olefin hydroarylation. The installation of NO ligand reduces the electron density of the Ru center, but, it also trigger biphenyl reductive elimination. A Ru(II) complex by the Tp^{Br3} ligand is not a catalyst for ethylene hydrophenylation, which might be due to the size of the Tp^{Br3} lignad inhibiting ethylene coordination.

The new cationic Ru(II) complexes supported by tris(triazolyl)methanol ligands, [(MeOTTM)Ru(P(OCH$_2$)$_3$CEt)(NCMe)Ph]$^+$ and [(PhTTM)Ru(P(OCH$_2$)$_3$CEt)(NCMe)Ph]$^+$, catalyze oxidative ethylene hydrophenylation to produce styrene as well as ethylbenzene under some conditions. In contrast, similar Ru(II)

catalysts with trispyrazolylborate (Tp) or trispyrazolylmethane ligands are highly selective for ethylbenzene production.[6, 28] The complex [(MeOTTM)Ru(P(OCH$_2$)$_3$CEt)(NCMe)Ph][BAr'$_4$] (**7**) produces 53 TON of styrene under 40 psig of ethylene at 150 °C, and the selectivity toward styrene production increases when higher ethylene pressures are used. Determination of reversible Ru(III/II) potentials using cyclic voltammetry indicate minor differences in electron-density at Ru for [(HC(pz^5)$_3$Ru(P(OCH$_2$)$_3$)CEt)(NCMe)Ph]$^+$, [(MeOTTM)Ru(P(OCH$_2$)$_3$CEt)(NCMe)Ph]$^+$ and [(PhTTM)Ru(P(OCH$_2$)$_3$CEt)(NCMe)Ph]$^+$. Thus, the change in selectivity for styrene versus ethylbenzene is likely a result of steric profile of the tristriazolyl ligands. That is, the benzyl and phenyl substituents on the MeOTTM and PhTTM ligands biases the catalysis toward styrene production. DFT calculations provide an explanation: the equilibrium between [(PhTMM)Ru(P(OCH$_2$)$_3$CEt)(H)(η^2-C$_2$H$_4$)]$^+$ to [(PhTMM)Ru(P(OCH$_2$)$_3$CEt)(H)(η^2-styrene)]$^+$ favors the ethylene complex, which ultimately leads to styrene formation. Furthermore, assessment under Curtin-Hammett conditions is consistent with favorable styrene production (see above). Since ethylene is produced directly from ethane, this new process for styrene production without an added external oxidant is promising as outlined in Scheme 2.15.

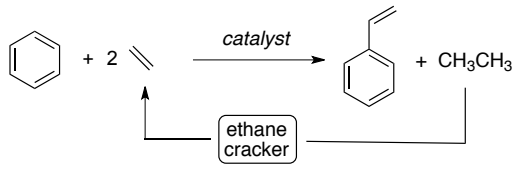

Scheme 2.15. Vision for a new process for styrene production.

2.7 Experimental Section

General Considerations. Unless otherwise noted, all synthetic procedures were performed under anaerobic conditions in a dinitrogen-filled glovebox or by using standard Schlenk techniques. Glovebox purity was maintained by periodic nitrogen purges and was monitored by an oxygen analyzer (O_2 < 15 ppm for all reactions). Tetrahydrofuran and diethyl ether were dried by distillation from sodium/benzophenone, respectively. Benzene, methylene chloride, and hexanes were purified by passage through a column of activated alumina. Benzene-d_6, acetone-d_6, CD_3CN, and THF-d_8 were used as received and stored under a dinitrogen atmosphere over 4 Å molecular sieves. ^{1}H NMR spectra were recorded on a Varian 600, Varian 500 MHz or a Bruker 600 MHz or 800 MHz spectrometer, and $^{13}C\{^1H\}$ NMR spectra were recorded on a Varian 600 MHz (operating frequency 125 MHz), Bruker 600 MHz (operating frequency = 150 MHz) or a Bruker 800 MHz (operating frequency = 201 MHz). All ^{1}H and ^{13}C spectra are referenced against residual proton signals (^{1}H NMR) or ^{13}C resonances (^{13}C NMR) of the deuterated solvents. $^{31}P\{^1H\}$ NMR spectra were obtained on a Varian 500 MHz (operating frequency = 201 MHz) or Varian 600 MHz (operating frequency = 243 MHz) spectrometer and referenced against an external standard of H_3PO_4 ($\delta = 0$). ^{19}F NMR spectra were obtained on a Varian 600 MHz (operating frequency = 565 MHz) spectrometer and referenced against an external standard of C_6F_6. GC/MS was performed using a Shimadzu GCMS-QP2010 Plus system with a 30 m x 0.25 mm RTx-Qbond column with 8 μm thickness using electron impact ionization. GC/FID was performed using a Shimadzu GC-2014 system with a 30 m x 90.25 mm HP5

column with 0.25 μm film thickness. Styrene production was quantified using linear regression analysis of gas chromatograms of standard samples of authentic product. A plot of peak area ratios versus molar ratios gave a regression line. For the GC/FID system, the slope and correlation coefficient of the regression line were 1.34 and 0.99, respectively. FID response factors for other products were determined in a similar fashion, using authentic standards of products. All other reagents were used as received from commercial sources. The preparation, isolation and characterization of $[(\eta^6\text{-}p\text{-cymene})Ru(Br)(\mu\text{-}Br)]_2$, $NaBAr'_4$ (sodium tetrakis[3,5-bis(trifluoromethyl)phenyl]borate), $Ph_2Mg[THF]_2$, MeOTTM {4, 4', 4"-(methoxymethanetriyl)-tris(1-benzyl-1H-1,2,3-triazole)}, PhTMM {4, 4' ,4"-(hydroxymethanetriyl)-tris(1-phenyl-1H-1,2,3-triazole)}, $(\eta^6\text{-}p\text{-cymene})Ru(P(OCH_2)_3CEt)(Br)Ph$ were performed according to literature procedures.[4, 6, 8, 34, 35] Elemental analyses were performed by Atlantic Microlab, Inc.

$TpRu(NO)Cl_2$ (1). This is a modified procedure based on the literature.[12] A solution of $Ru(NO)Cl_3$ monohydrate (2.37g, 10 mmol) and two equivalents of KTp (5.04 g, 20 mmol) in 150 mL of ethanol was stirred under inert atmosphere for two days to yield a dark brownish red mixture. The resulting suspension was filtered through a two inch pack of celite, and the filtrate was concentrated to dryness under reduced pressure to get a solid crude product. The resulting solid was dissolved in DCM and purified by column chromatography using a 5-inch plug of silica gel. The pink solution that eluted first is unreacted $Ru(NO)Cl_3$. The second fraction, which was brown, from the column is $TpRu(NO)Cl_2$. The solvent was then removed under reduced pressure to yield 2.2 g (53%)

of complex **1** as a purple solid. ^{1}H NMR (600 MHz, $CDCl_3$) δ 8.15 (dd, *J* = 2.3, 0.7 Hz, 1H, pyrazyl 3-H), 7.91 (d, *J* = 2.2 Hz, 2H, pyrazyl 3-H), 7.80 (dd, *J* = 2.5, 0.7 Hz, 2H, pyrazyl 5-H), 7.59 (dd, *J* = 2.4, 0.8 Hz, 1H, pyrazyl 5-H), 6.43 (t, *J* = 2.4 Hz, 2H, pyrazyl 4-H), 6.27 (t, *J* = 2.4 Hz, 1H, pyrazyl 4-H). IR (KBr): ν_{NO} = 1898 cm^{-1}.

TpRu(NO)Ph$_2$ (2). Stirring TpRu(NO)Cl_2 **(1)** (415 mg, 1 mmol) in THF under dinitrogen at −78 ºC results in a light purple solution. A cold THF solution of 4 equivalents of Ph_2Zn (880 mg, 4 mmol) was added dropwise to the solution of **1**. After the addition of the Ph_2Zn, the reaction was stirred at −78 ºC for additional 2 hours. Then, the reaction mixture was allowed to warm to 0 ºC and stirring was maintained for 48 hours. The reaction mixture turned brown during this time period. Next, the mixture was filtered though Celite, and the solvent was removed under reduced pressure. The resulting solid was dissolved in DCM and eluted through a plug of silica gel. The brown TpRu(NO)Ph_2 (**2**) solution, which eluted after complex **1**, was collected and the solvent was removed under reduced pressure to yield the product with 54% isolated yield (270 mg). ^{1}H NMR (600 MHz, $CDCl_3$) δ 7.78 (dd, *J* = 2.4, 0.7 Hz, 2H, pyrazyl 3-H), 7.64 (dd, *J* = 2.2, 0.7 Hz, 1H, pyrazyl 3-H), 7.39 (dd, *J* = 2.0, 0.6 Hz, 2H, pyrazyl 4-H), 7.16 (d, 4H, phenyl ortho-H), 7.11 (dd, *J* = 2.2, 0.7 Hz, 1H, pyrazyl 4-H), 7.05 (d, 4H, phenyl, meta-H), 7.00 (t, 2H, phenyl para-H), 6.26 (t, *J* = 2.1 Hz, 2H, pyrazyl 5-H), 6.10 (t, *J* = 2.3 Hz, 1H, pyrazyl 5-H). IR (KBr): ν_{NO} = 1826 cm^{-1}.

TpRu(NO)PhOTf (3). Adding a cold DCM solution of 0.9 equivalents of HOTf (27.1 mg, 0.18 mmol) into a DCM solution of TpRu(NO)Ph_2 (**2**) (100mg, 0.2 mmol) at –78 ºC

under inert atmosphere resulted in protonation of one of the phenyl groups. The reaction was performed at –78 ºC for 2 hours and then allowed to warm to room temperature. A color change of the reaction solution from light brownish red to purple was observed during warming. The solvent was removed under reduced pressure, and the resulting solid was dissolved in DCM and passed through a plug of silica gel using DCM as eluent. The light pink solution was collected, and solvent was evaporated to obtain TpRu(NO)PhOTf (**3**) in 80 % yield (91.2 mg). ^{1}H NMR (600 MHz, $CDCl_3$) δ 8.38 (d, *J* = 2.1 Hz, 1H, pyrazyl 3-H), 7.89 (dd, *J* = 2.6, 0.7 Hz, 1H, pyrazyl 3-H), 7.76 (dd, *J* = 2.4, 0.7 Hz, 1H, pyrazyl 3-H), 7.70 (dd, *J* = 2.4, 0.7 Hz, 1H, pyrazyl 4-H), 7.60 (d, 2H, phenyl ortho-H), 7.45 (d, 2H, phenyl meta-H), 7.35 (t, 1H, phenyl para-H), 6.95 (dd, *J* = 2.7, 1.3 Hz, 1H, pyrazyl 4-H), 6.94 (dd, *J* = 2.0, 1.3 Hz, 1H, pyrazyl 4-H), 6.39 (t, *J* = 2.2 Hz, 1H, pyrazyl 5-H), 6.36 (t, *J* = 2.4 Hz, 1H, pyrazyl 5-H), 6.19 (t, *J* = 2.3 Hz, 1H, pyrazyl 5-H).

$(Tp^{Br3})Ru(P(OCH_2)_3CEt)(NCMe)Ph$ (4). The complex (η^6-*p*-cymene)Ru(P(OCH_2)$_3$CEt)(Br)Ph (0.55 g, 1.0 mmol) was dissolved in NCMe (20 mL), added to a pressure tube, and heated for 3.5 h at 70 °C. The reaction was allowed to cool to room temperature. The mixture was filtered through Celite, and the filtrate was concentrated to dryness yielding the putative complex (NCMe)$_3$Ru(P(OCH_2)$_3$CEt)(Br)Ph.[3] The resulting solid was taken up in DCM (10 mL) and added to a 50 mL thick-wall glass pressure tube with $TlTp^{Br3}$ (1.24 g, 1.1 mmol) in DMSO (10 mL). The solution was heated to 70 °C for 15 h after which it was cooled to room temperature and filtered through Celite. The volatiles were removed from the filtrate under reduced pressure. Benzene was added,

and the mixture was stirred for 10 min. The solution was filtered through Celite, and the filtrate was discarded. The remaining white solid was dissolved in DCM and filtered through Celite. The filtrate was concentrated to 2 mL, and hexanes were added to induce precipitation. The colorless precipitate was collected on a fine porosity frit. The solid was washed with pentane and dried *in vacuo* to yield 1.2 g of tan solid (44%). ^{1}H NMR (600 MHz, DMSO-d_6) δ 7.56 (d, J = 7.6 Hz, 1H, phenyl ortho-H), 6.74 (s, 1H, phenyl meta-H), 6.59 (tt, J = 7.1, 1.3 Hz, 1H, phenyl para-H), 6.49 (s, 1H, phenyl meta-H), 6.11 (d, J = 7.8 Hz, 1H, phenyl ortho-H), 4.18 (d, J = 3.9 Hz, 6H, P(OCH_2)$_3$CCH$_2$CH$_3$), 2.40 (s, 3H, NCCH$_3$), 1.19 (q, J = 7.6 Hz, 2H, P(OCH$_2$)$_3$CCH_2CH$_3$), 0.77 (t, J = 7.7 Hz, 3H, P(OCH$_2$)$_3$CCH$_2$CH_3).

Catalytic Oxidative Hydrophenylation of Ethylene using (Tp^{Br3})Ru(P(OCH$_2$)$_3$CEt)(NCMe)Ph (4). A representative catalytic reaction is described. A stock solution containing **4** (0.023 mmol), hexamethylbenzene (74.5 mg, 0.46 mmol), and benzene (200 mL) was prepared in a volumetric flask. Thick-walled Fisher-Porter reactors were charged with stock solution (10 mL). The vessels were sealed, pressurized with ethylene, and subsequently stirred and heated to desired temperature in oil bath. The reaction was sampled every 1 h. At each time point, the reactors were cooled to room temperature, sampled, recharged with ethylene, and heated. Aliquots of the reaction mixture were analyzed by GC/FID using relative peak areas versus the internal standard.

(Ttz)Ru(P(OCH$_2$)$_3$CEt)(NCMe)Ph (5). The complex (η^6-*p*-cymene)Ru(P(OCH$_2$)$_3$CEt)(Br)Ph (0.55 g, 1.0 mmol) was dissolved in NCMe (20 mL),

added to a pressure tube, and heated for 3.5 h at 70 °C. The reaction was allowed to cool to room temperature. The mixture was filtered through Celite, and the filtrate was concentrated to dryness yielding the putative complex $(NCMe)_3Ru(P(OCH_2)_3CEt)(Br)Ph$.[3] The resulting solid was taken up in CH_2Cl_2 (10 mL) and added to a 50 mL thick-wall glass pressure tube with KTtz (0.28 g, 1.1 mmol) in DCM (10 mL). The solution was heated to 70 °C for 15 h after which it was cooled to room temperature and filtered through Celite. The volatiles were removed from the filtrate under reduced pressure. Benzene was added, and the mixture was stirred for 10 min. The solution was filtered through Celite, and the filtrate was discarded. The remaining white solid was dissolved in DCM and filtered through Celite. The filtrate was concentrated to 2 mL, and hexanes were added to induce precipitation. The colorless precipitate was collected on a fine porosity frit. The solid was washed with pentane and dried *in vacuo* to yield a off white solid (262 mg, 43%). ^{1}H NMR (600 MHz, $CDCl_3$) δ 8.32 (d, J = 2.4 Hz, 2H, triazole-H), 8.28 (s, 1H, triazole-H), 8.23 (s, 1H, triazole-H), 7.92 (s, 1H, triazole-H), 7.54 (s, 1H, triazole-H), 6.99 – 6.96 (m, 2H, phenyl-H), 6.89 – 6.80 (m, 3H, phenyl-H), 4.18 (dt, J = 5.2, 2.3 Hz, 6H, $P(OCH_2)_3CCH_2CH_3$), 2.31 (s, 3H, $NCCH_3$), 1.19 (q, J = 7.7 Hz, 2H, $P(OCH_2)_3CCH_2CH_3$), 0.82 (t, J = 7.7 Hz, 3H, $P(OCH_2)_3CCH_2CH_3$). ^{31}P{^{1}H} NMR (121 MHz, CD_2Cl_2) δ 133.3. Anal. Calcd for $C_{20}H_{26}O_3N_{10}PBRu$: C, 40.21; H, 4.39; N, 8.04. Found: C, 40.23; H, 4.29; N, 8.17.

Catalytic Oxidative Hydrophenylation of Ethylene using (Ttz)Ru(P(OCH$_2$)$_3$CEt)(NCMe)Ph (5). A representative catalytic reaction is described.

A stock solution containing **5** (0.023 mmol), hexamethylbenzene (74.5 mg, 0.46 mmol), and benzene (200 mL) was prepared in a volumetric flask. Thick-walled Fisher-Porter reactors were charged with stock solution (10 mL). The vessels were sealed, pressurized with 45 psig of ethylene, and subsequently stirred and heated to desired temperature (75, 90, 105 and 120 ºC) in oil bath. The reaction was sampled every 2 h. At each time point, the reactors were cooled to room temperature, sampled, recharged with ethylene, and heated. Aliquots of the reaction mixture were analyzed by GC/FID using relative peak areas versus the internal standard.

[(MeOTTM)Ru(P(OCH$_2$)$_3$CEt)(NCMe)Ph]Br (6). The complex (η^6-*p*-cymene)Ru(P(OCH$_2$)$_3$CEt)(Br)Ph (0.55 g, 1.0 mmol) was dissolved in NCMe (20 mL), added to a pressure tube, and heated for 3.5 h at 70 °C. The reaction was allowed to cool to room temperature. The mixture was filtered through Celite, and the filtrate was concentrated to dryness yielding the putative complex (NCMe)$_3$Ru(P(OCH$_2$)$_3$CEt)(Br)Ph.[3] The resulting solid was taken up in CH_2Cl_2 (10 mL) and added to a 50 mL thick-wall glass pressure tube with MeOTTM (0.57 g, 1.1 mmol) in CH_2Cl_2 (10 mL). The solution was heated to 70 °C for 15 h after which it was cooled to room temperature and filtered through Celite. The volatiles were removed from the filtrate under reduced pressure. Benzene was added, and the mixture was stirred for 10 min. The solution was filtered through Celite, and the filtrate was discarded. The remaining white solid was dissolved in CH_2Cl_2 and filtered through Celite. The filtrate was concentrated to 2 mL, and hexanes were added to induce precipitation. The colorless precipitate was collected on a fine porosity frit. The

solid was washed with pentane and dried *in vacuo* to yield a tan solid (73%). ^{1}H NMR (600 MHz, CD_2Cl_2) δ 8.38 (s, 1H, *triazole-H*), 8.36 (s, 1H, *triazole-H*), 8.21 (s, 1H, *triazole-H*), 7.38-7.29 (m, 15H, phenyl form benzyl), 6.91 (d, $^{3}J_{HH}$ = 7 Hz, 2H, phenyl *ortho-H*), 6.83-6.76 (m, 3H, phenyl *meta* and *para-H*), 5.65 (m, 1H, -CH_2-), 5.59-5.54 (m, 2H, -CH_2-), 5.53 (s, 1H, -CH_2-), 5.50 (s, 1H, -CH_2-), 5.46 (s, 1H, -CH_2-), 4.19-4.11 (m, 6H, P(OCH_2)$_3$CCH$_2$CH$_3$), 4.07 (s, 3H, -OCH_3), 2.30 (s, 3H, NCMe), 1.20 (q, $^{3}J_{HH}$ = 8 Hz, 2H, P(OCH$_2$)$_3$CCH_2CH$_3$), 0.83 (t, $^{3}J_{HH}$ = 8 Hz, 3H, P(OCH$_2$)$_3$CCH$_2$CH_3).^{31}P{^{1}H} NMR (121 MHz, CD_2Cl_2) δ 134.7. Anal. Calcd for $C_{43}H_{46}O_4N_{10}PBrRu$: C, 52.18; H, 4.80; N, 14.49. Found: C, 52.43; H, 4.92; N, 14.51.

[(MeOTTM)Ru(P(OCH$_2$)$_3$CEt)(NCMe)Ph][BAr'$_4$] (7). The Ru(II) complex (MeOTTM)Ru(P(OCH$_2$)$_3$CEt)(NCMe)Ph]Br (**6**) (0.978 g, 0.300 mmol) was suspended in THF (10 mL) in a round bottom flask to form a heterogeneous mixture. NaBAr'$_4$ (0.270, 0.303 mmol) dissolved in THF (5 mL) was slowly added, resulting in a colorless homogenous solution. The reaction was stirred at room temperature for 2.5 h during which time it turned from colorless to grey. The solution was filtered through Celite, and the filtrate was concentrated to dryness. The resulting solid was reconstituted in Et_2O and filtered through Celite. The filtrate was concentrated to dryness to yield a golden solid. The golden solid was reconstituted in benzene and filtered through Celite. The filtrate was concentrated to dryness to yield a golden foam solid (53%). ^{1}H NMR (600 MHz, CD_2Cl_2) δ 7.74 (br s, 8H, BAr'$_4$, *ortho-H*), 7.64 (s, 1H, *triazole-H*), 7.63 (s, 1H, *triazole-H*), 7.59 (s, 1H, t*riazole-H*), 7.57 (br s, 4H, BAr'$_4$, *para-H*), 7.38-7.31 (m, 6H, phenyl), 7.24-7.23 (m,

4H, phenyl), 6.95-6.94 (m, 2H, phenyl *ortho-H*), 6.87-6.83 (m, 3H, phenyl *meta* and *para-H*), 5.63 (d, $^{2}J_{HH}$ = 15 Hz, 2H, -C*H*$_2$-), 5.56 (d, $^{2}J_{HH}$ = 15 Hz, 2H, -C*H*$_2$-), 5.51 (d, $^{2}J_{HH}$ = 14 Hz, 2H, -C*H*$_2$-), 5.43 (m, 5H), 4.21 (m, 6H, P(OC*H*$_2$)$_3$CCH$_2$CH$_3$), 3.86 (s, 3H,-OCH$_3$), 2.33 (s, 3H, NCMe), 1.21 (q, 2H, $^{3}J_{HH}$ = 8 Hz, P(OCH$_2$)$_3$CC*H*$_2$CH$_3$), 0.84 (t, 3H, $^{3}J_{HH}$ = 8 Hz, P(OCH$_2$)$_3$CCH$_2$C*H*$_3$). ^{13}C NMR (151 MHz, CD_2Cl_2) δ 166.8 (d, $^{2}J_{CP}$ = 17 Hz, ipso of phenyl), 162.8, 162.5 , 162.2, 161.8 (four line pattern, $^{1}J_{CB}$ = 50 Hz, BAr'$_4$), 145.8, 145.8, 145.6, 142.4, 134.0 , 133.8, 129.9-129.6 (m) (each a s, phenyl groups of benzyl substituents), 135.4 (s, BAr'$_4$), 128.9 (d, $^{2}J_{CP}$ = 7 Hz), 126.1, 125.8, 124.3 (each a s,triazole-H), 121.1-120.9 (m, -*C*H$_2$-), 118.1 (s, N*C*CH$_3$), 74.6 (d, $^{2}J_{CP}$ = 7 Hz, P(O*C*H$_2$)$_3$CCH$_2$CH$_3$), 56.3-56.1 (m), 55.6 (s, -OCH$_3$), 35.8 (d, $^{3}J_{CP}$ = 31Hz, P(OCH$_2$)$_3$*C*CH$_2$CH$_3$), 24.1 (s, P(OCH$_2$)$_3$C*C*H$_2$CH$_3$), 7.5 (s, P(OCH$_2$)$_3$CCH$_2$*C*H$_3$), 4.9 (s, NC*C*H$_3$). ^{31}P{^{1}H} NMR (121 MHz, CD_2Cl_2) δ 134.6. ^{19}F NMR (282 MHz, CD_2Cl_2) δ -62.9. CV (NCMe): $E_{1/2}$ = 0.86 V. Anal. Calcd for $C_{75}H_{58}BO_4N_{10}PF_{24}Ru$: C, 51.12; H, 3.22; N, 7.95. Found: C, 50.88; H, 3.46; N, 8.17.

[(PhTTM)Ru(P(OCH$_2$)$_3$CEt)(NCMe)Ph]Br (8). Following the above procedure for [(MeOTTM)Ru(P(OCH$_2$)$_3$CEt)(NCMe)Ph]Br (**6)** and using PhTMM, **8** was obtained as a white powder (44% yield). ^{1}H NMR (600 MHz, CD_2Cl_2) δ 8.86 (s, 1H, *triazole-H*), 8.75 (s, 1H, *triazole-H*), 8.64 (s, 1H, *triazole-H*), 7.83-7.39 (m, 15H, phenyl from benzyl), 7.26 (d, $^{3}J_{HH}$= 7.4 Hz, 2H, phenyl *ortho-H*), 6.82 (t, $^{3}J_{HH}$ = 7.3 Hz, 2H, phenyl *meta-H*), 6.75 (t, $^{3}J_{HH}$ = 7.1 Hz, 1H, phenyl *para-H*), 4.27 (dt, $^{2}J_{HH}$ = 6.3, 2.8 Hz, 6H, P(OC*H*$_2$)$_3$CCH$_2$CH$_3$), 2.32 (s, 3H, NCMe), 1.21 (d, $^{3}J_{HH}$ = 8 Hz, 2H, P(OCH$_2$)$_3$CC*H*$_2$CH$_3$), 0.82 (t, $^{3}J_{HH}$ = 8 Hz,

3H, $P(OCH_2)_3CCH_2CH_3$). $^{31}P\{^1H\}$ NMR (121 MHz, CD_2Cl_2) δ 134.6. Anal. Calcd for $C_{39}H_{38}O_4N_{10}PBrRu$: C, 50.76; H, 4.15; N, 15.18. Found: C, 51.82; H, 4.15; N, 16.26.

Catalytic Oxidative Hydrophenylation of Ethylene using [(MeOTTM)Ru(P(OCH$_2$)$_3$CEt)(NCMe)Ph][BAr'$_4$] (7). A representative catalytic reaction is described. A stock solution containing **7** (0.040 g, 0.023 mmol), decane (88 μL, 0.46 mmol), and benzene (200 mL) was prepared in a volumetric flask. Thick-walled Fisher-Porter reactors were charged with stock solution (10 mL). The vessels were sealed, pressurized with ethylene (40 psig), and subsequently stirred and heated to 150 °C. The reaction was sampled every 1 h for the first 2 h, then every 2 h. At each time point, the reactors were cooled to room temperature, sampled, recharged with ethylene (40 psig), and heated. Aliquots of the reaction mixture were analyzed by GC/FID using relative peak areas versus the internal standard.

Catalytic Oxidative Hydrophenylation of Ethylene using [(MeOTTM)Ru(P(OCH$_2$)$_3$CEt)(NCMe)Ph][BAr'$_4$] (7) under Different Ethylene Pressure. A stock solution containing [(MeOTTM)Ru(P(OCH$_2$)$_3$CEt)(NCMe)Ph][BAr'$_4$] (**7**) (0.001 mol % relative to benzene), decane (20 equiv. relative to [(MeOTTM)Ru(P(OCH$_2$)$_3$CEt)(NCMe)Ph][BAr'$_4$]), and benzene (200 mL) was prepared in a volumetric flask. Thick-walled Fisher-Porter reactors were charged with stock solution (10 mL). The vessels were sealed, charged with ethylene (15, 25, 40, 50, or 75 psig, 3 reactors at each pressure), and subsequently stirred and heated to 150 °C. The reaction was sampled every 1 h for 6 h. At each time point, the reactors were cooled to room temperature,

sampled, recharged with ethylene pressure, and reheated. Aliquots of the reaction mixture were analyzed by GC/FID using relative peak areas versus the internal standard (decane).

Degenerate $NCCH_3/NCCD_3$ Exchange for [(MeOTTM)Ru(P(OCH$_2$)$_3$CEt)(NCMe)Ph][BAr'$_4$] (7). In a 1 mL volumetric flask **7** (0.054 g) was dissolved in CD_3CN. A small crystal of hexamethylbenzene was added as an internal standard. The solution was divided between three J. Young NMR tubes (300 μL per tube). ^{1}H NMR spectra were taken every 15 minutes. Each spectrum required 2 minutes to complete. Eight scans were acquired for each spectrum. The delay time was set to 12.8 s, and the acquisition time was set to 2.2 s. The exchange reaction was repeated at 70 °C, 90 °C and 110 °C with NMR tubes heated in a temperature-controlled oil baths. ^{1}H NMR spectra using a 12.8 s pulse delay time were acquired periodically. All reactions were monitored through at least three half-lives.

Kinetic Isotope Effect Experiments. A stock solution containing [(MeOTTM)Ru(P(OCH$_2$)$_3$CEt)(NCMe)Ph][BAr'$_4$] (**7**) (0.001 mol % relative to benzene) and a 1:1 molar mixture of C_6H_6 and C_6D_6 (30 mL) was prepared in a volumetric flask. Thick-walled Fisher-Porter reactors were charged with stock solution (10 mL). The vessels were sealed, charged with ethylene (40 psig), and subsequently stirred and heated to 150 °C. The reaction was sampled at 1, 2, and 4 h. At each time point, the reactors were cooled to room temperature, sampled, recharged with ethylene, and reheated. Aliquots of the reaction mixture were analyzed by GC/MS. The KIE was determined by examining the ratio of styrene (m/z = 104) to styrene-d_5 (m/z = 109) in the mass spectrum, accounting for the

initial isotopic distribution and natural abundance. No change in the isotopic distribution for benzene was observed over the course of the reaction, and the observed isotopic distribution of product was consistent with the initial distribution. No $d_{6\text{-}8}$ products were observed, except those predicted by the natural abundance of deuterium in ethylene.

2.8 References

1. Foley, N. A.; Lee, J. P.; Ke, Z.; Gunnoe, T. B.; Cundari, T. R., Ru(II) catalysts supported by hydridotris(pyrazolyl)borate for the hydroarylation of olefins: reaction scope, mechanistic studies, and guides for the development of improved catalysts. *Acc. Chem. Res.* **2009,** *42* (5), 585-597.
2. Foley, N. A.; Lail, M.; Gunnoe, T. B.; Cundari, T. R.; Boyle, P. D.; Petersen, J. L., Combined Experimental and Computational Study of TpRu{P(pyr)3}(NCMe)Me (pyr =N-pyrrolyl): Inter- and Intramolecular Activation of C−H Bonds and the Impact of Sterics on Catalytic Hydroarylation of Olefins. *Organometallics* **2007,** *26* (23), 5507-5516.
3. Foley, N. A.; Lail, M.; Lee, J. P.; Gunnoe, T. B.; Cundari, T. R.; Petersen, J. L., Comparative reactivity of TpRu(L)(NCMe)Ph (L = CO or PMe3): impact of ancillary ligand l on activation of carbon-hydrogen bonds including catalytic hydroarylation and hydrovinylation/oligomerization of ethylene. *J. Am. Chem. Soc.* **2007,** *129* (21), 6765-6781.
4. Joslin, E. E.; McMullin, C. L.; Gunnoe, T. B.; Cundari, T. R.; Sabat, M.; Myers, W. H., Catalytic Hydroarylation of Ethylene Using TpRu(L)(NCMe)Ph (L = 2,6,7-Trioxa-1-phosphabicyclo[2,2,1]heptane): Comparison to TpRu(L′)(NCMe)Ph Systems (L′ = CO, PMe3, P(pyr)3, or P(OCH2)3CEt). *Organometallics* **2012,** *31* (19), 6851-6860.
5. Lail, M.; Arrowood, B. N.; Gunnoe, T. B., Addition of arenes to ethylene and propene catalyzed by ruthenium. *J. Am. Chem. Soc.* **2003,** *125* (25), 7506-7507.

6. Burgess, S. A.; Joslin, E. E.; Gunnoe, T. B.; Cundari, T. R.; Sabat, M.; Myers, W. H., Hydrophenylation of ethylene using a cationic Ru(ii) catalyst: comparison to a neutral Ru(ii) catalyst. *Chem. Sci.* **2014,** *5* (11), 4355-4366.
7. Joslin, E. E.; Quillian, B.; Gunnoe, T. B.; Cundari, T. R.; Sabat, M.; Myers, W. H., C-H activation of pyrazolyl ligands by Ru(II). *Inorg. Chem.* **2014,** *53* (12), 6270-6279.
8. Ozkal, E.; Llanes, P.; Bravo, F.; Ferrali, A.; Pericàs, M. A., Fine-Tunable Tris(triazolyl)methane Ligands for Copper(I)- Catalyzed Azide-Alkyne Cycloaddition Reactions. *Adv. Synth. Catal.* **2014,** *356* (4), 857-869.
9. Wang, D.; Etienne, L.; Echeverria, M.; Moya, S.; Astruc, D., A highly active and magnetically recoverable tris(triazolyl)-Cu(I) catalyst for alkyne-azide cycloaddition reactions. *Chem. Eur. J* **2014,** *20* (14), 4047-4054.
10. Chen, H.; Hou, S.; Tan, Y., An 'in-water' halogen-ion compatible "click" catalyst for cucurbituril guest ligation. *Supramol. Chem.* **2016,** *28* (9-10), 801-809.
11. Arikawa, Y.; Yamaguchi, S.; Haige, R.; Oshiro, E.; Umakoshi, K.; Onishi, M., Methylation of a nitrosylruthenium complex bearing a hydridotris(pyrazolyl)borate ligand. *J. Organomet. Chem.* **2014,** *755*, 12-15.
12. Onishi, M., Syntheses and Spectral Properties of New Nitrosyl-[poly(1-pyrazolyl)borato]ruthenium Complexes. *Bull. Chem. Soc. Jpn.* **1991,** *64* (10), 3039-3045.
13. Chang, J.; Bergman, R. G., Reductive elimination leading to transient (. eta. 5-C5Me5) Ru (NO). Trapping, dimerization and oxidative addition reactions of this intermediate

and the effect of structural variation on its generation. *J. Am. Chem. Soc.* **1987,** *109* (14), 4298-4304.

14. Caballero, A.; Díaz-Requejo, M. M.; Belderraín, T. R.; Nicasio, M. C.; Trofimenko, S.; Pérez, P. J., Highly Regioselective Functionalization of Aliphatic Carbon−Hydrogen Bonds with a Perbromohomoscorpionate Copper(I) Catalyst. *J. Am. Chem. Soc.* **2003,** *125* (6), 1446-1447.
15. Dias, H. V. R.; Lovely, C. J., Carbonyl and Olefin Adducts of Coinage Metals Supported by Poly(pyrazolyl)borate and Poly(pyrazolyl)alkane Ligands and Silver Mediated Atom Transfer Reactions. *Chem. Rev.* **2008,** *108* (8), 3223-3238.
16. Bongiovanni, J. L.; Rowe, B. W.; Fadden, P. T.; Taylor, M. T.; Wells, K. R.; Kumar, M.; Papish, E. T.; Yap, G. P. A.; Zeller, M., Synthesis, structural studies and solubility properties of zinc(II), nickel(II) and copper(II) complexes of bulky tris(triazolyl)borate ligands. *Inorganica Chimica Acta* **2010,** *363* (10), 2163-2170.
17. Gardner, S. R.; Papish, E. T.; Monillas, W. H.; Yap, G. P. A., Tris(triazolyl)borate ligands of intermediate steric bulk for the synthesis of biomimetic structures with hydrogen bonding and solubility in hydrophilic solvents. *J. Inorg. Bio.* **2008,** *102* (12), 2179-2183.
18. Jernigan, F. E.; Sieracki, N. A.; Taylor, M. T.; Jenkins, A. S.; Engel, S. E.; Rowe, B. W.; Jové, F. A.; Yap, G. P. A.; Papish, E. T.; Ferrence, G. M., Sterically Bulky Tris(triazolyl)borate Ligands as Water-Soluble Analogues of Tris(pyrazolyl)borate. *Inorg. Chem.* **2007,** *46* (2), 360-362.

19. Kumar, M.; Papish, E. T.; Zeller, M.; Hunter, A. D., Zinc complexes of TtzR,Me with O and S donors reveal differences between Tp and Ttz ligands: acid stability and binding to H or an additional metal (TtzR,Me = tris(3-R-5-methyl-1,2,4-triazolyl)borate; R = Ph, tBu). *Dalton Trans.* **2011,** *40* (29), 7517-7533.

20. Papish, E. T.; Donahue, T. M.; Wells, K. R.; Yap, G. P. A., How are tris(triazolyl)borate ligands electronically different from tris(pyrazolyl)borate ligands? A study of (TtztBu,Me)CuCO [TtztBu,Me = tris(3-t-butyl-5-methyl-1,2,4-triazolyl)borate]. *Dalton Trans.* **2008,** (22), 2923-2925.

21. Dixon, N. A.; McQuarters, A. B.; Kraus, J. S.; Soffer, J. B.; Lehnert, N.; Schweitzer-Stenner, R.; Papish, E. T., Dramatic tuning of ligand donor properties in (Ttz)CuCO through remote binding of H+ (Ttz = hydrotris(triazolyl)borate). *Chem. Comm.* **2013,** *49* (49), 5571-5573.

22. Muller, P., Glossary of terms used in physical organic chemistry (IUPAC Recommendations 1994). *Pure Appl. Chem.* **1994,** *66* (5), 1077-1184.

23. Anderson, J. E., Conformational analysis of cyclohexane derivatives. The A value of a benzyl group. *Journal of the Chemical Society, Perkin Transactions 2* **1974,** (1), 10-13.

24. Vaughan, B. A.; Webster-Gardiner, M. S.; Cundari, T. R.; Gunnoe, T. B., Organic chemistry. A rhodium catalyst for single-step styrene production from benzene and ethylene. *Science* **2015,** *348* (6233), 421-424.

25. Vaughan, B. A.; Khani, S. K.; Gary, J. B.; Kammert, J. D.; Webster-Gardiner, M. S.; McKeown, B. A.; Davis, R. J.; Cundari, T. R.; Gunnoe, T. B., Mechanistic Studies of

Single-Step Styrene Production Using a Rhodium(I) Catalyst. *J. Am. Chem. Soc.* **2017,** *139* (4), 1485-1498.

26. Webster-Gardiner, M. S.; Chen, J.; Vaughan, B. A.; McKeown, B. A.; Schinski, W.; Gunnoe, T. B., Catalytic Synthesis of "Super" Linear Alkenyl Arenes Using an Easily Prepared Rh(I) Catalyst. *J. Am. Chem. Soc.* **2017,** *139* (15), 5474-5480.
27. McKeown, B. A.; Gonzalez, H. E.; Friedfeld, M. R.; Brosnahan, A. M.; Gunnoe, T. B.; Cundari, T. R.; Sabat, M., Platinum(II)-Catalyzed Ethylene Hydrophenylation: Switching Selectivity between Alkyl- and Vinylbenzene Production. *Organometallics* **2013,** *32* (9), 2857-2865.
28. Foley, N. A.; Ke, Z.; Gunnoe, T. B.; Cundari, T. R.; Petersen, J. L., Aromatic C−H Activation and Catalytic Hydrophenylation of Ethylene by TpRu{P(OCH2)3CEt}(NCMe)Ph. *Organometallics* **2008,** *27* (13), 3007-3017.
29. Frisch, M. J.; Trucks, G. W.; Schlegel, H. B.; Scuseria, G. E.; Robb, M. A.; Cheeseman, J. R.; Scalmani, G.; Barone, V.; Mennucci, B.; Petersson, G. A.; Nakatsuji, H.; Caricato, M.; Li, X.; Hratchian, H. P.; Izmaylov, A. F.; Bloino, J.; Zheng, G.; Sonnenberg, J. L.; Hada, M.; Ehara, M.; Toyota, K.; Fukuda, R.; Hasegawa, J.; Ishida, M.; Nakajima, T.; Honda, Y.; Kitao, O.; Nakai, H.; Vreven, T.; Montgomery, J. A.; Peralta, J. E.; Ogliaro, F.; Bearpark, M.; Heyd, J. J.; Brothers, E.; Kudin, K. N.; Staroverov, V. N.; Kobayashi, R.; Normand, J.; Raghavachari, K.; Rendell, A.; Burant, J. C.; Iyengar, S. S.; Tomasi, J.; Cossi, M.; Rega, N.; Millam, J. M.; Klene, M.; Knox, J. E.; Cross, J. B.; Bakken, V.; Adamo, C.; Jaramillo, J.; Gomperts, R.; Stratmann, R. E.; Yazyev, O.; Austin, A. J.;

Cammi, R.; Pomelli, C.; Ochterski, J. W.; Martin, R. L.; Morokuma, K.; Zakrzewski, V. G.; Voth, G. A.; Salvador, P.; Dannenberg, J. J.; Dapprich, S.; Daniels, A. D.; Farkas; Foresman, J. B.; Ortiz, J. V.; Cioslowski, J.; Fox, D. J., Gaussian 09, Revision B.01. Wallingford CT, 2009.

30. Becke, A. D., Density-functional exchange-energy approximation with correct asymptotic behavior. *Phys Rev A Gen Phys* **1988,** *38* (6), 3098-3100.
31. Lee, C.; Yang, W.; Parr, R. G., Development of the Colle-Salvetti correlation-energy formula into a functional of the electron density. *Phys Rev B Condens Matter* **1988,** *37* (2), 785-789.
32. Marenich, A. V.; Cramer, C. J.; Truhlar, D. G., Universal solvation model based on solute electron density and on a continuum model of the solvent defined by the bulk dielectric constant and atomic surface tensions. *J. Phys. Chem. B* **2009,** *113* (18), 6378-6396.
33. Grimme, S.; Ehrlich, S.; Goerigk, L., Effect of the damping function in dispersion corrected density functional theory. *J. Comput. Chem.* **2011,** *32* (7), 1456-1465.
34. Yakelis, N. A.; Bergman, R. G., Safe Preparation and Purification of Sodium Tetrakis [(3, 5-trifluoromethyl) phenyl] borate (NaBArF24): Reliable and Sensitive Analysis of Water in Solutions of Fluorinated Tetraarylborates. *Organometallics* **2005,** *24* (14), 3579-3581.

35. Lühder, K.; Nehls, D.; Madeja, K., A SIMPLE METHOD FOR THE PREPARATION OF DIALKYL-MAGNESIUMORGANO OR DIARYLMAGNESIUMORGANO COMPOUNDS. *JOURNAL FUR PRAKTISCHE CHEMIE* **1983,** *325* (6), 1027-1029.

3 Study of Palladium Catalysts for the Oxidative Alkenylation of Benzene

This chapter is adapted from Jia, X., Foley, A. M., Liu, C., Vaughan, B. A., McKeown, B. A., Zhang, S., & Gunnoe, T. B. Styrene Production from Benzene and Ethylene Catalyzed by Palladium (II): Enhancement of Selectivity toward Styrene via Temperature-dependent Vinyl Ester Consumption. Organometallics **2019**, *38,* 3532-3541. *Copyright 2019 American Chemical Society*

3.1 Introduction

3.1.1 Fujiwara-Moritani reaction

The Fujiwara–Moritani reaction, which was discovered by Yuzo Fujiwara and Ichiro Moritani in 1967, is a type of cross coupling reaction where an aromatic C–H bond is directly coupled to an olefinic C–H bond, generating a new C–C bond. This reaction is performed in the presence of a transition metal, typically palladium.[1-3] Although the mechanism of this reaction is not fully elucidated, a general mechanism that is widely accepted is shown in Scheme 3.1

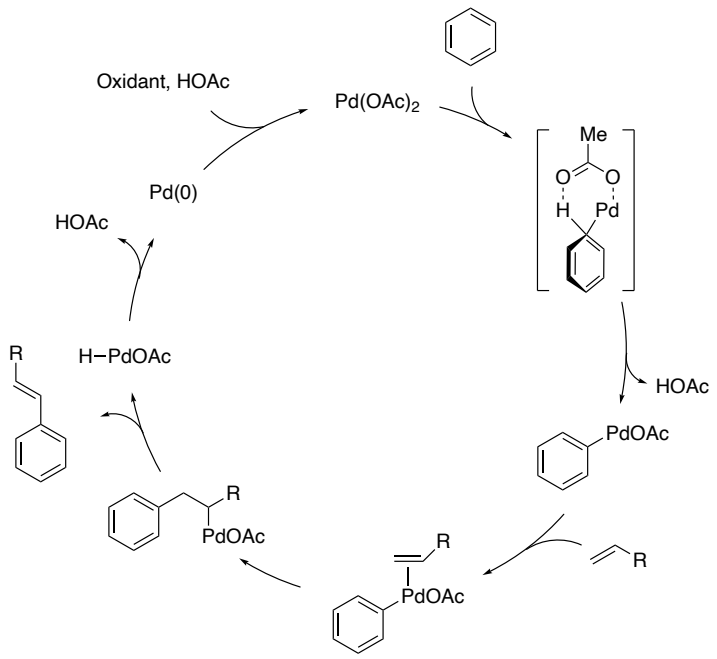

Scheme 3.1. Proposed catalytic cycle for Fujiwara-Moritani reaction.

The catalytic cycle begisn with the formation of a Pd–Ar bond via concerted deprotonation metalation process and produces one equivalent of acetic acid,[4] then a olefin is coordinated to the palladium and undergoes a migratory insertion to form a Pd–phenethyl species. Next, β-hydride elimination produces an alkenyl arene and palladium hydride. To recover the active catalyst, oxidation of Pd occurs, which is often proposed to involve the oxidation of Pd(0) to Pd(II).

The Fujiwara-Monritani reaction has traditionally been limited in substrate scope, as directing groups on the arene are often required.[5-17] Direct arene alkenylation using unactivated arenes and olefins (*e.g.*, benzene, toluene, ethylene, propylene, etc.) remains challenging with regard to selectivity, reaction rate and catalyst longevity. Examples of transition metal-based catalysts for arene alkylation of simple hydrocarbon substrates

include Pt,[18-27] Ru[28-37] and Ir.[38-40] In addition, catalytic oxidative arene alkenylation using Rh and Pd precursors has been reported.[41-44]

3.1.2 Olefin hydroarylation catalyzed by $Pd(OAc)_2$

Palladium(II) has a similar electronic structure as Rh(I) and can also catalyze oxidative hydroarylation of olefins, but selectivity is often low, as undesired products can dominate. Fujiwara and coworkers reported styrene production using $Pd(OAc)_2$ with AgOAc as the oxidant. This reaction produced a low yield (0.59 TOs) of styrene relative to the catalyst along with substantial amounts of stilbene and biphenyl.[1] Periana and coworkers reported styrene production using $Pd(OAc)_2$ with $Cu(OAc)_2$ and O_2 as the terminal oxidant, but they observed significant vinyl acetate production (~2.5 times the amount of styrene produced).[41, 45] This observation was perhaps not surprising, since Pd(II) is known to catalyze ethylene oxidation using $CuCl_2$ as an oxidant in commercial processes.[46-50] Sanford and coworkers reported that (3,5-dichloropyridyl)$Pd(OAc)_2$ affords styrene from benzene and ethylene with 100% selectivity; however, the process suffered from low yields (~33% relative to the limiting oxidant reagent) and used an expensive oxidant ($PhCO_3{}^tBu$) that cannot be regenerated aerobically.[51]

In this chapter, we report studies on the conversion of benzene and ethylene to styrene catalyzed by $Pd(OAc)_2$ with the air-recyclable oxidant $Cu(OPiv)_2$ (Piv = pivalate). The effects of olefin pressure, temperature, acid concentration, copper(II) loading, water and dioxygen on the reactivity and selectivity have been investigated. Under optimized

conditions, selectivity for benzene vinylation with high efficiency for aerobic oxidant recycling has been achieved. We propose that the conversion of benzene and vinyl pivalate, formed from ethylene and $Cu(OPiv)_2$, to styrene is central to the high selectivity for styrene formation.

3.2 Oxidative ethylene hydrophenylation catalyzed by palladium(II) acetate under anaerobic conditions

3.2.1 Induction period

For all reported experiments, the data provided are the average of at least three independent experiments with standard deviations given in parentheses. Heating 5 mL of 0.001 mol% $Pd(OAc)_2$ in a benzene solution with 240 equiv. of copper(II) pivalate under 45 psig of ethylene in a high pressure reactor, resulted in the formation of styrene and vinyl pivalate. Every 30 min, the reactors were cooled, sampled and analyzed on GC-FID, TOs were calculated relative to an internal standard, hexamethylbenzene, based on a calibration curve.

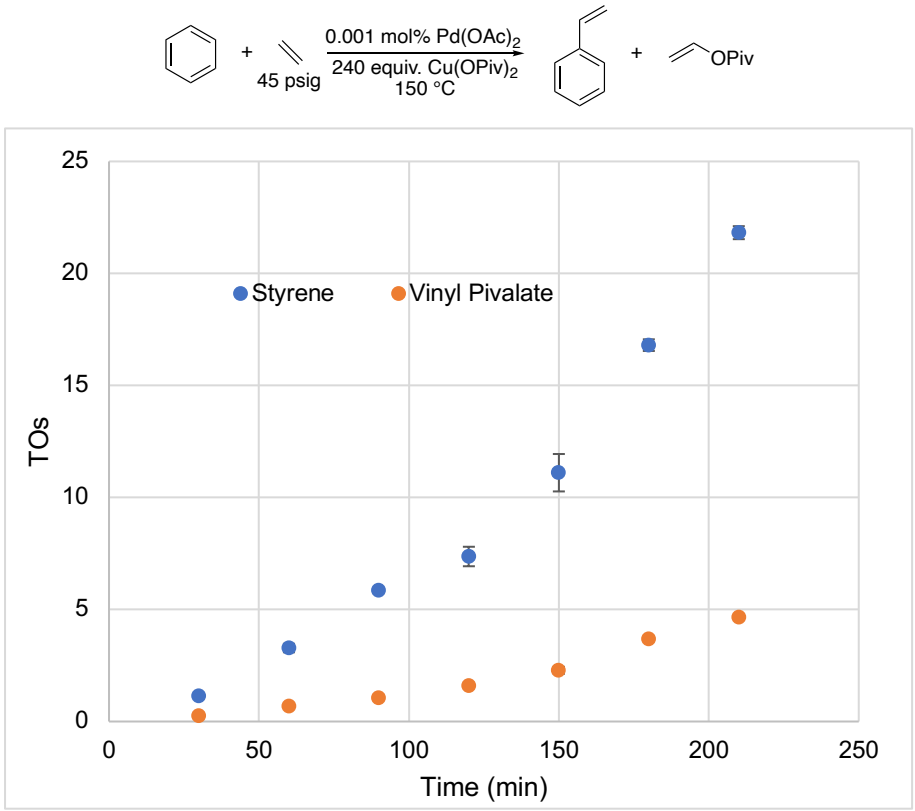

Figure 3.1. Turnovers of styrene versus time plot for anaerobic benzene ethenylation catalyzed by $Pd(OAc)_2$ with stoichiometric amount of $Cu(OPiv)_2$.

As shown in Figure 3.1, for both styrene and vinyl pivalate, an induction period was observed before entering the linear production region. Under the conditions describe above, the induction period was approximately 2 hours long. This observation of the induction period is consistent with our previous anaerobic Rh catalysis.

3.2.2 Influence of reaction temperature and olefin pressure on catalysis

The use of $Pd(OAc)_2$ as a catalyst precursor for oxidative ethylene hydrophenylation was investigated under various temperatures and ethylene pressures under anaerobic conditions (Figure 3.2). Under a dinitrogen atmosphere,10 mL benzene solutions of

$Pd(OAc)_2$ (0.001 mol% relative to benzene) with 240 equivalents of $Cu(OPiv)_2$ were heated at different temperatures (120-180 °C) and ethylene pressures (20-60 psig), which affords styrene production. Two equivalents of $Cu(OPiv)_2$ were required per equivalent of styrene; therefore, using 240 equivalents of $Cu(OPiv)_2$ the maximum theoretical turnovers for styrene production is 120 in the absence of oxidative regeneration of $Cu(OPiv)_2$. The catalytic reactions produced styrene, vinyl pivalate and stilbene. Under optimized conditions at 150 °C, 94% selectivity for styrene was obtained (Table 3.1). Using higher reaction temperature and ethylene pressure required less time for the reaction to reach completion, which was consistent with our observations for Rh catalyzed processes.[43, 44, 52] The selectivity for vinyl pivalate versus styrene varied with reaction conditions. As shown in Figure 3.2, the formation of styrene increased from 120 °C to 150 °C, but the production of styrene was reduced at 180 °C. There are two apparent issues at 180 °C: 1) the selectivity for stilbene was increased with ~10-fold more stilbene than observed at 150 °C, and 2) lower overall yields of all oxidation products were observed at 180 °C. At 150 °C and 20 psig of ethylene, a total of ~ 120 TOs were observed, while under the same ethylene pressure at 180 °C (entry 7) ~70 TOs were observed. The amount of vinyl pivalate increased with increasing ethylene pressure. For example, entries 1, 2 and 3 were using the same reaction temperature (120 °C) and varying pressures of ethylene; the reaction which used the highest ethylene pressure (60 psig) produced 142% more vinyl pivalate than at 20 psig of ethylene. When higher temperature was applied to the reaction systems (*e.g.*, entries

2, 5 and 8), the production of vinyl pivalate decreased by 96% with 25(3) TOs at 120 °C, 4.5(5) TOs at 150 °C and only 1.0(3) at 180 °C.

Table 3.1. Ethylene hydrophenylation under anaerobic conditions using $Pd(OAc)_2$ as a catalyst precursor and $Cu(OPiv)_2$ as the oxidant.

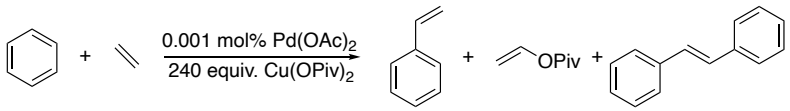

Entry[a]	Temperature (°C)	Ethylene Pressure (psig)	Time[b] (hours)	Styrene (TOs)	Vinyl pivalate (TOs)	Stilbene[c] (TOs)	Selectivity (% Styrene)
1	120	20	16	121(5)	14(1)	2(1)	88%
2	120	40	10	117(3)	25(3)	0.5(2)	82%
3	120	60	8	102.2(2)	34(1)	0.32(1)	77%
4	150	20	2	114(8)	3.6(5)	3.5(3)	94%
5	150	40	2	112(1)	4.5(5)	3.0(5)	94%
6	150	60	1	121(2)	10.9(6)	1.2(1)	91%
7	180	20	0.5	38(5)	0.2(1)	33(4)	51%
8	180	40	0.5	51(7)	1.0(3)	23(1)	67%
9	180	60	0.5	78(3)	2.5(2)	15(2)	84%

[a] Conditions: 0.001 mol % of $Pd(OAc)_2$ dissolved in 10 mL of benzene with HMB (hexamethylbenzene) as an internal standard, 240 equivalents (relative to Pd) of copper(II) pivalate are used. [b] The end point of reactions were determined by the color of the reaction mixture, the color change from blue to light brown indicates consumption of the Cu(II) oxidant (see Supporting Information). [c] Stilbene indicates *trans*-stilbene. The numbers in parentheses are standard deviations that are based on at least three independent experiments.

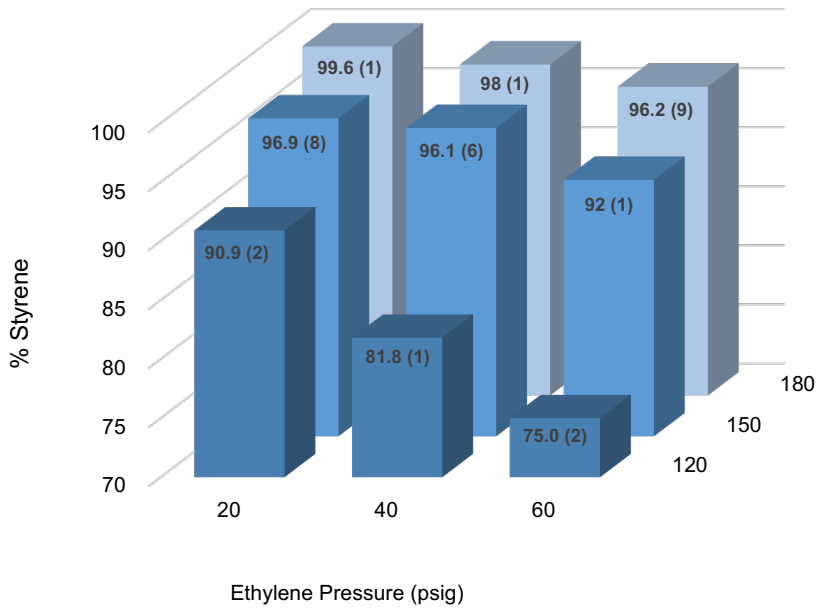

Figure 3.2. Selectivity for styrene production from oxidative ethylene hydrophenylation catalyzed by $Pd(OAc)_2$ as a function of temperature and ethylene pressure. Conditions: 0.001 mol % of $Pd(OAc)_2$ dissolved in 10 mL of benzene with HMB (hexamethylbenzene) as an internal standard and 240 equivalents (relative to Pd) of copper(II) pivalate are used. Percent styrene is the percentage of styrene versus vinyl pivalate production. The numbers in parentheses are standard deviations that are based on at least three independent experiments.

The influence of olefin pressure on stilbene production was investigated at 180 °C where vinyl pivalate production is negligible. As shown in Figure 3.3, the production of stilbene was highly dependent on ethylene pressure. The ratio of styrene versus stilbene increased dramatically when temperature was increased from 120 °C to 180 °C. Since stilbene is likely produced by the oxidative hydroarylation of styrene formed *in situ*, the dissociation of styrene from the Pd catalyst might play a key role in determining the styrene/stilbene ratio. As shown in Scheme 3.2, it is possible that the dissociation of styrene via ligand exchange with ethylene is important to minimize stilbene formation since the

ethylene/styrene exchange reaction likely depends on the concentration of ethylene. At higher temperature and lower ethylene pressure, the concentration of ethylene decreased,[53] which led to more stilbene production.

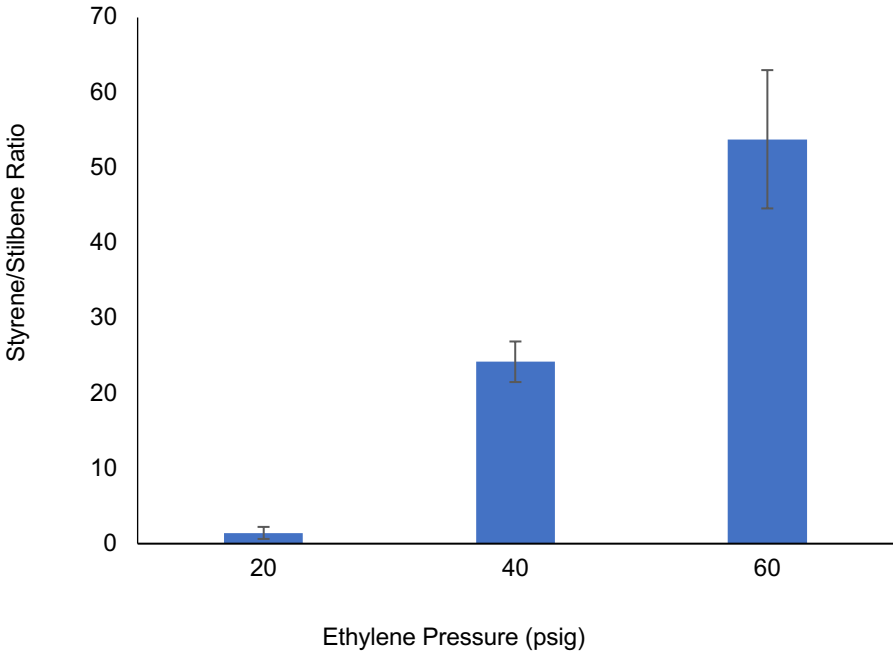

Figure 3.3. The ratio of styrene versus stilbene as a function of ethylene pressure at 180 °C. Conditions: 10 mL benzene solution of 0.001 mol% $Pd(OAc)_2$, 240 equivalent of $Cu(OPiv)_2$, 20, 40 or 60 psig ethylene, 180 °C for 30 minutes. Error bars represent standard deviations from at least three independent experiments.

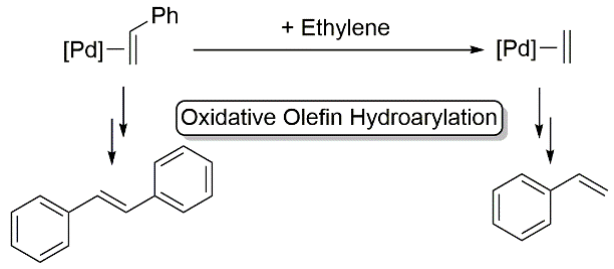

Scheme 3.2. Olefin exchange reaction between ethylene and styrene and subsequent olefin hydroarylation products. A higher ethylene concentration should facilitate styrene dissociation and reduce stilbene production.

3.2.3 Effect of Additives

It has been reported that the addition of carboxylate acid can enhance the catalytic performance of Rh catalyzed olefin hydroarylation reaction under both anaerobic and aerobic conditions by increasing the solubility of the copper salt and suppress the hydrolysis of Cu(II). The influence of additional pivalic acid was further investigated.

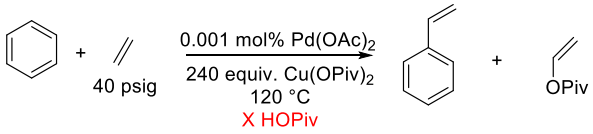

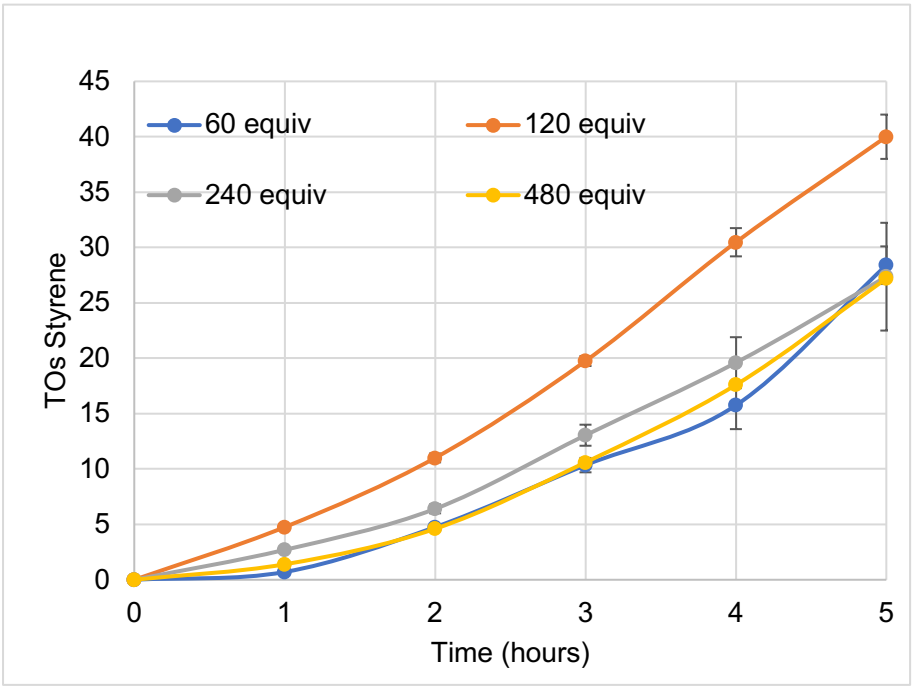

Figure 3.4. Turnovers of hydroarylation products versus time plot of anaerobic arene alkenylation catalyzed by $Pd(OAc)_2$ with stoichiometric amount of copper oxidant.

Figure 3.4 shows the Pd catalyzed arene alkenylation with the addition of different amounts of pivalic acid. The initial rate of the catalysis was very similar, but after 4 hours

the reaction with 120 equivalents of HOPiv gave 30.5 TOs of styrene, whereas 60, 240 and 480 equivalents gave about 15-20 TOs.

For some cases of C–H activation via the concerted metalation deprotonation (CMD) mechanism; the addition of carboxylate salt can have a positive impact on the reaction rate.[54] To investigate the impact of carboxylate salt on our Pd catalysis, 10 equivalents of KOAc were added to the catalytic process (Figure 3.5). No obvious change on the catalysis was observed.

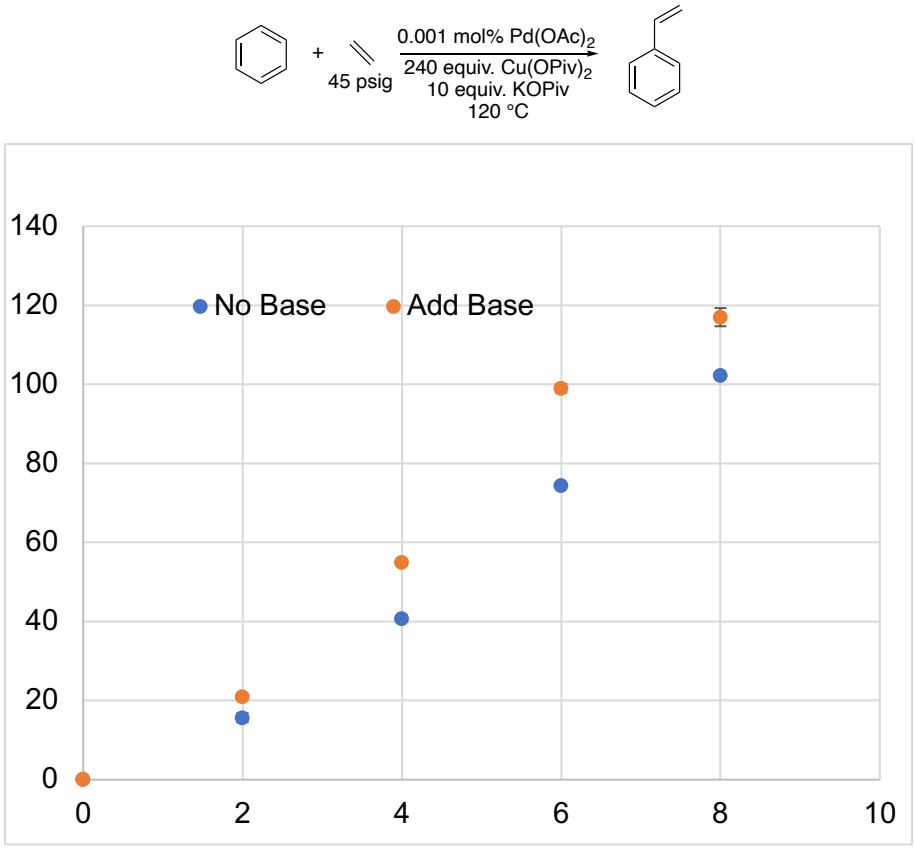

Figure 3.5. Turnovers of styrene versus time plot for anaerobic benzene ethenylation catalyzed by $Pd(OAc)_2$ with stoichiometric amount of $Cu(OPiv)_2$.

3.3 Oxidative ethylene hydrophenylation catalyzed by palladium(II) acetate under aerobic conditions

The conversion of CuX and HX to CuX_2 and water using air or purified dioxygen is efficient for many anions X (*e.g.*, X = chloride, acetate, or pivalate). This conversion forms one foundation of the commercial Hoechst-Wacker process for ethylene oxidation.[47-50] Since the Cu(II) oxidant can be efficiently recycled in air, the inclusion of air or pure dioxygen in the Pd catalyzed conversion of benzene and ethylene to styrene should enable higher product yields as the limiting reagent Cu(II) can be regenerated *in situ*. However, when the copper(I) salt is recycled by dioxygen, one equivalent of water will be generated per equivalent of copper, creating a potential problem for catalysis.

Heating 5 mL of 0.001 mol% of $Pd(OAc)_2$ solution in benzene with 240 equivalents of copper(II) pivalate salt under 40 psig ethylene and 15 psig of air at 150 ºC produced 190 TOs of styrene after 18 hours (Figure 3.6), which is a 158% yield relative to the copper(II) salt. This indicated the recycling of copper(II) was successful in the catalytic process; however, catalyst deactivation still occurred after 18 hours of reaction. One possible explanation of the catalyst deactivation is that water inhibits the formation of styrene. To examine this hypothesis, we added molecular sieves (4Å) at 18 hours to remove water from the reaction, and observed a reactivation of the catalyst with an enhanced reaction rate.

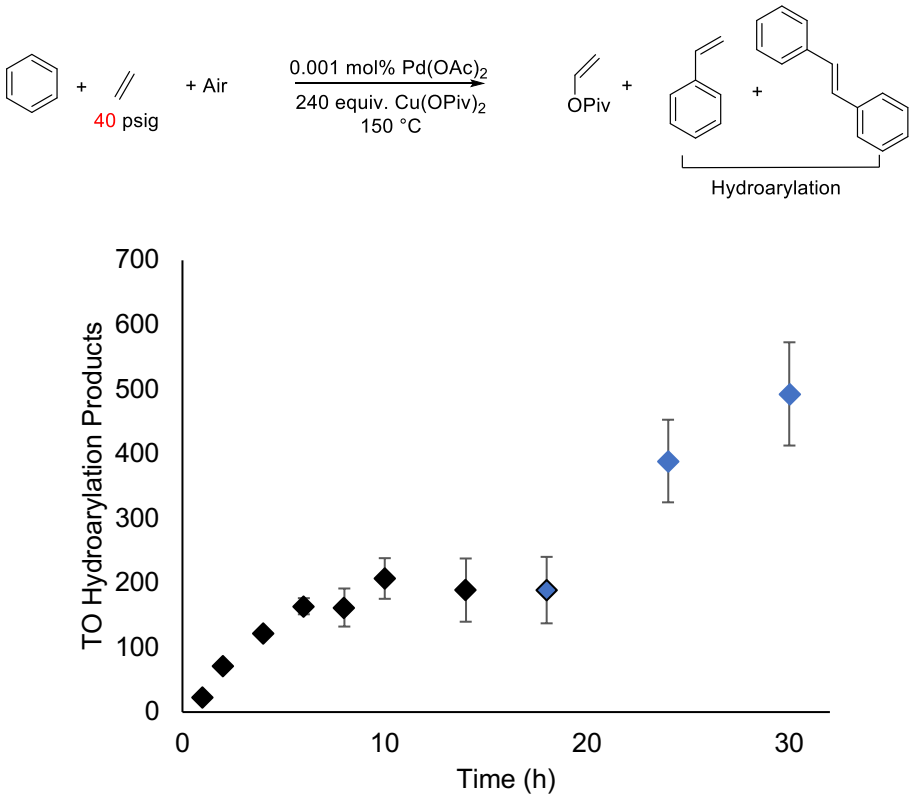

Figure 3.6. Turnovers of styrene versus time plot of aerobic oxidative ethylene hydrophenylation catalyzed by $Pd(OAc)_2$. Drying agent (molecular sieves) was added at the 18 hour time point. This plot shows the potential influence of water in the catalysis.

Table 3.2 shows the reaction optimization data for the oxidative ethylene hydrophenylation reaction under aerobic conditions. First, we compared the use of air and purified oxygen since the commercial ethylene oxidation process requires pure oxygen when used *in situ*.[50] More styrene production was observed when performing catalysis under pure dioxygen (Table 2, entries 1 and 2). The catalysis was also performed at different temperatures, and the same selectivity trend was observed as with the anaerobic catalysis. At 120 °C, vinyl pivalate production was relatively high, while at 180 °C stilbene and phenyl pivalate are the major byproducts (entries 3, 4 and 5). The production of phenyl

pivalate was observed as a minor byproduct for some conditions in our previously reported rhodium catalyzed oxidative olefin hydroarylation.[42-44] In our studies of Rh catalysis, we found that arene acetoxylation was likely mediated by CuX_2 (X = acetate, trimethylacetate, 2-ethylhexnonate) and was a side reaction when temperature is ≥ 150 °C.

Table 3.2. Condition optimization of ethylene hydrophenylation under aerobic conditions using $Pd(OAc)_2$ as catalyst precursor

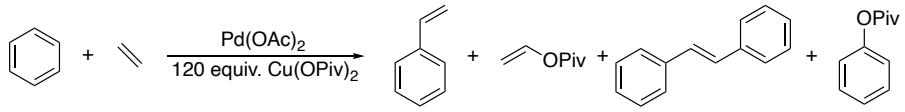

Entry	Catalyst loading[a] (mol%)	Oxygen Source[b]	Temp (°C)	Ethylene Pressure (psig)	4Å MS[c] (mg)	Time[b] (hours)	Styrene (TOs)	Vinyl pivalate (TOs)	Stilbene[c] (TOs)	Phenyl pivalate (TOs)	Selectivity (% Styrene)
1	0.001	Air	150	60	-	12	285(7)	32(1)	8.4(3)	4.3(1)	88%
2	0.001	O_2	150	60	-	12	343(3)	37(3)	11.4(6)	5.4[d]	86%
3	0.001	O_2	150	60	300	12	567(27)	26.4(4)	112(5)	4(1)	80%
4	0.001	O_2	120	60	300	48	282(18)	45(5)	7.0(3)	1.2(1)	84%
5	0.001	O_2	180	40	300	12	52(8)	0	146(6)	74(4)	19%
6	0.0001	O_2	150	60	300	24	2410(127)	98(6)	96(18)	156(15)	87%
7	0.0001	O_2	180	60	300	12	356(16)	0	281(23)	815(79)	24%

[a] Catalyst loading is relative to benzene (10 mL). [b] The reactions are purged by air or pure oxygen prior to the catalysis. [c] 4Å molecular sieves (powder) were dried at 200 °C under vacuum for 12 hours prior to use. [d] The standard deviation is lower than 0.1 TOs. The numbers in parentheses are standard deviations that are based on at least three independent experiments.

The effect of catalyst concentration on selectivity was also examined. When 0.0001 mol % catalyst (with respect to benzene) was used under optimized conditions, 2410 TOs of styrene were obtained with 87% selectivity after 24 hours (Scheme 3.2). This lower catalyst loading of 0.0001 mol % resulted in reduced stilbene production relative to styrene (Table 3.2, entry 6, styrene/stilbene = 24:1) compared to 0.001 mol % Pd loading (Table 2,

entry 3, styrene/stilbene = 5:1), but the selectivity for vinyl pivalate was similar with approximately 20:1 ratio when using 0.001 mol% Pd vs. approximately 26:1 for 0.0001 mol% loading. This observation was consistent with our hypothesis (Scheme 3.1) that stilbene production is suppressed when the ethylene to styrene ratio is high.

Table 3.3. Oxidative hydrophenylation of ethylene under optimized aerobic conditions using reduced catalyst loading at 150 °C, turnover numbers (TOs) are listed below products. Standard deviations, given in parentheses, are the result of at least three independent experiments.

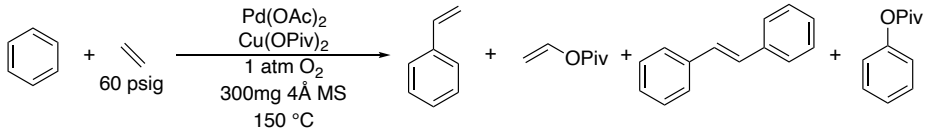

Entry	Catalyst loading (mol%)	$Cu(OPiv)_2$ (equiv.)	Time (hours)	Styrene (TOs)	Vinyl pivalate (TOs)	Stilbene (TOs)	Vinyl pivalate (TOs)
1	0.0001	1200	24	2410(127)	98(8)	96(18)	165(15)
2	0.00005	2400	48	6266(390)	254(7)	250(45)	500(77)

High catalytic turnovers could be achieved under reduced catalyst loading. As described in Table 3.3, under optimized condition, catalysis with 0.0001 mol% $Pd(OAc)_2$ produced 2410 TOs of styrene in a one day. 6266 TOs of styrene was produced under 0.00005 mol% $Pd(OAc)_2$ catalyst loading after 48 hours of catalysis. However, prolonged reaction time produced a large amount of the undesirable phenyl pivalate.

3.3 Dependence of the observed rate constants for the aerobic oxidative olefin hydrophenylation on the $Pd(OAc)_2$ concentration

The influence of catalyst loading on the reaction was examined by heating 10 mL benzene solutions with different amounts of $Pd(OAc)_2$ and 60 psig of ethylene, 1 atm of

pure dioxygen, 300 mg of 4Å molecular sieves and 0.54 mM of $Cu(OPiv)_2$. We estimated the k_{obs} under six different catalyst loadings (0.001, 0.0025, 0.005, 0.01, 0.02, 0.025 mol%) by using the average TOF calculated from 1 hour of catalysis (Figure 3.7).

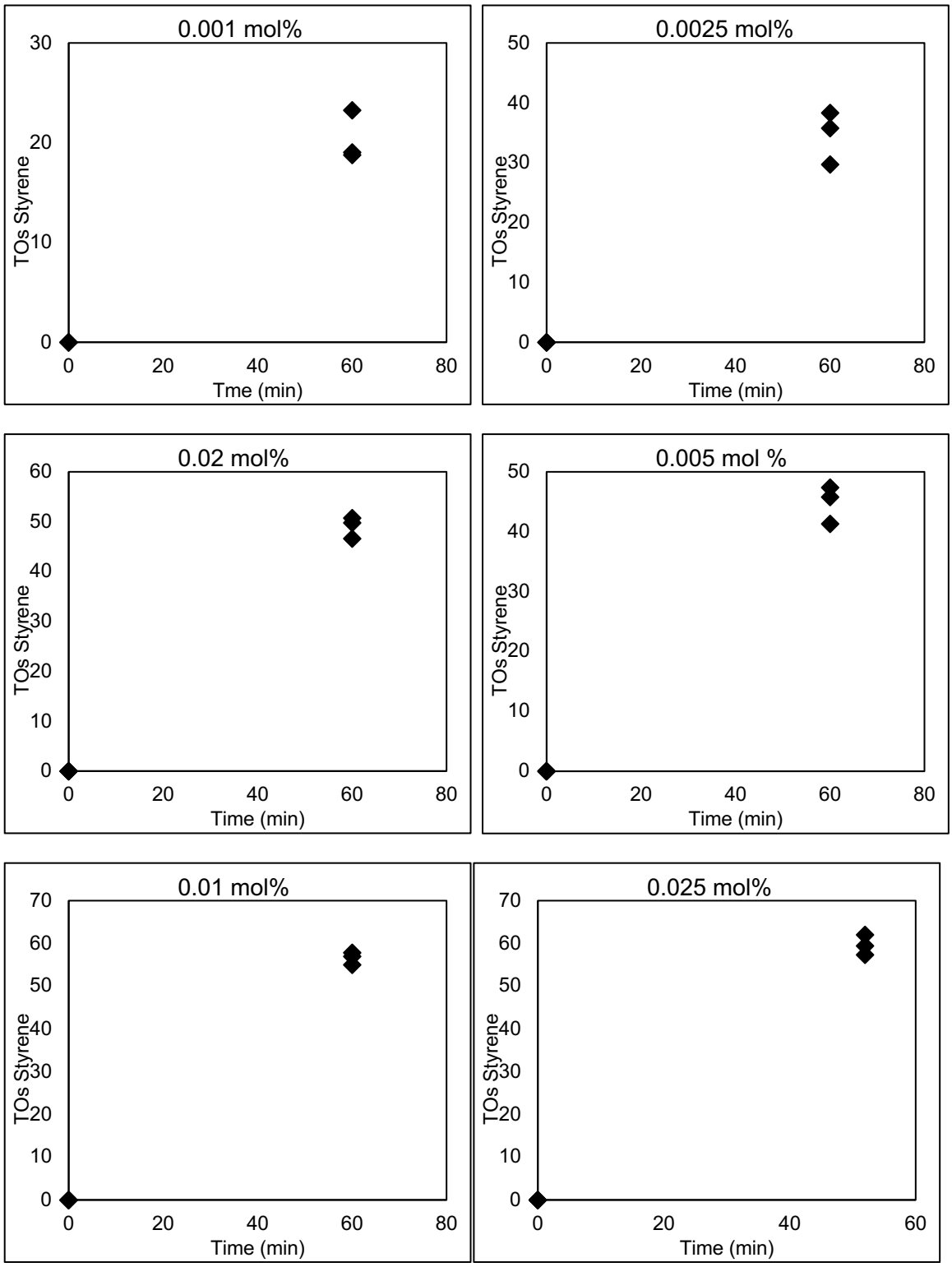

Figure 3.7. TOs of styrene vs. time plots for aerobic oxidative ethylene hydrophenylation under different $Pd(OAc)_2$ loading. Data from three runs are presented in each figure. Condition: 0.001, 0.0025, 0.005, 0.01, 0.02 or 0.025 mol% of $Pd(OAc)_2$, 60 psig of

ethylene, 1 atm of pure dioxygen, 300 mg of 4Å molecular sieves and 0.54 mM of $Cu(OPiv)_2$.

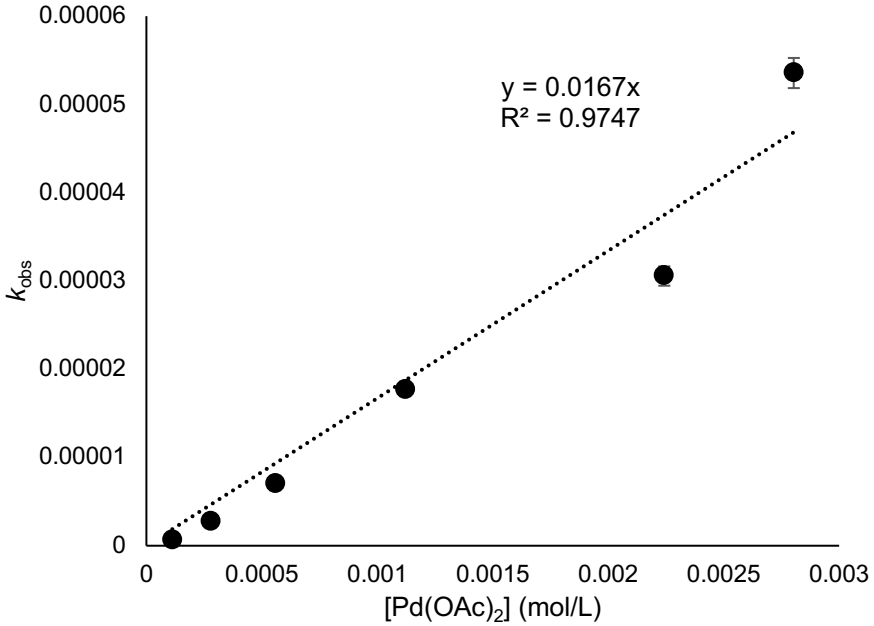

Figure 3.8. Concentrations of $Pd(OAc)_2$ versus observed rate constants (k_{obs}) plot. Condition: 0.001, 0.0025, 0.005, 0.01, 0.02 or 0.025 mol% of $Pd(OAc)_2$, 60 psig of ethylene, 1 atm of pure dioxygen, 300 mg of 4Å molecular sieves and 0.54 mM of $Cu(OPiv)_2$.

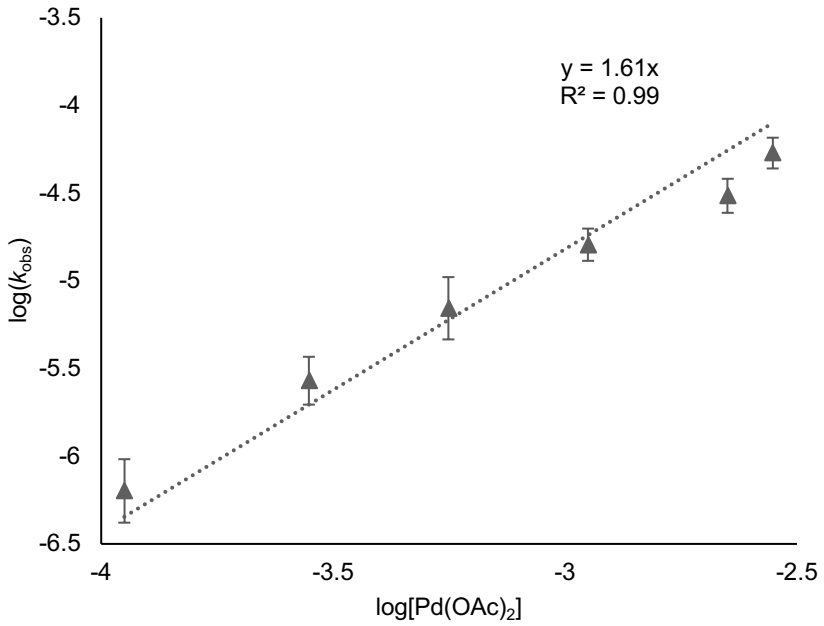

Figure 3.9. Log-log plot of the observed rate constant as a function of the concentration of $Pd(OAc)_2$ under aerobic conditions.

Figure 3.9 shows a log-log plot of k_{obs} versus Pd concentration. A slope of 1.61 shows a reaction order between 1.5 and 2.

3.4 Study of thermal decomposition of $Pd(OAc)_2$ under reaction condition

Previous work in our lab has demonstrated that, under some conditions, Rh catalyzed arene alkenylation reactions formed Rh(s).[55] Samples of thermal decomposition of $Pd(OAc)_2$ were prepared with or without copper(II) oxidants. Heating 10 mL of a benzene solution with 0.05 mol % $Pd(OAc)_2$ under 40 psig of ethylene pressure with or without 1 equivalent of $Cu(OPiv)_2$, the reaction color changed from blue to colorless in 5 minutes for the catalysis with $Cu(OPiv)_2$ and from light yellow to gray for the reaction without

$Cu(OPiv)_2$. Under both conditions, a black precipitate was formed. The reaction mixtures were filtered, and the solid was washed with benzene several times. Scanning electron microscope (SEM) analysis suggested that $Pd(OAc)_2$ was reduced to large spherical Pd particles with a size of ~300 μm (Figure 3.10, Figure 3.11). The identity of palladium was also confirmed by the energy dispersive X-ray spectroscopy (EDS). SEM images of the solid from the deactivation of $Pd(OAc)_2$ (Figure 3.12, Figure 3.13).

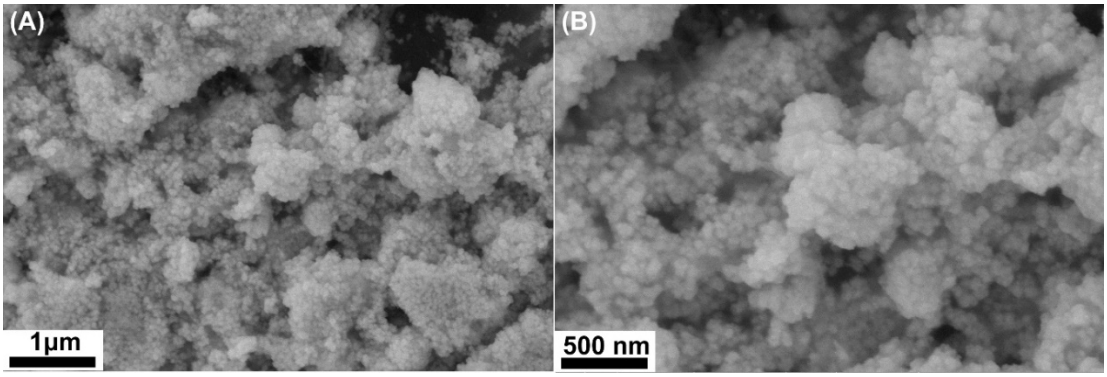

Figure 3.10. SEM images of the solid from the deactivation of $Pd(OAc)_2$ in benzene under catalytic conditions. A) 20,000 times magnification B) 40,000 times magnification.

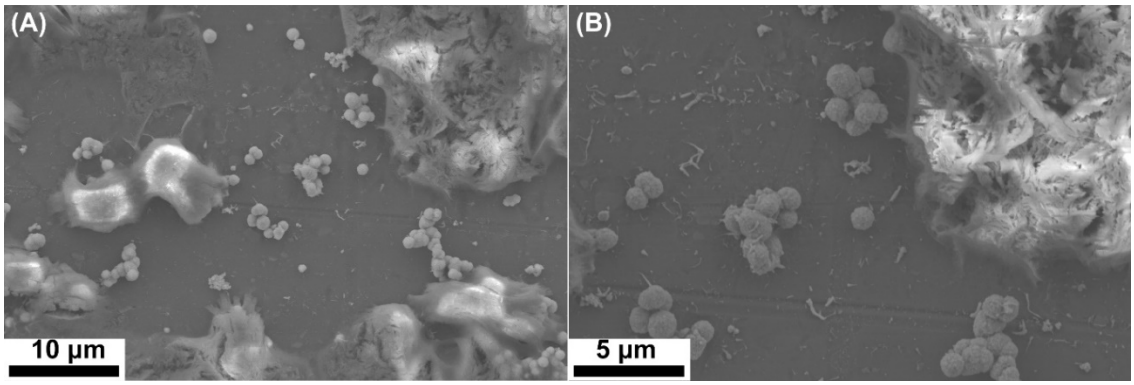

Figure 3.11. SEM images of the solid from the deactivation of $Pd(OAc)_2$ and 1 equiv. of $Cu(OPiv)_2$ in benzene under catalytic condition. A) 2,500 times magnification B) 5,000 times magnification

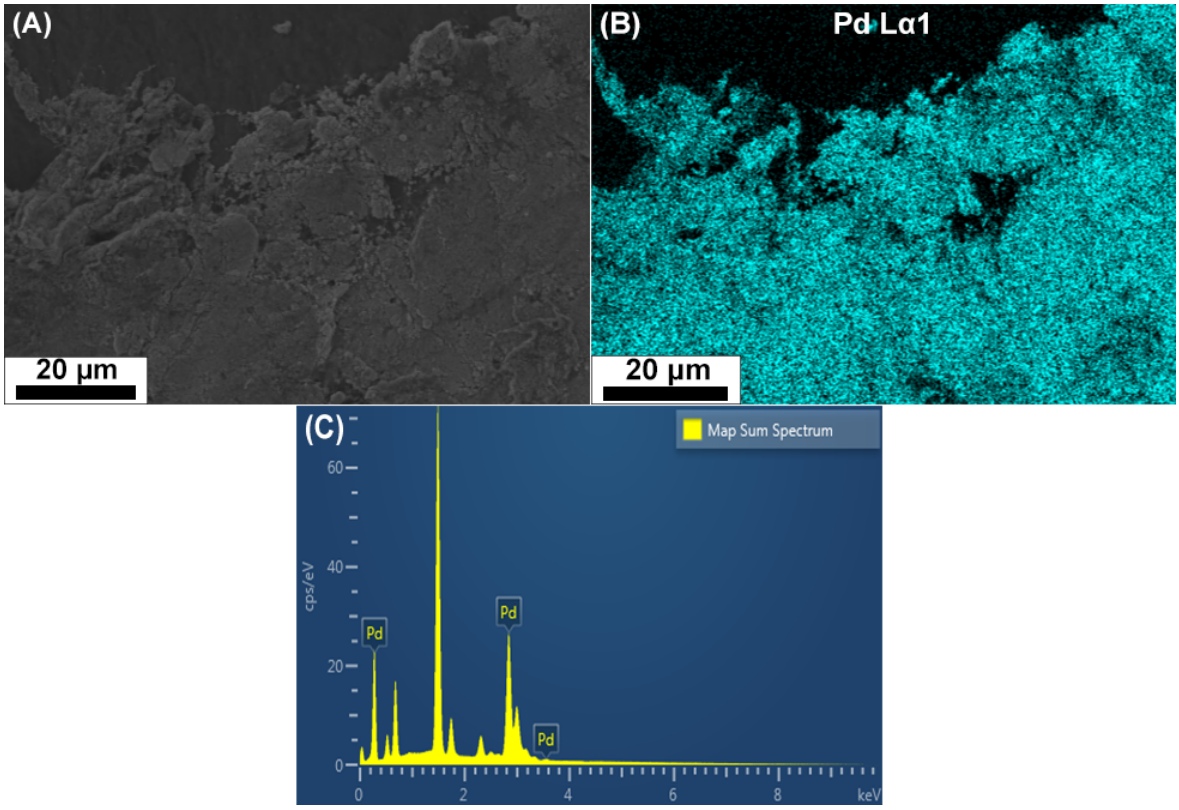

Figure 3.12. A) SEM images of the solid from the deactivation of $Pd(OAc)_2$ in benzene under catalytic conditions. B) Pd L edge EDS elemental mapping image of (A) C) EDS spectrum image for SEM image (A).

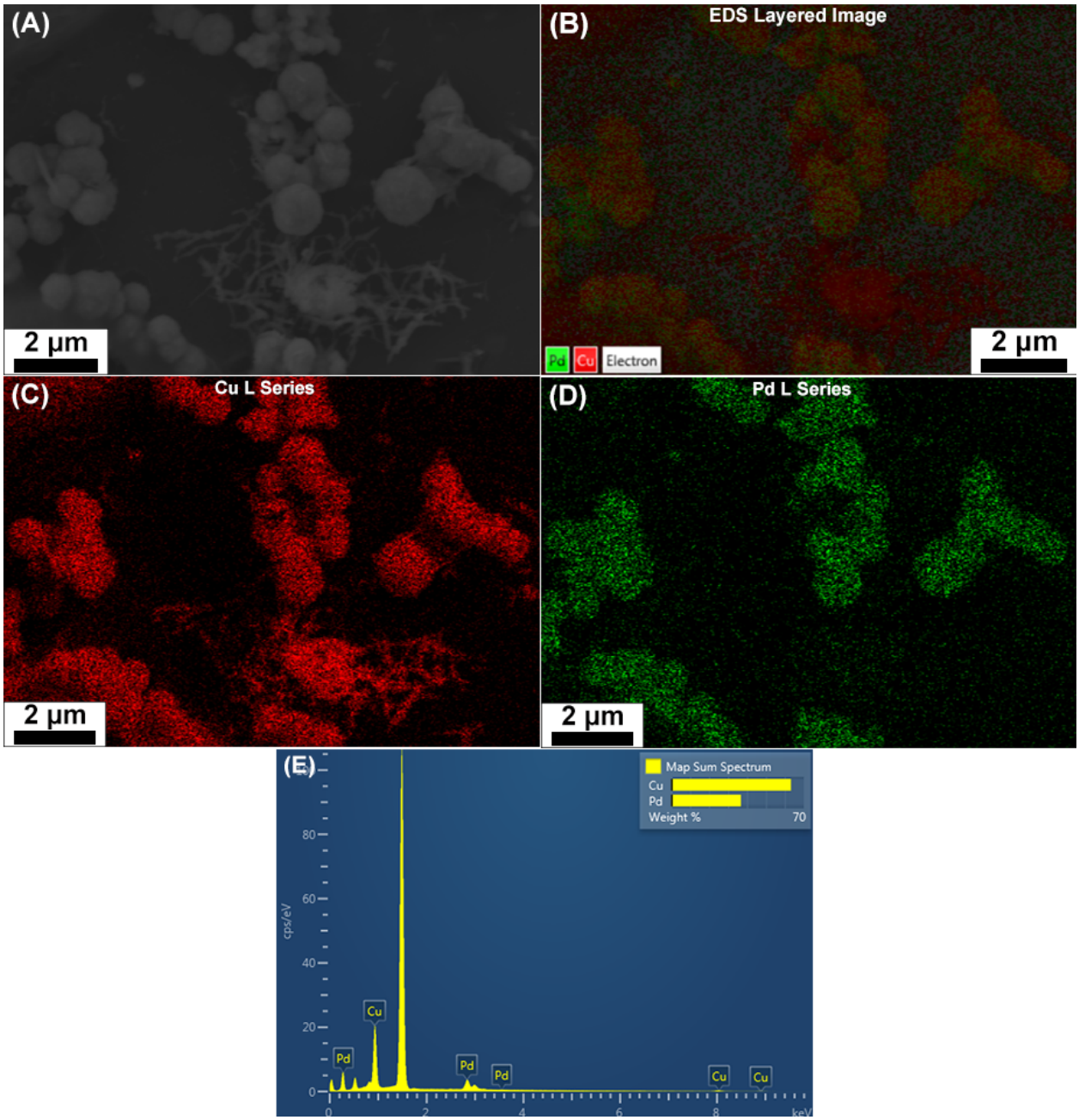

Figure 3.13. A) SEM images of the solid from the deactivation of $Pd(OAc)_2$ and 1 equiv. of $Cu(OPiv)_2$ in benzene under catalytic conditions. B) Pd, Cu EDS elemental mapping image of (A) C) Cu EDS elemental mapping image; D) Pd EDS elemental mapping image; E) EDS spectrum image for SEM image (A).

The decomposition of $Pd(OAc)_2$ was monitored by in situ ^1H NMR spectroscopy. A thick-wall J-Young tube was charged with a benzene-d_6 solution of $Pd(OAc)_2$ and 40 psig

of ethylene. The NMR spectrum prior to heating is shown in Figure 3.14. Then the NMR tube was heated to 90 °C in oil bath.

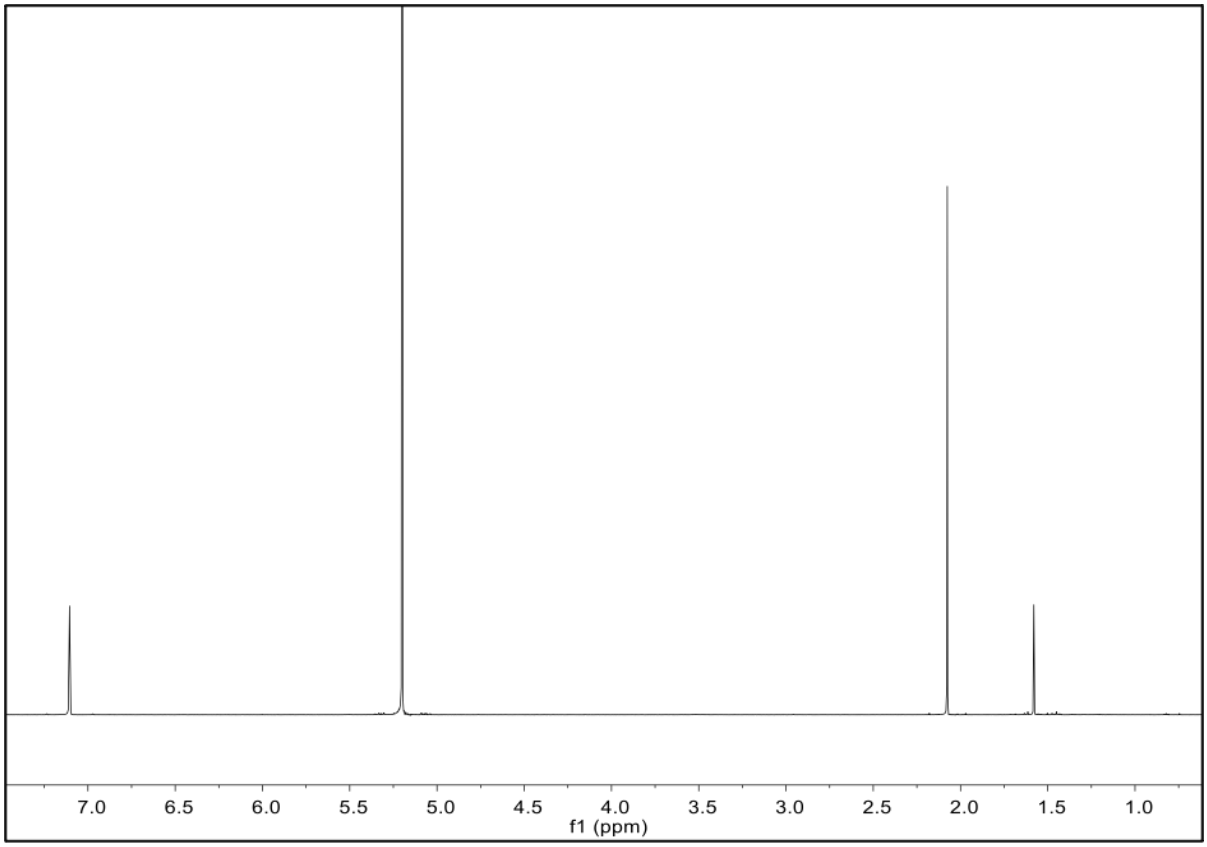

Figure 3.14. Representative ^{1}H NMR spectrum of the $Pd(OAc)_2$ thermal decomposition experiment. Conditions: $Pd(OAc)_2$ (0.057 mmol), 40 psig C_2H_4, 0.5 mL benzene-d_6, before heating. ^{1}H NMR (600 MHz, benzene-d_6) δ 7.16 (solvent residue), 5.25 (s, ethylene), 2.13 (s, hexamethylbenzene, internal standard), 1.63 (s, $Pd(OAc)_2$).

After 9 hours, a palladium(0) mirror formed on the wall of the NMR tubes, and ^{1}H NMR spectroscopy revealed the formation of styrene-d_5, vinyl acetate and free acetic acid (Figure 3.15). Scheme 3.3 outlines two overall processes that could lead to the decomposition of soluble Pd to Pd(s) that are consistent with our experimental observations.

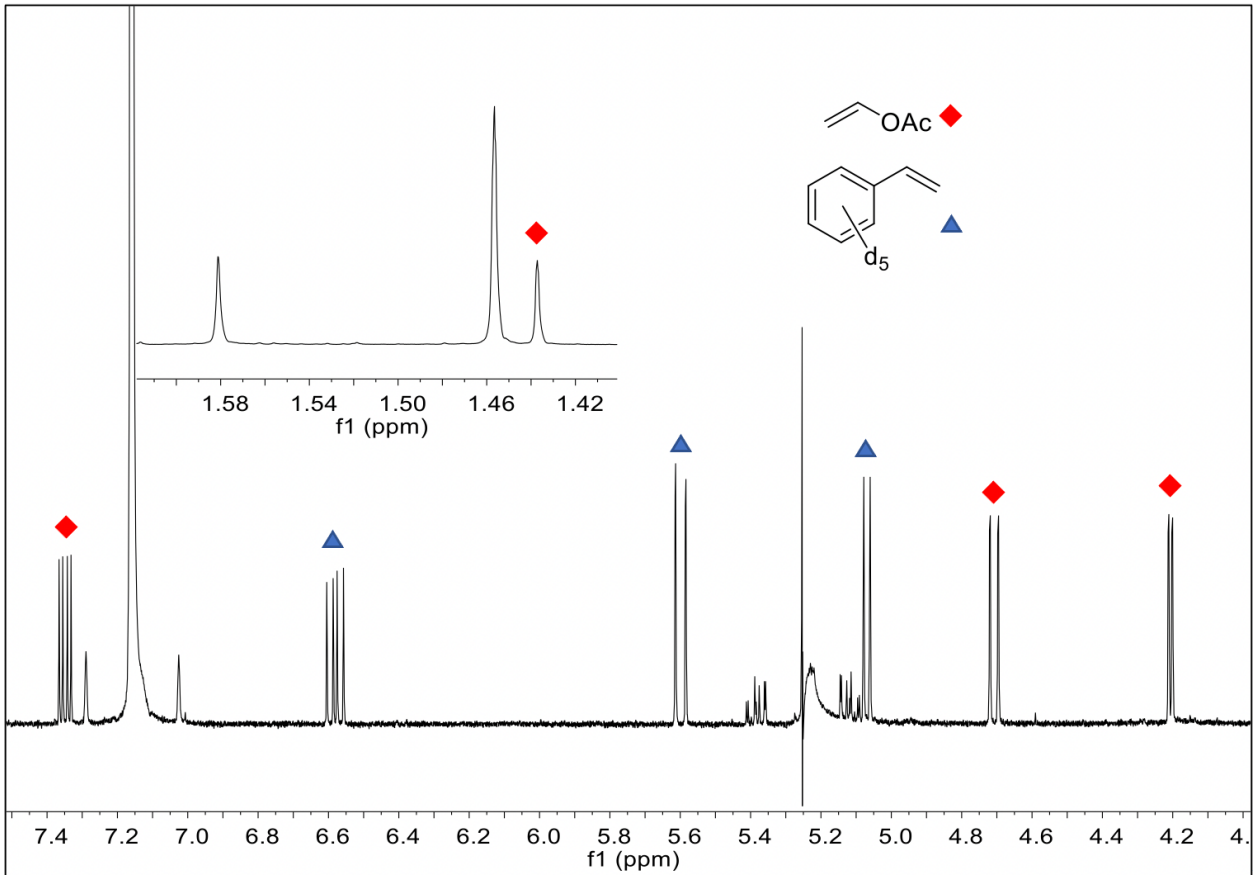

Figure 3.15. Representative ^{1}H NMR spectrum of the $Pd(OAc)_2$ thermal decomposition experiment. Conditions: $Pd(OAc)_2$ (0.057 mmol), 40 psig C_2H_4, 0.5 mL benzene-d_6, 90 °C, 510min. Ethylene peak was suppressed by applying a pre-saturation pulse. ^{1}H NMR (600 MHz, benzene-d_6) δ 7.35 (dd, J = 14.0, 6.3 Hz, CH_2=C*H*O(CO)CH_3), 6.58 (dd, J = 17.6, 10.8 Hz, $CH_2CHC_6D_5$), 5.60 (dd, J = 17.6, 1.0 Hz, $CH_2CHC_6D_5$), 5.07 (dd, J = 10.9, 1.0 Hz, $CH_2CHC_6D_5$), 4.71 (dd, J = 14.0, 1.5 Hz, CH_2=CHO(CO)CH_3), 4.21 (dd, J = 6.3, 1.5 Hz, CH_2=CHO(CO)CH_3), 1.46 (s, acetic acid, CH_3COOH), 1.44 (s, CH_2=CHO(CO)CH_3).

Kinetic studies of thermal decomposition of $Pd(OAc)_2$ were performed at 60, 90 and 120 °C. The kinetic plots show a zero order decay of $Pd(OAc)_2$ (Figure 3.16). An Eyring plot was constructed using the zero-order rate constants from four different temperatures (Figure 3.17), and the $\Delta H^{\ddagger}$ and $\Delta S^{\ddagger}$ were calculated to be 10(1) kcal/mol and 60(1)

cal/(mol·K), respectively. Additionally, when there was no ethylene added, the decomposition of $Pd(OAc)_2$ was much slower.

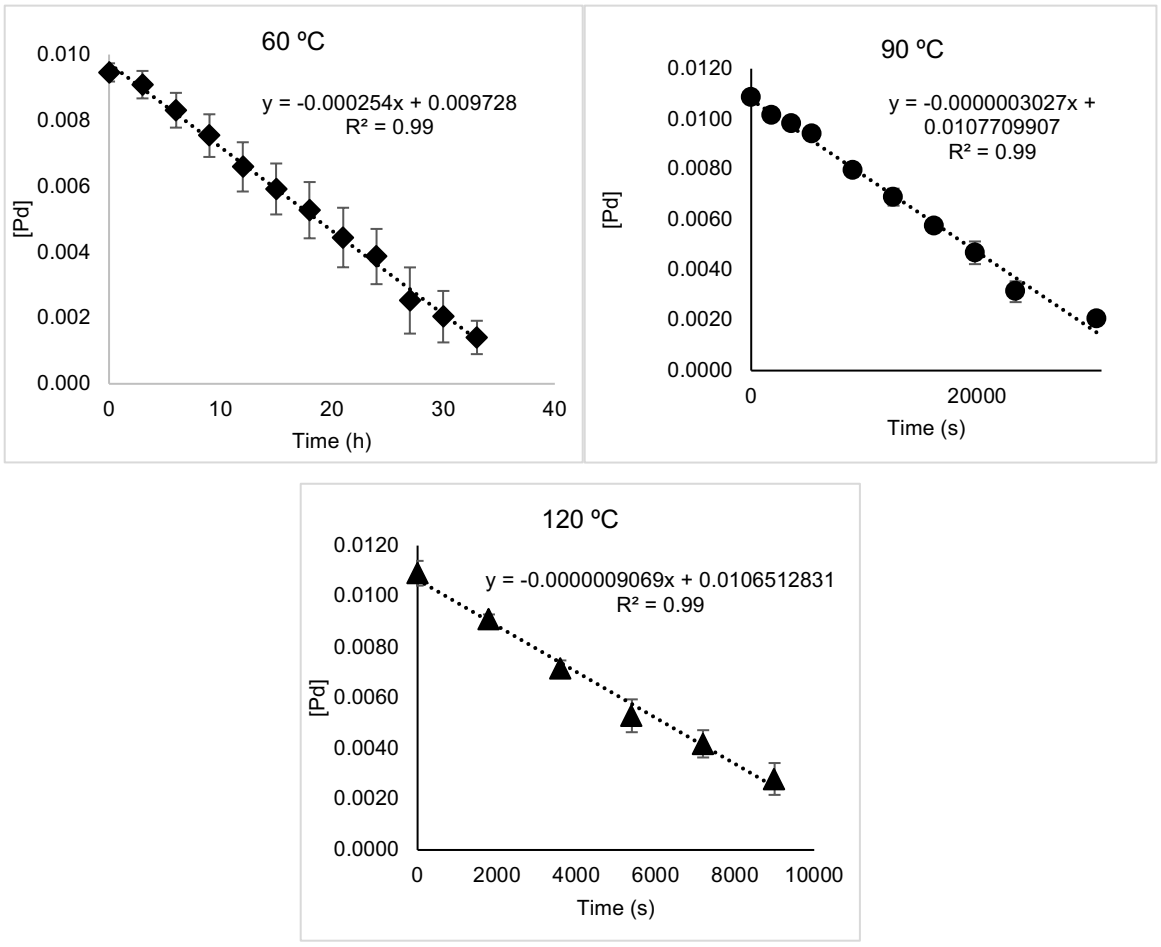

Figure 3.16. Plot of $Pd(OAc)_2$ concentration versus time for thermal decomposition in benzene-d_6 at different temperatures. Each data point is the average of three separate experiments. Error bars represent the standard deviation based on a minimum of three independent experiments.

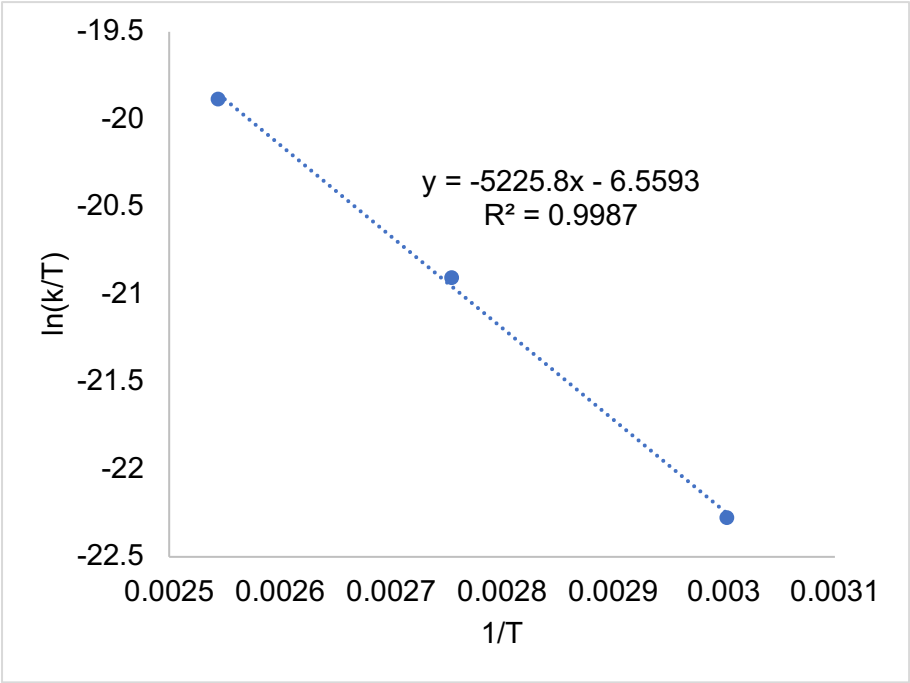

Figure 3.17.Eyring plot for $Pd(OAc)_2$ decomposition.

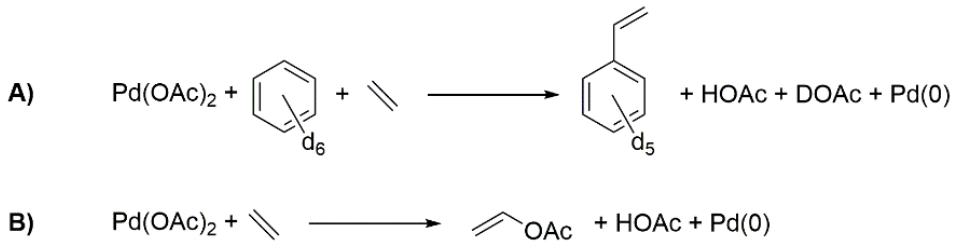

Scheme 3.3. Two proposed $Pd(OAc)_2$ decomposition processes that produce Pd(0) and acetic acid. A) decomposition of $Pd(OAc)_2$ via benzene C–H activation; B) decomposition of $Pd(OAc)_2$ via olefin C–H activation.

3.5 Kinetic isotope effect of the palladium(II) acetate catalyzed oxidative hydrophenylation of ethylene

The kinetic isotope effect (KIE) of the palladium catalyzed oxidative ethylene hydrophenylation reaction was measured for comparative rates in C_6H_6 and C_6D_6 using two methods (Scheme 3.4 and Figure 3.18). Catalysis was run at 150 °C using a 1:1 molar ratio mixture of benzene and benzene-d_6 with a catalyst loading of 0.001 mol% of

$Pd(OAc)_2$ and 240 equiv. of $Cu(OPiv)_2$ under 40 psig of ethylene pressure (Scheme 3.4). After 1 hour, the ratio of per-protio styrene [mass/charge ratio (m/z) = 104] to styrene-d_5 (m/z = 109) was determined by GC-MS and used to calculate the KIE of 3.35(1).

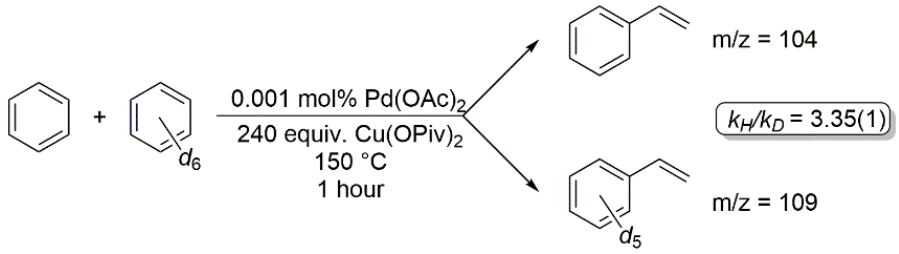

Scheme 3.4. Kinetic isotope effect measured using 1:1 ratio mixture of benzene and benzene-d_6, an observed KIE of 3.35(1) was obtained.

Catalytic reactions were also performed separately in C_6H_6 or C_6D_6 at 150 °C with a catalyst loading of 0.001 mol% of $Pd(OAc)_2$ and 240 equiv. of $Cu(OPiv)_2$ under 40 psig of ethylene pressure (Figure 3.20). The reaction solutions were analyzed by GC-FID to monitor TOs of styrene and styrene-d_5 every 30 minutes. Since we observed an apparent induction period during the first hour of the catalysis, the TOFs (TOFs = turnover frequencies) were determined from a linear fit of turnovers versus time for reactions between 1 and 3 hours (Figure 3.21).

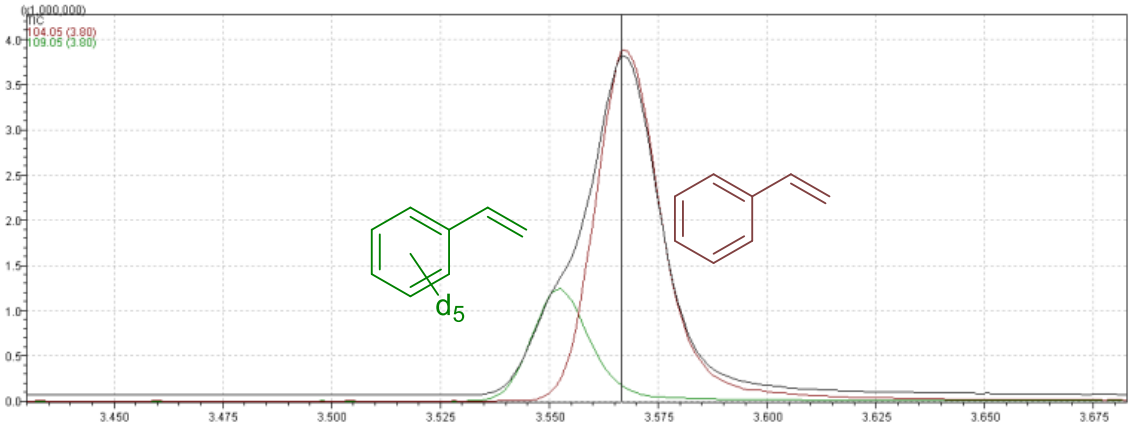

Figure 3.18. Styrene peak from the GC of the KIE experiment using a 1:1 molar ratio of C_6H_6 to C_6D_6. Peak of m/z = 109 (green, styrene-d_5) and m/z = 104 (red, styrene) was highlighted using GCSolution Postrun software by Shimazu. The following Mass-Spec data was collected using the average peak of both styrene-d_5 and styrene peaks

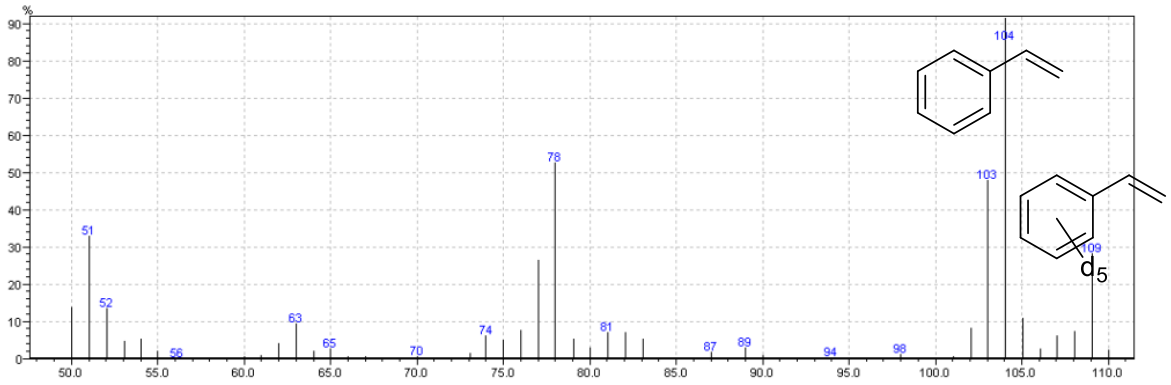

Figure 3.19. Representative mass spectrum of the KIE experiment using a 1:1 molar ratio of C_6H_6 to C_6D_6 after 3-hour reaction. m/z = 109 peak is correspondence to styrene-d_5, m/z 104 peak is correspondence to styrene. The KIE was determined by the intensity ratio of m/z = 109 versus m/z = 104 using GCSolution Postrun software by Shimadzu.

Using the slopes of TO vs. time plots from reactions in C_6H_6 and C_6D_6, a k_H/k_D of 3.5(2) was determined (Scheme 3.4). Thus, the KIEs calculated from the two independent methods, 3.35(1) and 3.5(2), were statistically identical. These KIEs are similar to reported KIEs from Crabtree and coworkers (4.1)[56] and Sanford and coworkers {4.5(4)}[57] for

palladium catalyzed arene acetoxylation and to those from Jones and coworkers (4.3 and 3.33)[58, 59] and our group {3.3(2)}[52] for Rh(I) catalyzed alkane isomerization and oxidative ethylene hydrophenylation. The observed primary KIE suggests that the palladium catalyzed oxidative olefin hydroarylation undergoes a Pd-mediated C–H activation pathway and that the C–H activation step occurs before or during the rate limiting step.[60, 61]

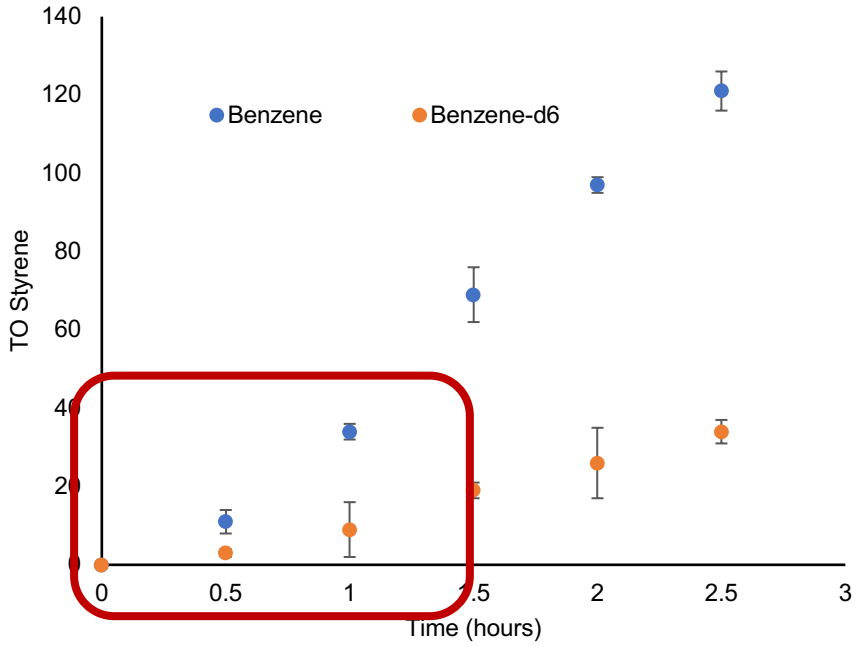

Figure 3.20. Plot of TOs of styrene and styrene-d_5 versus time for $Pd(OAc)_2$ catalyzed oxidative ethylene hydrophenylation reaction using benzene or benzene-d_6 as solvent. An induction period was observed for the first hour (in red). Conditions: 240 equiv. of $Cu(OPiv)_2$ was added to 10 mL benzene/benzene-d_6 solution of $Pd(OAc)_2$, the reactors were then pressurized by 40 psig of ethylene and heated to 150 °C

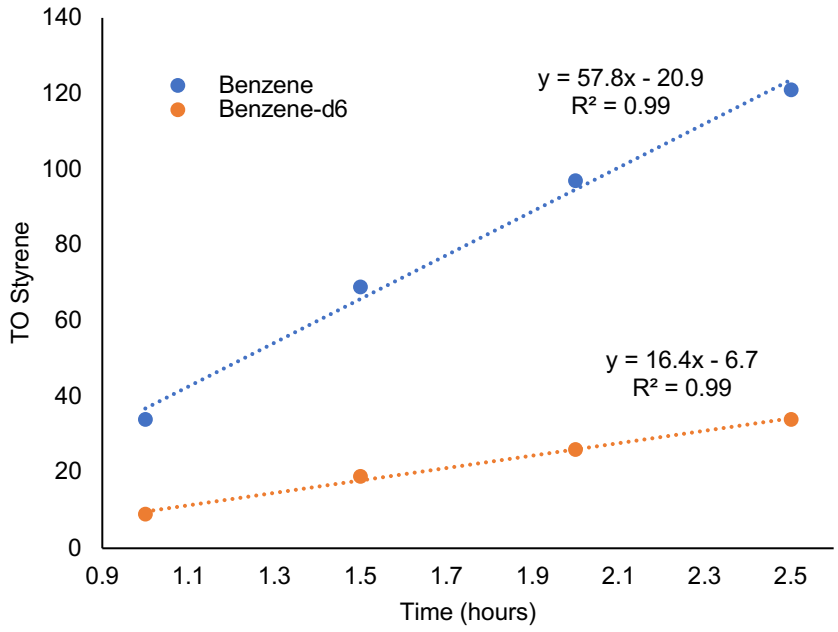

Figure 3.21. Linear fits of TOs of styrene and styrene-d_5 versus time for data between 1 and 3 hours of reaction. Conditions: 240 equiv. of $Cu(OPiv)_2$ was added to 10 mL benzene/benzene-d_6 solution of $Pd(OAc)_2$, the reactors were then pressurized by 40 psig of ethylene and heated to 150 °C

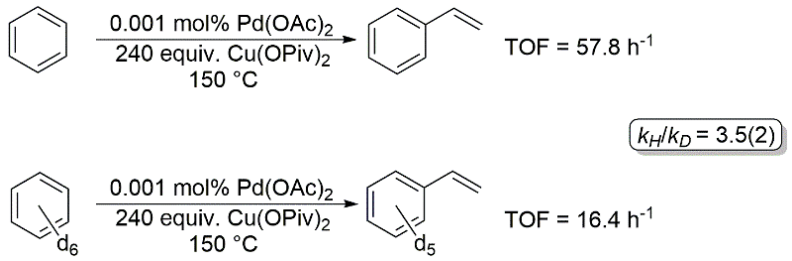

Scheme 3.5. Kinetic isotope effect measured by comparing the rates of catalysis in benzene versus benzene-d_6 after 2.5 hours.

3.6 Studies of vinyl ester production and consumption

One major byproduct in the palladium(II) acetate catalyzed oxidative ethylene hydrophenylation using $Cu(OPiv)_2$ is the olefin oxidation product, vinyl pivalate. We observed a significant decrease in the yield of vinyl pivalate when using higher reaction

temperatures (≥ 150 °C) or lower ethylene pressures (≤ 40 psig, Figure 3.1). The influence of ethylene pressure could be explained by a likely first order dependence on ethylene concentration for the ethylene oxidation reaction to produce vinyl pivalate; however, the influence of reaction temperature was less clear.

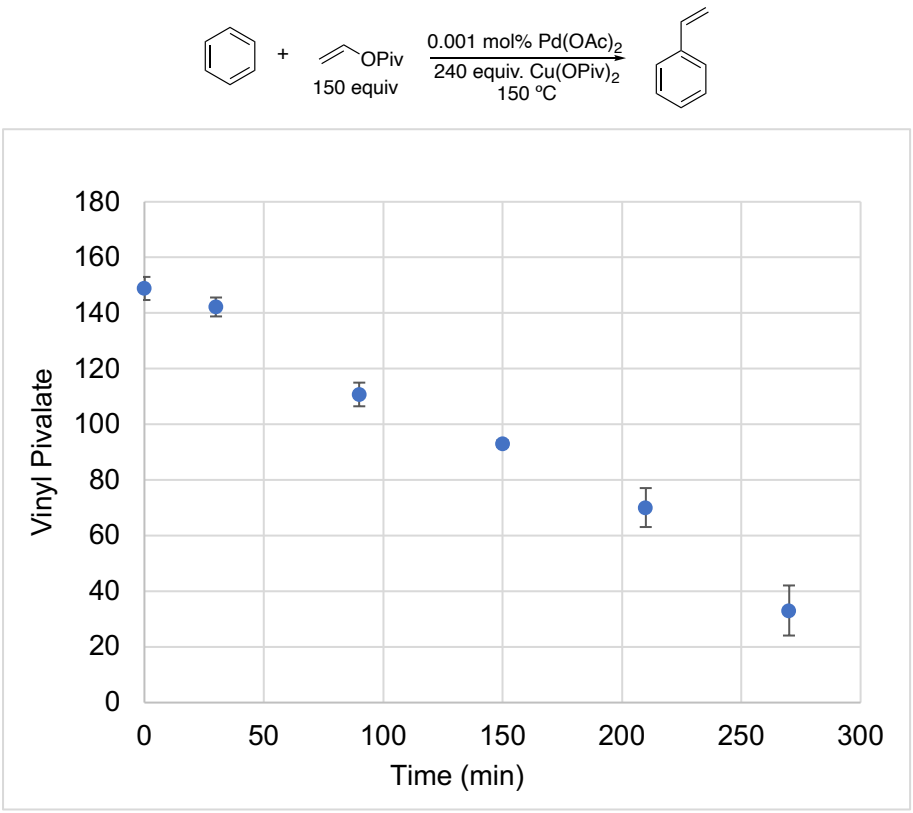

Figure 3.22. Turnovers of vinyl pivalate versus time plot of vinyl pivalate consumption catalyzed by $Pd(OAc)_2$.

We studied the ability of $Pd(OAc)_2$ to convert benzene and vinyl pivalate to styrene (Figure 3.22, Table 3.3). The conversion of vinyl pivalate and benzene to styrene was observed at ≥ 150 °C (Table 3.3, entries 1, 2 and 3). This process required both the palladium catalyst and copper(II) oxidant (Table 3.3, entries 4, 5 and 6). This discovery

helped rationalize the higher styrene selectivity at the higher reaction temperature (Figure 3.22, Table 3.2), since vinyl pivalate was rapidly converted to styrene.

In order gain insight into this palladium catalyzed ester consumption reaction, we studied other esters (Scheme 3.6). Only vinyl acetates were converted to the vinyl arene product. In addition to the production of styrene and stilbene, the formation of vinyl pivalate was observed when vinyl acetate and copper(II) pivalate were present in the reaction mixture. The ester exchange reaction was general, as indicated by the results shown in Table 3.4. For reactions of benzene using allyl acetate and methylacrylate, only oxidative hydrophenylation of allyl acetate or methylacrylate hydrophenylation were detected scheme 3.6). When alkyl acetates were used, no reaction was observed for ethyl acetate, *n*-propylacetate, and amyl acetate were used, no reaction was observed. These observations suggest that the conversion of ester and benzene to vinyl benzene requires a C(sp^2)-O bond.

Table 3.4. Conversion of benzene and vinyl pivalate to styrene catalyzed by $Pd(OAc)_2$.

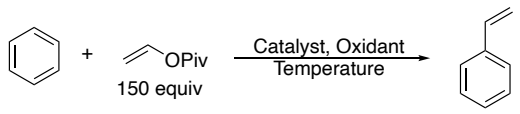

Entry[a]	Catalyst	Oxidant	Temperature (°C)	Time (min)	Vinylpivalate (equiv.)	Alkenylation Product (TOs)
1	$Pd(OAc)_2$	$Cu(OPiv)_2$	120	300	0	0
2	$Pd(OAc)_2$	$Cu(OPiv)_2$	150	270	115(4)	120(7)
3	$Pd(OAc)_2$	$Cu(OPiv)_2$	180	30	126(7)	117(6)
4	$Pd(OAc)_2$	$Cu(OPiv)_2$	150	30	27(3)	19(6)
5	$Pd(OAc)_2$	-	150	300	0	0

6	-	$Cu(OPiv)_2$	150	300	0	0

[a] Conditions: 0.001 mol % of $Pd(OAc)_2$ dissolved in 10 mL of benzene with HMB (hexamethylbenzene) as an internal standard, 150 equivalent. of vinyl pivalate, 240 equivalents of copper pivalate (if applicable). [b] vp = vinyl pivalate. [c] Hydroarylation products include: styrene, stilbene and 1,1,2-triphenylethylene. [d] 60 equivalents of copper(II) pivalate are used in entry 4.

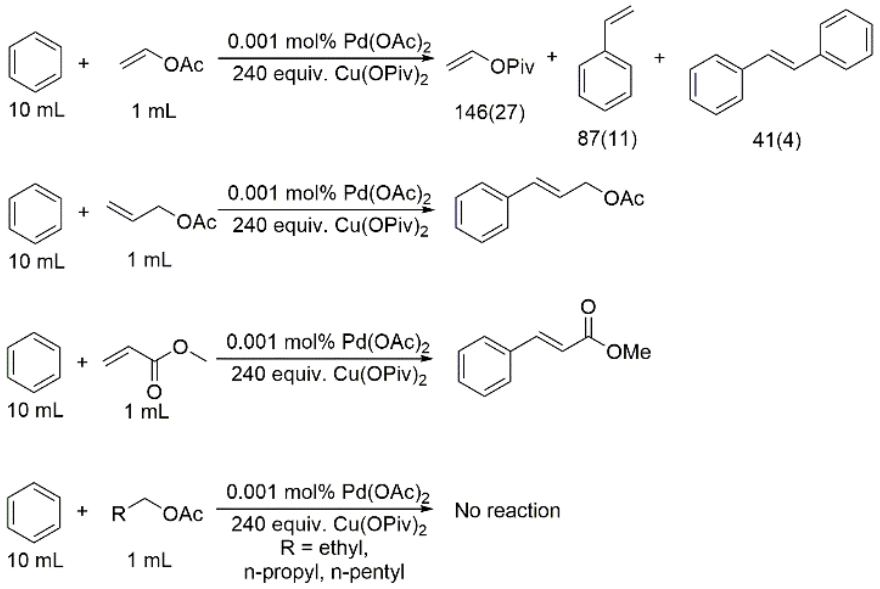

Scheme 3.6. Summary of attempted reactions with various acetates and benzene. Conditions: 0.001 mol% $Pd(OAc)_2$, 240 equiv. $Cu(OPiv)_2$, 1 mL corresponding ester, 150 °C 1h. Products were analyzed by GC-FID and GC-MS.

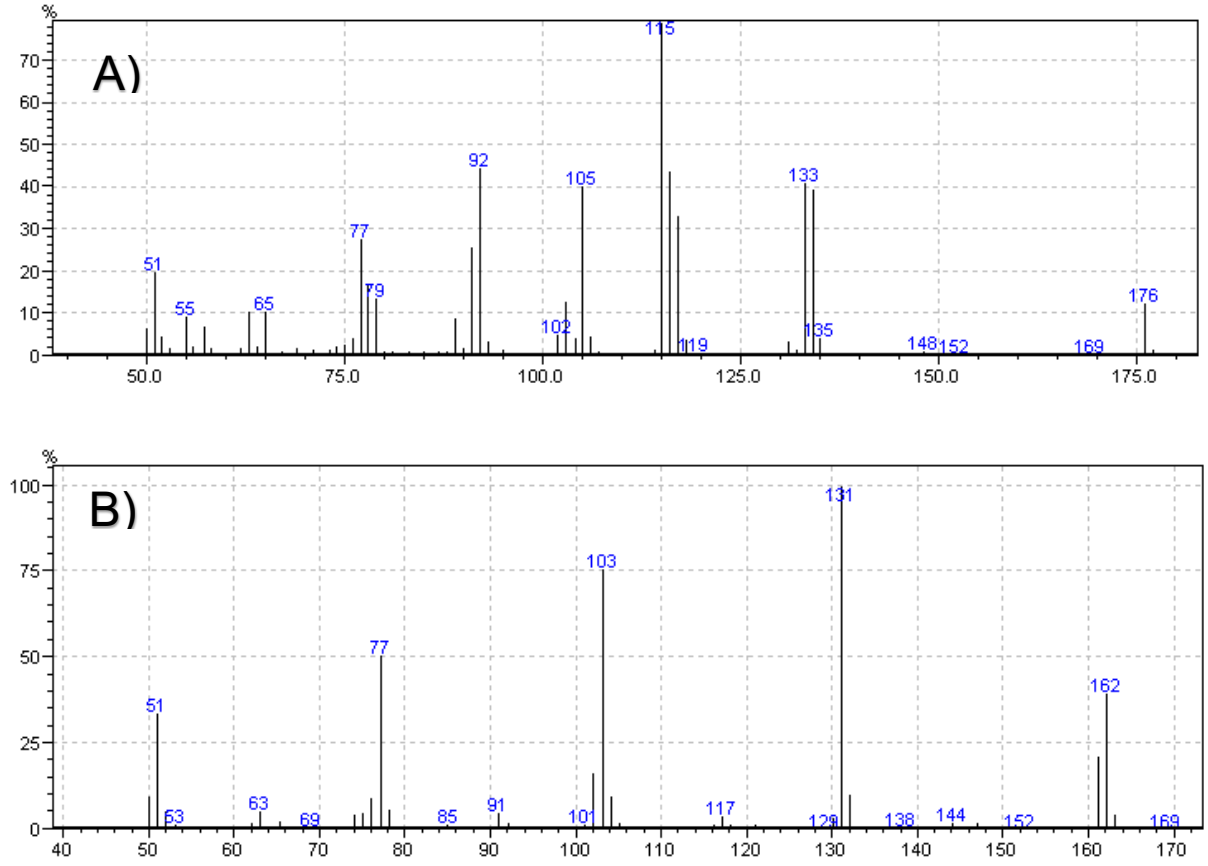

Figure 3.23. Mass spectra of the undesired product from Pd catalyzed ester consumption. A) cinnamyl acetate (From the reaction between allyl acetate and benzene under catalytic condition). B) methyl cinnamate (From the reaction between methyl acrylate and benzene under catalytic conditions). Both mass spec plots are consistent with the standard spectra by ≥ 98%.

Table 3.5. Vinyl ester metathesis using potassium salts as the acetate source.

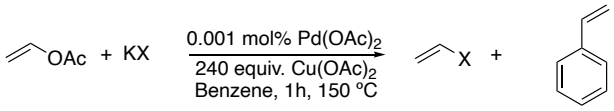

Entry	X	Vinyl-X (TOs)	Styrene (TOs)
1	trimethylacetate	18(1)	10(3)
2	trifluoroacetate	21(4)	11(1)
3	benzoate	9(1)	11(3)

3.7 Alternative oxidants

The use of alternative oxidants for Pd catalyzed alkenylation was also investigated. As shown in Table 3.5, cobalt(II) pivalate, manganese(IV) oxide, tris(acetylacetonato)iron(III), chromium trioxide, nickel(II) pivalate and 1,4-benzoquinone (BQ) were tested under the conditions for catalytic formation of styrene (Table 3.6).

Table 3.6. Pd catalyzed alkenylation using alternative oxidants

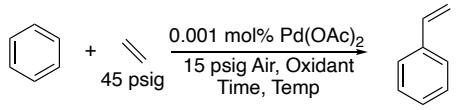

Entry	Oxidant	Temperature (°C)	Time (hours)	Styrene (TOs)	By-product(s)
1	60 equiv. $Co(OPiv)_2$	150	6	55(1)	45 TOs of biphenyl
2	60 equiv. MnO_2	150	6	5(1)	-
3	60 equiv. $Fe(acac)_3$	150/180	12	-	-
4	60 equiv. CrO3	150/180	12	-	-
5	60 equiv. $Ni(OPiv)_2$	150/180	12	-	-
6	120 equiv. BQ w/o O_2	150/180	18h	-	-
7	120 equiv. BQ	150/180	18h	-	-

The catalytic reaction using $Co(OPiv)_2$ (entry 1) gave 55 catalytic turnovers of styrene after 6 hours reaction; however, 45 TOs of biphenyl are also produced, possibly indicating that a Co-mediated aryl-aryl coupling reaction is competing with the arene alkenylation. The black solid manganese(IV) oxide (entry 2) did not dissolve in benzen, but, after 6 hours

reaction at 150 ^{o}C, 6 TOs of styrene were observed. Unfortunately, the reaction with tris(acetylacetonato)iron(III), chromium trioxide, nickel(II) pivalate and 1,4-benzoquinone (BQ) did not yield the desired product, styrene.

3.8 Summary and Conclusions

$Pd(OAc)_2$ catalyzed oxidative ethylene hydrophenylation, which directly converts benzene, ethylene, and Cu(II) oxidant to styrene, is shown to operate with high selectivity under optimized aerobic and anaerobic conditions. Our studies have revealed new insight into these reactions that led to conditions where > 2,400 TOs with > 85% selectivity for styrene were achieved. Our conclusions include:

(1) Ethylene pressures and reaction temperature play important roles for the ratio of vinyl pivalate to styrene. The production of vinyl pivalate has a positive correlation with ethylene pressure. Importantly, the increased selectivity for styrene versus vinyl pivalate as a function of temperature is likely a result of a Pd-catalyzed conversion of vinyl pivalate and benzene to styrene.

(2) The production of stilbene could not be avoided, but it can be limited by increasing the concentration of ethylene in the reaction mixture.

(3) Catalysis under aerobic conditions gives higher catalytic TOs, since Cu(II) is regenerated in situ; however, the reaction rate is slower than catalysis under anaerobic conditions.

(4) The identification of temperature dependent vinyl ester conversion to alkenyl arene provides a strategy to reduce vinyl ester production as well as a new synthetic method toward some more industrial valuable vinyl esters (e.g., vinyl benzoate).

3.9 Experimental Section

General Considerations. Unless otherwise noted, all synthetic procedures were performed under anaerobic conditions in a nitrogen-filled glovebox or by using standard Schlenk techniques. Glovebox purity was maintained by periodic nitrogen purges and was monitored by an oxygen analyzer (O_2 < 15 ppm for all reactions). Benzene was purified by passage through a column of activated alumina. ^{1}H NMR spectra were recorded on a Varian 600 spectrometer. ^{1}H NMR spectra are referenced against residual proton signals (^{1}H NMR) of the deuterated solvents. GC/MS was performed using a Shimadzu GCMS-QP2010 Plus system with a 30 m x 0.25 mm RTx-Qbond column with 8 μm thickness using electron impact ionization. GC/FID was performed using a Shimadzu GC-2014 system with a 30 m x 90.25 mm HP5 column with 0.25 μm film thickness. Styrene, vinyl pivalate, phenyl pivalate, biphenyl and stilbene production was quantified using linear regression analysis of gas chromatograms of standard samples of authentic product. The slope, correlation coefficient and the response factor of the regression lines were 2.59, 0.99 and 2.54 for vinyl pivalate, 1.78, 0.99 and 1.72 for styrene, 1.53, 0.99 and 1.50 for phenyl pivalate, 1.07, 0.99 and 1.03 for biphenyl and 0.83, 0.99 and 0.80 for stilbene, respectively. SEM images were taken from FEI Quanta 650 with energy dispersive X-ray spectroscopy (EDS). High

tension for imaging was 10 kV and spot size was 2.0-3.0. For EDS, the applied potential was still 10 kV but the spot size was larger, 4.0. Copper(II) pivalate was synthesized according to a published procedure.[62] All other reagents were used as received from commercial sources.

Catalytic Oxidative Ethylene Hydrophenylation under Anaerobic Condition: General procedure. A representative catalytic reaction under anaerobic condition is described. A stock solution containing $Pd(OAc)_2$ (0.063 g, 0.028 mmol), HMB (hexamethylbenzene) (0.091 g, 0.56 mmol), and benzene (250 mL) was prepared in a volumetric flask. Thick-walled Fisher-Porter reactors were charged with stock solution (10 mL) and $Cu(OPiv)_2$ (240 equiv. relative to $Pd(OAc)_2$). The vessels were sealed, pressurized with ethylene and subsequently stirred and heated in oil baths. The reactions were sampled after all the copper(II) was consumed, as indicated by a change in the color of the reaction from blue to colorless. Aliquots of the reaction mixture were analyzed by GC/FID using relative peak areas versus the internal standard.

Catalytic Oxidative Ethylene Hydrophenylation under Aerobic Conditions. General procedure: A representative catalytic reaction under aerobic condition is described. A stock solution containing $Pd(OAc)_2$ (0.063 g, 0.028 mmol), HMB (hexamethylbenzene) (0.091 g, 0.56 mmol), and benzene (250 mL) was prepared in a volumetric flask. Thick-walled Fisher-Porter reactors were charged with stock solution (10 mL), $Cu(OPiv)_2$ (240 equiv. relative to $Pd(OAc)_2$), and 300 mg of the drying agent 4Å

molecular sieves (molecular sieves (powder) were dried at 200 °C under vacuum for at least 12 hours prior to use). The vessels were sealed, purged by air/O_2 through a needle for 2 minutes and pressurized with different ethylene pressures and subsequently stirred and heated different temperatures. The reactions were sampled after all the copper(II) was consumed as indicated by a change in the color of the reaction from blue to brown. Aliquots of the reaction mixture were analyzed by GC/FID using relative peak areas versus the internal standard.

Scanning Electron Microscope (SEM) and Energy-dispersive X-ray spectroscopy (EDS) Studies of $Pd(OAc)_2$ Decomposition under Catalytic Conditions: Sample preparation. A stock solution containing 0.001 mol % $Pd(OAc)_2$ and benzene (100 mL) was prepared in a volumetric flask. Thick-walled Fisher-Porter reactors were charged with stock solution (10 mL) and $Cu(OPiv)_2$ (0 and 1 equiv. relative to $Pd(OAc)_2$). The vessels were sealed and pressurized with 60 psig of ethylene. After heating in oil bath at 150 °C for 1 hour, the reactor was allowed to cool and sonicated for 5 minutes for SEM sample preparation. The well-dispersed ink was dripped dropwise onto an aluminum foil covered SEM sample stage.

^{1}H NMR Spectroscopy Studies of Thermal Deactivation of $Pd(OAc)_2$ under Catalytic Conditions: General Procedure. A 10 mL stock solution containing 0.57 mmol of $Pd(OAc)_2$ and 10 mL C_6D_6 was prepared in volumetric flask. A thick-wall J-Young

NMR tube was charged with 0.5 mL of the stock solution and sealed. Then, the tube was pressurized with 40 psig of ethylene

Oxidative Hydrophenylation of Ethylene as a Function of $Pd(OAc)_2$ Loading: General Procedure. Six separate stock solutions were prepared in 10 mL volumetric flasks, each containing $Pd(OAc)_2$ (0.028, 0.022, 0.011, 0.0056, 0.0028 or 0.0011 mM), hexamethylbenzene (10 equiv. relative to $Pd(OAc)_2$) and benzene (10 mL). Fisher-Porter reactors (3 reactors per concentration level) were charged with stock solution (10 mL) and copper(II) pivalate (0.54 mM), 300 mg of 4Å molecular sieves and purged with dioxygen for 2 minutes. The vessels were sealed, pressurized with ethylene (60 psig), and stirred while heating in an oil bath at 150 °C. The reactions were sampled after 1 hour. Aliquots of the reaction mixture were analyzed by GC/FID using relative peak area vs. an internal standard (hexamethylbenzene).

Kinetic Isotope Effect (KIE) Experiment of Pd(II) Catalyzed Oxidative Ethylene Hydrophenylation: General procedure for KIE experiments (A) Using a 1:1 molar mixture of C_6H_6 and C_6D_6. A stock solution containing $Pd(OAc)_2$ (0.112 mM) and a 1:1 molar mixture of C_6H_6 and C_6D_6 (100 mL) was prepared in a volumetric flask. Fisher-Porter reactors were charged with stock solution (10 mL) and $Cu(OPiv)_2$ (240 equiv. relative to $Pd(OAc)_2$). The vessels were sealed, pressurized with ethylene (50 psig), and stirred while heated in an oil bath to 150 °C. The reactions were sampled at 1, 2 and 3 h. At each time point the reactors were cooled to room temperature, sampled, recharged with

ethylene, and reheated. Aliquots of the reaction mixture were analyzed by GC/MS. KIEs were determined by examining the ratio of styrene (m/z = 104) to styrene-d_5 (m/z = 109) in the mass spectrum, accounting for the initial isotopic distribution and natural abundance. No change in the isotopic distribution for benzene was observed over the course of the reaction, and the observed isotopic distribution of product was consistent with the initial distribution. No $d_{6–8}$ products were observed, except those predicted by the natural abundance of deuterium in ethylene.

General procedure for KIE experiments (B): Oxidative hydrophenylation of ethylene using $Pd(OAc)_2$ in C_6D_6. A stock solution containing $Pd(OAc)_2$ (0.112 mM), hexamethylbenzene (20 equiv. relative to $Pd(OAc)_2$), and C_6D_6 (50 mL) was prepared in a volumetric flask. Fisher-Porter reactors were charged with stock solution (20 mL) and copper (II) pivalate (26.9 mM). The vessels were sealed, pressurized with ethylene (50 psig), and stirred while heating in an oil bath to 150 °C. The reactions were sampled every 30 min for 3 h. At each time point the reactors were cooled to room temperature, sampled, recharged with ethylene, and reheated. Aliquots of the reaction mixture were analyzed by GC/FID using relative peak area vs an internal standard (hexamethylbenzene).

Conversion of Benzene and Vinyl Ester to Alkenyl Arene Catalyzed by $Pd(OAc)_2$: General Procedure. A representative catalytic reaction of vinyl ester consumption is described. A stock solution containing 0.001 mol % $Pd(OAc)_2$, internal standard (HMB) and benzene (250 mL) was prepared in a volumetric flask. Thick-walled Fisher-Porter

reactors were charged with stock solution (10 mL), $Cu(OPiv)_2$ (240 equiv. relative to $Pd(OAc)_2$), and 1 mL of ester substrate. The vessels were sealed, pressurized with 70 psig of N_2 and subsequently stirred and heated in oil baths.

3.10 Reference

1. Fujiwara, Y.; Moritani, I.; Danno, S.; Asano, R.; Teranishi, S., Aromatic substitution of olefins. VI. Arylation of olefins with palladium(II) acetate. *J. Am. Chem. Soc.* **1969,** *91* (25), 7166-9.
2. Fujiwara, Y.; Moritani, I.; Matsuda, M.; Teranishi, S., Aromatic substitution of styrene-palladium chloride complex. II effect of metal acetate. *Tetrahedron Lett.* **1968,** *9* (5), 633-636.
3. Fujiwara, Y.; Moritani, I.; Danno, S.; Asano, R.; Teranishi, S., Aromatic substitution of olefins. VI. Arylation of olefins with palladium(II) acetate. *Journal of the American Chemical Society* **1969,** *91* (25), 7166-7169.
4. García-Cuadrado, D.; Braga, A. A. C.; Maseras, F.; Echavarren, A. M., Proton Abstraction Mechanism for the Palladium-Catalyzed Intramolecular Arylation. *Journal of the American Chemical Society* **2006,** *128* (4), 1066-1067.
5. Whisler, M. C.; MacNeil, S.; Snieckus, V.; Beak, P., Beyond thermodynamic acidity: a perspective on the complex-induced proximity effect (CIPE) in deprotonation reactions. *Angew. Chem. Int. Ed. Engl.* **2004,** *43* (17), 2206-25.
6. Dick, A. R.; Sanford, M. S., Transition metal catalyzed oxidative functionalization of carbon–hydrogen bonds. *Tetrahedron* **2006,** *62* (11), 2439-2463.

7. Chen, X.; Engle, K. M.; Wang, D. H.; Yu, J. Q., Palladium(II)-catalyzed C-H activation/C-C cross-coupling reactions: versatility and practicality. *Angew. Chem. Int. Ed. Engl.* **2009,** *48* (28), 5094-115.

8. Daugulis, O.; Do, H. Q.; Shabashov, D., Palladium- and copper-catalyzed arylation of carbon-hydrogen bonds. *Acc. Chem. Res.* **2009,** *42* (8), 1074-86.

9. Ackermann, L., Carboxylate-Assisted Transition-Metal-Catalyzed C−H Bond Functionalizations: Mechanism and Scope. *Chem. Rev.* **2011,** *111* (3), 1315-1345.

10. Colby, D. A.; Bergman, R. G.; Ellman, J. A., Rhodium-Catalyzed C−C Bond Formation via Heteroatom-Directed C−H Bond Activation. *Chem. Rev.* **2010,** *110* (2), 624-655.

11. Lyons, T. W.; Sanford, M. S., Palladium-catalyzed ligand-directed C-H functionalization reactions. *Chem. Rev.* **2010,** *110* (2), 1147-69.

12. Rouquet, G.; Chatani, N., Katalytische Funktionalisierung von C(sp2)-H- und C(sp3)-H-Bindungen unter Verwendung von zweizähnigen dirigierenden Gruppen. *Angew. Chem.* **2013,** *125* (45), 11942-11959.

13. Engle, K. M.; Mei, T. S.; Wasa, M.; Yu, J. Q., Weak coordination as a powerful means for developing broadly useful C-H functionalization reactions. *Acc. Chem. Res.* **2012,** *45* (6), 788-802.

14. Bruckl, T.; Baxter, R. D.; Ishihara, Y.; Baran, P. S., Innate and guided C-H functionalization logic. *Acc. Chem. Res.* **2012,** *45* (6), 826-39.

15. Yeung, C. S.; Dong, V. M., Catalytic dehydrogenative cross-coupling: forming carbon-carbon bonds by oxidizing two carbon-hydrogen bonds. *Chem. Rev.* **2011,** *111* (3), 1215-92.

16. Wencel-Delord, J.; Droge, T.; Liu, F.; Glorius, F., Towards mild metal-catalyzed C-H bond activation. *Chem. Soc. Rev.* **2011,** *40* (9), 4740-61.

17. Davis, H. J.; Phipps, R. J., Harnessing non-covalent interactions to exert control over regioselectivity and site-selectivity in catalytic reactions. *Chem Sci* **2017,** *8* (2), 864-877.

18. Clement, M. L.; Grice, K. A.; Luedtke, A. T.; Kaminsky, W.; Goldberg, K. I., Platinum(II) olefin hydroarylation catalysts: tuning selectivity for the anti-Markovnikov product. *Chem. Eur. J* **2014,** *20* (52), 17287-91.

19. Luedtke, A. T.; Goldberg, K. I., Intermolecular hydroarylation of unactivated olefins catalyzed by homogeneous platinum complexes. *Angew. Chem. Int. Ed. Engl.* **2008,** *47* (40), 7694-6.

20. Bowring, M. A.; Bergman, R. G.; Tilley, T. D., Disambiguation of Metal and Brønsted Acid Catalyzed Pathways for Hydroarylation with Platinum(II) Catalysts. *Organometallics* **2011,** *30* (6), 1295-1298.

21. Karshtedt, D.; Bell, A. T.; Tilley, T. D., Pt−Ag Catalyst System for Hydroarylations with Unactivated Arenes and Olefins. *Organometallics* **2004,** *23* (18), 4169-4171.

22. Karshtedt, D.; McBee, J. L.; Bell, A. T.; Tilley, T. D., Stoichiometric and Catalytic Arene Activations by Platinum Complexes Containing Bidentate Monoanionic Nitrogen-Based Ligands. *Organometallics* **2006,** *25* (7), 1801-1811.

23. McKeown, B. A.; Foley, N. A.; Lee, J. P.; Gunnoe, T. B., Hydroarylation of Unactivated Olefins Catalyzed by Platinum(II) Complexes. *Organometallics* **2008,** *27* (16), 4031-4033.

24. McKeown, B. A.; Gonzalez, H. E.; Friedfeld, M. R.; Brosnahan, A. M.; Gunnoe, T. B.; Cundari, T. R.; Sabat, M., Platinum(II)-Catalyzed Ethylene Hydrophenylation: Switching Selectivity between Alkyl- and Vinylbenzene Production. *Organometallics* **2013,** *32* (9), 2857-2865.

25. McKeown, B. A.; Gonzalez, H. E.; Friedfeld, M. R.; Gunnoe, T. B.; Cundari, T. R.; Sabat, M., Mechanistic studies of ethylene hydrophenylation catalyzed by bipyridyl Pt(II) complexes. *J. Am. Chem. Soc.* **2011,** *133* (47), 19131-52.

26. McKeown, B. A.; Gonzalez, H. E.; Gunnoe, T. B.; Cundari, T. R.; Sabat, M., PtII-Catalyzed Ethylene Hydrophenylation: Influence of Dipyridyl Chelate Ring Size on Catalyst Activity and Longevity. *ACS Catal.* **2013,** *3* (6), 1165-1171.

27. McKeown, B. A.; Gonzalez, H. E.; Michaelos, T.; Gunnoe, T. B.; Cundari, T. R.; Crabtree, R. H.; Sabat, M., Control of Olefin Hydroarylation Catalysis via a Sterically and Electronically Flexible Platinum(II) Catalyst Scaffold. *Organometallics* **2013,** *32* (14), 3903-3913.

28. Burgess, S. A.; Joslin, E. E.; Gunnoe, T. B.; Cundari, T. R.; Sabat, M.; Myers, W. H., Hydrophenylation of ethylene using a cationic Ru(ii) catalyst: comparison to a neutral Ru(ii) catalyst. *Chem. Sci.* **2014,** *5* (11), 4355-4366.

29. Foley, N. A.; Ke, Z.; Gunnoe, T. B.; Cundari, T. R.; Petersen, J. L., Aromatic C−H Activation and Catalytic Hydrophenylation of Ethylene by TpRu{P(OCH2)3CEt}(NCMe)Ph. *Organometallics* **2008,** *27* (13), 3007-3017.

30. Foley, N. A.; Lail, M.; Gunnoe, T. B.; Cundari, T. R.; Boyle, P. D.; Petersen, J. L., Combined Experimental and Computational Study of TpRu{P(pyr)3}(NCMe)Me (pyr =N-pyrrolyl): Inter- and Intramolecular Activation of C−H Bonds and the Impact of Sterics on Catalytic Hydroarylation of Olefins. *Organometallics* **2007,** *26* (23), 5507-5516.

31. Foley, N. A.; Lail, M.; Lee, J. P.; Gunnoe, T. B.; Cundari, T. R.; Petersen, J. L., Comparative reactivity of TpRu(L)(NCMe)Ph (L = CO or PMe3): impact of ancillary ligand l on activation of carbon-hydrogen bonds including catalytic hydroarylation and hydrovinylation/oligomerization of ethylene. *J. Am. Chem. Soc.* **2007,** *129* (21), 6765-81.

32. Foley, N. A.; Lee, J. P.; Ke, Z.; Gunnoe, T. B.; Cundari, T. R., Ru(II) catalysts supported by hydridotris(pyrazolyl)borate for the hydroarylation of olefins: reaction scope, mechanistic studies, and guides for the development of improved catalysts. *Acc. Chem. Res.* **2009,** *42* (5), 585-97.

33. Jia, X.; Gary, J. B.; Gu, S.; Cundari, T. R.; Gunnoe, T. B., Oxidative Hydrophenylation of Ethylene Using a Cationic Ru(II) Catalyst: Styrene Production with Ethylene as the Oxidant. *Isr. J. Chem.* **2017,** *57* (10-11), 1037-1046.

34. Joslin, E. E.; McMullin, C. L.; Gunnoe, T. B.; Cundari, T. R.; Sabat, M.; Myers, W. H., Catalytic Hydroarylation of Ethylene Using TpRu(L)(NCMe)Ph (L = 2,6,7-Trioxa-1-phosphabicyclo[2,2,1]heptane): Comparison to TpRu(L′)(NCMe)Ph Systems (L′ = CO, PMe3, P(pyr)3, or P(OCH2)3CEt). *Organometallics* **2012,** *31* (19), 6851-6860.

35. Joslin, E. E.; Quillian, B.; Gunnoe, T. B.; Cundari, T. R.; Sabat, M.; Myers, W. H., C-H activation of pyrazolyl ligands by Ru(II). *Inorg. Chem.* **2014,** *53* (12), 6270-9.

36. Lail, M.; Arrowood, B. N.; Gunnoe, T. B., Addition of arenes to ethylene and propene catalyzed by ruthenium. *J. Am. Chem. Soc.* **2003,** *125* (25), 7506-7.

37. Lail, M.; Bell, C. M.; Conner, D.; Cundari, T. R.; Gunnoe, T. B.; Petersen, J. L., Experimental and Computational Studies of Ruthenium(II)-Catalyzed Addition of Arene C−H Bonds to Olefins. *Organometallics* **2004,** *23* (21), 5007-5020.

38. Periana, R. A.; Liu, X. Y.; Bhalla, G., Novel bis-acac-O,O-Ir(III) catalyst for anti-Markovnikov, hydroarylation of olefins operates by arene CH activation. *Chem. Commun.* **2002,** (24), 3000-1.

39. Bhalla, G.; Oxgaard, J.; Goddard, W. A.; Periana, R. A., Anti-Markovnikov Hydroarylation of Unactivated Olefins Catalyzed by a Bis-tropolonato Iridium(III) Organometallic Complex. *Organometallics* **2005,** *24* (13), 3229-3232.

40. Oxgaard, J.; Muller, R. P.; Goddard, W. A., 3rd; Periana, R. A., Mechanism of homogeneous Ir(III) catalyzed regioselective arylation of olefins. *J. Am. Chem. Soc.* **2004,** *126* (1), 352-63.

41. Matsumoto, T.; Periana, R. A.; Taube, D. J.; Yoshida, H., Direct Synthesis of Styrene by Rhodium-Catalyzed Oxidative Arylation of Ethylene with Benzene. *J. Catal.* **2002,** *206* (2), 272-280.

42. Chen, J.; Nielsen, R. J.; Goddard, W. A., 3rd; McKeown, B. A.; Dickie, D. A.; Gunnoe, T. B., Catalytic Synthesis of Superlinear Alkenyl Arenes Using a Rh(I) Catalyst Supported by a "Capping Arene" Ligand: Access to Aerobic Catalysis. *J. Am. Chem. Soc.* **2018,** *140* (49), 17007-17018.

43. Webster-Gardiner, M. S.; Chen, J.; Vaughan, B. A.; McKeown, B. A.; Schinski, W.; Gunnoe, T. B., Catalytic Synthesis of “Super” Linear Alkenyl Arenes Using an Easily Prepared Rh(I) Catalyst. *J. Am. Chem. Soc.* **2017,** *139* (15), 5474-5480.

44. Vaughan, B. A.; Webster-Gardiner, M. S.; Cundari, T. R.; Gunnoe, T. B., Organic chemistry. A rhodium catalyst for single-step styrene production from benzene and ethylene. *Science* **2015,** *348* (6233), 421-4.

45. Taube, D.; Periana, R.; Matsumoto, T., Oxidative coupling of olefins and aromatics using a rhodium catalyst and a copper (II) redox agent. Google Patents: 2000.

46. Keith, J. A.; Henry, P. M., The mechanism of the Wacker reaction: a tale of two hydroxypalladations. *Angewandte Chemie International Edition* **2009,** *48* (48), 9038-9049.

47. Jira, R., Acetaldehyde from ethylene--a retrospective on the discovery of the Wacker process. *Angew. Chem. Int. Ed. Engl.* **2009,** *48* (48), 9034-7.

48. Hafner, W.; Jira, R.; Sedlmeier, J.; Smidt, J., Über die Reaktionen von Olefinen mit wäßrigen Lösungen von Palladiumsalzen. *Chem. Ber.* **1962,** *95* (7), 1575-1581.

49. Smidt, J.; Hafner, W.; Jira, R.; Sedlmeier, J.; Sieber, R.; Rüttinger, R.; Kojer, H., Katalytische Umsetzungen von Olefinen an Platinmetall-Verbindungen Das Consortium-Verfahren zur Herstellung von Acetaldehyd. *Angew. Chem.* **1959,** *71* (5), 176-182.

50. Smidt, J.; Hafner, W.; Jira, R.; Sieber, R.; Sedlmeier, J.; Sabel, A., The Oxidation of Olefins with Palladium Chloride Catalysts. *Angew. Chem. Int. Ed.* **1962,** *1* (2), 80-88.

51. Kubota, A.; Emmert, M. H.; Sanford, M. S., Pyridine ligands as promoters in PdII/0-catalyzed C–H olefination reactions. *Org. Lett.* **2012,** *14* (7), 1760-1763.

52. Vaughan, B. A.; Khani, S. K.; Gary, J. B.; Kammert, J. D.; Webster-Gardiner, M. S.; McKeown, B. A.; Davis, R. J.; Cundari, T. R.; Gunnoe, T. B., Mechanistic Studies of Single-Step Styrene Production Using a Rhodium(I) Catalyst. *J. Am. Chem. Soc.* **2017,** *139* (4), 1485-1498.

53. Holder, G. A.; Macauley, D., Solubility of ethylene in benzene at pressures to 9 MPa and temperatures from 353 to 433 K. *Journal of Chemical & Engineering Data* **1992,** *37* (1), 100-104.

54. Miura, M.; Tsuda, T.; Satoh, T.; Pivsa-Art, S.; Nomura, M., Oxidative Cross-Coupling of N-(2‘-Phenylphenyl)benzene- sulfonamides or Benzoic and Naphthoic Acids with Alkenes Using a Palladium−Copper Catalyst System under Air. *The Journal of Organic Chemistry* **1998,** *63* (15), 5211-5215.

55. Zhu, W.; Luo, Z.; Chen, J.; Liu, C.; Yang, L.; Dickie, D. A.; Liu, N.; Zhang, S.; Davis, R. J.; Gunnoe, T. B., Mechanistic Studies of Single-Step Styrene Production Catalyzed by Rh Complexes with Diimine Ligands: An Evaluation of the Role of Ligands and Induction Period. *ACS Catal.* **2019,** *9* (8), 7457-7475.

56. Yoneyama, T.; Crabtree, R. H., Pd(II) catalyzed acetoxylation of arenes with iodosyl acetate. *J. Mol. Catal. A: Chem.* **1996,** *108* (1), 35-40.

57. Cook, A. K.; Sanford, M. S., Mechanism of the palladium-catalyzed arene C-H acetoxylation: a comparison of catalysts and ligand effects. *J. Am. Chem. Soc.* **2015,** *137* (8), 3109-18.

58. Northcutt, T. O.; Wick, D. D.; Vetter, A. J.; Jones, W. D., Investigation of the mechanism of alkane reductive elimination and skeletal isomerization in Tp'Rh(CNneopentyl)(R)H complexes: the role of alkane complexes. *J. Am. Chem. Soc.* **2001,** *123* (30), 7257-70.

59. Vetter, A. J.; Flaschenriem, C.; Jones, W. D., Alkane coordination selectivity in hydrocarbon activation by [Tp'Rh(CNneopentyl)]: the role of alkane complexes. *J. Am. Chem. Soc.* **2005,** *127* (35), 12315-22.

60. Simmons, E. M.; Hartwig, J. F., On the interpretation of deuterium kinetic isotope effects in C-H bond functionalizations by transition-metal complexes. *Angew. Chem. Int. Ed. Engl.* **2012,** *51* (13), 3066-72.

61. Cundari, T. R.; Grimes, T. V.; Gunnoe, T. B., Activation of carbon-hydrogen bonds via 1,2-addition across M-X (X = OH or NH(2)) bonds of d(6) transition metals as a potential key step in hydrocarbon functionalization: a computational study. *J. Am. Chem. Soc.* **2007,** *129* (43), 13172-82.

62. Xie, L.; Suh, M. P., Flexible metal-organic framework with hydrophobic pores. *Chem. Eur. J* **2011,** *17* (49), 13653-6.

4 Direct Comparison between Pd(II) and Rh(I) Catalyzed Oxidative Olefin Hydroarylation

4.1 Introduction

The Gunnoe lab has performed extensive studies of rhodium catalyzed arene alkenylation.[1-8] We have studied Rh catalyzed arene alkenylation using olefins and α-olefins under anaerobic and aerobic conditions and have applied this methodology for the synthesis of stilbene and its derivatives (see Chapter 5). Palladium, which is adjacent to rhodium on the periodic table, has also been proven to be an excellent catalyst for C–C coupling and C–H activation reactions.[9-42] Pd catalyzed oxidative olefin hydroarylation is emerging as a useful tool for organic synthesis.[43-48] We have recently reported an optimized process for palladium(II) acetate catalyzed oxidative olefin hydroarylation using unactivated benzene and ethylene with high selectivity for the benzene alkenylation product.[2] Since Pd(II) and Rh(I) share similar electronic structures, we hypothesized that oxidative hydroarylation catalyzed by Pd and Rh may involve similar reaction pathways (Scheme 4.1). Herein, we sought to delineate differences in catalysis using closely related Rh(I) and Pd(II) catalyst precursors.

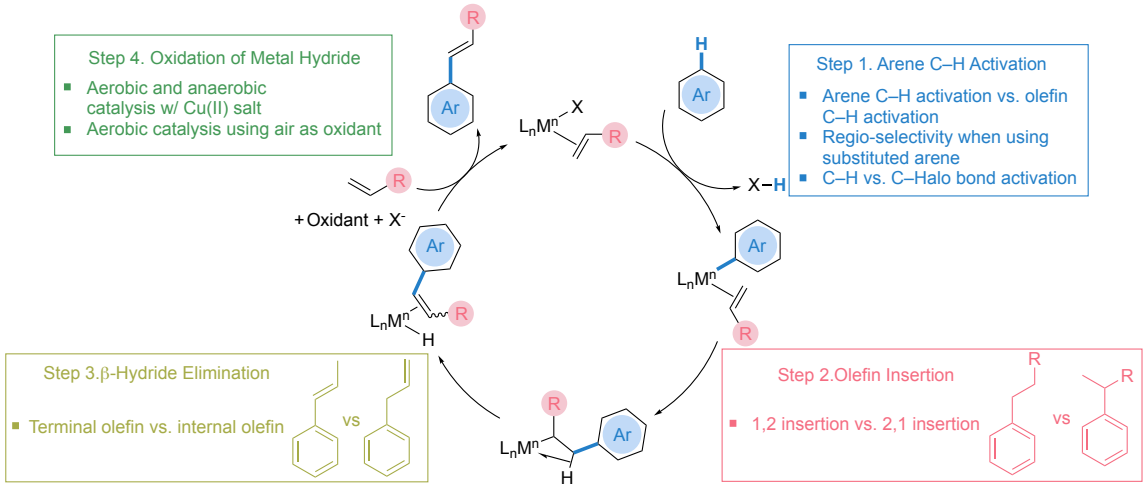

Scheme 4.1. Possible catalytic cycles for Rh(I) and Pd(II) catalyzed arene alkenylation, X = carboxylate (e.g., acetate, trimethylacetate/pivalate, trifluoroacetate, etc.).

Four basic steps are involved in the possible arene alkenylation catalytic cycles shown in Scheme 4.1, including: 1) concerted metalation deprotonation (CMD) C–H activation of the arene mediated by the Rh or Pd carboxylate catalyst, 2) olefin insertion into the metal-aryl bond to form a Rh- or Pd-phenethyl intermediate, 3) β-hydride elimination of the metal-phenethyl intermediate to generate a metal olefin hydride complex, and 4) release of the alkenylated product and oxidation of the metal hydride to regenerate the metal catalyst.

Previously, the Gunnoe group reported that a Rh ethylene acetate dimer complex $[Rh(\mu\text{-}OAc)(\eta^2\text{-}C_2H_4)]_2$ serves as a catalyst precursor that converts α-olefins and arenes to alkenyl arenes with high anti-Markovnikov (i.e., linear) selectivity in the presence of Cu(II) carboxylate oxidants (Scheme 4.2).[6] Oxidative hydroarylation of benzene and propylene with the Rh complex are selective for linear products, and the Rh-catalyzed reactions of benzene with isobutylene and neohexene are selective linear alkenyl arenes. We have also

discovered that Rh catalysis has shown different regioselectivity when using substituted arenes as substrates when compared to Friedel Crafts alkylation. Rh catalysis gives almost no ortho-functionalization as approximately 2:1 meta: para selectivity is generally observed. In contrast, for Friedel-Crafts alkylation, the o:m:p selectivity is dependent on the electronic properties of the functional group(s) on the arene.

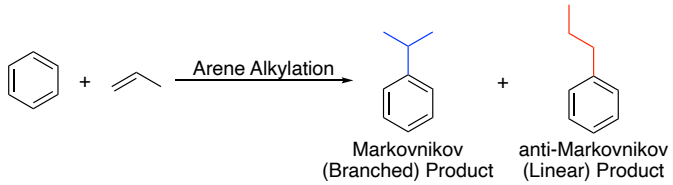

Scheme 4.2. Selectivity in catalytic benzene alkylation using propylene to produce propylbenzenes.

In this chapter, we detail experimental comparisons of catalytic arene alkenylation using Rh(I) and Pd(II) catalyst precursors. Specifically, we compared: 1) catalytic styrene production from benzene and ethylene; 2) catalytic conversion from vinyl ester and arene to alkenyl arene using vinyl pivalate/acetate and benzene; 3) catalytic alkenylation of mono-substituted arene; 4) catalytic alkenylation of halogenated arene; 5) catalytic alkenylation of benzene using α-olefins.

4.2 Catalytic Styrene Production via C–H activation

4.2.1 Arene C–H activation vs. olefin C–H activation

It has been demonstrated that both Rh and Pd can serve as catalysts for oxidative ethylene hydrophenylation to produce styrene. [1, 4-8, 49] Under the conditions we discussed in the previous Pd catalysis chapter (see Chapter 3), one of the major byproducts in Pd

catalyzed arene alkenylation using CuX_2 (X = carboxylate) as the oxidant is the vinyl ester, which is produced from olefin functionalization by the Pd catalyst. [49] A large amount of vinyl acetate production has been observed at high ethylene pressure and low reaction temperature. We have shown in Chapter 3 that at higher reaction temperatures, the Pd catalysis produces less vinyl pivalate, which is due to a palladium catalyzed reaction that converts vinyl pivalate and benzene to styrene. However, under most conditions in our previous Rh studies, only a trace amount of vinyl ester product was observed, and the conversion of vinyl esters to alkenyl arenes was minimal (Scheme 4.3). To probe the differences in arene vs alkene C–H bond functionalization selectivity, Rh and Pd catalyzed ethylene hydrophenylation reactions were studied under identical conditions (Table 4.1).

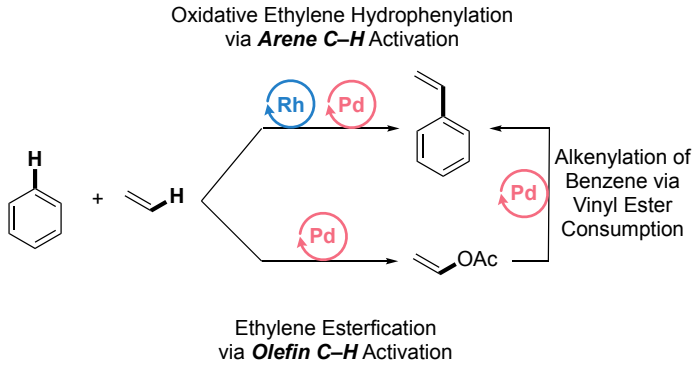

Scheme 4.3. Benzene C–H, ethylene C–H functionalization and vinyl ester consumption mediated by Rh and/or Pd complexes.

Table 4.1. Anaerobic ethylene hydrophenylation using $Pd(OAc)_2$ or $[Rh(\eta^2\text{-}C_2H_4)_2(\mu\text{-}OAc)]_2$ as the catalyst precursor with copper(II) pivalate as oxidant. Conditions: 0.001 mol%

$Pd(OAc)_2$ or $[Rh(\eta^2\text{-}C_2H_4)_2(\mu\text{-}OAc)]_2$, 240 equivalents of copper(II) pivalate, 45 psig of ethylene.

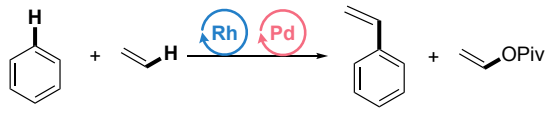

[M]	Temperature (°C)	Styrene (TOs)	Vinyl pivalate (TOs)	Selectivity (% Styrene)
[Pd]	120	88(2)	19(1)	82
	150	112(1)	4.5(5)	96
[Rh]	120	97(4)	2.0(7)	98
	150	110(4)	3.0(1)	97

As shown in Table 4.1, both Rh and Pd complexes catalyzed the oxidative ethylene hydrophenylation to produce styrene at 120 °C and 150 °C. At 120 ºC, after complete consumption of copper(II) oxidant (as indicated by color change from blue to colorless), Pd catalysis produced more vinyl acetate, the olefin functionalization byproduct, than rhodium (19 TOs vs. 2 TOs of vinyl acetate), revealing relatively poor selectivity for the Pd catalyzed process compared to use of Rh as catalyst. The differences in the selectivity between Pd and Rh catalysis were less significant at 150 ºC, where only 4.5 TOs of vinyl acetate was produced by Pd catalysis and 3 TOs by Rh catalysis. We attribute this selectivity change to a Pd-catalyzed side reaction that converts vinyl ester and benzene to alkenyl benzene, which previous study revealed only occurs at temperatures > 135 ºC under our reaction conditions (Chapter 3).[49] Generally, Pd catalysis has shown a greater propensity for olefin functionalization than rhodium catalysis has.

4.2.2 Vinyl ester consumption and metathesis using Pd catalyst

The discovery of Pd catalyzed conversion of vinyl ester and benzene to alkenyl benzene (Chapter 3) has provided a rationale for the higher styrene selectivity that has been observed at high reaction temperatures (e.g., > 135 °C).[49] Vinyl ester consumption reaction was performed at different temperatures with both Pd and Rh catalyst precursors in the presence of vinyl ester and benzene to probe the differences in reactivity between Pd and Rh (Table 4.2). As shown in Table 4.2, Pd converts vinyl acetate and benzene to styrene at temperatures > 135 ºC. In addition to the desired product styrene, stilbene was also observed, which is a product of an additional benzene alkenylation reaction using styrene as the olefin substrate.

Table 4.2. Catalytic conversion of vinyl acetate to styrene under different temperatures and amount of vinyl acetate in benzene. Conditions: 0.001 mol% $Pd(OAc)_2$ or $[Rh(\eta^2\text{-}C_2H_4)_2(\mu\text{-}OAc)]_2$, 240 equivalents of copper(II) pivalate and 100 or 5000 equivalents of vinyl acetate.

[M]	Temperature (°C)	Vinyl acetate (equiv.)	Styrene (TOs)	Vinyl Pivalate (TOs)
[Pd]	120	100	0	0
	135	100	17(2)	2
	150	100	95(2)	2
[Rh]	120	100	0	0
	135	100	0	4(2)
	150	100	0	-
	150	5000	9(2)	40(7)

4.2.3 Comparison of turnover frequencies for the Rh and Pd catalyzed processes for the consumption of vinyl ester

Table 4.3. Turnover frequencies of the Rh and Pd catalyzed conversion of vinyl pivalate to styrene in benzene. Conditions: 0.001 mol% $Pd(OAc)_2$ or $[Rh(\eta\text{-}C_2H_4)_2(\mu\text{-}OAc)]_2$, 240 equivalents of copper pivalate and 150 equivalents of vinyl pivalate. The TOF is calculated from the slope of TOs vs. time plots.

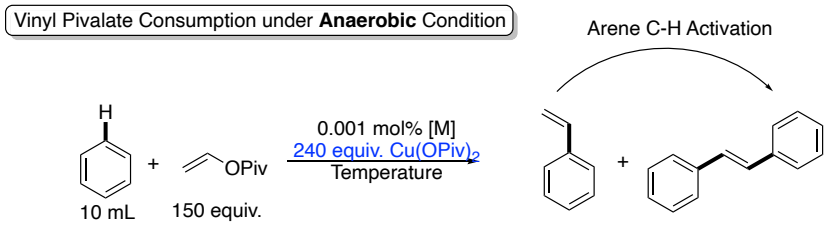

[M]	Temperature (°C)	TOF for styrene formation (s^{-1})	TOF of Alkenylation[a] (s^{-1})
[Pd]	150	0.0039	0.0062
	180	-	0.0139
[Rh]	150	-	0.00014
	180	-	0.00035

[a] TOF of Alkenylation is the total TOF of catalytic styrene and stilbene production.

The turnover frequencies of the Rh/Pd catalyzed consumption of vinyl pivalate are shown in Table 4.3. At both 150 °C and 180 °C, Pd catalysis is significantly faster than Rh catalysis. With the Rh catalyst, styrene was not observed in the final reaction mixture, indicating that the Rh catalyzed styrene production reaction proceeded faster than the conversion of vinyl ester to alkenylbenzene in benzene.

4.2.4 Regioselectivity for arene alkenylation reactions with substituted arenes

Unlike acid-based alkylation chemistry where regioselectivity is determined by the electronic properties of arene functional groups, the regioselectivity of transition metal-catalyzed arene alkenylation of substituted arenes can be catalyst directed. As a result, consistent regioselectivity for a single catalyst can be achieved, potentially, for different substituted arenes.

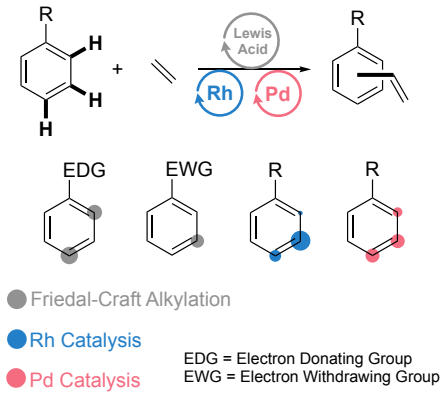

Scheme 4.4. Regioselectivities in acid-based Friedel-Craft alkylation, and Rh/Pd catalyzed arene alkenylation.

As shown in Scheme 4.4, the regioselectivity Friedel-Crafts alkylation reaction favors the generation of *ortho* and *para* products for substrates with EDG substituents and *meta* products for substrates with EWG substituents. In our previous studies about Rh mediated oxidative propylene hydroarylation, a 2:1 meta:para ratio is observed when we use mono-substituted benzene.[1, 3, 6] The regioselectivity differences between Pd and Rh catalyzed

alkenylation was probed using toluene, chlorobenzene, and anisole as the arene candidates, and ethylene, styrene and methyl acrylate as the olefins (Table 4.4).

Table 4.4. Distribution of regioisomers for the alkenylation of mono-substituted arenes using Rh or Pd catalysts. The table shows percent selectivity for alkenylation of each position. Conditions: 5 mL arene, 45 psig of ethylene or 1 mmol of olefin, 0.001 mol% of [Rh] or [Pd] ([Rh] = $[Rh(C_2H_4)_2OAc]_2$; [Pd] = $Pd(OAc)_2$), 240 equiv. of $Cu(OPiv)_2$, 480 equiv. of HOPiv, 15 psig of air, 150 °C, 12 hours.

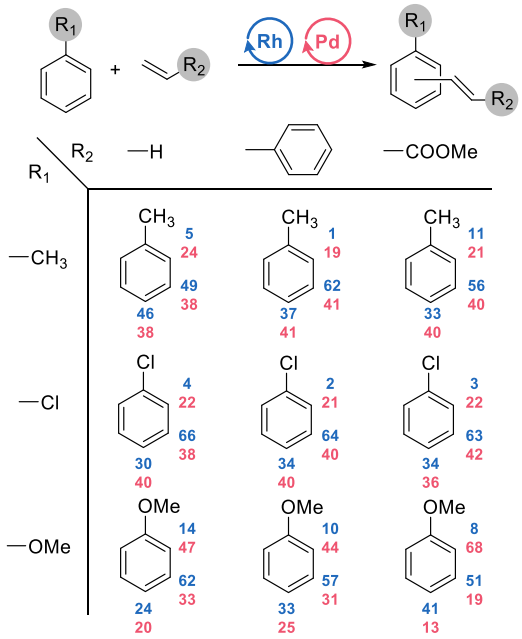

The reactions with toluene and chlorobenzene gave very consistent results. The ortho functionalization in Rh catalysis is minimal in both cases and the *meta*:*para* functionalization ratio is very close to 2:1. When using anisole as the arene substrate, we observed an small increase in the generation of the ortho-substituted product for both Rh and Pd catalysis. We attribute this change to the weak coordination (directing) effect of the -OMe to the Rh and Pd center that allowes for more ortho functionalization. Using Pd catalysis, ortho functionalization was more significant than using Rh catalysis for all of the

studied substrates. Using $Pd(OAc)_2$ as catalyst precursor, the reaction with toluene and chlorobenzene resulted in an ~1:2:2 ortho:meta:para ratio of functionalized products. Because of the directing effect of the methoxy substituent, the reaction with anisole produced greater ortho functionalization, and, in the case of ethylene, styrene and methyl arylate as olefin, the ortho product was the major product. In both Rh and Pd catalysis, electronic effects have a minimal influence on regioselectivity, as shown by similar results for the electron-rich arenes, toluene and anisole, and the electron deficient chlorobenzene.

4.2.5 Comparison of C–X and C–H bond activation

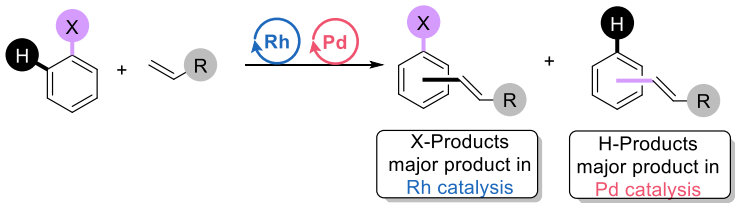

Scheme 4.5. C–H vs. C–X functionalization. (X = Br and I)

A variety of catalytic C–C bond coupling reaction that operate through C–X (X = halogen) bond activation have been developed based on Suzuki, Sonogashira, Stille, Heck and related reactions.[22, 24, 26, 27, 31, 35, 40, 50-55]The Pd catalyzed C–C bond coupling reaction has been broadly studied and Pd(0) species have demonstrated the ability to activate C–X bonds via oxidative addition.[43] Rhodium(I) catalyst precursors, however, have shown better tolerance of C–X bonds and more readily activate C–H bonds. For example, we have demonstrated that Rh-catalyzed stilbene production that Rh catalysis is tolerant of some halogenation functionalities.[2]

For arene alkenylation, we sought to compare tolerance of halogen functionality for Pd versus Rh catalysis. Thus, arene alkenylation catalysis was examined using $Pd(OAc)_2$ as catalyst precursor. Using chlorobenzene, the desired product mixture (*ortho*, *meta* and *para* isomers) can be obtained after 24 hours at reaction conditions with the same product distribution (approximately 1:2:2 *ortho*:*meta*:*para* ratio is observed). When using bromobenzene and iodobenzene as the substrates, Pd catalysis shows lower tolerance of halide functionality. The reaction of bromobenzene with $Pd(OAc)_2$ produces a large amount of stilbene, with a 1:1 ratio of stilbene:bromostilbene, which likely results from C–Br bond activation in lieu of C–H bond activation. When using iodobenzene, the reaction produces trace amounts of iodostilbene, which indicates that Pd favors activation of C–I versus C–H bonds.

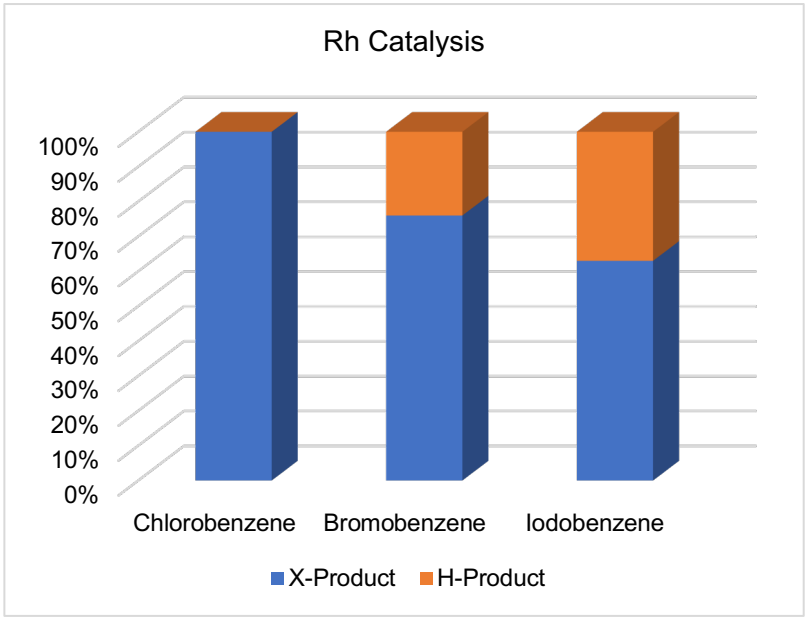

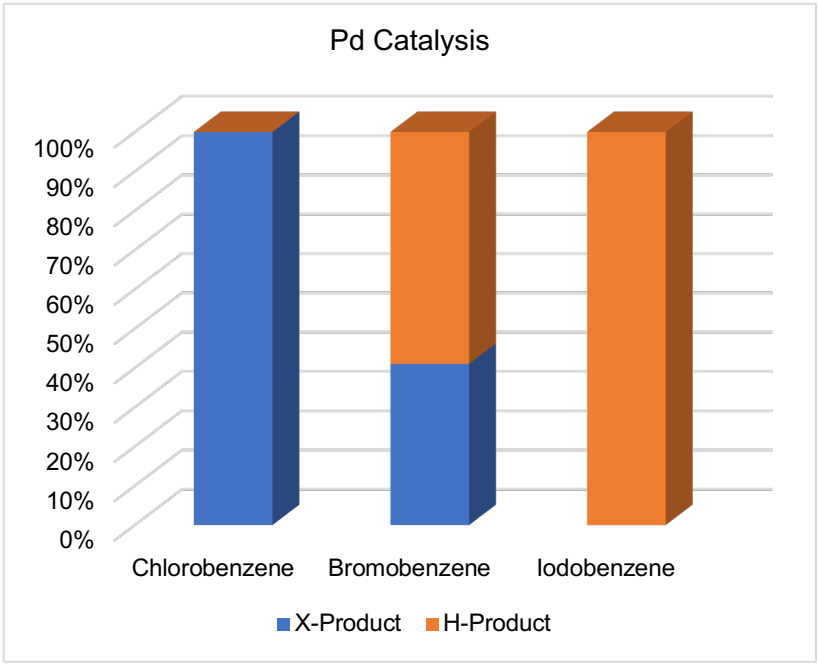

Figure 4.1. Products distrubution of the chloro-, bromo- and Iodobenzene alkenylation using methyl acrylate catalyzed by Pd or Rh. Conditions: 5 mL arene, 1 mmol of methylacrylate, 0.001 mol% of [Rh] or [Pd] ([Rh] = $[Rh(C_2H_4)_2OAc]_2$; [Pd] = $Pd(OAc)_2$), 240 equiv. of $Cu(OPiv)_2$, 480 equiv. of HOPiv, 15 psig of air, 150 °C, 12 hours.

Figure 4.1 shows the selectivity of the reaction with halogenated arenes catalyzed by Rh(top figure) and Pd(bottom figure) catalyst precursors. The same trend is observed from the rection. Rh catalysis has shown better functional group tolerance when reacting with bromobenzene and iodobenzene where 76% and 63% C–H activation products were observed, respectively. Pd catalysis, however, produced only 41% C–H activation products with bromobenzene, and exclusively activates C–I bonds in the reaction with iodobenzene.

4.3 Selectivities for arene alkenylation using α-olefins

The Gunnoe group has studied Rh(I) catalysts for arene alkenylation using α-olefins extensively in recent years.[1, 6] High selectivity for anti-Markovnikov linear alkenyl arene products, which cannot be synthesized using Friedel-Crafts acid-based reactions, has been demonstrated, providing a route to "super" linear alkyl arenes (1-phenyl-n-alkanes) upon hydrogenation. [6] Recently we have supported Rh(I) with a carefully designed "capping arene" ligand, making the catalysis more tolerant of aerobic conditions.[1] Regardless of the Rh(I) catalyst precursor used, our study of Rh catalyzed arene alkenylation shows selectivity for linear product with linear:branched (L:B) ratios of 8:1 up to 18:1 (depending on specific conditions).

4.3.1 Reaction optimization for Pd catalyzed propylene hydrophenylation

We first investigated the linear to branched selectivity of the $Pd(OAc)_2$ catalyzed propylene hydrophenylation reaction, which gives three major benzene alkenylation

products including two linear products: allylbenzene, β-methylstyrene, and one branched product, α-methylstyrene. The Pd catalyzed propylene hydrophenylation operates under anaerobic conditions. Heating 5 mL benzene solutions of $Pd(OAc)_2$ in the presence of 240 equivalents of $Cu(OPiv)_2$ under 0 (saturate benzene solution of propylene with 1 atm top pressure of propylene) or 35 psig of propylene, results in complete reaction after 2 hours at 150 ºC, as indicated by the change in color from blue, due to Cu(II), to pale bronze, due to Cu(I), with an approximate 75% yield (relative to $Cu(OPiv)_2$) of propylenebenzenes (Table 4.5).

Table 4.5. Product distribution in Rh and Pd catalyzed propylene hydrophenylation. Conditions: 5 mL benzene, 0.001 mol% of [Pd] ([Pd] = $Pd(OAc)_2$), 240 equiv. of $Cu(OPiv)_2$, 150 °C, 12 hours.

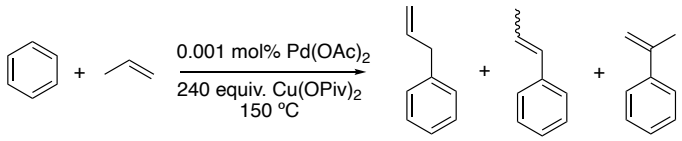

Propylene pressure (psig)	Allylbenzene (TOs)	β-methylstyrenes	α-methylstyrene	L:B
0	4.0(1)	74.2(7)	14.7(2)	5.4 : 1
35	3.3(2)	65.7(9)	13.0(2)	5.3 : 1

As shown in Table 4.5, all three propenylbenzene products were observed. The catalysis favored production of linear products, and β-methylstyrene was the major product. Oxidative propylene hydrophenylation reaction was performed under air with 4Å molecular sieves as a drying agent gave very little propenylbenzene production under 35 psig propylene pressure (127 TOs). The yield is improved when a lower pressure of

propylene is used: 269 TOs of propenylbenzenes under 15 psig propylene, 398 TOs under 5 psig and 420 TOs under 0 psig of propylene pressure (saturate benzene solution of propylene with 1 atm propylene pressure) were observed.

This inverse dependence on ethylene pressure had been observed in our previously reported Pt(II) and Ru(II) catalyzed ethylene hydrophenylation reactions. In those studies, we attribute the suppression of the catalysis by ethylene to the off-cycle $M(CH_2CH_2Ph)(\eta^2\text{-}C_2H_4)$ (M = Pt, Ru) [56, 57]. A similar observation has been made by Periana, Goddard and coworkers for Ir catalysis.(REF) In the Pd catalysis, although further studies are required to determine why the higher propylene suppresses the catalysis, but we hypothesize that high olefin concentration under reaction condition might facilitate olefin functionalization to produce vinyl ester. Another observation from these experiments is, under aerobic conditions, the L:B ratio is independent of olefin pressure but higher than under anaerobic conditions.

Table 4.6. Aerobic $Pd(OAc)_2$ catalyzed propylene hydrophenylation at different propylene pressures. Conditions: 5 mL benzene, 0.001 mol% of [Pd] ([Pd] = $Pd(OAc)_2$), 240 equiv. of $Cu(OPiv)_2$, 400 mg 4Å molecular sieves 150 °C, 12 hours.

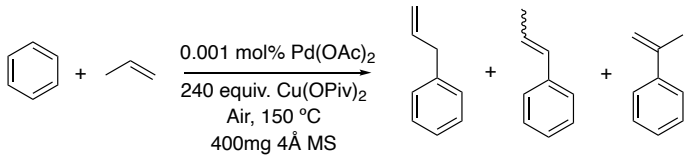

propylene pressure (psig)	allylbenzene (TOs)	β-methylstyrenes (TOs)	α-methylstyrene (TOs)	L:B
35	9(1)	101(7)	17(2)	6.5 : 1

15	12(4)	222(11)	35(1)	6.7 : 1
5	10(1)	335(9)	53(2)	6.5 : 1
0*	3(1)	363(17)	54	6.8 : 1

The effect of the pivalic acid additive was also investigated. The reactions were performed aerobically with different amounts of HOPiv, but no significant change in L:B ratio was observed (Table 4.7).

Table 4.7. Aerobic $Pd(OAc)_2$ catalyzed propylene hydrophenylation using different amount of HOPiv. Conditions: 5 mL benzene, 0.001 mol% of [Pd] ([Pd] = $Pd(OAc)_2$), 240 equiv. of $Cu(OPiv)_2$, 400 mg 4Å molecular sieves 150 °C, 12 hours.

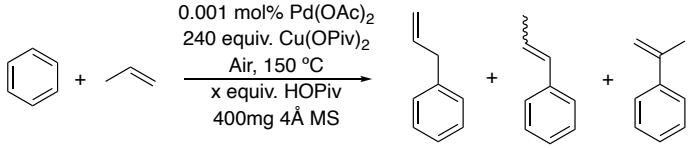

HOPiv (equiv)	Allylbenzene (TOs)	β-methylstyrenes	α-methylstyrene	L:B
0	3(1)	363(17)	54(7)	6.8 : 1
240	2.0(4)	249(1)	36(1)	7 : 1
480	6.1(7)	309(7)	46(5)	6.8 : 1
960	7.0(4)	353(21)	54(9)	6.7
2400	3.2(4)	379(8)	55(4)	6.9

4.3.2 Comparison of Pd and Rh catalyzed propylene hydrophenylation

The summary of Rh and Pd catalyzed propylene hydrophenylation is shown in **Figure 4.2**. Under identical conditions, propylene hydrophenylation catalyzed by Pd(II) and Rh(I) salts both favored the generation of linear products (*i.e.*, allylbenzene and β-methylstyrenes); however, the distribution of the products was different. Rh catalysis gave a higher L:B of 9: while Pd gave a L:B of 5:1. Moreover, the selectivity for allyl benzene versus β-methylstyrenes is different for Rh versus Pd. The major linear product in the Pd

catalysis is β-methylstyrenes (> 90%), while Rh catalysis gave ~1:1 ratio of β-methylstyrenes to allylbenzene.

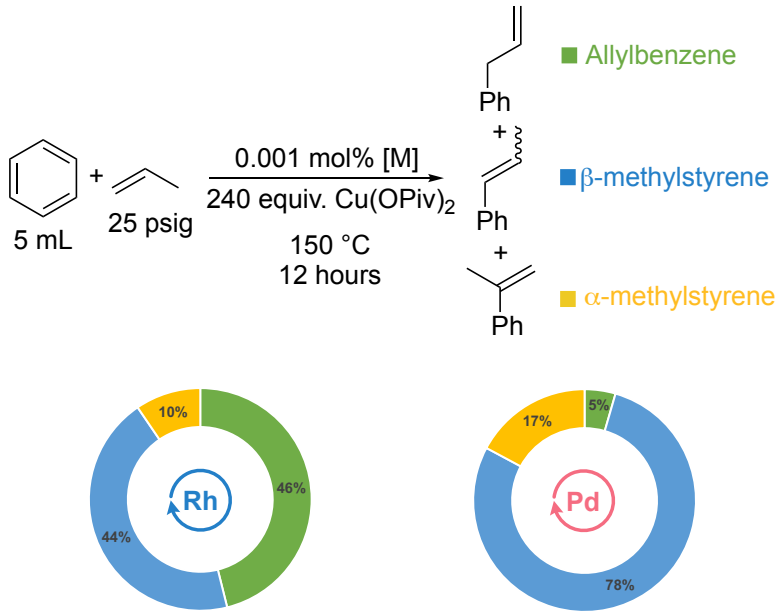

Figure 4.2. Product distributions of propylene hydrophenylation catalyzed by $Pd(OAc)_2$ and $[Rh(\eta^2\text{-}C_2H_4)_2(\mu\text{-}OAc)]_2$ Conditions: Catalyst loading: 0.001 mol%, 240 equiv. $Cu(OPiv)_2$, 25 psig propylene, 150 °C, reaction run to completion (all copper consumed)

Previous work has revealed that for the Rh(I) complex (5-FP)Rh(TFA)(η^2-C_2H_4) (5-FP = 1,2-bis(N-7-azaindolyl)benzene; TFA = trifluoroacetate), the L:B ratio of products increases from 11:1 to 18:1 when the temperature is decreased from 150 °C to 80 °C[1] We probed the anaerobic propylene hydrophenylation reaction using Rh(I) and Pd(II) salts under different reaction temperatures and found a similar trend (Figure 4.3). Also, the allylbenzene : β-methylstyrenes ratios were affected by the temperature.

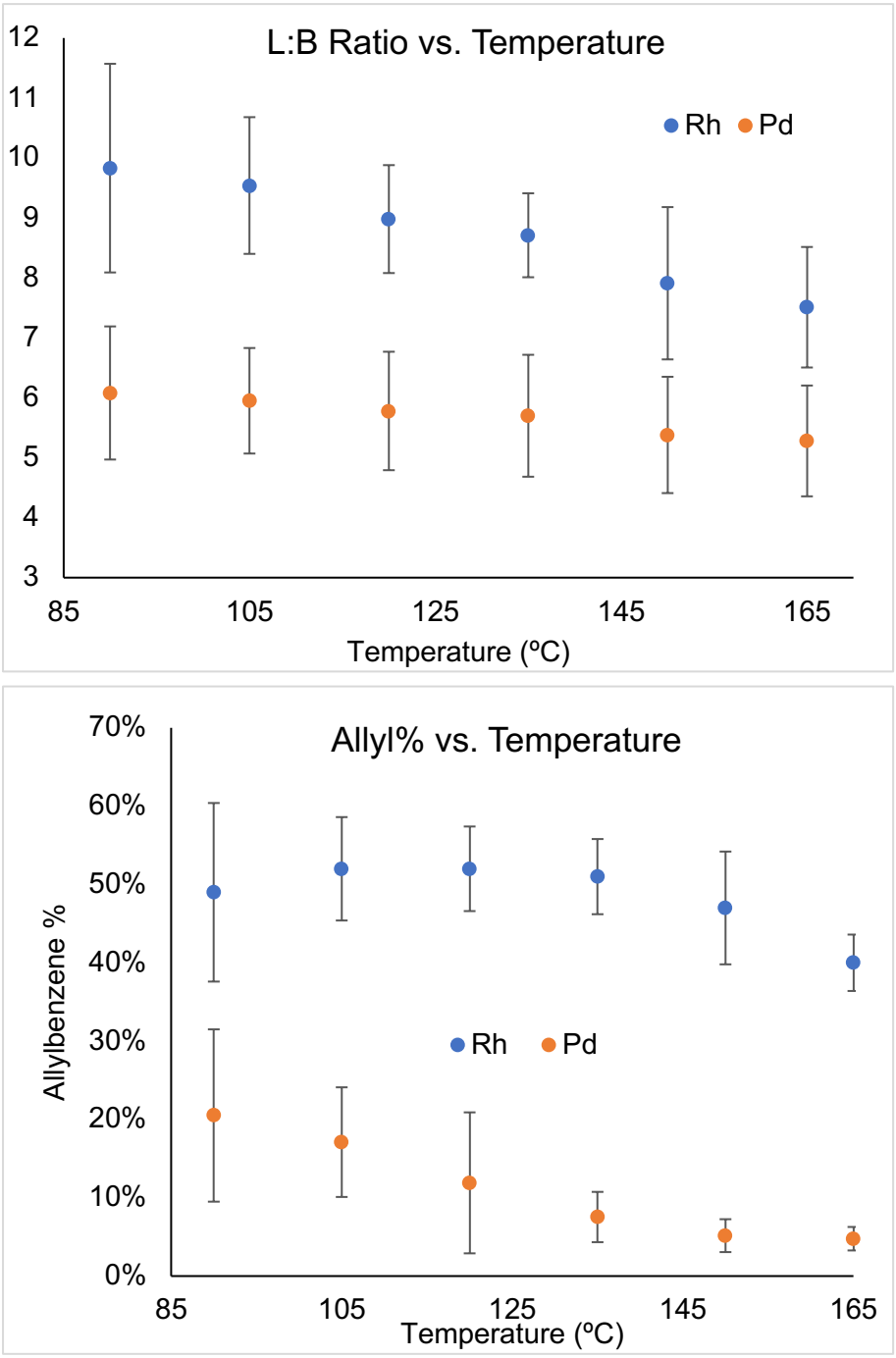

Figure 4.3. L:B ratio and allylbenzene % (of total linear products) to temperature plot from oxidaive propylene hydrophenylation reactions. Conditions: 5 mL benzene, 25 psig of

propylene, 0.001 mol% of [Rh] or [Pd] ([Rh] = $[Rh(C_2H_4)_2OAc]_2$; [Pd] = $Pd(OAc)_2$), 240 equiv. of $Cu(OPiv)_2$, 480 equiv. of HOPiv.

As shown in Figure 4.3, varying the temperature had an impact on the L:B ratio for both Rh and Pd catalysis. At 90 ºC, the catalysis is very slow. After 24 hours, only 16 TOs and 21 TOs of propenylbenzene products were observed for Pd and Rh catalysis, respectively, resulting in a large deviation of L:B ratio. The linear to branched ratio is 9.8:1 for Rh catalysis and 6.1:1 for Pd. Higher reaction temperatures (105 ºC, 120 ºC, 135 ºC, 150 ºC and 165 ºC) were studied for both Rh and Pd, and a decreased L:B ratio was observed with increasing reaction temperature. At 165 ºC, L:B ratios of 7.5:1 and 5.3:1 were observed for Rh and Pd catalysis, respectively. In addition to the L:B ratio, temperature also influences the linear product distribution. Figure 4.3b shows the percent allylbenzene, which is the percentage of allylbenzene in total linear product (β-methylstyrenes + allylbenzene), versus temperature. At 85 ºC, 49% of linear products from Rh catalysis is allylbenzene and 20% of linear products from Pd catalysis is allylbenzene. At higher temperature, the percentage of allylbenzene decreases for both Rh and Pd catalysis. At 165 ºC, the percent allylbenzene product decreases to 40% and 5% for Rh and Pd catalysis, respectively. This observation could be explained by the higher reaction temperature facilitating the formation of β-methylstyrenes through metal catalyzed isomerization. To evaluate the thermodynamic composition of the different alkenes at the equilibrium, DFT calculations of allylbenzene and respective isomers of β-methylstyrenes

have been reported previously (Table 4.8).[58] As shown in Table 4.8, β-transmethylstyrene is the most thermodynamically favored product. It is ~6 kcal/mol lower energy than allylbenzene.

Table 4.8. Energy values for the different alkene isomers calculated for allylbenzene.[50]

	Relative energies (kcal/mol)		
Temperature (°C)	**allylbenzene**	**β-trans-methylstyrene**	**β-cis-methylstyrene**
0	7.74	0	2.84
25	6.58	0	3.39
50	6.59	0	3.21

4.3.3 Allylbenzene isomerization studies

Additional studies were performed to quantify the linear to branched ratio and selectivity for allylbenzene versus β-methylstyrenes. It has been reported that late transition metals can catalyze isomerization between propenylbenzene species.[59] Accordingly, we considered that both Pd(II) and Rh(I) salts could produce the kinetic product allylbenzene in an early stage of the reaction, and then Pd(II) catalyzes an isomerization of allylbenzene to yield the more thermodynamically favorable β-methylstyrenes.[58]

To examine this hypothesis, allylbenzene was added to the oxidative propylene hydrophenylation reaction (Scheme 4.6). Only minimal isomerization of allylbenzene was detected, and the majority of the allylbenzene served as an olefin substrate and was converted to the oxidative hydroarylation product 1,3-diphenylpropylene which is identified by GC-MS.

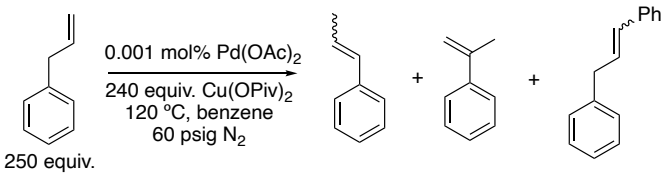

Scheme 4.6. Study of possible allylbenzene isomerization in the presence of $Pd(OAc)_2$. Conditions: 5 mL benzene, 0.001 mol% of [Pd] ([Pd] = $Pd(OAc)_2$), 250 equiv. allylbenzene, 240 equiv. of $Cu(OPiv)_2$, 120 °C. 12 h

Additional studies of allylbenzene isomerization were performed in the presence of ethylene. Ethylene was pressurized to the reaction mixture that contain allylbenzene and Rh catalysts to suppress allylbenzene oxidative hydroarylation by replacing allylbenzene as the olefin (assuming that ethylene would compete with allylbenzene kinetically).[5] The product of oxidative ethylene hydroarylation, styrene, will not affect the propenylbenzene distribution. The results showed no isomerization of allylbenzene (Figure 4.4). Under our catalytic conditions, there is no evidence of allylbenzene isomerization by Pd catalysis.

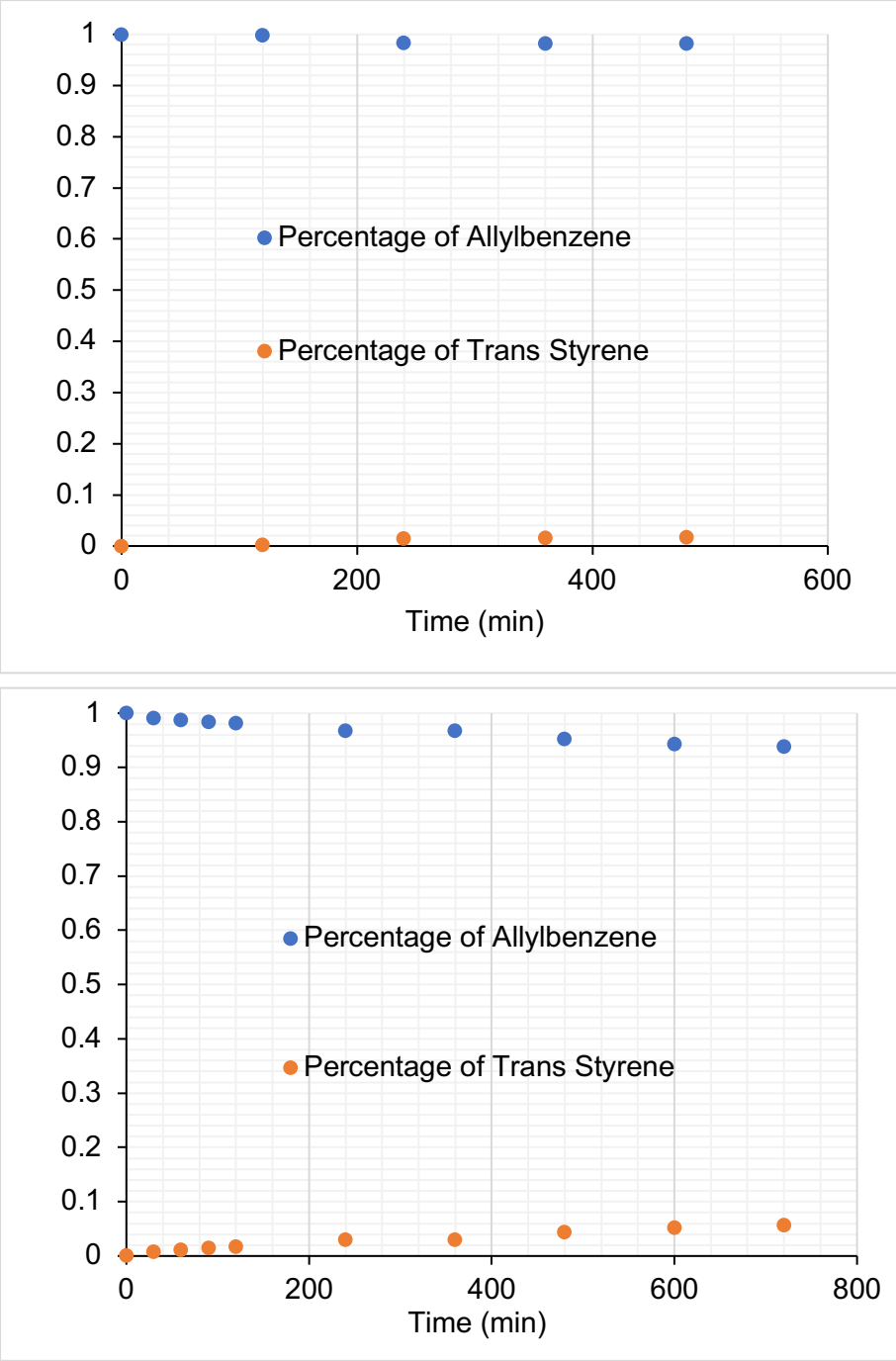

Figure 4.4. Product distribution of Pd-mediated allylbenzene isomerizatoin

4.4 Summary

In this chapter, we have compared the differences in catalytic performances and selectivities for palladium and rhodium catalyzed arene alkenylation reactions.

1) Pd catalysis shows a greater propensity for olefin functionalization to form vinyl acetates than rhodium catalysis. But, at 150 °C Pd is more reactive than Rh for the conversion of vinyl ester and benzene to alkenylarenes.
2) For catalysis using mono-substituted arene, an approximate 2:1 meta:para (very little ortho) ratio is observed for Rh catalysis whereas an appoximate 1:2:2 ortho:meta:para ratio is observed for Pd catalysis.
3) For the reaction with bromo- and iodo benzene, Rh catalysis shows tolerance of the halogenated functionalities to give C–H alkenylation products; however, Pd favors activation of C–I versus C–H bonds.
4) In propylene hydrophenylation reaction, Rh catalysis gives higher L:B ratio (linear = anti-Markovnikov products; branched = Markovnikov products) than the Pd catalyzed processes; ratio of allylbenzene to β-trans-methylstyrene varies greatly between Rh (1.2) and Pd (0.06).

4.5 Experimental Section

General Considerations Unless otherwise noted, all synthetic procedures were performed under anaerobic conditions in a nitrogen-filled glovebox or by using standard Schlenk techniques. Glovebox purity was maintained by periodic nitrogen purges and was

monitored by an oxygen analyzer (O_2 < 15 ppm for all reactions). Benzene was purified by passage through a column of activated alumina. ^{1}H NMR spectra were recorded on a Varian 600 spectrometer. ^{1}H NMR spectra are referenced against residual proton signals (^{1}H NMR) of the deuterated solvents. GC/MS was performed using a Shimadzu GCMS-QP2010 Plus system with a 30 m x 0.25 mm RTx-Qbond column with 8 μm thickness using electron impact ionization. GC/FID was performed using a Shimadzu GC-2014 system with a 30 m x 90.25 mm HP5 column with 0.25 μm film thickness. Ethylbenzene, cumene, styrene, phenylacetate, phenyl pivalate, cumene, allylbenzene, α-methylstyrene, trans-β-methylstyrene, cis-β-methylstyrene, and biphenyl production was quantified using linear regression analysis of gas chromatograms of standard samples of an authentic product. A plot of peak area ratios versus molar ratios gave a regression line using hexamethylbenzene as the internal standard. For the GC/FID instrument, the slope and correlation coefficient of the regression lines were 1.72 and 0.99 (ethylbenzene), 1.67 and 0.99 (styrene), 0.87 and 0.99 (trans-stilbene), 1.67 and 0.99 (phenylacetate), 1.22 and 0.99 (phenyl pivalate), 1.99 and 0.99 (cumene), 1.40 and 0.99 (allylbenzene), 1.23 and 0.99 (α-methylstyrene), 1.47 and 0.99 (cis-β-methylstyrene), 1.38 and 0.99 (trans-β-methylstyrene), and 0.96 and 0.99 (biphenyl), respectively. Propylene and ethylene were purchased in gas cylinders from GTSWelco and used as received. Copper(II) pivalate and di-μ-acetatotetrakis(dihaptoethene)dirhodium(I) ([Rh(*h*-C_2H_4)(*m*-OAc)]$_2$) was synthesized

according to a published procedure.[60, 61] All other reagents were used as received from commercial sources.

Catalytic Oxidative Ethylene Hydrophenylation under Anaerobic Condition using Pd or Rh as Catalyst A representative catalytic reaction under anaerobic condition is described. Stock solutions containing (6.3 mg, 0.028 mmol) $Pd(OAc)_2$ or (6.1mg 0.014 mmol) $[Rh(\eta\text{-}C_2H_4)(\mu\text{-}OAc)]_2$, HMB (hexamethylbenzene) (0.091 g, 0.56 mmol), and benzene (250 mL) was prepared in two volumetric flasks. Thick-walled Andrews Glass™ Lab-Crest® Fisher-Porter tube with a stir bar reactors were charged with stock solution (10 mL) and $Cu(OPiv)_2$ (240 equiv. relative to metal). The vessels were sealed, pressurized with ethylene, and subsequently stirred and heated in oil baths under 120 and 150 °C. The reactions were sampled after all copper was consumed, as indicated by a change in the color of the reaction from blue to colorless. Aliquots of the reaction mixture were analyzed by GC/FID using relative peak areas versus the internal standard.

Catalytic Vinyl Acetate Consumption using Pd or Rh Catalyst under Anaerobic condition A representative catalytic reaction under anaerobic condition is described. Stock solutions containing (6.3 mg, 0.028 mmol) $Pd(OAc)_2$ or (6.1mg 0.014 mmol) $[Rh(\eta\text{-}C_2H_4)(\mu\text{-}OAc)]_2$, HMB (hexamethylbenzene) (0.091 g, 0.56 mmol), and benzene (250 mL) was prepared in two volumetric flasks. Thick-walled Andrews Glass™ Lab-Crest® Fisher-Porter tube with a stir bar reactors were charged with stock solution (10 mL), 100 or 1000 equiv. of vinyl acetate and $Cu(OPiv)_2$ (240 equiv. relative to metal). The vessels were

sealed, pressurized with ethylene, and subsequently stirred and heated in oil baths under 120, 135 and 150 °C. The reactions were sampled after all copper was consumed, as indicated by a change in the color of the reaction from blue to colorless. Aliquots of the reaction mixture were analyzed by GC/FID using relative peak areas versus the internal standard.

Turnover Frequencies of Pd and Rh Catalyzed Vinyl Acetate Consumption A representative catalytic reaction under anaerobic condition is described. Stock solutions containing (6.3 mg, 0.028 mmol) $Pd(OAc)_2$ or (6.1mg 0.014 mmol) $[Rh(\eta\text{-}C_2H_4)(\mu\text{-}OAc)]_2$, HMB (hexamethylbenzene) (0.091 g, 0.56 mmol), and benzene (250 mL) was prepared in two volumetric flasks. Thick-walled Andrews Glass™ Lab-Crest® Fisher-Porter tube with a stir bar reactors were charged with stock solution (10 mL), 150 equiv. of vinyl acetate and $Cu(OPiv)_2$ (240 equiv. relative to metal). The vessels were sealed, pressurized with ethylene, and subsequently stirred and heated in oil baths under 150 and 180 °C. The reactions were sampled after 30 minutes Aliquots of the reaction mixture were analyzed by GC/FID using relative peak areas versus the internal standard. Turnover frequencies are calculated by the average rate of the first 30 minutes of the reaction.

Catalytic mono substituted Arene Alkenylation Catalyzed by Pd and Rh Under an atmosphere of dry nitrogen, $[Rh(\eta\text{-}C_2H_4)(\mu\text{-}OAc)]_2$ (1.25 μmol, 550 μg) or $Pd(OAc)_2$ (2.5 μmol, 560 μg), copper(II) pivalate (400 μmol, 106 mg), and pivalic acid (2 mmol, 204 mg) were added into a dried Andrews Glass™ Lab-Crest® Fisher-Porter tube with a stir

bar. Then olefin (500 μmol, styrene or methyl acrylate or 45 psig ethylene) and mono substituted arene (5 mL) were added by syringe. Then the tube was opened to air, sealed, and pressurized with dinitrogen (60 psig for the experiments with styrene and methyl acrylate, 15 psig for the experiments with ethylene). The mixture was stirred at 165 °C. After 24 h, the reaction was allowed to cool to room temperature. The resultant mixture was diluted with ethyl acetate (40 mL) and washed with saturated sodium carbonate solution (50 mL). The crude reaction mixtures were analyzed by GC/FID using relative peak areas. The aqueous and organic layers were separated. The aqueous layer was extracted with ethyl acetate (3 × 40 mL) and the combined organic layers were washed with water, (3 × 10 mL), dried over magnesium sulfate, filtered, and concentrated under vacuum. ^{1}H NMR of the purified solid was taken using $CDCl_3$ as solvent to get the accurate ratio of each regio isomers

Catalytic Halogenated Arene Alkenylation Catalyzed by Pd and Rh Under an atmosphere of dry nitrogen, $[Rh(\eta\text{-}C_2H_4)(\mu\text{-}OAc)]_2$ (1.25 μmol, 550 μg) or $Pd(OAc)_2$ (2.5 μmol, 560 μg), copper(II) pivalate (400 μmol, 106 mg), and pivalic acid (2 mmol, 204 mg) were added into a dried Andrews Glass™ Lab-Crest® Fisher-Porter tube with a stir bar. Then olefin (500 μmol, styrene or methyl acrylate or 45 psig ethylene) and halogenated arene (5 mL) were added by syringe. Then the tube was opened to air, sealed, and pressurized with dinitrogen (60 psig for the experiments with styrene and methyl acrylate, 15 psig for the experiments with ethylene). The mixture was stirred at 165 °C. After 24 h,

the reaction was allowed to cool to room temperature. The resultant mixture was diluted with ethyl acetate (40 mL) and washed with saturated sodium carbonate solution (50 mL). The crude reaction mixtures were analyzed by GC/FID using relative peak areas. The aqueous and organic layers were separated. The aqueous layer was extracted with ethyl acetate (3 × 40 mL) and the combined organic layers were washed with water, (3 × 10 mL), dried over magnesium sulfate, filtered, and concentrated under vacuum. ^{1}H NMR of the purified solid was taken using $CDCl_3$ as solvent to get the accurate ratio of each product.

Catalytic Oxidative Propylene Hydrophenylation under Anaerobic Condition using $Pd(OAc)_2$ as Catalyst A representative catalytic reaction under anaerobic condition is described. A stock solution containing $Pd(OAc)_2$ (0.063 g, 0.028 mmol), HMB (hexamethylbenzene) (0.091 g, 0.56 mmol), and benzene (250 mL) was prepared in a volumetric flask. Thick-walled Fisher-Porter reactors were charged with stock solution (10 mL) and $Cu(OPiv)_2$ (240 equiv. relative to $Pd(OAc)_2$). The vessels were sealed, pressurized with 0 or 35 psig of propylene and subsequently stirred and heated in oil baths. The reactions were sampled after all copper was consumed, as indicated by a change in the color of the reaction from blue to colorless. Aliquots of the reaction mixture were analyzed by GC/FID using relative peak areas versus the internal standard.

Catalytic Oxidative Propylene Hydrophenylation under Aerobic Condition using $Pd(OAc)_2$ as Catalyst A representative catalytic reaction under anaerobic condition is described. A stock solution containing $Pd(OAc)_2$ (0.063 g, 0.028 mmol), HMB

(hexamethylbenzene) (0.091 g, 0.56 mmol), and benzene (250 mL) was prepared in a volumetric flask. Thick-walled Fisher-Porter reactors were charged with stock solution (10 mL) and $Cu(OPiv)_2$ (240 equiv. relative to $Pd(OAc)_2$). The vessels was opened to air and then were sealed, pressurized with 0 or 35 psig of propylene and subsequently stirred and heated in oil baths. The reactions were sampled after 12 hours. Aliquots of the reaction mixture were analyzed by GC/FID using relative peak areas versus the internal standard.

Catalytic Oxidative Propylene Hydrophenylation under Aerobic Condition using $Pd(OAc)_2$ as Catalyst with different amount of HOPiv A representative catalytic reaction under anaerobic condition is described. A stock solution containing $Pd(OAc)_2$ (0.063 g, 0.028 mmol), HMB (hexamethylbenzene) (0.091 g, 0.56 mmol), and benzene (250 mL) was prepared in a volumetric flask. Thick-walled Fisher-Porter reactors were charged with stock solution (10 mL), $Cu(OPiv)_2$ (240 equiv. relative to $Pd(OAc)_2$) and 0, 240, 480, 960 and 2400 equiv. of HOPiv. The vessels was opened to air and then were sealed, pressurized with 0 or 35 psig of propylene and subsequently stirred and heated in oil baths. The reactions were sampled after 12 hours. Aliquots of the reaction mixture were analyzed by GC/FID using relative peak areas versus the internal standard.

Catalytic Oxidative Propylene Hydrophenylation under Aerobic Condition using Pd and Rh: The Influence of Reaction Temperature A representative catalytic reaction under anaerobic condition is described. Stock solutions containing (6.3 mg, 0.028 mmol) $Pd(OAc)_2$ or (6.1mg 0.014 mmol) $[Rh(\eta\text{-}C_2H_4)(\mu\text{-}OAc)]_2$, HMB (hexamethylbenzene)

(0.091 g, 0.56 mmol), and benzene (250 mL) was prepared in two volumetric flasks. Thick-walled Andrews Glass™ Lab-Crest® Fisher-Porter tube with a stir bar reactors were charged with stock solution (10 mL), 480 equiv. of HOPiv and $Cu(OPiv)_2$ (240 equiv. relative to metal). The vessels were sealed, pressurized with propylene, and subsequently stirred and heated in oil baths under 90, 105, 120, 135, 150 and 165 °C. The reactions were sampled after all copper was consumed, as indicated by a change in the color of the reaction from blue to colorless. Aliquots of the reaction mixture were analyzed by GC/FID using relative peak areas versus the internal standard.

Catalytic Isomerization of Allylbenzene using Pd using $Pd(OAc)_2$ as Catalyst A representative catalytic reaction under anaerobic condition is described. A stock solution containing $Pd(OAc)_2$ (0.063 g, 0.028 mmol), HMB (hexamethylbenzene) (0.091 g, 0.56 mmol), and benzene (250 mL) was prepared in a volumetric flask. Thick-walled Fisher-Porter reactors were charged with stock solution (10 mL), 250 equiv. of allylbenzene and $Cu(OPiv)_2$ (240 equiv. relative to $Pd(OAc)_2$). The vessels were sealed, pressurized with 60 psig of dinitrogen and subsequently stirred and heated in oil baths. The reactions were sampled every 30 minutes. Aliquots of the reaction mixture were analyzed by GC/FID using relative peak areas versus the internal standard.

4.6 Reference

1. Chen, J.; Nielsen, R. J.; Goddard, W. A., 3rd; McKeown, B. A.; Dickie, D. A.; Gunnoe, T. B., Catalytic Synthesis of Superlinear Alkenyl Arenes Using a Rh(I) Catalyst Supported by a "Capping Arene" Ligand: Access to Aerobic Catalysis. *J. Am. Chem. Soc.* **2018,** *140* (49), 17007-17018.

2. Jia, X.; Frye, L. I.; Zhu, W.; Gu, S.; Gunnoe, T. B., Synthesis of Stilbenes by Rhodium-Catalyzed Aerobic Alkenylation of Arenes via C–H Activation. *Journal of the American Chemical Society* **2020,** *142* (23), 10534-10543.

3. Liebov, N. S.; Zhu, W.; Chen, J.; Webster-Gardiner, M. S.; Schinski, W. L.; Gunnoe, T. B., Rhodium-Catalyzed Alkenylation of Toluene Using 1-Pentene: Regioselectivity To Generate Precursors for Bicyclic Compounds. *Organometallics* **2019,** *38* (19), 3860-3870.

4. Vaughan, B. A.; Khani, S. K.; Gary, J. B.; Kammert, J. D.; Webster-Gardiner, M. S.; McKeown, B. A.; Davis, R. J.; Cundari, T. R.; Gunnoe, T. B., Mechanistic Studies of Single-Step Styrene Production Using a Rhodium(I) Catalyst. *J. Am. Chem. Soc.* **2017,** *139* (4), 1485-1498.

5. Vaughan, B. A.; Webster-Gardiner, M. S.; Cundari, T. R.; Gunnoe, T. B., Organic chemistry. A rhodium catalyst for single-step styrene production from benzene and ethylene. *Science* **2015,** *348* (6233), 421-424.

6. Webster-Gardiner, M. S.; Chen, J.; Vaughan, B. A.; McKeown, B. A.; Schinski, W.; Gunnoe, T. B., Catalytic Synthesis of "Super" Linear Alkenyl Arenes Using an Easily Prepared Rh(I) Catalyst. *J. Am. Chem. Soc.* **2017,** *139* (15), 5474-5480.

7. Zhu, W.; Gunnoe, T. B., Advances in Rhodium-Catalyzed Oxidative Arene Alkenylation. *Acc. Chem. Res.* **2020,** *53* (4), 920-936.

8. Zhu, W.; Luo, Z.; Chen, J.; Liu, C.; Yang, L.; Dickie, D. A.; Liu, N.; Zhang, S.; Davis, R. J.; Gunnoe, T. B., Mechanistic Studies of Single-Step Styrene Production Catalyzed by Rh Complexes with Diimine Ligands: An Evaluation of the Role of Ligands and Induction Period. *ACS Catal.* **2019,** *9* (8), 7457-7475.

9. Culkin, D. A.; Hartwig, J. F., Palladium-Catalyzed α-Arylation of Carbonyl Compounds and Nitriles. *Acc. Chem. Res.* **2003,** *36* (4), 234-245.

10. Hartwig, J. F., Electronic Effects on Reductive Elimination To Form Carbon−Carbon and Carbon−Heteroatom Bonds from Palladium(II) Complexes. *Inorg. Chem.* **2007,** *46* (6), 1936-1947.

11. Johns, A. M.; Utsunomiya, M.; Incarvito, C. D.; Hartwig, J. F., A Highly Active Palladium Catalyst for Intermolecular Hydroamination. Factors that Control Reactivity and Additions of Functionalized Anilines to Dienes and Vinylarenes. *Journal of the American Chemical Society* **2006,** *128* (6), 1828-1839.

12. Kuwano, R.; Utsunomiya, M.; Hartwig, J. F., Aqueous Hydroxide as a Base for Palladium-Catalyzed Amination of Aryl Chlorides and Bromides. *The Journal of Organic Chemistry* **2002,** *67* (18), 6479-6486.

13. Lee, S. Y.; Hartwig, J. F., Palladium-Catalyzed, Site-Selective Direct Allylation of Aryl C–H Bonds by Silver-Mediated C–H Activation: A Synthetic and Mechanistic Investigation. *Journal of the American Chemical Society* **2016,** *138* (46), 15278-15284.

14. Nettekoven, U.; Hartwig, J. F., A New Pathway for Hydroamination. Mechanism of Palladium-Catalyzed Addition of Anilines to Vinylarenes. *Journal of the American Chemical Society* **2002,** *124* (7), 1166-1167.

15. Cook, A. K.; Sanford, M. S., Mechanism of the palladium-catalyzed arene C-H acetoxylation: a comparison of catalysts and ligand effects. *J. Am. Chem. Soc.* **2015,** *137* (8), 3109-3118.

16. Dick, A. R.; Kampf, J. W.; Sanford, M. S., Platinum Model Studies for Palladium-Catalyzed Oxidative Functionalization of C−H Bonds. *Organometallics* **2005,** *24* (4), 482-485.

17. Lotz, M. D.; Camasso, N. M.; Canty, A. J.; Sanford, M. S., Role of Silver Salts in Palladium-Catalyzed Arene and Heteroarene C–H Functionalization Reactions. *Organometallics* **2017,** *36* (1), 165-171.

18. Lyons, T. W.; Sanford, M. S., Palladium-catalyzed ligand-directed C-H functionalization reactions. *Chem. Rev.* **2010,** *110* (2), 1147-1169.

19. Neufeldt, S. R.; Sanford, M. S., Controlling site selectivity in palladium-catalyzed C-H bond functionalization. *Acc. Chem. Res.* **2012,** *45* (6), 936-946.

20. Remy, M. S.; Cundari, T. R.; Sanford, M. S., Computational and Experimental Studies of Methyl Group Exchange between Palladium(II) Centers. *Organometallics* **2010,** *29* (7), 1522-1525.

21. Stowers, K. J.; Sanford, M. S., Mechanistic comparison between Pd-catalyzed ligand-directed C-H chlorination and C-H acetoxylation. *Org. Lett.* **2009,** *11* (20), 4584-4587.

22. Albeniz, A. C.; Espinet, P.; Martin-Ruiz, B.; Milstein, D., Catalytic system for Heck reactions involving insertion into Pd-(perfluoro-organyl) bonds. *J. Am. Chem. Soc.* **2001,** *123* (46), 11504-11505.

23. Albéniz, A. C.; Espinet, P.; Martín-Ruiz, B.; Milstein, D., Catalytic System for the Heck Reaction of Fluorinated Haloaryls. *Organometallics* **2005,** *24* (15), 3679-3684.

24. Andrus, M. B.; Liu, J.; Meredith, E. L.; Nartey, E., Synthesis of resveratrol using a direct decarbonylative Heck approach from resorcylic acid. *Tetrahedron Lett.* **2003,** *44* (26), 4819-4822.

25. Aouf, C.; Thiery, E.; Le Bras, J.; Muzart, J., Palladium-catalyzed dehydrogenative coupling of furans with styrenes. *Org. Lett.* **2009,** *11* (18), 4096-4099.

26. Beletskaya, I. P.; Cheprakov, A. V., The heck reaction as a sharpening stone of palladium catalysis. *Chem. Rev.* **2000,** *100* (8), 3009-3066.

27. Botella, L.; Nájera, C., Synthesis of methylated resveratrol and analogues by Heck reactions in organic and aqueous solvents. *Tetrahedron* **2004,** *60* (26), 5563-5570.

28. Eberhard, M. R., Insights into the Heck Reaction with PCP Pincer Palladium(II) Complexes. *Org. Lett.* **2004,** *6* (13), 2125-2128.

29. Girase, T. R.; Kapdi, A. R., Novel Carbazole-Based N-Heterocyclic Carbene Ligands to Access Synthetically Relevant Stilbenes in Pd-Catalyzed Coupling Processes. *Chem Asian J* **2019,** *14* (15), 2611-2619.

30. Han, G.; Xia, J.; Gao, J.; Inagaki, Y.; Tang, W.; Kokudo, N., Anti-tumor effects and cellular mechanisms of resveratrol. *Drug Discov Ther* **2015,** *9* (1), 1-12.

31. Heck, R. F.; Nolley, J. P., Palladium-Catalyzed Vinylic Hydrogen Substitution Reactions with Aryl, Benzyl, and Styryl Halides. *J. Org. Chem.* **1972,** *37* (14), 2320-&.

32. Kumar, B. S.; Anbarasan, R.; Amali, A. J.; Pitchumani, K., Isolable C@Fe3O4 nanospheres supported cubical Pd nanoparticles as reusable catalysts for Stille and Mizoroki-Heck coupling reactions. *Tetrahedron Lett.* **2017,** *58* (33), 3276-3282.

33. Le Bras, J.; Muzart, J., Intermolecular dehydrogenative Heck reactions. *Chem. Rev.* **2011,** *111* (3), 1170-1214.

34. Li, H.; He, K. H.; Liu, J.; Wang, B. Q.; Zhao, K. Q.; Hu, P.; Shi, Z. J., Straightforward synthesis of phenanthrenes from styrenes and arenes. *Chem Commun (Camb)* **2012,** *48* (56), 7028-7030.

35. McGlacken, G. P.; Bateman, L. M., Recent advances in aryl-aryl bond formation by direct arylation. *Chem. Soc. Rev.* **2009,** *38* (8), 2447-2464.

36. Moro, A. V.; Cardoso, F. S. P.; Correia, C. R. D., Heck arylation of styrenes with arenediazonium salts: short, efficient, and stereoselective synthesis of resveratrol, DMU-212, and analogues. *Tetrahedron Lett.* **2008,** *49* (39), 5668-5671.

37. Rodriguez, N.; Goossen, L. J., Decarboxylative coupling reactions: a modern strategy for C-C-bond formation. *Chem. Soc. Rev.* **2011,** *40* (10), 5030-5048.

38. Wang, S. M.; Song, H. X.; Wang, X. Y.; Liu, N.; Qin, H. L.; Zhang, C. P., Palladium-catalyzed Mizoroki-Heck-type reactions of [Ph2SRfn][OTf] with alkenes at room temperature. *Chem Commun (Camb)* **2016,** *52* (80), 11893-11896.

39. Wang, Y.-P.; Lee, H. M., Catalytic application of zwitterionic palladium complexes in Mizoroki–Heck reactions using ionic liquid as solvent. *J. Organomet. Chem.* **2015,** *791*, 90-98.

40. Yamada, Y. M.; Takeda, K.; Takahashi, H.; Ikegami, S., Assembled catalyst of palladium and non-cross-linked amphiphilic polymer ligand for the efficient heterogeneous Heck reaction. *Tetrahedron* **2004,** *60* (18), 4097-4105.

41. Ying, C.; Yan, S.; Duan, W., 2-Hydroxy-1,10-phenanthroline vs 1,10-phenanthroline: significant ligand acceleration effects in the palladium-catalyzed oxidative Heck reaction of arenes. *Org. Lett.* **2014,** *16* (2), 500-503.

42. Zhou, A.; Guo, R.-M.; Zhou, J.; Dou, Y.; Chen, Y.; Li, J.-R., Pd@ZIF-67 Derived Recyclable Pd-Based Catalysts with Hierarchical Pores for High-Performance Heck Reaction. *ACS Sustainable Chemistry & Engineering* **2018,** *6* (2), 2103-2111.

43. Chen, X.; Engle, K. M.; Wang, D. H.; Yu, J. Q., Palladium(II)-catalyzed C-H activation/C-C cross-coupling reactions: versatility and practicality. *Angew. Chem. Int. Ed. Engl.* **2009,** *48* (28), 5094-5115.

44. Engle, K. M.; Mei, T. S.; Wasa, M.; Yu, J. Q., Weak coordination as a powerful means for developing broadly useful C-H functionalization reactions. *Acc. Chem. Res.* **2012,** *45* (6), 788-802.

45. Shi, B.-F.; Zhang, Y.-H.; Lam, J. K.; Wang, D.-H.; Yu, J.-Q., Pd(II)-Catalyzed Enantioselective C−H Olefination of Diphenylacetic Acids. *Journal of the American Chemical Society* **2010,** *132* (2), 460-461.

46. Vora, H. U.; Silvestri, A. P.; Engelin, C. J.; Yu, J.-Q., Rhodium(II)-catalyzed nondirected oxidative alkenylation of arenes: arene loading at one equivalent. *Angew. Chem. Int. Ed. Engl.* **2014,** *53* (10), 2683-2686.

47. Wang, P.; Verma, P.; Xia, G.; Shi, J.; Qiao, J. X.; Tao, S.; Cheng, P. T. W.; Poss, M. A.; Farmer, M. E.; Yeung, K.-S.; Yu, J.-Q., Ligand-accelerated non-directed C-H functionalization of arenes. *Nature* **2017,** *551* (7681), 489-493.

48. Yang, Y.-F.; Cheng, G.-J.; Liu, P.; Leow, D.; Sun, T.-Y.; Chen, P.; Zhang, X.; Yu, J.-Q.; Wu, Y.-D.; Houk, K. N., Palladium-Catalyzed Meta-Selective C–H Bond Activation with a Nitrile-Containing Template: Computational Study on Mechanism and Origins of Selectivity. *Journal of the American Chemical Society* **2014,** *136* (1), 344-355.

49. Jia, X.; Foley, A. M.; Liu, C.; Vaughan, B. A.; McKeown, B. A.; Zhang, S.; Gunnoe, T. B., Styrene Production from Benzene and Ethylene Catalyzed by Palladium(II): Enhancement of Selectivity toward Styrene via Temperature-dependent Vinyl Ester Consumption. *Organometallics* **2019,** *38* (19), 3532-3541.

50. Stille, J. K., The Palladium-Catalyzed Cross-Coupling Reactions of Organotin Reagents with Organic Electrophiles [New Synthetic Methods (58)]. *Angewandte Chemie International Edition in English* **1986,** *25* (6), 508-524.

51. Sonogashira, K., Development of Pd–Cu catalyzed cross-coupling of terminal acetylenes with sp2-carbon halides. *J. Organomet. Chem.* **2002,** *653* (1), 46-49.

52. Miyaura, N.; Suzuki, A., Palladium-Catalyzed Cross-Coupling Reactions of Organoboron Compounds. *Chem. Rev.* **1995,** *95* (7), 2457-2483.

53. Nomura, K.; Suzuki, N.; Matsumoto, S., *Biochemistry* **1990,** *29*, 4525.

54. Yoshida, J. i.; Suga, S.; Suzuki, S.; Kinomura, N.; Yamamoto, A.; Fujiwara, K., *J. Am. Chem. Soc.* **1999,** *121*, 9546.

55. Lautens, M.; Piguel, S., A New Route to Fused Aromatic Compounds by Using a Palladium-Catalyzed Alkylation – Alkenylation Sequence. *Angew. Chem. Int. Ed.* **2000,** *39* (6), 1045-1046.

56. McKeown, B. A.; Gonzalez, H. E.; Friedfeld, M. R.; Gunnoe, T. B.; Cundari, T. R.; Sabat, M., Mechanistic studies of ethylene hydrophenylation catalyzed by bipyridyl Pt(II) complexes. *J. Am. Chem. Soc.* **2011,** *133* (47), 19131-19152.

57. Foley, N. A.; Lee, J. P.; Ke, Z.; Gunnoe, T. B.; Cundari, T. R., Ru(II) catalysts supported by hydridotris(pyrazolyl)borate for the hydroarylation of olefins: reaction scope, mechanistic studies, and guides for the development of improved catalysts. *Acc. Chem. Res.* **2009,** *42* (5), 585-597.

58. Scarso, A.; Colladon, M.; Sgarbossa, P.; Santo, C.; Michelin, R. A.; Strukul, G., Highly Active and Selective Platinum(II)-Catalyzed Isomerization of Allylbenzenes: Efficient Access to (E)-Anethole and Other Fragrances via Unusual Agostic Intermediates. *Organometallics* **2010,** *29* (6), 1487-1497.

59. Hassam, M.; Taher, A.; Arnott, G. E.; Green, I. R.; van Otterlo, W. A., Isomerization of allylbenzenes. *Chem. Rev.* **2015,** *115* (11), 5462-5569.

60. Xie, L.; Suh, M. P., Flexible metal-organic framework with hydrophobic pores. *Chem. Eur. J* **2011,** *17* (49), 13653-13656.

61. Werner, H.; Poelsma, S.; Schneider, M. E.; Windmüller, B.; Barth, D., Synthesis and Reactivity of Bis(ethene) Rhodium(I) and Iridium(I) Carboxylato Complexes. *Chem. Ber.* **1996,** *129* (6), 647-652.

5 Synthesis of Stilbenes by Rhodium-Catalyzed Aerobic Alkenylation of Arenes via C–H Activation

5.1 Introduction

5.1.1 Stilbene and its derivatives

The name for stilbene (1,2-diphenylethylene) was derived from the Greek work *stilbos*, which means shining. Stilbene has two geometric isomers, (E)-stilbene (*trans*-stilbene) and (Z)-stilbene (*cis*-stilbene) (Figure 6.1). Due to the large steric interaction between two phenyl groups in (Z)-stilbene, (E)-stilbene is more stable, but the two isomers can interconvert when irradiated with light (Scheme 5.1).

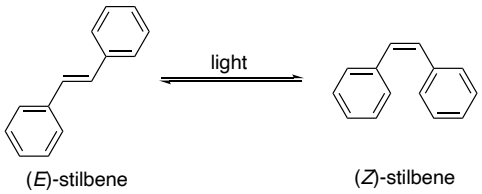

Scheme 5.1. Two isomers of stilbene.

Stilbene and its derivatives have unique intense absorption and fluorescence properties as a result of their extended π-conjugation, and the chemistry and photochemistry of stilbenes has been widely investigated for decades.[1-6] Their photophysical and photochemical properties render them useful in dyes, liquid crystals and LEDs. [7-10] In addition, some products of medicinal interest possess core stilbene (*i.e.*, 1,2-diarylethylene) structures. Given limitations of current synthetic methods, innovative synthetic routes to

stilbenes are of interest as the products are potentially applicable in the pharmaceutical industry and materials science.[11]

5.1.2 Current syntheses of stilbene products

Traditional synthetic routes to stilbenes feature cross-coupling of arenes and styrenes,[12, 13] but these methods frequently require pre-functionalized substrates, which are activated with a functional group, and result in the formation of undesired byproducts (Scheme 5.2). These specialized substrates are not always commercially available and often require multi-step synthesis.[14]

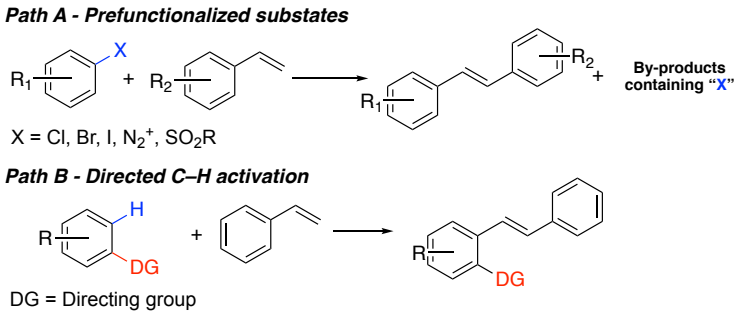

Scheme 5.2. Current synthetic routes for stilbenes. Path A required pro-installation of functional group X and will produce X-containing undesired product. Path B involves direct arene C–H activation, but a directing group is often required.

For example, the synthesis of alkenyl arenes has been achieved with halo-, diazonium- and sulfone-substituted arenes, as well as carboxyl- and nitroalkenes, but these processes produce stoichiometric amounts of waste.[15-20] In addition, there are synthetic inefficiencies associated with the generation of the initial functionalized substrates. Thus, coupling arenes and olefins through C–C bond forming processes via C–H bond breaking (rather than C–halogen bond activation, for example) offers potential advantages. But, in many cases of

arene alkenylation involving transition metal-mediated C–H activation, directing groups are required to enhance reactivity toward arene C–H activation and/or promote regioselectivity (Scheme 5.2). For example, amines, amides and carbamates have been used to allow site-selective functionalization of C–H bonds with C–H activation and subsequent alkenylation typically occurring at the ortho position. [21] The requirement of a directing group limits the scope of substrates that can be used for arene alkenylation via C–H bond breaking reactions and the directing group may stay in the product and limit the use of this reaction

5.1.3 Resveratrol and its derivatives

Resveratrol (3,5,4'-trihydroxylstilbene) is a natural polyphenol present in a variety of medicinal plants and grapes; it protects plants against pathogenic attack and environmental stress. Because it is present in grape skin, resveratrol is found in red wine. The first evidence of the beneficial effect of resveratrol on human health was shown by its ability to protect against cardiovascular diseases. [22] Also, it has been reported that polyphenolic compounds and methyl ether derivatives, such as DMU-212 (3,4,5,4'-tetramethoxystilbene), possess anti-cancer bioactivity and have been shown to possess cytotoxic activity that varies in cell lines derived from the same type of cancer (*i.e.*, ovarian, breast, and colorectal) (Figure 5.1). [22-43] Resveratrol is commonly used as a dietary supplement that possesses chemopreventive and cytostatic properties against a variety of human tumor cell lines, including several prostate cancer cell lines.[37-39, 44-46]

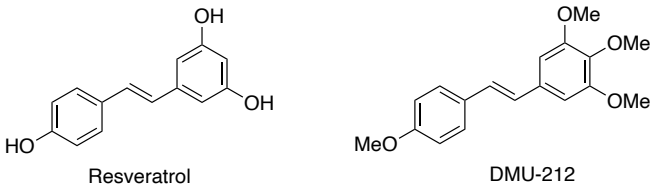

Figure 5.1. Examples of bioactive stilbene derivatives: Resveratrol and DMU-212.

5.1.4 Synthesis of stilbene and derivatives via a Rh-catalyzed arene alkenylation reaction

Oxidative olefin hydroarylation provides an opportunity to enable more atom-economical formation of carbon–carbon bonds between inexpensive arenes and alkenes through undirected C–H activation. It has been reported and discussed in Chapter 3 that Pd[47-53] and Rh[54-61] catalyze oxidative arene alkenylation using oxidants with functionalized olefins. Thus, it was proposed that a reaction between arenes and styrenes in the presence of a rhodium catalyst precursor and sub-stoichiometric amount of Cu(II) salt would form stilbene products via a Rh-mediated direct C–H activation with no directing group/prefunctionalization required (Scheme 5.3).

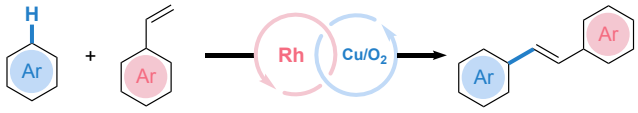

Scheme 5.3. Proposed one-step synthesis of stilbene and its derivatives via an aerobic Rh-catalyzed arene alkenylation which O_2 is serves as the oxidant.

The proposed catalytic cycle is shown below in Scheme 5.4. Four major steps are involved in this catalytic cycle including: 1) Arene C–H activation of the arene mediated

by a Rh carboxylate species via a carboxylate-assisted concerted C–H activation to form Rh–Ar; 2) vinyl arene coordination and insertion to form a Rh–diphenylethyl species; 3) β-hydride elimination to yield the stilbene product and a Rh–H intermediate; and 4) Rh–H oxidation by a Cu(II) carboxylate salt to regenerate the catalyst.

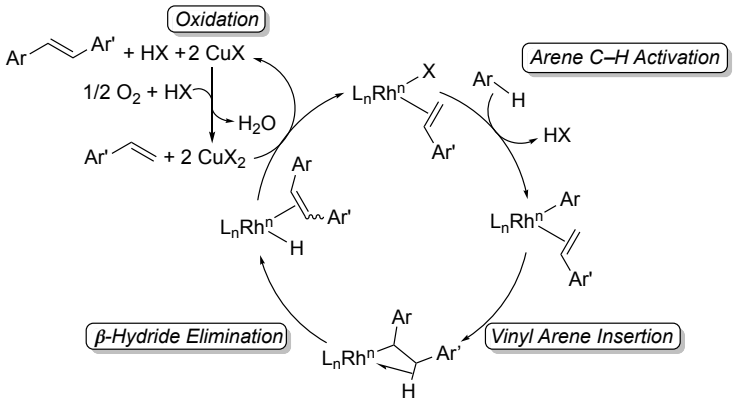

Scheme 5.4. Proposed catalytic cycle alkenylation using vinyl arene to produce stilbenes and its derivatives.

As discussed in Chapter 3, the use of Cu carboxylate salts allows *in situ* recycling of the salt by introducing air/O_2 into the reaction system. With the efficient recycling of the Cu salt, O_2 serves as the oxidant in the proposed process.

5.2 Reaction Optimization

5.2.1 Catalyst precursor

The reaction between benzene and styrene to produce stilbene was used as a model to determine the effect of using various Rh catalyst precursors on the reaction (Table 5.1). The reaction mixture was analyzed by GC-FID to quantify the yield based on a stilbene calibration curve. Commercially available $RhCl_3•H_2O$, $[Rh(COD)Cl]_2$ (COD =

cyclooctadiene) and easily-synthesized [Rh(μ-OAc)(η^2-C_2H_4)$_2$]$_2$ were examined. The Rh(I) acetate dimer, [Rh(μ-OAc)(η^2-C_2H_4)$_2$]$_2$, gave the best yield of 82% {based on amount of Cu(II)}, possibly due to the presence of the acetate groups that can facilitate C–H activation via a concerted metalation/deprotonation (CMD) mechanism. [55, 62-66] Previous studies by the Gunnoe group have shown that Rh-catalyzed arene alkenylation using hydrocarbons does not occur in the absence of a carboxylate source (*e.g.*, Cu(II) carboxylate salt).[54-58] The absence of chloride in [Rh(μ-OAc)(η^2-C_2H_4)$_2$]$_2$ also prevents the formation of undesired chlorinated product, which led to a cleaner separation.

Table 5.1. Catalyst precursor screening.

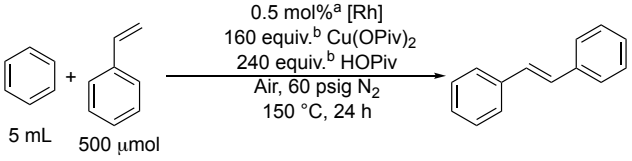

Entry	[Rh]	Yield (%)
1	$RhCl_3 \cdot H_2O$	69
2	[Rh(COD)Cl]$_2$	72
3	[Rh(μ-OAc)(η^2-C_2H_4)$_2$]$_2$	81

[a] 0.25 mol% [Rh(μ-OAc)(η^2-C_2H_4)$_2$]$_2$ (0.5 mol% based on rhodium relative to styrene. [b] Amount of copper(II) salt and acid is relative to Rh. [c] Yield is GC yield based on calibration curve using hexamethylbenzene as internal standard and relative to amount of Cu(II).

5.2.2 Reaction temperature

In previous studies, reaction temperature plays a critical role in the olefin hydroarylation reaction rate as well as its selectivity.[55, 67-69] The use of a higher reaction (up 200 °C) temperature results in faster reaction rate, but also leads to the formation of

undesired by-products. In Table 5.2, when the reaction temperature is raised from 135 °C to 165 °C (entries 1-3), the yield after 24 hours increases from 43% to 92%. However, the higher temperature also results in the conversion of arene to aryl ester (i.e., phenyl pivalate) due to a background reaction with copper(II) pivalate. The yield of stilbenes is minimally affected when styrene is used as a limiting reagent (compare entries 2 and 3). However, when the reaction temperature reached 180 °C (entry 4), oxidation of styrene to benzaldehyde is observed, which leads to a lower yield of stilbene.

Table 5.2. Reaction temperature screening.

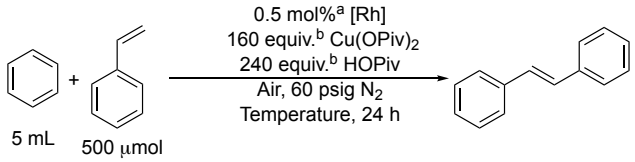

Entry	Temperature (ºC)	Time (h)	Yield (%)
1	135	48	43
2	150	24	81
3	165	24	92
4	180	24	68

[a] 0.25 mol% [Rh(μ-OAc)(η^2-C_2H_4)$_2$]$_2$ (0.5 mol% based on rhodium). [b] Amount of copper(II) salt and acid is relative to Rh. Yield is calculated using GC-FID based on calibration curve.

5.2.3 Reaction solvent

Previous studies have shown that the Rh-catalyzed arene alkenylation reaction is efficient in neat arene solution.[49, 54-59, 68-73] Efforts have been made to find an alternative solution for the arene alkenylation reaction to produce stilbene. As shown in Table 5.3, stilbene is not produced when using DMF, MeOH, 1,4-dioxane or hexanes is the solvent (entries 1-4). The lower concentrations of arene when using these solvents might result in

slower arene C–H activation. The reaction in mesitylene and hexafluorobenzene (entries 5 and 8) gave 10-20 % yield, but neither solvent could not compete with the reaction in neat benzene (entry 10). The Gunnoe lab recently reported that benzene alkenylation could proceed in acetic acid to produce styrene however, due to the lower reaction rate, the yield is poor, 2.6% (entry 9).

Table 5.3. Reaction solvent screening.

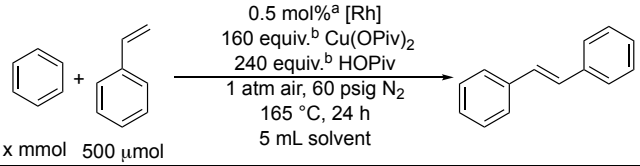

Entry	Solvent	Benzene Loading (mmol)	Yield (%)
1	DMF	3	0
2	MeOH	3	0.2
3	1,4-dioxane	3	3
4	hexanes	3	7
5	mesitylene	3	10.9
6	mesitylene	5	17.4
7	hexafluorobenzene	3	12.1
8	hexafluorobenzene	5	21.7
9	acetic acid	3	2.6
10	benzene	/	81

[a] 0.25 mol% [Rh(μ-OAc)(η^2-C_2H_4)$_2$]$_2$ (0.5 mol% based on rhodium). [b] Amount of copper(II) salt and acid is relative to Rh. [c] Yield is GC yield based on calibration curve using hexamethylbenzene as internal standard.

5.2.4 Dioxygen source

Some components in air (*e.g.*, water, carbon dioxide) can influence late transition metal-mediated reactions. Thus, catalysis has been conducted under atmospheres of air and purified dioxygen (Table 5.4). No major differences on the yield were observed.

Table 5.4. Dioxygen source screening.

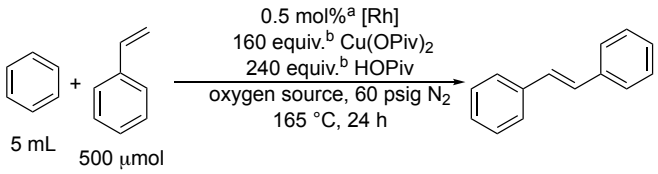

Entry	Oxygen sourse	Yield (%)
1	1 atm air	92
2	1 atm oxygen	91

[a] 0.25 mol% [Rh(μ-OAc)(η^2-C_2H_4)$_2$]$_2$ (0.5 mol% based on rhodium) [b] amount of copper salt and acid is relative to Rh [c] Yield is GC yield based on calibration curve using hexamethylbenzene as internal standard

5.2.5 Effects of copper(II) loading and added acid

The influence of copper(II) and acid loading has been investigated. Stilbene is not produced in the absence of copper(II) salt (Table 5.5, entry 1) under anaerobic conditions, and the reaction yield increases with increased copper(II) loading (entries 2 and 3). The reaction with 160 equiv. of Cu(OPiv)$_2$ gave the best yield, 81% (entry 3). When increasing the copper(II) loading further to 320 equiv., which is beyond the solubility of copper(II) pivalate under the reaction conditions, a lower yield of 71% was observed. In previous studies, the addition of the pivalic acid has been shown to facilitate aerobic catalysis,[55]

which is likely due to 1) improved solubility of copper(II) pivalate; and 2) suppression of hydrolysis of copper(I) salt. As shown in entries 3, 5 and 6, the optimal HOPiv loading is 800 equivalents, which results in a 92% yield; yields are lower when 240 or 1600 equiv. of HOPiv are added.

Table 5.5. Copper pivalate and pivalic acid loading screening.

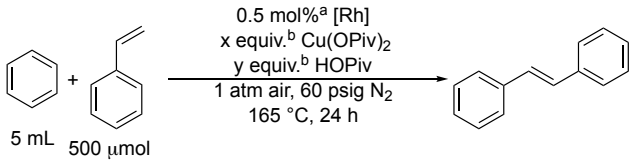

Entry	x equiv. $Cu(OPiv)_2$	y equiv. HOPiv	Yield (%)
1	0	240	0
2	20	240	52
3	160	240	81
4	320	240	71
5	160	800	92
6	160	1600	20

[a] 0.25 mol% $[Rh(\mu\text{-}OAc)(\eta^2\text{-}C_2H_4)_2]_2$ (0.5 mol% based on rhodium) [b] amount of copper salt and acid is relative to Rh [c] Yield is GC yield based on calibration curve using hexamethylbenzene as internal standard

5.2.6 Drying agent

Under aerobic conditions, where Cu(II) salt in recycled *in situ*, two equivalents of water are generated per equivalent of dioxygen. It was observed in previous studies that adding drying agent to catalytic system, the catalysis is improved as water is removed by the drying agent *in situ*.[49] Different types of drying agent have been examined to investigate their effects on catalysis.

Table 5.6. Effect of drying agents.

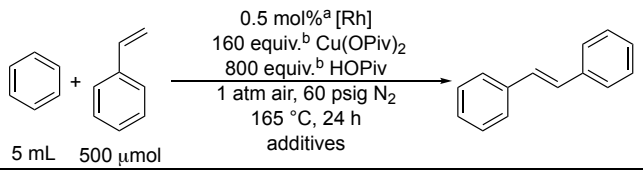

Entry	Additive	Yield (%)
1	3Å molecular sieve	91
2	4Å molecular sieve	72
3	V_2O_5	90
4	Graphene Oxide[c]	91
5	Ac_2O[d]	5
6	No additive	92

[a] 0.25 mol% [Rh(μ-OAc)(η^2-C_2H_4)$_2$]$_2$ (0.5 mol% based on rhodium) [b] amount of copper salt and acid is relative to Rh [c] Graphene oxide was synthesized by a modified Hummer method[74] [d] 5 mL of Ac_2O (acetic anhydrate)was added.

The reaction yield was not improved on addition of various drying agents. Molecular sieves, both 3Å and 4Å, have minimal (entry 1) or inhibitive effect (Table 5.6, entry 2) on the catalysis. It has been reported that vanadium(V) oxide can facilitate arene alkenylation reaction under some reaction conditions, but no influence on catalytic stilbene formation was observed. In previous unpublished results by the Gunnoe group, the addition of graphene oxide has been shown to have a positive effect on arene alkenylation catalysis. Graphene oxide was added to the catalytic reaction. No enhancement of the yield is observed (entry 4).

5.2.7 Temperature optimization for polymethoxybenzenes

Due to the importance of the methoxy substituted stilbenes in the pharmaceutical industry, an optimization of reaction conditions for methoxy benzene substrates were performed. Alkenylation of 1,3-dimethoxybenzene using styrene was used as a model reaction (Table 5.7). As shown in Table 5.7, temperature plays an important role in the reaction. It is possible that at higher reaction temperature, the copper(II) salt reacts with the methoxy functional group. The highest yield of 71% was observed for the reaction at 135 °C after 96 h.

Table 5.7. Optimization of the reaction with methoxy-containing substrates.

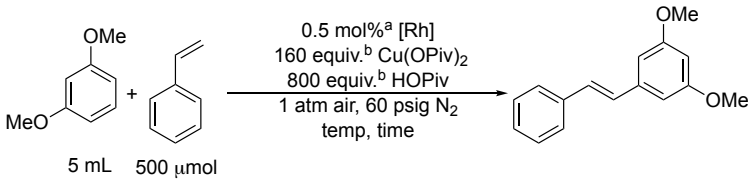

Entry	Temperature (ºC)	Time (h)	Yield (%)
1	165	24	31
2	150	24	41
3	150	48	47
4	135	24	17
5	135	48	37
6	135	72	52
7	135	96	71
8	135	108	71

[a] 0.25 mol% [Rh(μ-OAc)(η^2-C_2H_4)$_2$]$_2$ (0.5 mol% based on rhodium) [b] Reactors were cooled down and purged with air every 24 hours [c] Yield is GC yield based on calibration curve using hexamethylbenzene as internal standard

5.2.8 Progress of the reaction

In order to understand the progress of the reaction under optimized conditions, catalysis with a lower loading of Rh catalyst loading was performed (Figure 5.2). Reaction mixtures were sampled and analyzed every 24 hours.

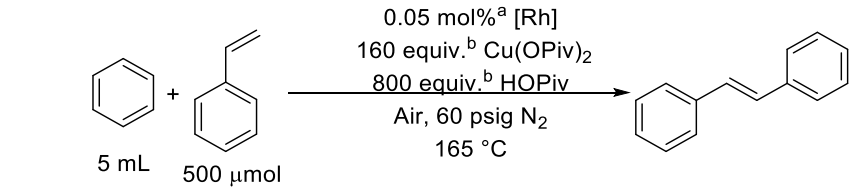

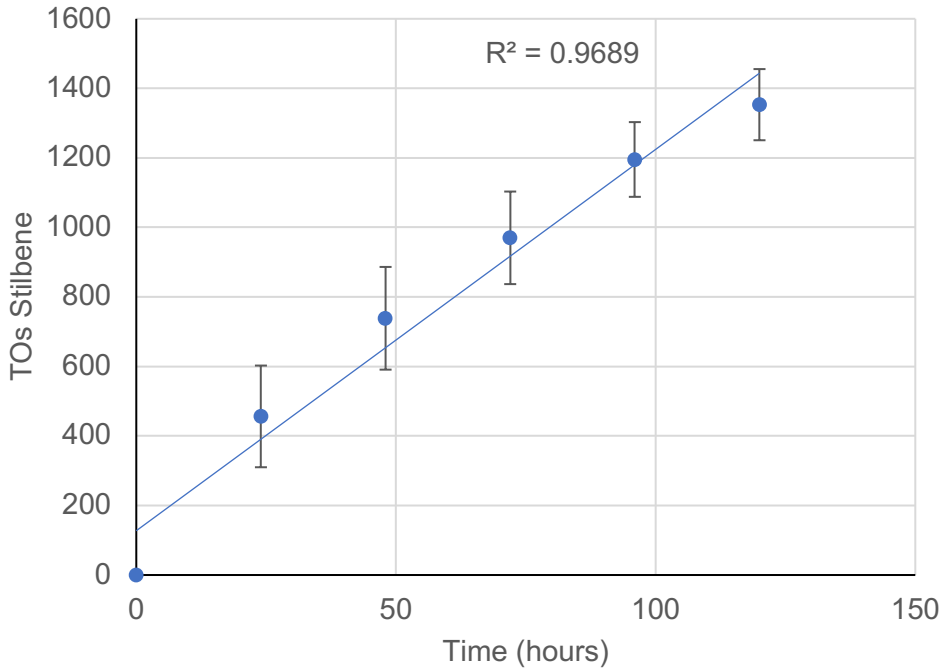

Figure 5.2.Progress of the model reaction (*i.e.*, benzene alkenylation to produce stilbene) using low catalyst loading. [a] 0.25 mol% [Rh(μ-OAc)(η^2-C_2H_4)$_2$]$_2$ (0.5 mol% based on rhodium) [b] amount of copper salt and acid is relative to Rh

The reaction profile is shown in Figure 5.2. A relatively linear relationship between stilbene production and time is observed ($R^2 = 0.97$), indicating that no significant catalyst deactivation has occurred after 120 h. A stilbene yield of 68% is achieved after 120 h of reaction. This yield can be explained by a side reaction that oxidizes styrene to the benzaldehyde. The amount of aldehyde is significant after approximately 36 hours.

A major side product from this catalysis is benzaldehyde, which is produced by a styrene oxidation side reaction (Figure 5.3). It has been reported that this reaction could be catalyzed by Rh or/and Cu(II) in the presence of dioxygen. The production of benzaldehyde has been shown to be linear with respect to time ($R^2 = 0.99$). In summary, these experiments have shown that under the optimized conditions, catalysis proceeds smoothly and selectively without significant decomposition of the Rh catalyst.

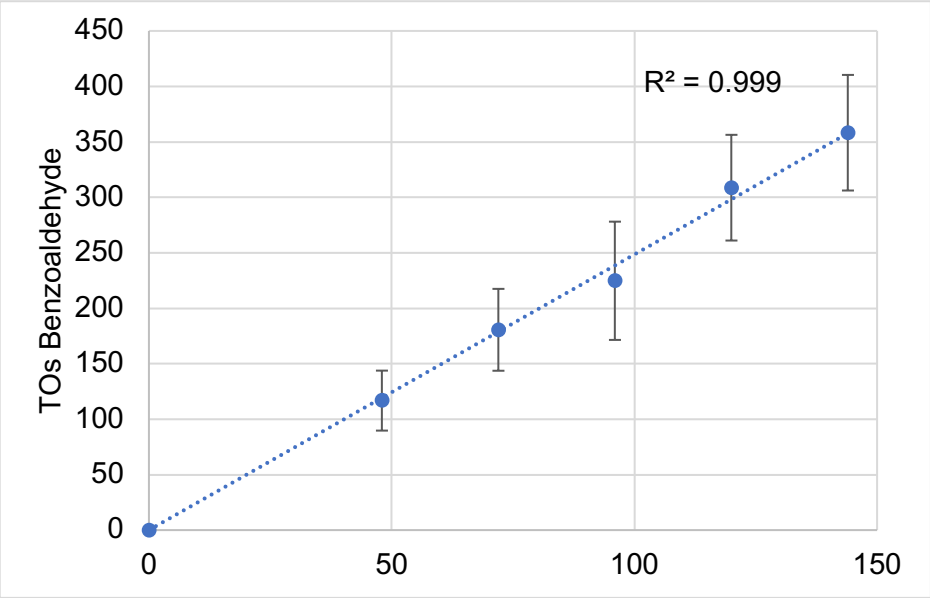

Figure 5.3. Benzaldehyde production under the reaction conditions in Figure 5.2.

5.3 Vinyl arene scope

Under optimized conditions, the scope of the Rh-catalyzed process was studied with a variety of substituted styrene precursors (Table 5.8). The reactions between substituted styrenes and benzene show good functional group tolerance and isolated yields. The reactions with halogenated styrenes afford the expected stilbene derivatives **1f**-**1k** with isolated yields > 60% for fluoride, chloride and iodide, but a lower yield of 30% for bromide. Thus, rhodium catalysis is tolerant of some halogen groups. The reaction also leaves alkoxy groups in **1o**-**1s** untouched, which affords an opportunity to synthesize protected resveratrol and derivatives using this approach (see below). In the reaction of benzene with β-nitrostyrene, biphenyl is observed as the major product, and the expected stilbene is not observed. Thus, benzene C–H activation occurs, but the olefin coordination and/or olefin insertion step(s) appear to be inhibited.

Table 5.8. Vinyl arene scope for benzene alkenylation catalyzed by $[Rh(\mu\text{–}OAc)(\eta^2\text{–}C_2H_4)_2]_2$ in neat benzene and isolated yields.

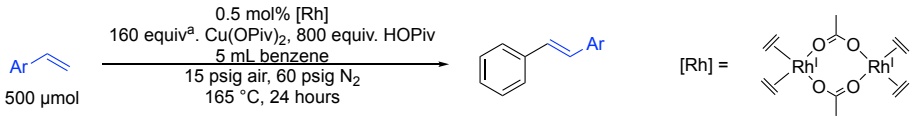

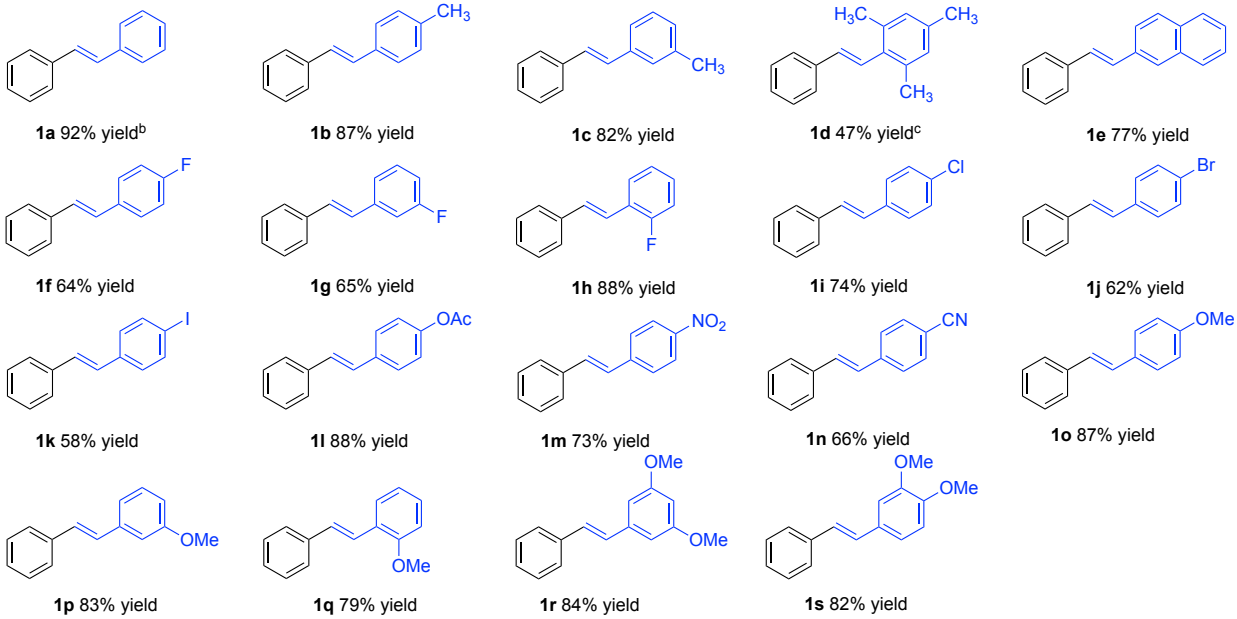

[a] Relative to [Rh]. [b] All yields in this table are isolated yields. [c] Reaction is performed for 48 hours.

The extension of this method to α- and β-substituted styrenes (Scheme 5.5) shows that both α-methylstyrene and trans-β-methylstyrene give the desired product **1t** and along with products **1u** and **1v**, which are likely produced by a rhodium-mediated isomerization reaction. Two possible olefin isomerization routes to generate **1u** and **1v** have been proposed (Scheme 5.6). The production of **1u** is attributed to a side isomerization reaction from product **1u** to **1v** via a Rh-hydride mediated process, and production of **1v** is proposed to occur by a similar process that converts β-methylstyrene to allyl benzene, which likely served as the precursor to **1v**.

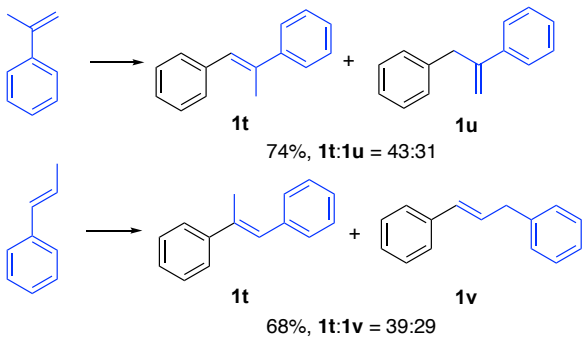

Scheme 5.5. Alkenylation using vinyl substituted styrene of benzene. Condition: 0.25 mol% [Rh(μ-OAc)(η^2-C_2H_4)$_2$]$_2$ (0.5 mol% for single rhodium), 160 equiv. copper pivalate, 800 equiv. pivalic acid, 60 psig N_2, 15 psig air, 5 mL benzene as solvent, 165 ˚C, 24 hours.

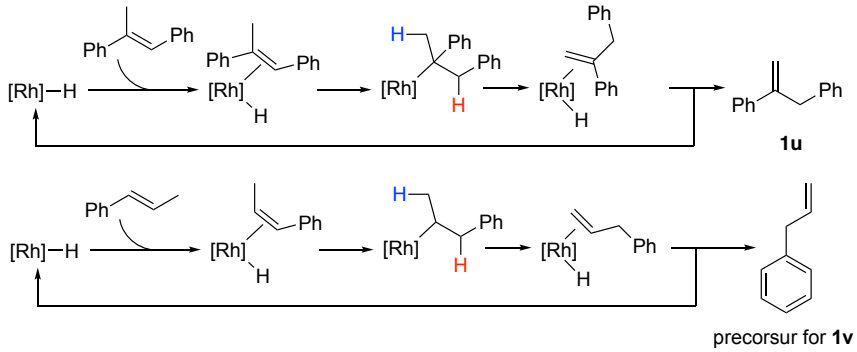

Scheme 5.6. Rh-mediated olefin isomerization that produces unexpected products **1v** and **1w**.

5.4 Arene scope

Table 5.9 shows isolated yields for catalytic reactions using substituted arenes and styrene. A range of monosubstituted arenes are functionalized to give products **2a–2d**, **2i–2n**, **2r**, **2u** and **2v**, which range from electron-rich anisole (**2r**) to electron deficient α,α,α-trifluorotoluene. Regardless of the identity of the arene substituent, the Rh catalysis is regioselective for the formation of *meta* and *para* products with an approximate ratio of

2:1. For **2a**, **2j**, **2l** and **2v**, the *meta*- and *para*-functionalized isomers were separated using column chromatography to give ~2:1 isolated yields of *meta*:*para* products. These results indicate that the C–H activation step is sensitive to steric hindrance, with even small fluoro or methyl groups (**2a** and **2k**, respectively) almost completely suppressing *ortho* functionalization. When dialkylbenzenes and trialkylbenzene **2e–2h** were used as the substrate, the same influence of sterics on the selectivity was observed. Since all four arene C–H bonds in *p*-xylene **2e** are adjacent to a methyl group, the reaction gives a low yield of only 22%. For *m*-xylene (**2f**) and *o*-xylene (**2g**), better yields (> 70%) are obtained since they have more sterically accessible arene C–H bonds. The substrate 1,2,3-trimethylbenzene has a similar steric profile to *meta*-xylene (*i.e.*, an accessible C–H bond that is meta to methyl groups), and the reaction gave 67% isolated yield of the desired product (**2h**) after prolonged reaction time (48 hours).

Table 5.9. Arene scope of oxidative styrene hydroarylation catalyzed by $[Rh(\mu\text{–}OAc)(\eta^2\text{–}C_2H_4)_2]_2$ in neat arene solution. All yields are isolated.

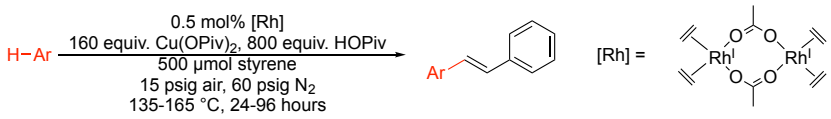

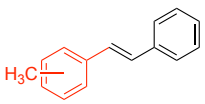

2a 76% total yield[a]
para **1b** 21% yield
meta **1c** 47% yield
o:*m*:*p*[b] = 1:28:13

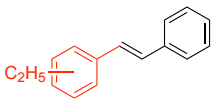

2b 81% total yield
o:*m*:*p* = 0:3:1

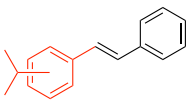

2c 77% total yield
o:*m*:*p* = 0:2:1

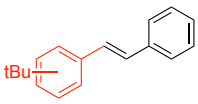

2d 81% total yield
o:*m*:*p* = 0:2:1

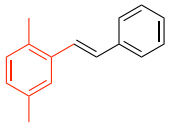

2e 22% yield[c]

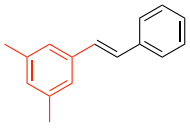

2f 77% yield[c]

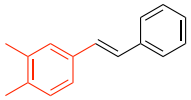

2g 71% yield

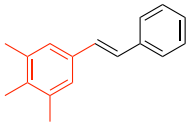

2h 67% yield[c]

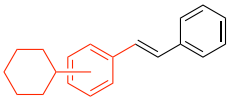

2i 81% total yield
o:*m*:*p* = 0:3:1

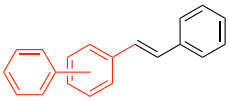

2j[d] 81% total yield
para **2ja** 24% yield
meta **2jb** 51% yield
o:*m*:*p* = 0:3:1

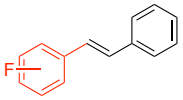

2k 82% total yield
o:*m*:*p*[e] = 1:28:23

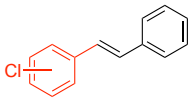

2l 87% total yield
para **2la** 25% yield
meta **2lb** 56% yield
o:*m*:*p* = 0:2:1

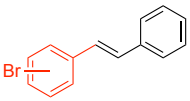

2m 21% total yield
o:*m*:*p* = 0:2:1

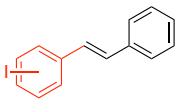

2n 17% NMR yield[f]
o:*m*:*p* = 0:2:1

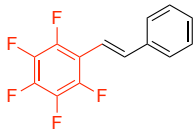

2o 61% yield[c]

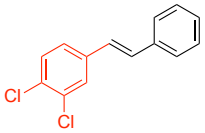

2p 74% yield

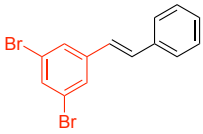

2q 74% yield

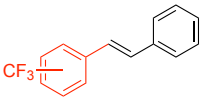

2r 87% total yield
o:*m*:*p* = 0:2:1

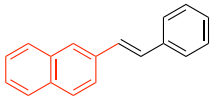

2s[d] 75% total yield

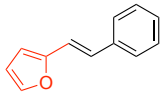

2t 49% yield

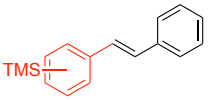

2u 91% total yield
o:*m*:*p* = 0:2:1

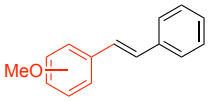

2v[g] 81% total yield
para **2va** 19% yield
meta **2vb** 43% yield
o:*m*:*p* = 0:3:1

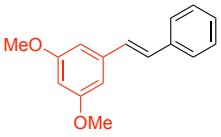

2w[g] 74% yield[g]

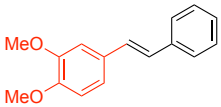

2x[g] 73% yield

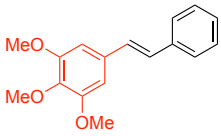

2y[d,g] 73% yield

[a] Total yield is calculated prior to isomer separation. [b] The o:m:p value is calculated based on GC-FID peak areas. [c] Reaction was performed for 48 hours. [d] Mesitylene (2.5 mL) was added to the reaction mixture. [e] The o:m:p value is calculated based on ^{19}F NMR spectroscopy due to poor resolution of isomers in the GC. [f] The crude reaction mixture was washed with base and analyzed by ^{1}H NMR spectroscopy. The yield was calculated based on the integration of the vinyl protons of iodostilbene relative to the internal standard

CH_3NO_2. [g] Reactions were performed at 135 ˚C for 96 hours, reactors were purged with air every 24 hours.

With respect to halogenated arenes, the reactions proceed for fluoro- and chlorobenzene with total isolated yields (all isomers) of 82% (**2k**) and 87% (**2l**), respectively. However, reactions are less successful with bromo- and iodobenzene due to C–X bond functionalization competing with C–H activation. Thus, along with the desired products bromo- (**2m**) and iodostilbene (**2n**), (*E*)-stilbene (**1a**) is formed. The observed ratio of halostilbene to stilbene are 4:1 for bromo and 1.1:1 for iodobenzene under 165 °C. The reaction works well for pentafluorobenzene (**2o**), *ortho*-dichlorobenzene (**2p**) and *meta*-dibromobenzene (**2q**, under 135 ˚C) giving 61%, 74% and 74% isolated yields, respectively. When using the arenes with methoxy groups (**2v**-**2y**), a decrease in yield at 165 ˚C is observed. But the yields can be improved by lowering the reaction temperature to 135 ˚C for 96 hours. We expanded the scope of the catalysis to polycyclic arenes and heteroaromatic substrates. The reactions with naphthalene (**2u**) and furan (**2v**) are selective and generate the expected alkenylation products in moderate to good yields.

5.5 Synthesis of bioactive molecules

Current synthetic routes for resveratrol and its derivates use Wittig or Horner-Wadsworth-Emmons reactions, Perkin condensations, alkene metathesis, and cross-coupling.[24, 26, 32, 35, 75-77] Using this method, DMU-212 and resveratrol can be prepared from

poly-methoxybenzene and vinyl anisole in 68% and 71% yields by a single- or two-step conversion, respectively (Scheme 5.7).

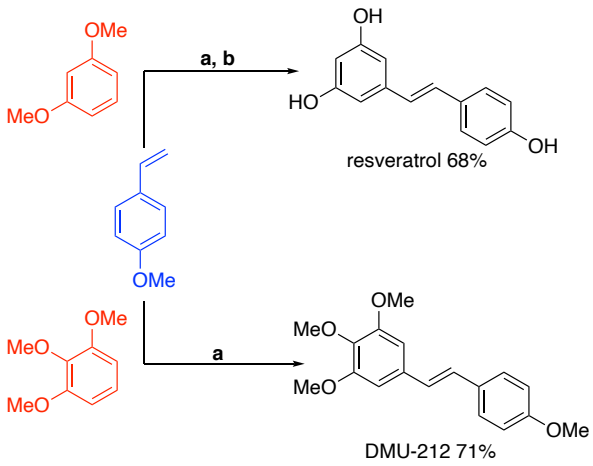

Scheme 5.7. Rh-catalyzed direct synthesis of bioactive molecules, resveratrol and DMU-212. Yields are isolated. [a] Conditions: (a): 0.25 mol% $[Rh(\mu\text{-}OAc)(\eta^2\text{-}C_2H_4)_2]_2$ (0.5 mol% based on rhodium), 160 equiv. copper pivalate, 800 equiv. pivalic acid, 60 psig N_2, 15 psig air, 5 mL arene as solvent, 500 µmol of 4-vinylanisole, 135 °C, 96 hours, reactors were open to air every 24 hours; (b) BBr_3, 0-30 °C, quant, overnight.

In addition to resveratrol and DMU-212, many other polyphenolics and their methyl esters can be synthesized using this strategy as studies have demonstrated that this method works well on polymethoxybenzenes (**2v**-**2y**) and vinyl-methoxybenzenes (**1p**-**1t**). Reactions between these substrates could produce more than 20 different polymethoxystilbenes.

5.6 Single step conversion from arene and ethylene to stilbenes

Stilbene has previously been observed as a byproduct in Rh- and Pd-catalyzed oxidative ethylene hydrophenylation to produce styrene. Using low ethylene pressure and high temperature, the production of stilbene is substantial. For example, palladium(II)

acetate-catalyzed oxidative ethylene hydrophenylation reaction gave a styrene:stilbene ratio of 1.4:1 at 180 °C with 20 psig ethylene pressure.[42] This observation indicates that stilbene could be produced from ethylene and benzene in a one pot reaction (Scheme 5.8). As shown in Table 5.10, this reaction has been tested using several arene substrates. Stilbenes are produced from benzene, 1,2-dichlorobenzene, and *meta*-xylene, with 37%, 39% and 23% of desired product relative to the limiting reagent ethylene. In all reaction solutions, vinyl arenes are found in approximately 10% yield (based on GC-FID analysis of crude reaction mixtures). Aryl aldehydes are also observed in approximately 10% yield, which likely results from undesired oxidation of vinyl arenes.

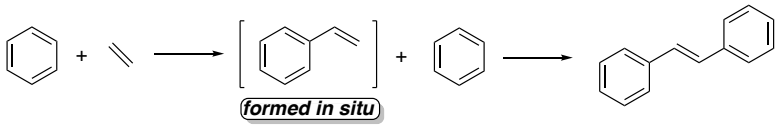

Scheme 5.8. Single-step conversion of ethylene and benzene to stilbene.

Table 5.10. Single step conversion from ethylene and arenes to stilbene derivatives catalyzed by [Rh(μ–OAc)(η^2–C_2H_4)$_2$]$_2$ via a dual C-H activation pathway.

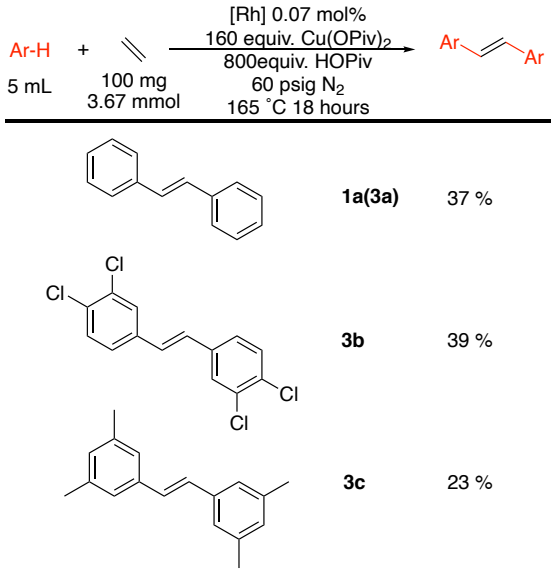

5.7 Large-scale synthesis of stilbene derivatives

For selected high-boiling-point arene substrates, large-scale catalysis could be performed under ambient pressure with a continuous air feed in larger scale. As shown in Scheme 5.8, the reaction between 1,3-dimethoxybenzene and 4-vinylanisole results in 62% yield of the desired product *(E)*-1,3-dimethoxy-5-(4-methoxystyryl)benzene (trimethylresveratrol). The continuous air flow created a stable O_2 concentration, and a lower copper loading can be used. The copper(II) salt loading was reduced to 8 equiv.

relative to Rh in the reaction between dichlorobenzene and an 84% yield of desired product **2p** is observed.

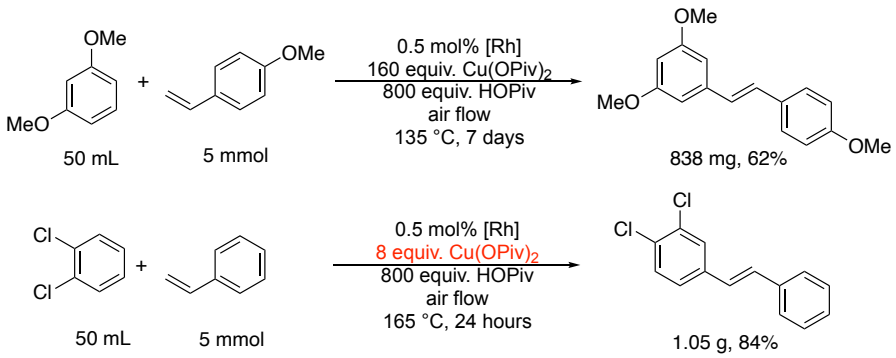

Scheme 5.9. Large scale synthesis of *(E)*-1,3-dimethoxy-5-(4-methoxystyryl)benzene and *(E)*-1,2-dichloro-4-styrylbenzene (2p).

5.8 Comparison of Pd and Rh catalysis

5.8.1 Regioselectivity

Previously, it was reported that $Pd(OAc)_2$, despite its low selectivity, could also serve as the catalyst for arene alkenylation. [49, 50] Thus, aerobic arene alkenylation for stilbene production has been examined using $Pd(OAc)_2$ in order to compare the results with those using rhodium catalysts. First, the palladium catalysis was tested with monosubstituted arenes. As shown in Table 5.11, reactions with toluene and chlorobenzene gave a different ratio of *ortho*:*meta*:*para* functionalization compared to the rhodium catalysis where *ortho* functionalization is minimum.

Table 5.11. Regioselectivity comparison between Rh and Pd catalysis.

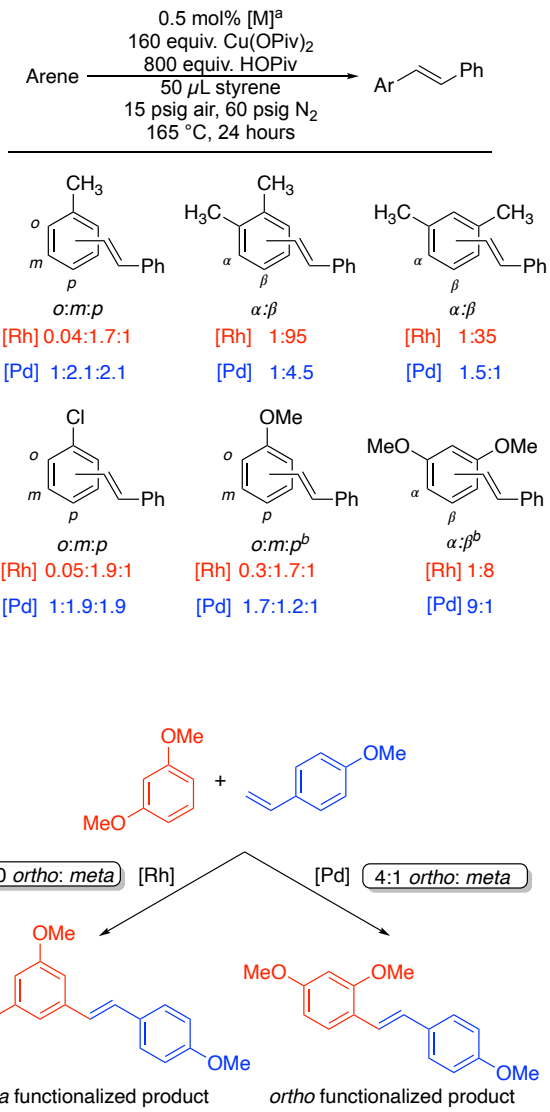

Scheme 5.10. Synthesis of new polyphenolics by Rh and Pd catalysis.

A directing group effect was observed when using anisole as the substrate, but this effect was more heavily pronounced for Pd than Rh. Using $Pd(OAc)_2$ as the catalyst precursor, the *ortho*:*meta* selectivity for 1,3-dimethyoxybenzene with 4-methoxystyrene is 4:1 in favor of *ortho* functionalization. In contrast, *ortho*:*meta* selectivity for anisole using the Rh catalysts gives a 1:10 ratio in favor of *meta* functionalization (Scheme 5.10).

5.8.2 C–X and C–H bond activation

Pd catalysis using halogenated arenes as substrate has also been examined (Table 5.12). Using chlorobenzene, the desired product mixture (*ortho*, *meta* and *para* isomers) can be obtained after 24 hours under optimized reaction conditions and the same differences in product distribution (approximately 1:2:2 *ortho*:*meta*:*para* ratio) is observed. When using bromobenzene and iodobenzene as the substrate, Pd shows much lower tolerance toward the halide functionality. The reaction of bromobenzene with $Pd(OAc)_2$ produces a large amount of stilbene, with a 1:1 ratio of stilbene:bromostilbene, which likely results from C–Br bond activation in lieu of C–H bond activation. When using iodobenzene, the reaction produces trace amounts of iodostilbene, which indicates that Pd favors activation of C–I bonds versus C–H bonds. In contrast, Rh has shown better tolerance on the bromo- and iodo-functionalities. Catalysis with Rh using bromobenzene favors C-H activation product bromostilbene over C–Br product stilbene by a ratio of 4:1, respectively. The reaction with iodobenzene is less selective, but slightly favors production of the C–H activation product. The observed ratio of iodostilbene to stilbene is 1.1 : 1.

Table 5.12. Difference in regioselectivity between rhodium and palladium catalysis with haloarenes, comparing C–X vs. C–H bond activation via product distribution.

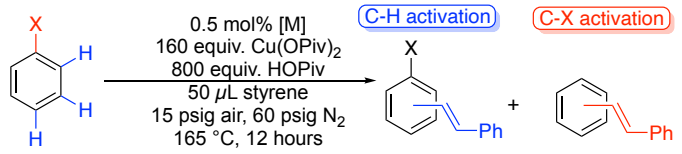

X	[M]	X-Stilbene	Stilbene
X = Cl	$Pd(OAc)_2$	1	N.D.
	$[Rh(\eta^2\text{-}C_2H_4)(\mu\text{-}OAc)]_2$	1	N.D.
X = Br	$Pd(OAc)_2$	1	6
	$[Rh(\eta^2\text{-}C_2H_4)(\mu\text{-}OAc)]_2$	4	1
X = I	$Pd(OAc)_2$	trace	1
	$[Rh(\eta^2\text{-}C_2H_4)(\mu\text{-}OAc)]_2$	1.1	1

5.9 Limitations

Although the Rh catalyzed stilbene synthesis has been demonstrated for a wide range of functional group tolerance, there are some limitations (Figure 5.4). 1) We have observed that Rh has very limited ability to functionalize ortho-C–H bonds, so the reaction with more substituted substrates (mesitylene and para-cymene) gave minimal yield of products. 2) Reactions with substrates in the phenol and aniline families did not yield the desired stilbene products. Instead, a large amount of arene-arene coupling products were observed, which is likely due to the oxidatively induced C–C coupling. 3) The reaction with benzonitrile gives ery little desired product; however, it produces a large amount of benzamide, which might be generated from the reaction of benzonitrile with water, which is produced during the reoxidation of the copper(II) salt. 4) The reaction with benzoic acid and benzaldehyde did not yield the desired products. This limitation is attributed to the oxidation/decarboxylation of -COOH and -CHO groups that may be catalyzed by Rh/Cu(II)

system. 5) Surprisingly, the reaction with phenyl acetate did not give the stilbene product. Only acetate metathesis occurs, which produces a large amount of phenylpivalate when copper(II) pivalate is the Cu(II) oxidant. 6) Benzylmethylsulfone seems to react with copper(II) and none of the desired product was observed. 7) The reaction with pyridine failed. It seems as though copper(II) binds pyridine and prevents copper(II) from serving as the necessary oxidant. Increasing the amount of acid in order to quench the coordination ability of pyridine did not enable functionalization. 8) Reactions with pyrrole, *N*-methylpyrrole, *N*-Boc pyrrole, thiophene and acetoaniline did not yield the corresponding stilbene products. These substrates appear to be oxidized by copper(II). 9) Nitrostilbene production could be observed when analyzing the neat reaction mixture immediately after completion; however, due to the light sensitivity of nitrostilbene, purification and isolation of the product were unsuccessful. 10) Phenanthrene and anthracene have high melting points and barely dissolve in mesitylene, so the alkenylation reaction does not occur under conditions tested. 11) The catalysis with 1,2,3,4-tetrahydronaphthalene, 2,3-dihydro-1H-indene, 2,3-dihydrobenzofuran and 1,3-benzodioxole also gives little desired product, likely due to the aerobic oxidation of methylene groups to form α-ketone. 12) Production of arene-arene coupling products is significant when using indole, *N*-methylindole and benzofuran, and leads to little desire product. 13) Reaction with the first five styrene derivatives in Figure 5.4 yield no alkenylation. 14) The alkenylation of ferrocene is

observed under our optimized conditions, but, oxidation of styrene to form benzaldehyde is also observed.

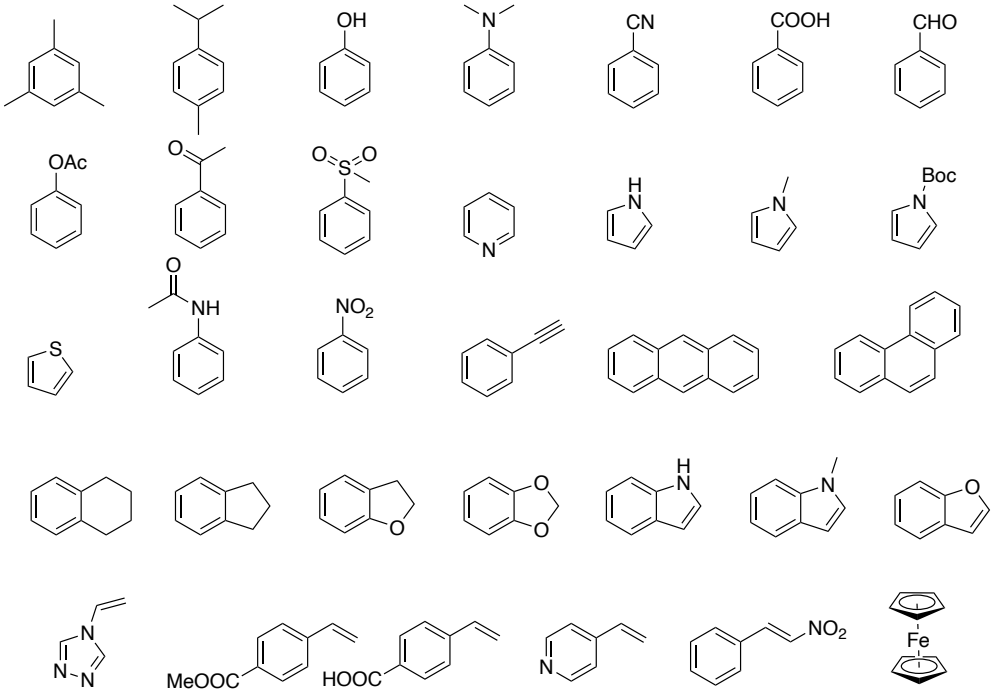

Figure 5.4. Substrates that did not survive under catalytic conditions.

5.10 Conclusion

In conclusion, a simple, one-pot aerobic Rh-catalyzed arene alkenylation reaction to produce stilbenes via direct C–H bond activation in the absence of directing groups has been developed. The reaction has shown wide functional group tolerance and presents an opportunity for larger-scale organic synthesis. Additionally, a method to synthesize stilbenes directly from arenes and ethylene has been reported.

5.11 Experimental detail and spectroscopy of the products

5.11.1 Optimization of reaction conditions

General procedure for Rh(I)-catalyzed oxidative hydrophenylation of styrene with benzene. Under an atmosphere of dry nitrogen, di-μ-acetatotetrakis(dihaptoethene)dirhodium(I) (2.5 μmol, 550 μg), copper(II) pivalate (400 μmol, 106 mg), and pivalic acid (2 mmol, 204 mg) were added into a dried Andrews Glass™ Lab-Crest® Fisher-Porter tube with a stir bar. Styrene (500 μmol, 57 μL), and benzene (5 mL) were then added by syringe. The tube was opened to air, sealed and pressurized with dinitrogen (60 psig), and the mixture was stirred at 165 °C. After 24 h, the reaction was allowed to cool to room temperature. The resultant mixture was diluted with ethyl acetate (40 mL), washed with saturated sodium carbonate solution (50 mL). The aqueous and organic layers were separated. The aqueous layer was extracted with ethyl acetate (3 × 40 mL), and the combined organic layers were washed with water (3 × 10 mL) and dried over magnesium sulfate. The resulting sample was subjected to GC-FID analysis. All yields and ratios given during the optimization studies were determined by GC-FID analysis of the crude reaction mixture using hexamethylbenzene as an internal standard.

5.11.2 Scope of vinyl arenes

General procedure for Rh(I)-catalyzed oxidative hydrophenylation of vinyl arenes with benzene.

Under an atmosphere of dry nitrogen, di-μ-acetatotetrakis(dihaptoethene)dirhodium(I) (**1**) (2.5 μmol, 550 μg), copper(II) pivalate (400 μmol, 106 mg), and pivalic acid (2 mmol, 204 mg) were added into a dried Andrews Glass™ Lab-Crest® Fisher-Porter tube with a stir bar. Then vinyl arene (500 μmol) and benzene (5 mL) were added by syringe. Then the tube was opened to air, sealed and pressurized with dinitrogen (60 psig). The mixture was stirred at 165 °C. After 24 h, the reaction was allowed to cool to room temperature. The resultant mixture was diluted with ethyl acetate (40 mL) and washed with saturated sodium carbonate solution (50 mL). The aqueous and organic layers were separated. The aqueous layer was extracted with ethyl acetate (3 × 40 mL) and the combined organic layers were washed with water, (3 × 10 mL), dried over magnesium sulfate, filtered, and concentrated under vacuum.

Alkenylation of benzene using styrene

(*E*)-Stilbene (1a)

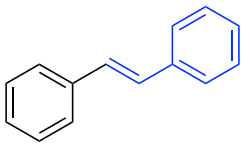

Following the general procedure described above and using styrene as the vinyl arene, the target compound **1a** was obtained as a white solid (83 mg, 92%). The product was purified by flash column chromatography using hexanes as the eluent. This compound was reported in literature.[78] **^{1}H NMR (600 MHz, $CDCl_3$):** δ 7.53 (d, J = 7.3 Hz, 4H), 7.37 (t, J = 7.7 Hz, 4H), 7.27 (t, J = 7.4 Hz, 2H), 7.12 (s, 2H) ppm. **^{13}C NMR (201 MHz, $CDCl_3$):** δ 137.5, 128.8, 127.8, 126.7 ppm. **HRMS (HAPCI) m/z:** Calcd for = $C_{14}H_{12}^+$ = 180.0939, Found = 180.0935.

Alkenylation of benzene using 4-methylstyrene

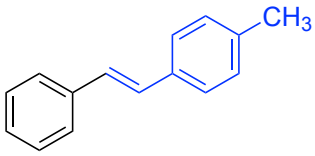

***(E)*-4-methyl-1-styrylbenzene (1b)**

Following the general procedure described above and using 4-methylstyrene as the vinyl arene, the target compound **1b** was obtained as a white solid (84 mg, 87%). The product was purified by flash column chromatography using hexanes as the eluent. This compound was reported in literature.[79] **^{1}H NMR (600 MHz, $CDCl_3$):** δ 7.53 (m, 2H), 7.45 (m, 2H), 7.38 (m, 2H), 7.28 (m, 1H), 7.20 (m, 2H), 7.13 (d, *J* = 16.4 Hz, 1H), 7.09 (d, *J* = 16.4 Hz, 1H), 2.39 (s, 3H) ppm. **^{13}C NMR (201 MHz, $CDCl_3$):** δ 137.7, 134.7, 129.53, 128.8, 128.8, 128.7, 127.8, 127.5, 126.5, 21.4, 21.4 ppm. **HRMS (HAPCI) m/z:** Calcd for $C_{15}H_{14}^+$ = 194.1096, Found Mass = 194.1098.

Alkenylation of benzene using 3-methylstyrene

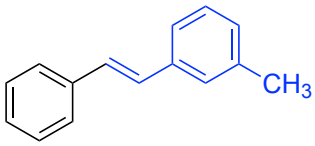

***(E)*-3-methyl-1-styrylbenzene (1c)**

Following the general procedure described above and using 4-methylstyrene as the vinyl arene, the target compound **1c** was obtained as a white solid (80 mg, 82%). The product was purified by flash column chromatography using hexanes as the eluent. This compound was reported in literature.[79] **^{1}H NMR (600 MHz, $CDCl_3$):** δ 7.54 (m, 2H), 7.41 – 7.33 (m, 4H), 7.31 – 7.26 (m, 2H), 7.16 – 7.08 (m, 3H), 2.41 (s, 3H) ppm. **^{13}C NMR (201 MHz, $CDCl_3$):** δ 138.4, 137.6, 137.4, 129.0, 128.8, 128.7, 128.7, 128.6, 128.6, 128.6, 127.7, 127.4, 126.6, 123.9, 21.6 ppm. **HRMS (HAPCI) m/z:** Calcd for $C_{15}H_{14}^+$ = 194.1096, Found Mass = 194.1083.

Alkenylation of benzene using 2,4,6-trimethylstyrene

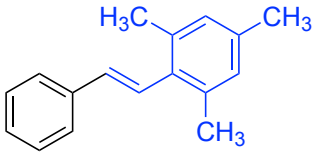

(*E*)-2,4,6-trimethyl-1-styrylbenzene (1d) Following the general procedure described above and using 2,4,6-trimethylstyrene as the vinyl arene, the target compound **1d** was obtained as a white solid (52 mg, 47%) after 48 hours reaction. The product was purified by flash column chromatography using hexanes as the eluent. This compound was reported in literature.[80] **^{1}H NMR (600 MHz, $CDCl_3$):** δ 7.47 (m, 2H), 7.41 (dd, *J* = 1.9, 0.6 Hz, 1H), 7.35 (m, 2H), 7.25 (m, 1H), 7.05 (d, *J* = 16.3 Hz, 1H), 6.91 (d, *J* = 16.2 Hz, 1H), 6.43 (dd, *J* = 3.3, 1.8 Hz, 1H), 6.36 (dd, *J* = 3.3, 0.4 Hz, 1H) ppm. **^{13}C NMR (151 MHz, $CDCl_3$):** δ 153.4, 142.3, 137.2, 128.8, 127.7, 127.3, 126.5, 116.7, 111.8, 108.7 ppm. **HRMS (HAPCI) m/z:** Calcd for $C_{17}H_{19}^+$ = 223.1487, Found Mass = 223.1486.

Alkenylation of benzene using 2-vinylnaphthalene

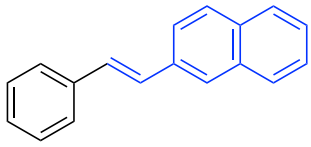

***(E)*-2-styrylnaphthalene (1e)** Following the general procedure described above and using 2-vinylnaphthalene as the vinyl arene, the target compound **1e** was obtained as a white solid (88 mg, 77%). The product was purified by flash column chromatography using hexanes as the eluent. This compound was reported in literature.[12] **^{1}H NMR (600 MHz, $CDCl_3$):** δ 7.86 (br, s, 1H), 7.85 – 7.79 (m, 3H), 7.75 (dd, *J* = 8.6, 1.8 Hz, 1H), 7.57 (m, 2H), 7.50 – 7.42 (m, 2H), 7.38 (m, 2H), 7.29 (d, *J* = 16.4 Hz, 2H), 7.28 (m, 2H), 7.24 (d, *J* = 16.3 Hz, 1H) ppm. **^{13}C NMR (151 MHz, $CDCl_3$):** δ 137.5, 135.0, 133.9, 133.2, 129.2, 128.9, 128.9, 128.5, 128.1, 127.8, 127.8,

126.8, 126.7, 126.5, 126.0, 123.7 ppm. **HRMS (HAPCI) m/z:** Calcd for $C_{18}H_{15}^+$ = 231.1174, Found Mass = 231.1169.

Alkenylation of benzene using 4-fluorostyrene

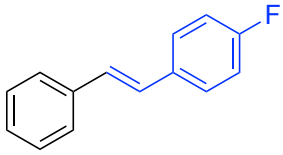

***(E)*-4-fluoro-1-styrylbenzene 1f)** Following the general procedure described above and using 4-fluorostyrene as the vinyl arene, the target compound **1f** was obtained as a white solid (64 mg, 64%). The product was purified by flash column chromatography using hexanes as the eluent. This compound was reported in literature.[79] **^{1}H NMR (600 MHz, $CDCl_3$):** δ 7.49 (m, 4H), 7.36 (t, *J* = 7.6 Hz, 2H), 7.28 (s, 1H), 7.09 – 7.00 (m, 4H) ppm. **^{13}C NMR (201 MHz, $CDCl_3$)**: δ 162.3 (d, *J* = 247.3 Hz), 137.2, 133.5 (d, *J* = 3.3 Hz), 128.70, 128.5 (d, *J* = 2.3 Hz), 128.0 (d, *J* = 7.9 Hz), 127.7, 127.5, 126.4, 115.6 (d, *J* = 21.6 Hz) ppm. **^{19}F NMR (564 MHz, $CDCl_3$)**: δ -112.5 (tt, *J* = 8.6, 5.4 Hz) ppm. **HRMS (HAPCI) m/z:** Calcd for $C_{14}H_{11}F^+$ = 198.0845, Found Mass = 198.0839.

Alkenylation of benzene of 3-fluorostyrene

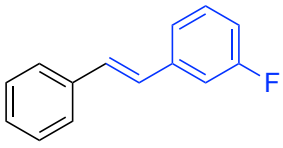

***(E)*-3-fluoro-1-styrylbenzene (1g)** Following the general procedure described above and using 3-fluorostyrene as the vinyl arene, the target compound **1g** was obtained as a white solid (65 mg, 64%). The product was purified by flash column chromatography using hexanes as the eluent. This compound was reported in literature.[12] **^{1}H NMR (600 MHz, $CDCl_3$):** δ 7.52 (d, *J* = 7.7 Hz, 2H), 7.37 (t, *J* = 7.6 Hz, 2H), 7.33 –7 .27 (m, 3H), 7.22 (d, *J* = 10.0 Hz, 1H), 7.11, 7.07 (ABq, $\Delta\nu_{AB}$

= 24 Hz, J_{AB} = 18 Hz, 2H), 6.95 (t, J = 7.8 Hz, 1H) ppm. **^{13}C NMR (201 MHz, $CDCl_3$):** δ 163.3 (d), 139.9 (d), 137.0, 130.2 (d), 130.2, 128.9, 128.2, 127.6 (d), 126.8, 122.6 (d), 114.5 (d), 112.9 (d) ppm. **^{19}F NMR (564 MHz, $CDCl_3$):** δ -111.8 (td, J = 9.3, 6.2 Hz, 1F) ppm. **HRMS (HAPCI) m/z:** Calcd for $C_{14}H_{11}F^+$ = 198.0845, Found Mass = 198.0836.

Alkenylation of benzene using 2-fluorostyrene

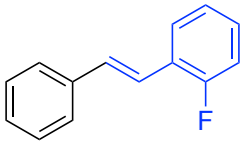

***(E)*-2-fluoro-1-styrylbenzene (1h)** Following the general procedure described above and using 2-fluorostyrene as the vinyl arene, the target compound **1h** was obtained as a white solid (87 mg, 88%). The product was purified by flash column chromatography using hexanes as the eluent. This compound was reported in literature.[81] **^{1}H NMR (600 MHz, $CDCl_3$):** δ 7.63 (td, J = 7.7, 1.8 Hz, 1H), 7.56 (m, 2H), 7.39 (m, 2H), 7.33 – 7.28 (m, 2H), 7.27 – 7.23 (m, 1H), 7.21 (d, J = 16.5 Hz, 1H), 7.16 (td, J = 7.5, 1.3 Hz, 1H), 7.10 (ddd, J = 10.8, 8.2, 1.3 Hz, 1H) ppm. **^{13}C NMR (201 MHz, $CDCl_3$):** δ 159.8(d, J = 249.3 Hz), 137.4, 131.1 (d, J = 4.9 Hz), 128.9 (d, J = 8.5 Hz), 128.9, 128.1, 127.2 (d, J = 3.9 Hz), 126.8, 125.4 (d, J = 11.6 Hz), 124.3 (d, J = 3.4 Hz), 121.1 (d, J = 3.5 Hz), 115.9 (d, J = 22.0 Hz) ppm. **^{19}F NMR (564 MHz, $CDCl_3$):** δ -116.3 (ddd, J = 11.0, 7.6, 5.1 Hz, 1F) ppm. **HRMS (HAPCI) m/z:** Calcd for $C_{14}H_{11}F^+$ = 198.0845, Found Mass = 198.0844.

Alkenylation of benzene using 4-chlorostyrene

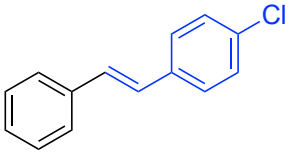

***(E)*-4-chloro-1-styrylbenzene (1i)** Following the general procedure described above and using 4-chlorostyrene as the vinyl

arene, the target compound **1i** was obtained as a white solid (79 mg, 74%). The product was purified by flash column chromatography using hexanes as the eluent. This compound was reported in literature.[79] **^{1}H NMR (600 MHz, $CDCl_3$):** δ 7.51 (d, *J* = 7.6 Hz, 2H), 7.44 (d, *J* = 8.6 Hz, 2H), 7.37 (t, *J* = 7.7 Hz, 2H), 7.33 (d, *J* = 8.5 Hz, 2H), 7.28 (t, *J* = 7.3 Hz, 1H), 7.08, 7.05 (ABq, $\Delta\nu_{AB}$ = 13.4 Hz, J_{AB} = 12 Hz, 2H) ppm. **^{13}C NMR (201 MHz, $CDCl_3$):** δ 137.1, 136.0, 133.3, 129.5, 129.0, 128.9, 128.0, 127.8, 127.5, 126.7 ppm. **HRMS (HAPCI) m/z:** Calcd for $C_{14}H_{11}Cl^+$ = 214.0549, Found Mass = 214.0558.

Alkenylation of benzene using 4-bromostyrene

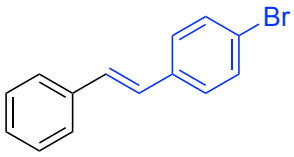

***(E)*-4-bromo-1-styrylbenzene (1j)** Following the general procedure described above and using 4-bromostyrene as the vinyl arene, the target compound **1j** was obtained as a white solid (87 mg, 68%). The product was purified by flash column chromatography using hexanes as the eluent. This compound was reported in literature.[79] **^{1}H NMR (600 MHz, $CDCl_3$):** δ 7.56 – 7.46 (m, 4H), 7.41 – 7.33 (m, 4H), 7.28 (m, 1H), 7.10 (d, *J* = 16.3 Hz, 1H), 7.04 (d, *J* = 16.3 Hz, 1H) ppm. **^{13}C NMR (201 MHz, $CDCl_3$):** δ 137.1, 136.4, 131.9, 129.6, 128.9, 128.12, 128.05, 127.6, 126.7, 121.5 ppm.

Alkenylation of benzene using 4-iodostyrene

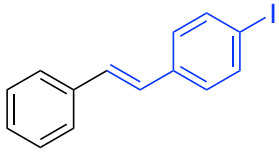

***(E)*-4-iodo-1-styrylbenzene (1k)** Following the general procedure described above and using 4-iodostyrene as the vinyl arene, the target compound **1k** was obtained as a white solid (104 mg, 68%). The product

was purified by flash column chromatography using hexanes as the eluent. This compound was reported in literature.[78] **^{1}H NMR (600 MHz, $CDCl_3$):** δ 7.68 (m, 1H), 7.51 (m, 1H), 7.36 (m, 2H), 7.28 (m, 1H), 7.25 (m, 2H), 7.11 (d, *J* = 16.3 Hz, 1H), 7.02 (d, *J* = 16.3 Hz, 1H) ppm. **^{13}C NMR (151 MHz, $CDCl_3$):** δ 137.9, 137.1, 137.0, 129.7, 128.9, 128.4, 128.1, 127.6, 126.7, 92.9 ppm.

Alkenylation of benzene using 4-vinylphenylacetate

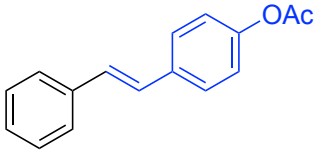

***(E)*-4-styrylphenylacetate (1l)** Following the general procedure described above and using 4-chlorostyrene as the vinyl arene, the target compound **2i** was obtained as a white solid (105 mg, 88%). The product was purified by flash column chromatography using hexanes and ethyl acetate (v/v = 95:5) as the eluent. This compound was reported in literature.[78] **^{1}H NMR (600 MHz, $CDCl_3$):** δ 7.52 (m, 4H), 7.37 (m, 2H), 7.27 (m, 2H), 7.10 (m, 3H), 7.06 (d, *J* = 16.4 Hz, 1H), 2.31 (s, 3H) ppm. **^{13}C NMR (151 MHz, $CDCl_3$):** δ 169.60, 150.20, 137.31, 135.30, 129.10, 128.84, 127.85, 127.80, 127.56, 126.65, 121.94, 21.30 ppm.

Alkenylation of benzene using 4-nitrostyrene

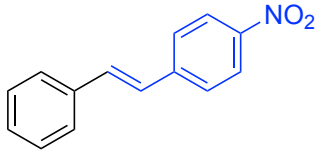

***(E)*-4-styryl-nitrobenzene (1m)** Following the general procedure described above and using 4-nitrostyrene as the vinyl arene, the target compound **1m** was obtained as a yellow solid (82 mg, 73%). The product was purified by flash column chromatography using hexanes as the eluent. This compound was reported in literature.[82] **^{1}H NMR (600 MHz, $CDCl_3$):** δ 8.22 (td, *J* = 8.8, 2.5 Hz, 2H),

7.63 (td, J = 8.5, 2.3 Hz, 2H), 7.56 (m, 2H), 7.41 (m, 2H), 7.34 (m, 1H), 7.30 – 7.25 (m, 1H), 7.15 (d, J = 16.3 Hz, 1H) ppm. **^{13}C NMR (151 MHz, $CDCl_3$):** δ 146.9, 144.0, 136.3, 133.5, 129.0, 129.0, 127.2, 127.0, 126.4, 124.3 ppm. **HRMS (HAPCI) m/z:** Calcd for $C_{14}H_{12}NO_2^+$ = 226.0868, Found Mass = 226.0861.

Alkenylation of benzene using 4-vinylbenzonitrile

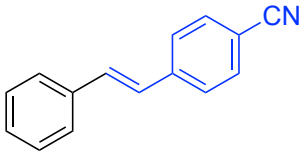

***(E)*-4-styrylbenzonitrile (1n)** Following the general procedure described above and using 4-vinylbenzonitrile as the vinyl arene, the target compound **1n** was obtained as a white solid (85 mg, 66%). The product was purified by flash column chromatography using hexanes and ethyl acetate (v/v = 85:15) as the eluent. This compound was reported in literature.[83] **^{1}H NMR (600 MHz, $CDCl_3$):** δ 7.64 (m, 2H), 7.58 (m, 2H), 7.54 (m, 2H), 7.40 (m, 2H), 7.33 (m, 1H), 7.22 (d, J = 16.2 Hz, 1H), 7.09 (d, J = 16.3 Hz, 1H) ppm. **^{13}C NMR (151 MHz, $CDCl_3$):** δ 142.0, 136.4, 132.6, 132.5, 129.0, 128.8, 127.0, 127.0, 126.9, 119.2, 110.7 ppm. **HRMS (HAPCI) m/z:** Calcd for $C_{15}H_{11}N^+$ = 205.0891, Found Mass = 205.0898.

Alkenylation of benzene using 4-methoxystyrene

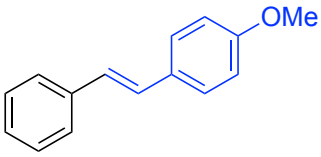

***(E)*-4-styrylanisole (1o)** Following the general procedure described above and using 4-vinylanisole as the vinyl arene, the target compound **1o** was obtained as a white solid (91 mg, 87%). The product was purified by flash column chromatography using hexanes and ethyl acetate (v/v = 9:1) as the eluent. This compound was reported in literature.[79] **^{1}H NMR (600 MHz, $CDCl_3$):** δ

7.48 (dd, J = 20.1, 8.0 Hz, 4H), 7.35 (t, J = 7.5 Hz, 2H), 7.24 (t, J = 7.4 Hz, 1H), 7.07, 6.98 (ABq, $\Delta\nu_{AB}$ = 52.6 Hz, J_{AB} = 16.3 Hz, 2H), 6.91 (d, J = 8.4 Hz, 2H), 3.84 (s, 3H) ppm. **^{13}C NMR (201 MHz, $CDCl_3$):** δ 159.4, 137.8, 130.3, 128.8, 128.4, 127.9, 127.4, 126.8, 126.4, 114.3, 77.2, 55.5 ppm. **HRMS (HAPCI) m/z:** Calcd for $C_{15}H_{15}O^+$ = 211.1123, Found Mass = 211.1116.

Alkenylation of benzene using 3-methoxystyrene

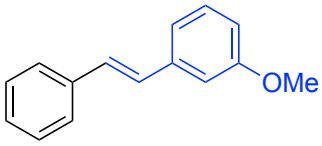

***(E)*-3-styrylanisole (1p)** Following the general procedure described above and using 3-vinylanisole as the vinyl arene, the target compound **1p** was obtained as a white solid (87 mg, 83%). The product was purified by flash column chromatography using hexanes and ethyl acetate (v/v = 9:1) as the eluent. This compound was reported in literature.[12] **^{1}H NMR (600 MHz, $CDCl_3$):** δ 7.55 (m, 2H), 7.40 (m, 2H), 7.35 – 7.28 (m, 2H), 7.19 – 7.12 (m, 3H), 7.10 (dd, J = 2.6, 1.0 Hz, 1H), 6.87 (ddd, J = 8.2, 2.5, 0.9 Hz, 1H), 3.88 (s, 3H) ppm. **^{13}C NMR (151 MHz, $CDCl_3$):** δ 160.0, 138.9, 137.4, 129.8, 129.1, 128.8, 128.7, 127.8, 126.7, 119.4, 113.4, 111.9, 55.3 ppm. **HRMS (HAPCI) m/z:** Calcd for $C_{15}H_{15}O^+$ = 211.1123, Found Mass = 211.1128.

Alkenylation of benzene using 2-methoxystyrene

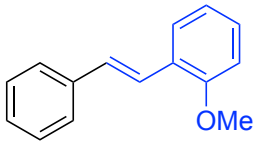

***(E)*-3-styrylanisole (1)** Following the general procedure described above and using 2-vinylanisole as the vinyl arene, the target compound **1q** was obtained as a white solid (83 mg, 79%). The product was purified by

flash column chromatography using hexanes and ethyl acetate (v/v = 9:1) as the eluent. This compound was reported in literature.[84] **^{1}H NMR (600 MHz, $CDCl_3$):** δ 7.63 (dd, *J* = 7.7, 1.7 Hz, 1H), 7.57 (m, 2H), 7.53 (d, *J* = 16.4 Hz, 1H), 7.38 (m, 2H), 7.30 – 7.25 (m, 2H), 7.15 (d, *J* = 16.5 Hz, 1H), 7.00 (m, 1H), 6.92 (m, 1H), 3.91 (s, 3H) ppm. **^{13}C NMR (151 MHz, $CDCl_3$):** δ 157.0, 138.1, 129.2, 128.8, 128.7, 127.5, 126.7, 126.6, 126.5, 123.6, 120.9, 111.0, 55.6 ppm. **HRMS (HAPCI) m/z:** Calcd for $C_{15}H_{15}O^+$ = 211.1123, Found Mass = 211.1116.

Alkenylation of benzene using 3,5-dimethoxystyrene

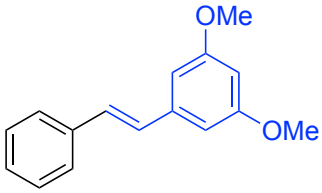

(*E*)-3,5-dimethoxyl-1-styrylbenzene (1r) Following the general procedure described above and using 3,5-dimethoxybenzene as the vinyl arene, the target compound **1r** was obtained as a colorless liquid (95 mg, 84%). The product was purified by flash column chromatography using hexanes and ethyl acetate (v/v = 9:1) as the eluent. This compound was reported in literature.[12] **^{1}H NMR (600 MHz, $CDCl_3$):** δ 7.52 (m, 2H), 7.37 (m, 2H), 7.28 (m, 1H), 7.11 (d, *J* = 16.3 Hz, 1H), 7.05 (d, *J* = 16.3 Hz, 1H), 6.70 (d, *J* = 2.3 Hz, 2H), 6.42 (t, *J* = 2.3 Hz, 1H), 3.85 (s, 6H) ppm. **^{13}C NMR (151 MHz, $CDCl_3$)**: δ 161.1, 139.5, 137.3, 129.3, 128.8, 127.9, 126.7, 104.7, 100.1, 55.5 ppm. **HRMS (HAPCI) m/z:** Calcd for $C_{16}H_{17}O_2^+$ = 241.1229, Found Mass = 241.1221.

Alkenylation of benzene using 3,5-dimethoxystyrene

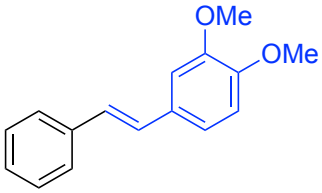

(*E*)-3,4-dimethoxyl-1-styrylbenzene (1s) Following the general procedure described above and using 3,4-dimethoxybenzene as the vinyl arene, the target compound **1s** was obtained as a colorless liquid (92 mg, 82%). The product was purified by flash column chromatography using hexanes and ethyl acetate (v/v = 9:1) as the eluent. This compound was reported in literature.[79] **^{1}H NMR (600 MHz, $CDCl_3$):** δ 7.50 (m, 2H), 7.35 (m, 2H), 7.25 (m, 1H), 7.09 – 7.03 (m, 3H), 6.98 (d, *J* = 16.3 Hz, 1H), 6.87 (d, *J* = 8.2 Hz, 1H), 3.95 (s, 3H), 3.91 (s, 3H) ppm. **^{13}C NMR (151 MHz, $CDCl_3$):** δ 149.3, 149.1, 137.7, 130.6, 128.8, 128.6, 127.4, 127.0, 126.4, 120.0, 111.4, 108.9, 56.1, 56.0 ppm. **HRMS (HAPCI) m/z:** Calcd for $C_{16}H_{16}O_2^+$ = 240.1150, Found Mass = 240.1144.

Alkenylation of benzene using α-methylstyrene

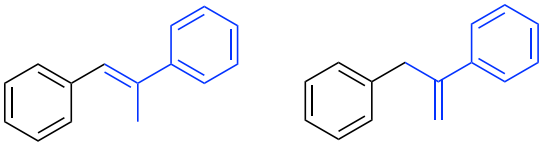

(*E*)-α-methyl stilbene (1t) and 2,3-diphenylpropene (1u) Following the general procedure described above and using α-methylstyrene as the vinyl arene, the target compound **1t** and **1u** were obtained as a white solid (72 mg, 74%, **1t**:**1u** = 43:31). The products were separated and purified by flash column chromatography using hexanes as the eluent. Both compounds were reported in literature.[85] **Characterizations for 1t: ^{1}H NMR (600 MHz, $CDCl_3$):** δ 7.54 (m, 2H), 7.42 – 7.35 (m, 6H), 7.30 (m, 1H), 7.28 – 7.22 (m, 1H), 6.85 (q, *J* = 1.4 Hz, 1H), 2.30 (d, *J* = 1.4 Hz, 3H) ppm. **^{13}C NMR (151 MHz, $CDCl_3$):** δ 144.12, 138.51, 137.57, 129.29, 128.47, 128.32, 127.85, 127.33, 126.61, 126.15,

17.63 ppm. **Characterizations for 1u: ^{1}H NMR (600 MHz, $CDCl_3$):** δ 7.44 (m, 2H), 7.32 – 7.27 (m, 4H), 7.25 – 7.21 (m, 3H), 7.19 (m, 1H), 5.50 (d, *J* = 1.3 Hz, 1H), 5.02 (q, *J* = 1.3Hz, 1H), 3.84 (d, *J* = 1.3 Hz, 2H) ppm. **HRMS (HAPCI) m/z:** Calcd for $C_{15}H_{14}^+$ = 194.1096, Found Mass = 194.1093.

Alkenylation of benzene using β-transmethylstyrene

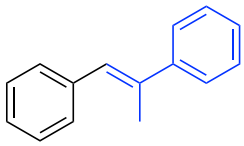
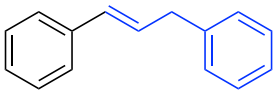

(*E*)-α-methyl stilbene (1t) and (*E*)-1,3-diphenylpropene (1v) Following the general procedure described above and using b-methylstyrene as the vinyl arene, the target compound **1u** and **1v** were obtained as a white solid (72 mg, 74%, **1u**:**1w** = 39:29). The products were separated and purified by flash column chromatography using hexanes as the eluent. Both compounds were reported in literature.[85, 86] **Characterizations for 1v: ^{1}H NMR (600 MHz, $CDCl_3$):** δ 7.37 (m, 2H), 7.34 – 7.27 (m, 4H), 7.27 – 7.23 (m, 2H), 7.23 – 7.18 (m, 2H), 6.47 (dt, *J* = 15.9, 1.5 Hz, 1H), 6.37 (dt, *J* = 15.7, 6.8 Hz, 1H), 3.58 – 3.54 (m, 2H) ppm. **HRMS (HAPCI) m/z:** Calcd for $C_{15}H_{14}^+$ = 194.1096, Found Mass = 194.1098.

5.11.3Scope of arenes

General procedure for Rh(I)-catalyzed oxidative hydroarylation of styrene with arenes. Under an atmosphere of dry nitrogen, di-μ-

acetatotetrakis(dihaptoethene)dirhodium(I) (2.5 μmol, 550 μg), copper(II) pivalate (400 μmol, 106 mg) and pivalic acid (2 mmol, 204 mg) were added to a dried Andrews Glass™ Lab-Crest® Fisher-Porter tube with a stir bar. Then styrene (500 μmol) and arene (5 mL) were added by syringe. The tube was opened to air, sealed and pressurized with dinitrogen (60 psig). The mixture was stirred at 165 °C. After 24 h, the reaction was allowed to cool to room temperature. The resultant mixture was diluted with ethyl acetate (40 mL) and washed with saturated sodium carbonate solution (50 mL). The aqueous and organic layers were separated. The aqueous layer was extracted with ethyl acetate (3 × 40 mL), and the combined organic layers were washed with water (3 × 10 mL) and dried over magnesium sulfate, filtered, and concentrated under vacuum. The concentrate was purified by column chromatography using hexanes as eluent.

Alkenylation of toluene

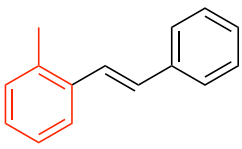

2a-*ortho*

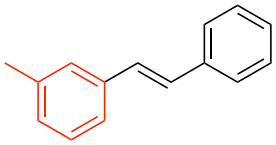

2a-*meta*

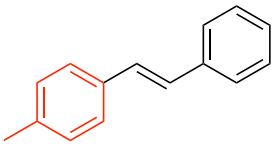

2a-*para*

Following the general procedure described above and using toluene as the arene, the target compounds mixture of **2a** were obtained as a white solid (74 mg, 76%, *ortho*:*para*:*meta* = 1:28:13). The products were separated and purified by flash column chromatography using hexanes as the eluent. However, due to the production of only a small quantity of **2a**-*ortho*, we were unable to isolate this compound. **Characterization of 2a-meta (1c)** (This

compound was reported in literature.[79]): **^{1}H NMR (600 MHz, $CDCl_3$):** δ 7.54 (m, 2H), 7.41 – 7.33 (m, 4H), 7.31 – 7.26 (m, 2H), 7.16 – 7.08 (m, 3H), 2.41 (s, 3H) ppm. **^{13}C NMR (201 MHz, $CDCl_3$):** δ 138.4, 137.6, 137.4, 129.0, 128.8, 128.7, 128.7, 128.6, 128.6, 128.6, 127.7, 127.4, 126.6, 123.9, 21.6 ppm. **Characterization of 3a-para (1b)** (This compound was reported in literature.[79]): **^{1}H NMR (600 MHz, $CDCl_3$):** δ 7.53 (m, 2H), 7.45 (m, 2H), 7.38 (m, 2H), 7.28 (m, 1H), 7.20 (m, 2H), 7.13 (d, J = 16.4 Hz, 1H), 7.09 (d, J = 16.4 Hz, 1H), 2.39 (s, 3H) ppm. **^{13}C NMR (201 MHz, $CDCl_3$):** δ 137.7, 134.7, 129.5, 128.8, 128.8, 128.7, 127.8, 127.5, 126.5, 21.4, 21.4 ppm.

Alkenylation of ethylbenzene

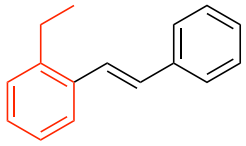

2b-*ortho*

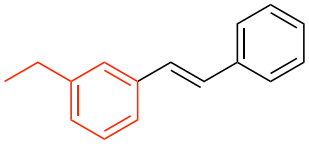

2b-*meta*

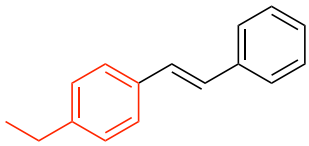

2c-*para*

Following the general procedure described above and using ethylbenzene as the arene, the target compounds mixture of **2b** were obtained as a white solid (82 mg, 81%, *ortho*:*para*:*meta* = 0:3:1). The product mixture was purified by flash column chromatography using hexanes as the eluent. However, due to the production of only a small quantity of **2b**-*ortho*, we were unable to see this compound from NMR.

Characterization of 2b mixture (2b-*meta* + 2b-*para*): ^{1}H NMR (600 MHz, $CDCl_3$) δ 7.54 – 7.48 (m, $2H^{meta}$+$2H^{para}$), 7.45 (m, $2H^{para}$), 7.39 – 7.33 (m, $3H^{meta}$+$2H^{para}$), 7.30 – 7.23 (m, $3H^{meta}$+$1H^{para}$), 7.20 (m, $2H^{para}$), 7.14 – 7.04 (m, $3H^{meta}$+$2H^{para}$),

2.72 – 2.63 (m, $4H^{meta}$+$4H^{para}$), 1.30 – 1.23 (m, $6H^{meta}$+$6H^{para}$) ppm. **HRMS (HAPCI) m/z:** Calcd for $C_{16}H_{16}^{+}$ = 208.1252, Found Mass = 208.1232.

Alkenylation of cumene

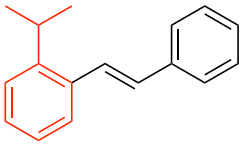

2c-*ortho*

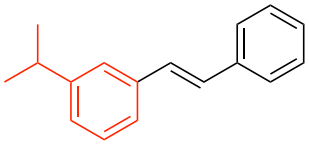

2c-*meta*

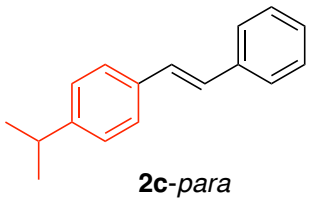

2c-*para*

Following the general procedure described above and using cumene as the arene, the target compounds mixture of **2c** were obtained as a white solid (88 mg, 77%, *ortho*:*para*:*meta* = 0:2:1). The products mixture was purified by flash column chromatography using hexanes as the eluent. However, due to the production of only a small quantity of **2c**-*ortho*, we were unable to see this compound from NMR. **Characterization of 2c mixture (2c-*meta* + 2c-*para*): ^{1}H NMR (600 MHz, $CDCl_3$):** δ 7.54 – 7.49 (m, $2H^{meta}$+$2H^{para}$), 7.46 (m, $2H^{para}$), 7.39 – 7.33 (m, $3H^{meta}$+$2H^{para}$), 7.31 – 7.21 (m, $3H^{meta}$+$3H^{para}$), 7.17 – 7.14 (m, $1H^{meta}$), 7.14 – 7.05 (m, $2H^{meta}$+$2H^{para}$), 2.94 (m, $1H^{meta}$+$1H^{para}$), 1.30 (d, J = 6.9 Hz, $6H^{para}$), 1.27 (d, J = 7.0 Hz, $6H^{meta}$) ppm. **HRMS (HAPCI) m/z:** Calcd for = $C_{17}H_{19}^{+}$ =223.1487, Found Mass = 223.1476.

Alkenylation of tert-butylbenzene

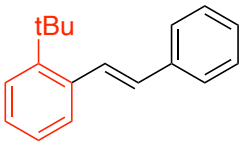

2d-*ortho*

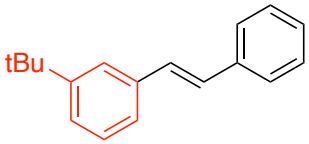

2d-*meta*

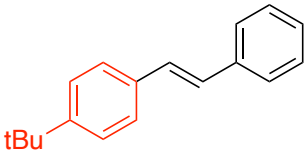

2d-*para*

Following the general procedure described above and using tert-butylbenzene as the arene, the target compounds mixture of **2d** were obtained as a white solid (96 mg, 81%, *ortho*:*para*:*meta* = 0:2:1). The products mixture was purified by flash column chromatography using hexanes as the eluent. However, due to the production of only a small quantity of **2d**-*ortho*, we were unable to see this compound from NMR. The assignment of peaks was achieved by comparison with the literature.[3] **Characterization of 2d mixture (2d-*meta* + 2d-*para*): ^{1}H NMR (600 MHz, $CDCl_3$):** δ 7.57 – 7.49 (m, $2H^{meta}$+$2H^{para}$), 7.48 – 7.44 (m, $2H^{para}$), 7.43 – 7.33 (m, $4H^{meta}$+$2H^{para}$), 7.33 – 7.28 (m, $2H^{para}$), 7.28 – 7.23 (m, $1H^{meta}$+$1H^{para}$), 7.18 – 7.03 (m, $2H^{meta}$+$2H^{para}$), 1.36 (s, $9H^{meta}$), 1.34 (s, $9H^{para}$) ppm. **HRMS (HAPCI) m/z:** Calcd for $C_{17}H_{19}^+$ =223.1487, Found Mass = 223.1476

Alkenylation of *para*-xylene

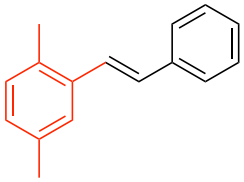

(*E*)-2,5-dimethyl-1-styrylbenzene (2e) Following the general procedure described above and using *para*-xylene as the arene, the target compound **2e** was obtained as a white solid (23 mg, 22%) after 48 hours reaction. The product was purified by flash column chromatography using hexanes as the eluent. This compound was reported in literature.[80] **^{1}H NMR (600 MHz,**

$CDCl_3$): δ 7.53 (m, 2H), 7.42 (d, *J* = 1.8 Hz, 1H), 7.37 (m, 2H), 7.32 (d, *J* = 16.2 Hz, 1H), 7.26 (m, 2H), 7.08 (d, *J* = 7.7 Hz, 1H), 7.03 – 6.97 (m, 2H), 2.39 (s, 3H), 2.36 (s, 3H) ppm. **^{13}C NMR (151 MHz, $CDCl_3$):** δ 137.9, 136.3, 135.7, 132.9, 130.5, 129.8, 128.8, 128.5, 127.7, 126.8, 126.7, 126.1, 21.2, 19.6 ppm. **HRMS (HAPCI) m/z:** Calcd for $C_{16}H_{16}^+$ =208.1252, Found Mass = 208.1243.

Alkenylation of *meta*-xylene

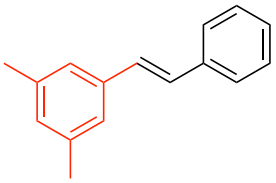

(*E*)-3,5-dimethyl-1-styrylbenzene (2f) Following the general procedure described above and using *meta*-xylene as the arene, the target compound **2f** was obtained as a white solid (88 mg, 77%) after 48 hours reaction. The product was purified by flash column chromatography using hexanes as the eluent. This compound was reported in literature.[79] **^{1}H NMR (600 MHz, $CDCl_3$):** δ 7.53 (m, 2H), 7.38 (m, 2H), 7.27 (tt, *J* = 7.3, 1.3 Hz, 1H), 7.17 (s, 2H), 7.11 (s, *J* = 16.3 Hz, 1H), 7.07 (d, *J* = 16.4 Hz, 1H), 6.93 (s, 1H), 2.36 (s, 6H). **^{13}C NMR (151 MHz, $CDCl_3$):** δ 138.2, 137.7, 137.4, 129.6, 129.0, 128.8, 127.6, 126.6, 124.6, 21.5 ppm. **HRMS (HAPCI) m/z:** Calcd for $C_{16}H_{16}^+$ =208.1252, Found Mass = 208.1246.

Alkenylation of *ortho*-xylene

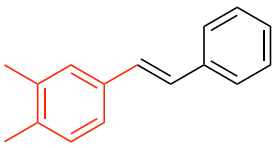

(*E*)-3,4-dimethyl-1-styrylbenzene (2g) Following the general procedure described above and using *ortho*-xylene as the arene, the target compound **2g** was obtained as a white solid (81 mg, 71%). The product was purified by flash column chromatography using hexanes as the eluent. This compound was

reported in literature.[87] **^{1}H NMR (600 MHz, $CDCl_3$):** δ 7.53 (m, 2H), 7.38 (m, 2H), 7.33 (s, 1H), 7.29 (dd, *J* = 7.5, 1H), 7.27 (m,1H), 7.15 (d, *J* = 7.7 Hz, 1H), 7.09 (m, 2H), 2.32 (s, 3H), 2.30 (s, 3H) ppm. **^{13}C NMR (151 MHz, $CDCl_3$):** δ 137.7, 136.9, 136.4, 135.1, 130.1, 128.9, 128.8, 127.9, 127.7, 127.5, 126.5, 124.2, 20.0, 19.7 ppm. **HRMS (HAPCI) m/z:** Calcd for $C_{16}H_{16}^+$ =208.1252, Found Mass = 208.1239.

Alkenylation of 1,2,3-trimethylbenzene

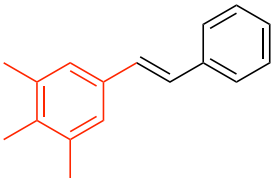

(*E*)-3,4,5-trimethyl-1-styrylbenzene (2h) Following the general procedure described above and using 1,2,3-trimethylbenzene as the arene, the target compound **2h** was obtained as a white solid (75 mg, 67%). The product was purified by flash column chromatography using hexanes as the eluent. This compound was reported in literature.[88] **^{1}H NMR (600 MHz, $CDCl_3$):** δ 7.51 (m, 2H), 7.35 (m, 2H), 7.25 (m, 2H), 7.19 (s, 2H), 7.07 (d, *J* = 16.2 Hz, 1H), 7.04 (d, *J* = 16.3 Hz, 1H), 2.33 (s, 6H), 2.20 (s, 3H) ppm. **^{13}C NMR (151 MHz, $CDCl_3$):** δ 137.8, 136.8, 135.0, 134.4, 128.9, 128.8, 127.5, 127.4, 126.5, 125.9, 20.8, 15.5 ppm. **HRMS (HAPCI) m/z:** Calcd for $C_{17}H_{19}^+$ =223.1487, Found Mass = 223.1481.

Alkenylation of cyclohexylbenzene

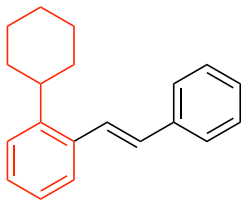

2i-*ortho*

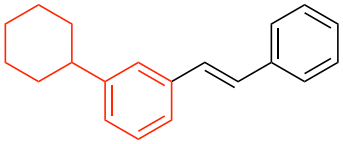

2i-*meta*

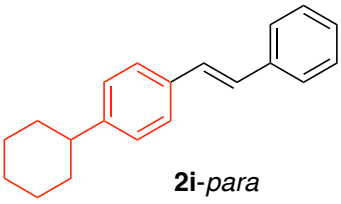

2i-*para*

Following the general procedure described above and using cyclohexylbenzene as the arene, the target compounds mixture of **2i** were obtained as a white solid (106 mg, 81%, *ortho*:*para*:*meta* = 0:3:1). The products mixture was purified by flash column chromatography using hexanes as the eluent. However, due to the production of only a small quantity of **2i**-*ortho*, we were unable to see this compound from NMR. **Characterization of 2i mixture (2i-*meta* + 2i-*para*):** ^{1}H NMR (600 MHz, $CDCl_3$) δ 7.56 – 7.51 (m, $2H^{meta}$+$2H^{para}$), 7.46 (m, $2H^{para}$), 7.41 – 7.25 (m, $6H^{meta}$+$3H^{para}$), 7.23 (m, $2H^{para}$), 7.17 – 7.04 (m, $3H^{meta}$+$2H^{para}$), 2.55 (m, $1H^{meta}$+$1H^{para}$), 2.02 – 1.73 (m, $5H^{meta}$+$5H^{para}$), 1.53 – 1.21 (m, $5H^{meta}$+$5H^{para}$) ppm. **HRMS (HAPCI) m/z:** Calcd for $C_{20}H_{22}^{+}$ = 262.1722, Found Mass = 262.1709.

Alkenylation of biphenyl

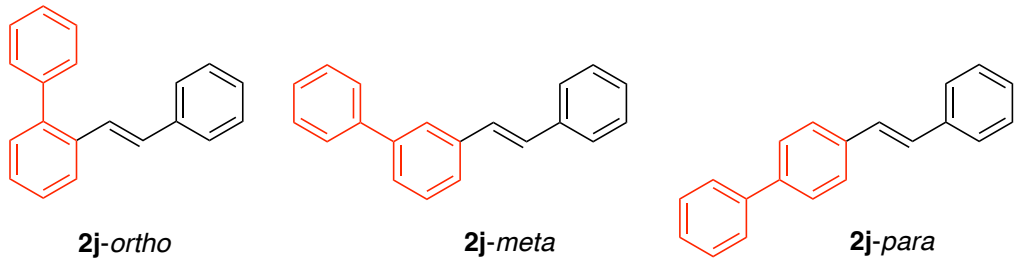

2j-*ortho* **2j**-*meta* **2j**-*para*

Following the general procedure described above and using biphenyl as the arene, 2.5mL of mesitylene was added to the reaction mixture as the co-solvent, the target compounds mixture of **2j** were obtained as a white solid (96 mg, 81%, *ortho*:*para*:*meta* = 0:2:1). The products were separated and purified by flash column chromatography using hexanes as the eluent. However, due to the production of only a small quantity of **2j**-*ortho*, we were

unable to isolate this compound. **Characterization of 2j-*meta*** (This compound was reported in literature.[12])**: ^{1}H NMR (600 MHz, $CDCl_3$):** δ 7.74 (t, *J* = 1.8 Hz, 1H), 7.64 (m, 2H), 7.55 (m, 2H), 7.53 – 7.43 (m, 5H), 7.38 (m, 3H), 7.29 (m, 1H), 7.19 (s, 2H) ppm. **^{13}C NMR (151 MHz, $CDCl_3$):** δ 141.9, 141.3, 138.0, 137.4, 129.24, 129.22, 128.93, 128.86, 128.8, 127.9, 127.6, 127.4, 126.71, 126.68, 125.6, 125.5 ppm. **Characterization of 2j-*para*** (This compound was reported in literature.[89])**: ^{1}H NMR (600 MHz, $CDCl_3$):** δ 7.65 – 7.57 (m, 6H), 7.54 (m, 2H), 7.48 (m, 2H), 7.40 – 7.34 (m, 3H), 7.38 (m, 1H), 7.16 (s, 2H) ppm. **^{13}C NMR (151 MHz, $CDCl_3$):** δ 140.8, 140.5, 137.5, 136.6, 129.0 (d, *J* = 1.8 Hz), 128.92, 128.86, 128.4, 127.51, 127.48, 127.1, 127.1, 126.7 ppm. **HRMS (HAPCI) m/z:** Calcd for $C_{20}H_{16}^{+}$ = 256.1252, Found Mass = 256.1250.

Alkenylation of fluorobenzene

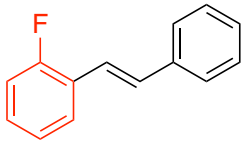

2k-*ortho*

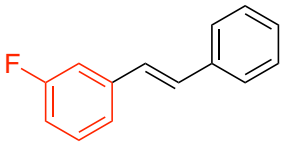

2k-*meta*

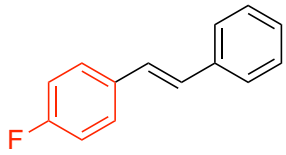

2k-*para*

Following the general procedure described above and using fluorobenzene as the arene, the target compounds mixture of **2k** were obtained as a white solid (81 mg, 82%, *ortho*:*para*:*meta* = 1:28:23). The products mixture was purified by flash column chromatography using hexanes as the eluent. However, due to the production of only a small quantity of **2k**-*ortho*, we were unable to see this compound in NMR. **Characterization of 2k-*meta*: ^{1}H NMR (600 MHz, $CDCl_3$):** δ 7.52 (d, *J* = 7.7 Hz, 2H),

7.37 (t, J = 7.6 Hz, 2H), 7.33–7.27 (m, 3H), 7.22 (d, J = 10.0 Hz, 1H), 7.11, 7.07 (ABq, $\Delta\nu_{AB}$ = 24 Hz, J_{AB} = 18 Hz, 2H), 6.95 (t, J = 7.8 Hz, 1H) ppm. **^{13}C NMR (201 MHz, $CDCl_3$):** δ 163.3 (d), 139.9 (d), 137.0, 130.2 (d), 130.2, 128.9, 128.2, 127.6 (d), 126.8, 122.6 (d), 114.5 (d), 112.9 (d) ppm. **^{19}F NMR (564 MHz, $CDCl_3$):** δ -111.8 (td, J = 9.3, 6.2 Hz, 1H) ppm. **Characterization of 2k-*para*: ^{1}H NMR (600 MHz, $CDCl_3$):** δ 7.49 (m, 4H), 7.36 (t, J = 7.6 Hz, 2H), 7.28 (s, 1H), 7.09 – 7.00 (m, 4H) ppm. **^{13}C NMR (201 MHz, $CDCl_3$)**: δ 162.3 (d, J = 247.3 Hz), 137.2, 133.5 (d, J = 3.3 Hz), 128.7, 128.5 (d, J = 2.3 Hz), 128.0 (d, J = 7.9 Hz), 127.7, 127.5, 126.4, 115.6 (d, J = 21.6 Hz) ppm. **^{19}F NMR (564 MHz, $CDCl_3$)**: δ -112.5 (tt, J = 8.6, 5.4 Hz) ppm. **HRMS (HAPCI) m/z:** Calcd for $C_{14}H_{11}F^+$ = 198.0845, Found Mass = 198.0842.

Alkenylation of chlorobenzene

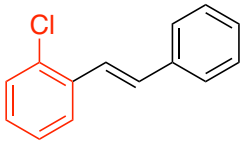

2l-*ortho*

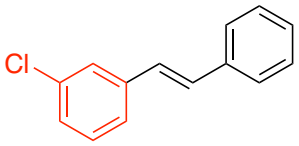

2l-*meta*

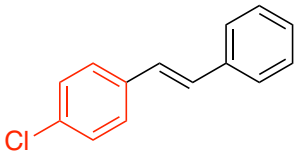

2l-*para*

Following the general procedure described above and using chlorobenzene as the arene, the target compounds mixture of **2l** were obtained as a white solid (94 mg, 87%, *ortho*:*para*:*meta* = 0:2:1). The products were separated and purified by flash column chromatography using hexanes as the eluent. However, due to the production of only a small quantity of **2l**-*ortho*, we were unable to isolate this compound. **Characterization of 2l-*meta*: ^{1}H NMR (600 MHz, $CDCl_3$):** δ 7.55 – 7.50 (m, 3H), 7.42 – 7.36 (m, 3H), 7.33 –

7.28 (m, 2H), 7.25 (ddd, J = 7.9, 2.1, 1.2 Hz, 1H), 7.13 (d, J = 16.3 Hz, 1H), 7.05 (d, J = 16.3 Hz, 1H) ppm. **^{13}C NMR (201 MHz, $CDCl_3$):** δ 139.4, 136.9, 134.8, 130.3, 130.0, 128.9, 128.2, 127.6, 127.3, 126.8, 126.4, 124.9 ppm. **Characterization of 2l-*para*: ^{1}H NMR (600 MHz, $CDCl_3$):** δ 7.51 (d, J = 7.6 Hz, 2H), 7.44 (d, J = 8.6 Hz, 2H), 7.37 (t, J = 7.7 Hz, 2H), 7.33 (d, J = 8.5 Hz, 2H), 7.28 (t, J = 7.3 Hz, 1H), 7.08, 7.05 (ABq, $\Delta\nu_{AB}$ = 13.4 Hz, J_{AB} = 12 Hz, 2H) ppm. **^{13}C NMR (201 MHz, $CDCl_3$):** δ 137.1, 136.0, 133.3, 129.5, 129.0, 128.9, 128.0, 127.8, 127.5, 126.7 ppm.

HRMS (HAPCI) m/z: Calcd for $C_{14}H_{11}Cl^+$ = 214.0549, Found Mass = 214.0539.

Alkenylation of bromobenzene

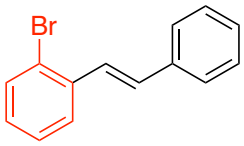

2m-*ortho*

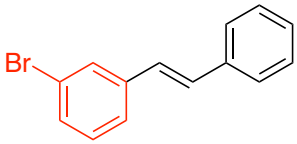

2m-*meta*

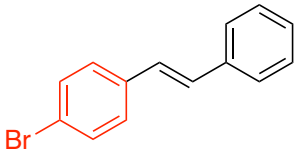

2m-*para*

Following the general procedure described above and using bromobenzene as the arene, the target compounds mixture of **2m** and undesired product stilbene **1a** were obtained as a white solid. The products were separated and purified by flash column chromatography using hexanes as the eluent. Only 21 mg 21% of **2m**-*para* was cleanly separated.

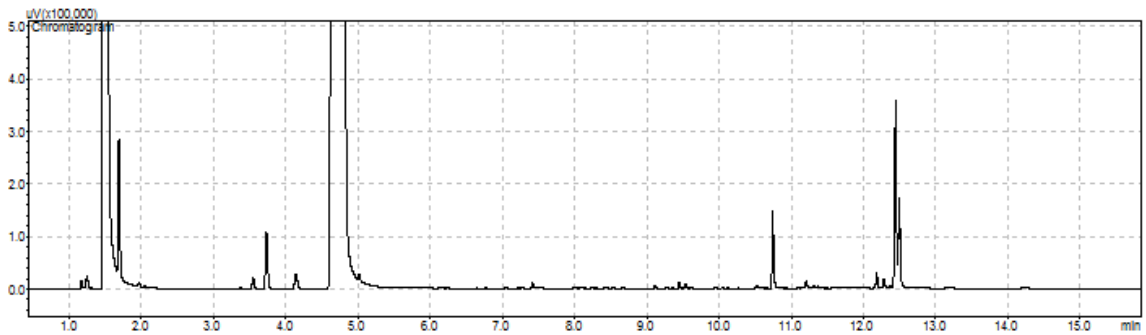

Representative GC-FID chromatogram of a reaction mixture from the reaction between bromobenzene and styrene. Peak assignments: 1-2 minutes dichloromethane, acetone and benzene; 4.1 minutes styrene; 4.6-5 minutes bromobenzene; 10.8 minutes trans-stilbene; 12-13 minutes mixture of bromostilbenes. GC-FID Parameters: starting temperature: 50 °C; time at starting temp: 2.5 min; ramp1: 20 °C/min up to 240 °C; hold for 6 min; flow rate (carrier): 3.01 mL/min (He); split ratio: 35:1; inlet temperature: 200 °C; detector temperature: 240 °C.**Characterization of 2m-*para*: ^{1}H NMR (600 MHz, $CDCl_3$):** δ 7.56 – 7.46 (m, 4H), 7.41 – 7.33 (m, 4H), 7.28 (m, 1H), 7.10 (d, *J* = 16.3 Hz, 1H), 7.04 (d, *J* = 16.3 Hz, 1H) ppm. **^{13}C NMR (201 MHz, $CDCl_3$):** δ 137.1, 136.4, 131.9, 129.6, 128.9, 128.12, 128.05, 127.6, 126.7, 121.5 ppm.

Alkenylation of iodobenzene

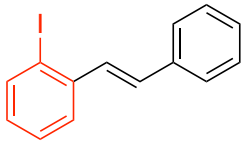

2n-*ortho*

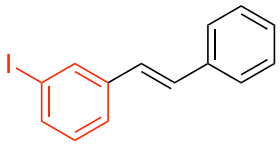

2n-*meta*

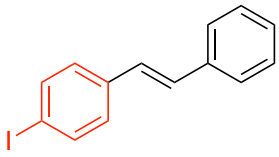

2n-*para*

Following the general procedure described above and using iodobenzene as the arene, the target compounds mixture of **2n** and undesired product stilbene **1a** were obtained as a white solid. The products were separated and purified by flash column chromatography using hexanes as the eluent.

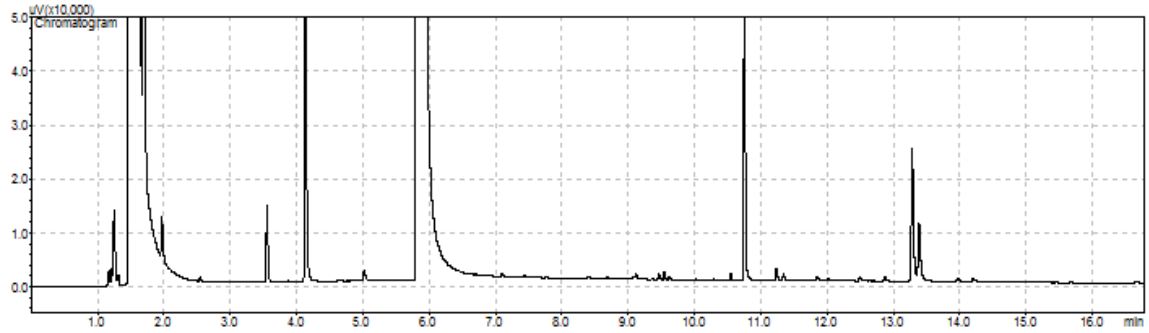

Representative GC-FID chromatogram of a reaction mixture from the reaction between iodobenzene and styrene. Peak assignments: 1-2 minutes dichloromethane, acetone and benzene; 4.1 minutes styrene; 5.6-7 minutes iodobenzene; 10.8 minutes trans-stilbene; 13-14 minutes mixture of iodostilbenes. GC-FID Parameters: starting temperature: 50 °C; time at starting temp: 2.5 min; ramp1: 20 °C/min up to 240 °C; hold for 6 min; flow rate (carrier): 3.01 mL/min (He); split ratio: 35:1; inlet temperature: 200 °C; detector temperature: 240 °C.

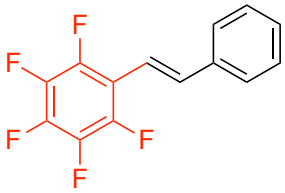

Alkenylation of pentafluorobenzene

(*E*)-2,3,4,5,6-pentafluoro-1-styrylbenzene (2o) Following the general procedure described above and using pentafluorobenzene as arene, the target compound **2o** was obtained as a white solid (82 mg, 61%). The product was purified by flash column chromatography using hexanes as the eluent. **^{1}H NMR (600 MHz, $CDCl_3$):** δ 7.54 (m, 2H), 7.46 – 7.38 (m, 3H), 7.35 (m, 1H), 6.99 (d, J = 16.8 Hz, 1H). **^{13}C NMR (201 MHz, $CDCl_3$):** δ 145.2 (dm, J = 250.1 Hz), 139.5 (dm, J = 254.9 Hz), 137.8 (dm, J = 252.1 Hz), 137.2 (t, J = 8.2 Hz), 136.5, 129.0, 128.9, 126.9, 112.7, 112.4

(td, J = 13.7, 4.5 Hz) ppm. **^{19}F NMR (564 MHz, $CDCl_3$):** δ -143.3 (dd, J = 21.2 Hz, 7.1 Hz, 2F), -157.2 (t, J = 20.8 Hz, 1F), -163.6 (td, J=20.8Hz, 6.8Hz, 2F) ppm. **HRMS (HAPCI) m/z:** Calcd for = $C_{14}H_7F_5^+$ = 270.0468, Found Mass = 270.0465。

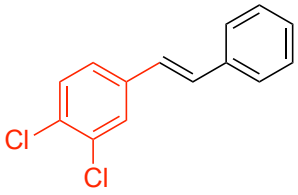

Alkenylation of 1,2-dichlorobenzene

(*E*)-3,4-dichloro-1-styrylbenzene (2p) Following the general procedure described above and using pentafluorobenzene as arene, the target compound **2p** was obtained as a white solid (81 mg, 74%). The product was purified by flash column chromatography using hexanes as the eluent. This compound was reported in literature.[82] **^{1}H NMR (600 MHz, $CDCl_3$):** δ 7.59 (d, J = 2.1, 1H), 7.50 (m, 2H), 7.42 (d, J = 8.3 Hz, 1H), 7.38 (m, 2H), 7.33 (dd, J = 8.3, 2.1, 1H), 7.30 (m, 1H), 7.09 (d, J = 16.3 Hz, 1H), 6.99 (d, J = 16.3 Hz, 1H) ppm. **^{13}C NMR (151 MHz, $CDCl_3$):** δ 137.6, 136.7, 132.9, 131.3, 130.7, 130.7, 128.9, 128.4, 128.2, 126.8, 126.3, 125.8 ppm. **HRMS (HAPCI) m/z:** Calcd for $C_{14}H_{10}Cl_2^+$ = 248.0160, Found Mass = 248.0163.

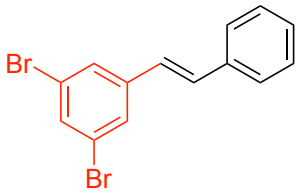

Alkenylation of 1,3-dibromobenzene

(*E*)-3,5-dibromo-1-styrylbenzene (2q) Following the general procedure described above and using 1,3-dibromobenzene as arene, the target compound **2q** was obtained as a white solid (125 mg, 74%). The product was purified by flash column chromatography using hexanes as the eluent. This compound was reported in literature.[90] **^{1}H NMR (600 MHz, $CDCl_3$):** δ 7.57 (d, J = 1.6 Hz, 2H), 7.54

(t, J = 1.7 Hz, 1H), 7.50 (m, 2H), 7.38 (m, 2H), 7.31 (m, 1H), 7.10 (d, J = 16.3 Hz, 1H), 6.93 (d, J = 16.3 Hz, 1H) ppm. **^{13}C NMR (151 MHz, $CDCl_3$):** δ 141.2, 136.4, 132.8, 131.7, 129.0, 128.6, 128.2, 127.0, 125.8, 123.4 ppm. **HRMS (HAPCI) m/z:** Calcd for $C_{14}H_{10}Br_2^+$ = 335.9149, Found Mass = 335.9142.

Alkenylation of α, α, α-trifluorotoluene

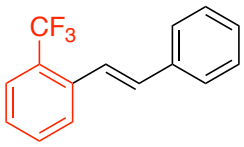

2r-*ortho*

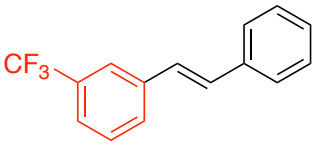

2r-*meta*

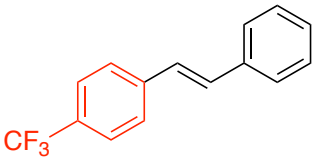

2r-*para*

Following the general procedure described above and using α, α, α-trifluorotoluene as the arene, the target compounds mixture of **2r** were obtained as a white solid (108 mg, 87%, *ortho*:*para*:*meta* = 0:2:1). The product was purified by flash column chromatography using hexanes as the eluent. The assignment of peaks was achieved by comparison with the literature.[3] **^{1}H NMR (600 MHz, $CDCl_3$)**: δ 7.78 (s, 1H^{meta}), 7.69 (d, J = 7.0, 1H^{meta}), 7.65 – 7.59 (m , 4H^{para}), 7.58 – 7.51 (m, 3H^{meta}+2H^{para}), 7.48 (t, J = 7.7 Hz, 1H^{meta}), 7.43 – 7.37 (m, 2H^{meta}+2H^{para}), 7.35 – 7.29 (m, 1H^{meta}+1H^{para}), 7.23 – 7.09 (m, 2H^{meta}+2H^{para}). **^{19}F NMR (564 MHz, $CDCl_3$):** δ -60.84 (s, 3F^{para}), -61.14 (s, 3F^{meta}) ppm.**HRMS (HAPCI) m/z:** Calcd for = $C_{15}H_{11}F_3^+$ = 248.0813, Found Mass = 248.0813.

Alkenylation of naphathalene

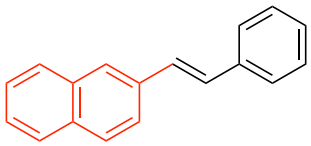

(*E*)-2-styrylnaphthalene (2s) Following the general procedure described above and using naphthalene as the arene, 2.5mL of mesitylene was added to the reaction mixture as the co-solvent, the target compound **3s** was obtained as a white solid (86 mg, 75%). The product was purified by flash column chromatography using hexanes as the eluent. This compound was reported in literature.[12] **^{1}H NMR (600 MHz, $CDCl_3$):** δ 7.86 (br, s, 1H), 7.85 – 7.79 (m, 2H), 7.75 (dd, *J* = 8.6, 1.8 Hz, 1H), 7.57 (m, 2H), 7.50 – 7.42 (m, 2H), 7.38 (m, 2H), 7.29 (d, *J* = 16.4 Hz, 1H), 7.28 (m, 2H).7.24 (d, *J* = 16.3 Hz, 1H) ppm. **^{13}C NMR (151 MHz, $CDCl_3$):** δ 137.5, 135.0, 133.9, 133.2, 129.2, 128.9, 128.9, 128.5, 128.1, 127.8, 127.8, 126.8, 126.7. 126.5, 126.0, 123.7 ppm. **HRMS (HAPCI) m/z:** Calcd for $C_{18}H_{14}^+$ = 230.1096, Found Mass = 230.1084.

Alkenylation of furan

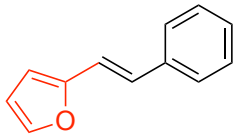

(*E*)-2-styrylfuran (2t) Following the general procedure described above and using furan as the arene, the target compound **2t** was obtained as a white solid (42 mg, 49%). The product was purified by flash column chromatography using hexanes as the eluent. This compound was reported in literature.[79] **^{1}H NMR (600 MHz, $CDCl_3$):** δ 7.47 (m, 2H), 7.41 (dd, *J* = 1.8, 0.7 Hz, 1H), 7.35 (m, 2H), 7.26 (m, 1H), 7.05 (d, *J* = 16.3 Hz, 1H), 6.91 (d, *J* = 16.3 Hz, 1H), 6.43 (dd, *J* = 3.3, 1.8 Hz, 1H), 6.36 (dd, *J* = 3.3, 0.7 Hz, 1H). **HRMS (HAPCI) m/z:** Calcd for $C_{12}H_{11}O^+$ = 171.0810, Found Mass = 171.0787.

Alkenylation of trimethylsilyl benzene

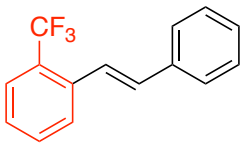

2r-*ortho*

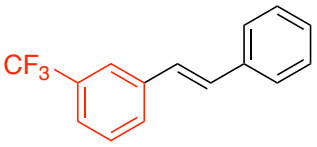

2r-*meta*

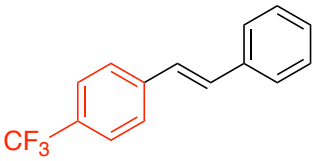

2r-*para*

Following the general procedure described above and using trimethylsilyl benzene as the arene, the target compounds mixture of **2u** were obtained as a white solid (115 mg, 91%, *ortho*:*para*:*meta* = 0:2:1). The product was purified by flash column chromatography using hexanes as the eluent. **Characterization of 3u mixture (3u-*meta* + 3u-*para*): ^{1}H NMR (600 MHz, $CDCl_3$):** δ 7.70 (m, $1H^{meta}$), 7.61 – 7.52 (m, $2H^{meta}$+$6H^{para}$), 7.48 (dt, *J* = 7.3, 1.2 Hz, $1H^{meta}$), 7.41 (m, $3H^{meta}$+$2H^{para}$), 7.33 – 7.29 (m, $1H^{meta}$ +$1H^{para}$), 7.22 – 7.13 (m, $3H^{meta}$+$2H^{para}$), 0.37 (s, $9H^{meta}$), 0.34 (s, $9H^{para}$) ppm. **HRMS (HAPCI) m/z:** Calcd for $C_{17}H_{20}Si^+$ = 252.1334, Found Mass = 252.1329.

Alkenylation of anisole

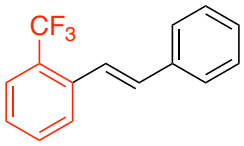

2r-*ortho*

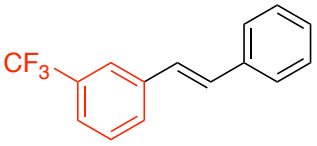

2r-*meta*

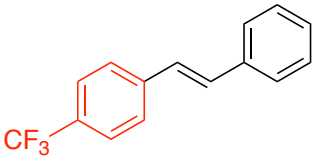

2r-*para*

Following the general procedure described above and using anisole as the arene, reaction was run under 135 °C for 96 hours, the reactor was cooled down and purge by fresh air every 24 hours, the target compounds mixture of **2v** were obtained as a colorless liquid (85 mg, 81%, *ortho*:*para*:*meta* = 0.3:1.7:1) The product was purified by flash column chromatography using hexanes and ethyl acetate (v/v = 9:1) as the eluent. However, due to

the production of only a small quantity of **3v**-*ortho*, we were unable to isolate this compound. **Characterization of 2v-*meta*: ^{1}H NMR (600 MHz, $CDCl_3$):** δ 7.55 (m, 2H), 7.40 (m, 2H), 7.35 – 7.28 (m, 2H), 7.19 – 7.12 (m, 3H), 7.10 (dd, J = 2.6, 1.0 Hz, 1H), 6.87 (ddd, J = 8.2, 2.5, 0.9 Hz, 1H), 3.88 (s, 3H) ppm. **^{13}C NMR (151 MHz, $CDCl_3$):** δ 160.0, 138.9, 137.4, 129.8, 129.1, 128.8, 128.7, 127.8, 126.7, 119.4, 113.4, 111.9, 55.3 ppm. **Characterization of 2v-*para*: ^{1}H NMR (600 MHz, $CDCl_3$):** δ 7.48 (dd, J = 20.1, 8.0 Hz, 4H), 7.35 (t, J = 7.5 Hz, 2H), 7.24 (t, J = 7.4 Hz, 1H), 7.07, 6.98 (ABq, $\Delta\nu_{AB}$ = 52.6 Hz, J_{AB} = 16.3 Hz, 2H), 6.91 (d, J = 8.4 Hz, 2H), 3.84 (s, 3H) ppm. **^{13}C NMR (201 MHz, $CDCl_3$):** δ 159.4, 137.8, 130.3, 128.78, 128.4, 127.9, 127.4, 126.8, 126.4, 114.3, 77.2, 55.5 ppm. **Characterization of 2v mixture: HRMS (HAPCI) m/z:** Calcd for $C_{15}H_{15}O^+$ = 211.1123, Found Mass = 211.1122.

Alkenylation of 1,3-dimethoxybenzene

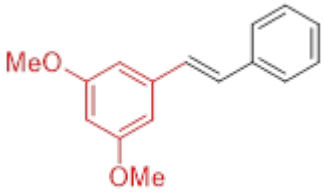

(*E*)-3,5-dimethoxyl-1-styrylbenzene (1w) Following the general procedure described above and using 1,3-dimethoxybenzene as the arene, reaction was run under 135 °C for 96 hours, the reactor was cooled down and purge by fresh air every 24 hours, the target compound of **1w** were obtained as a colorless liquid (89 mg, 74%). The product was purified by flash column chromatography using hexanes and ethyl acetate (v/v = 9:1) as the eluent. This compound was reported in literature.[4] **^{1}H NMR (600 MHz, $CDCl_3$):** δ 7.52

(m, 2H), 7.37 (m, 2H), 7.28 (m, 1H), 7.11 (d, J = 16.3 Hz, 1H), 7.05 (d, J = 16.3 Hz, 1H), 6.70 (d, J = 2.3 Hz, 2H), 6.42 (t, J = 2.3 Hz, 1H), 3.85 (s, 6H) ppm.**^{13}C NMR (151 MHz, $CDCl_3$)**: δ 161.1, 139.5, 137.3, 129.3, 128.8, 127.9, 126.7, 104.7, 100.1, 55.5 ppm. **HRMS (HAPCI) m/z:** Calcd for $C_{16}H_{16}O_2^+$ = 240.1150, Found Mass = 240.1158.

Alkenylation of 1,2-dimethoxybenzene

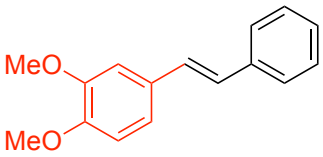

(*E*)-3,4-dimethoxyl-1-styrylbenzene (1x) Following the general procedure described above and using 1,2-dimethoxybenzene as the arene, reaction was run under 135 °C for 96 hours, the reactor was cooled down and purge by fresh air every 24 hours, the target compound of **1x** were obtained as a colorless liquid (88 mg, 73%). The product was purified by flash column chromatography using hexanes and ethyl acetate (v/v = 9:1) as the eluent. This compound was reported in literature.[79] **^{1}H NMR (600 MHz, $CDCl_3$):** δ 7.50 (m, 2H), 7.35 (m, 2H), 7.25 (m, 1H), 7.09 – 7.03 (m, 3H), 6.98 (d, J = 16.3 Hz, 1H), 6.87 (d, J = 8.2 Hz, 1H), 3.95 (s, 3H), 3.91 (s, 3H) ppm. **^{13}C NMR (151 MHz, $CDCl_3$):** δ 149.3, 149.1, 137.7, 130.6, 128.8, 128.6, 127.4, 127.0, 126.4, 120.0, 111.4, 108.9, 56.1, 56.0ppm. **HRMS (HAPCI) m/z:** Calcd for $C_{16}H_{16}O_2^+$ = 240.1150, Found Mass = 240.1149.

Alkenylation of 1,2,3-trimethoxybenzene

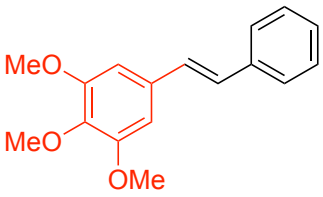

(*E*)-3,4,5-trimethoxyl-1-styrylbenzene (1y) Following the general procedure described above and using 1,2,3-trimethoxybenzene as the arene, reaction was run under 135 °C for 96 hours, the reactor was cooled down and purge by fresh air every 24 hours, the target compound of **1y** were obtained as a light yellow liquid (99 mg, 73%). The product was purified by flash column chromatography using hexanes and ethyl acetate (v/v = 9:1) as the eluent. This compound was reported in literature.[79] **^{1}H NMR (600 MHz, $CDCl_3$):** δ 7.51 (m, 2H), 7.36 (m, 2H), 7.27 (m, 1H), 7.05 (d, *J* = 16.3 Hz, 1H), 7.01 (d, *J* = 16.2 Hz, 1H), 3.92 (s, 6H), 3.88 (s, 3H) ppm. **^{13}C NMR (151 MHz, $CDCl_3$):** δ 153.6, 137.4, 133.2, 128.9, 128.8, 128.4, 127.8, 126.6, 103.8, 81.0, 61.1, 56.3 ppm. **HRMS (HAPCI) m/z:** Calcd for $C_{17}H_{18}O_3^+$ = 270.1256, Found Mass = 270.1254.

5.11.4 Synthesis of bioactive stilbenes derivatives

Under an atmosphere of dry nitrogen, di-μ-acetatotetrakis(dihaptoethene)dirhodium(I) (2.5 μmol, 550 μg), copper(II) pivalate (400 μmol, 106 mg) and pivalic acid (2 mmol, 204 mg) were added to a dried Andrews Glass™ Lab-Crest® Fisher-Porter tube with a stir bar. Then, vinyl arene (500 μmol) and arene (5 mL) were added by syringe. The tube was opened to air, sealed and pressurized with dinitrogen (60 psig). The mixture was stirred at 135 °C for 96 hours. After every 24 h, the reaction was allowed to cool to room temperature and fresh air was purged into the reactor via a long needle. After the reaction finished, the

resultant mixture was diluted with ethyl acetate (40 mL) and washed with saturated sodium carbonate solution (50 mL). The aqueous and organic layers were separated. The aqueous layer was extracted with ethyl acetate (3 × 40 mL), and the combined organic layers were washed with water (3 × 10 mL), dried over magnesium sulfate, filtered and concentrated under vacuum. The concentrate was purified by column chromatography using 9:1 hexanes:ethyl acetate as eluent.

Alkenylation of 1,3-dimethoxybenzene using 4-methoxystyrene, synthesis of *(E)*-1,3-dimethoxy-5-(4- methoxystyryl)benzene

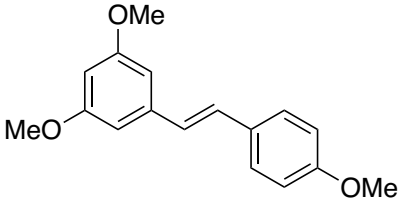

Following the general procedure described above and using 1,3-dimethoxybenzene as the arene, 4-vinylanisole as the vinylarene, reaction was run under 135 °C for 96 hours, the reactor was cooled down and purge by fresh air every 24 hours, the target compound of *(E)*-1,3-dimethoxy-5-(4- methoxystyryl)benzene was obtained as a light yellow liquid (92 mg, 68%). The product was purified by flash column chromatography using hexanes and ethyl acetate (v/v = 9:1) as the eluent. This compound was reported in literature.[12] **^{1}H NMR (600 MHz, $CDCl_3$):** δ 7.45 (m, 2H), 7.04 (d, *J* = 16.3 Hz, 1H), 6.93 – 6.89 (m, 3H), 6.66 (d, *J* = 2.3 Hz, 2H), 6.38 (t, *J* = 2.2 Hz, 1H), 3.83 (s, 9H) ppm. **^{13}C NMR (151 MHz, $CDCl_3$):** δ 161.1, 159.6, 139.9, 130.1, 128.9, 127.9, 126.7, 114.3, 104.5,

99.8, 55.50, 55.47ppm. **HRMS (HAPCI) m/z:** Calcd for $C_{17}H_{18}O_3^+$ = 270.1256, Found Mass = 270.1259.

Deprotection of trimethyl resveratrol

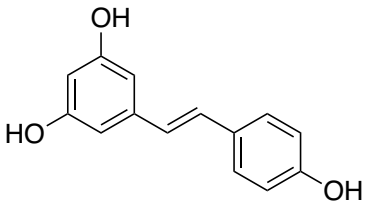

We followed a published with some modification.[4] *(E)*-1,3-dimethoxy-5-(4- methoxystyryl)benzene (92 mg, 340 µmol, 1.0 equiv) was dissolved in CH_2Cl_2 (15 mL) and a solution of BBr_3 (1.0 M in CH_2Cl_2, 3.3 mmol, 3.3 mL, 9.0 equiv) was added at –78 °C. The mixture was stirred for 1 h at –78 °C. Then the reaction was allowed to warm to room temperature, H_2O (25 mL) was added and the mixture was poured into H_2O (25 mL). Extraction with EtOAc (3 × 25 mL), washing of the combined organic layers with H_2O (25 mL), brine (25 mL), drying over $MgSO_4$ and concentration under reduced pressure gave the crude product which was purified by flash column chromatography using hexanes and ethyl acetate (v/v = 9:1) as the eluent. The target compound of resveratrol was obtained as a white solid (74 mg, 96%). **^{1}H NMR (600 MHz, DMSO-d_6):** δ 9.53 (s, 1H), 9.17 (s, 2H), 7.39 (m, 2H), 6.92 (d, J = 16.3 Hz, 1H), 6.81 (d, J = 16.3 Hz, 1H), 6.75 (m, 2H), 6.37 (d, J = 2.1 Hz, 2H), 6.11 (t, J = 2.1 Hz, 1H) ppm. **^{13}C NMR (201 MHz, DMSO-d_6):** δ 158.5, 157.2, 139.2, 128.1, 127.8, 127.8, 125.6, 115.5, 104.3, 101.7 ppm.

Synthesis of *(E)*-1,2,3-trimethoxy-5-(4-methoxystyryl)benzene (DMU-212)

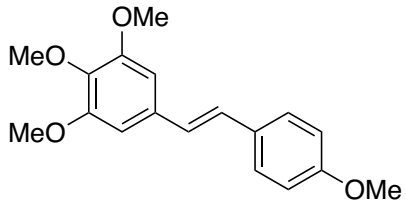

Following the general procedure described above and using 1,2,3-trimethoxybenzene as the arene, reaction was performed at 135 °C for 96 hours, the reactor was allowed to cool to room temperature and purged with air every 24 hours. The target compound DMU-212 was obtained as a light yellow liquid (106.6 mg, 71%). The product was purified by flash column chromatography using hexanes and ethyl acetate (v/v = 9:1) as the eluent. This compound was reported in literature.[35] **^{1}H NMR (600 MHz, $CDCl_3$):** δ 7.45 (m, 2H), 6.97 (d, *J* = 16.2 Hz, 1H), 6.94 – 6.87 (m, 3H), 6.72 (s, 2H), 3.92 (s, 6H), 3.87 (s, 3H), 3.83 (s, 3H) ppm. **^{13}C NMR (151 MHz, $CDCl_3$):** δ 159.4, 153.5, 137.8, 133.6, 130.2, 127.9, 127.8, 126.7, 114.3, 103.4, 61.1, 56.5, 55.5 ppm.

5.11.5 Synthesis of *(E)*-1,3-dimethoxy-5-(4-methoxystyryl)benzene – gram scale.

An oven dried 250 mL two-neck round bottom flask was charge with di-μ-acetatotetrakis(dihaptoethene)dirhodium(I) (25 μmol, 5.5 mg, 0.5 mol%), copper(II) pivalate (4 mmol, 1.06 g) and pivalic acid (20 mmol, 2.04 g). To the flask 50 mL of 1,3-dimethoxybenzene were added. The solution was stirred at room temperature for 10 minutes to dissolve all of the copper salt. Then, 0.665 mL of 4-methoxystyrene (5 mmol) were added to the reaction mixture. The reaction flask was connected to compressed air via

an adapter and a condenser (note: the air flow will facilitate the removal of the reaction solvent, thus a long condenser is needed). The reaction mixture was stirred at 135 °C for 96 hours. After completion of the reaction, the flask was allowed to cool to room temperature. The resultant mixture was diluted with ethyl acetate (150 mL) and washed with saturated sodium carbonate solution (200 mL). The aqueous and organic layers were separated. The aqueous layer was extracted with ethyl acetate (3 × 200 mL), and the combined organic layers were washed with water (3 × 200 mL), dried over magnesium sulfate, filtered, and concentrated under vacuum. The product was purified by flash column chromatography using hexanes and ethyl acetate (v/v = 9:1) as the eluent. 838 mg of desired product *(E)*-1,3-dimethoxy-5-(4-methoxystyryl)benzene (62%) was isolated.

5.11.6Synthesis of *(E)*-1,2-dichloro-4-styrylbenzene gram scale

An oven dried 250 mL two-neck round bottom flask was charge with di-μ-acetatotetrakis(dihaptoethene)dirhodium(I) (25 μmol, 5.5 mg, 0.5 mol%), copper(II) pivalate (0.2 mmol, 53 mg) and pivalic acid (20 mmol, 2.04 g). To the flask 50 mL of 1,2-dichlororbenzene were added. The solution was stirred at room temperature for 10 minutes to dissolve all of the copper salt. Then, 0.573 mL of styrene (5 mmol) were added to the reaction mixture. The reaction flask was connected to compressed air via an adapter and a condenser (note: the air flow will facilitate the removal of the reaction solvent, thus a long condenser is needed). The reaction mixture was stirred at 135 °C for 96 hours. After completion of the reaction, the flask was allowed to cool to room temperature. The resultant

mixture was diluted with ethyl acetate (150 mL) and washed with saturated sodium carbonate solution (200 mL). The aqueous and organic layers were separated. The aqueous layer was extracted with ethyl acetate (3 × 200 mL), and the combined organic layers were washed with water (3 × 200 mL), dried over magnesium sulfate, filtered, and concentrated under vacuum. The product was purified by flash column chromatography using hexanes as the eluent. 1.05g of the desired product *(E)*-1,2-dichloro-4-styrylbenzene was isolated (84%).

5.12 References:

1. Waldeck, D. H., Photoisomerization dynamics of stilbenes. *Chem. Rev.* **1991,** *91* (3), 415-436.
2. Whitten, D. G., Photochemistry and photophysics of trans-stilbene and related alkenes in surfactant assemblies. *Acc. Chem. Res.* **1993,** *26* (9), 502-509.
3. Papper, V.; Likhtenshtein, G. I., Substituted stilbenes: a new view on well-known systems: New applications in chemistry and biophysics. *J. Photochem. Photobio. A* **2001,** *140* (1), 39-52.
4. Gütlich, P.; Garcia, Y.; Woike, T., Photoswitchable coordination compounds. *Coord. Chem. Rev.* **2001,** *219*, 839-879.
5. Grabowski, Z. R.; Rotkiewicz, K.; Rettig, W., Structural changes accompanying intramolecular electron transfer: focus on twisted intramolecular charge-transfer states and structures. *Chem. Rev.* **2003,** *103* (10), 3899-4032.
6. Momotake, A.; Arai, T., Photochemistry and photophysics of stilbene dendrimers and related compounds. *Journal of Photochemistry and Photobiology C: Photochemistry Reviews* **2004,** *5* (1), 1-25.
7. Wong-Wah-Chung, P.; Mailhot, G.; Bolte, M., 4,4′-Diaminostilbene-2,2′-disulfonate (DSD) behaviour: under irradiation in water. *J. Photochem. Photobio. A* **2001,** *138* (3), 275-280.

8. Ichimura, K., Photoalignment of Liquid-Crystal Systems. *Chem. Rev.* **2000,** *100* (5), 1847-1874.

9. Halim, M.; Samuel, I. D. W.; Pillow, J. N. G.; Monkman, A. P.; Burn, P. L., Control of colour and charge injection in conjugated dendrimer/polypyridine bilayer leds. *Synth. Met.* **1999,** *102* (1-3), 1571-1574.

10. Morrall, J. P.; Dalton, G. T.; Humphrey, M. G.; Samoc, M., Organotransition Metal Complexes for Nonlinear Optics. In *Adv. Organomet. Chem.*, West, R.; Hill, A. F.; Fink, M. J., Eds. Academic Press: 2007; Vol. 55, pp 61-136.

11. Likhtenshtein, G., *Stilbenes: applications in chemistry, life sciences and materials science*. Wiley-VCH Verlag GmbH & Co. KGaA: 2009.

12. Mochida, S.; Hirano, K.; Satoh, T.; Miura, M., Synthesis of stilbene and distyrylbenzene derivatives through rhodium-catalyzed ortho-olefination and decarboxylation of benzoic acids. *Org. Lett.* **2010,** *12* (24), 5776-5779.

13. Zhang, N.; Quan, Z.; Zhang, Z.; Da, Y.; Wang, X., Synthesis of stilbene derivatives via visible-light-induced cross-coupling of aryl diazonium salts with nitroalkenes using -NO2 as a leaving group. *Chem. Commun.* **2016,** *52* (99), 14234-14237.

14. Le Bras, J.; Muzart, J., Intermolecular dehydrogenative Heck reactions. *Chem. Rev.* **2011,** *111* (3), 1170-1214.

15. Heck, R. F.; Nolley, J. P., Palladium-Catalyzed Vinylic Hydrogen Substitution Reactions with Aryl, Benzyl, and Styryl Halides. *J. Org. Chem.* **1972,** *37* (14), 2320

16. Schroll, P.; Hari, D. P.; Konig, B., Photocatalytic arylation of alkenes, alkynes and enones with diazonium salts. *ChemistryOpen* **2012,** *1* (3), 130-133.

17. Baudin, J. B.; Hareau, G.; Julia, S. A.; Ruel, O., A direct synthesis of olefins by reaction of carbonyl compounds with lithio derivatives of 2-[alkyl- or (2′-alkenyl)- or benzyl-sulfonyl]-benzothiazoles. *Tetrahedron Lett.* **1991,** *32* (9), 1175-1178.

18. Albéniz, A. C.; Espinet, P.; Martín-Ruiz, B.; Milstein, D., Catalytic System for the Heck Reaction of Fluorinated Haloaryls. *Organometallics* **2005,** *24* (15), 3679-3684.

19. Albeniz, A. C.; Espinet, P.; Martin-Ruiz, B.; Milstein, D., Catalytic system for Heck reactions involving insertion into Pd-(perfluoro-organyl) bonds. *J. Am. Chem. Soc.* **2001,** *123* (46), 11504-11505.

20. Albeniz, A. C.; Espinet, P.; Foces-Foces, C.; Cano, F. H., "Pd(C6F5)Br", a convenient precursor for studying the endo attack of nucleophiles on olefins. X-ray structure of bis(.mu.-bromo)bis(4-(pentafluorophenyl)-1-3-.eta.3-cyclohexenyl)dipalladium(II). *Organometallics* **1990,** *9* (4), 1079-1085.

21. Kuhl, N.; Hopkinson, M. N.; Wencel-Delord, J.; Glorius, F., Beyond directing groups: transition-metal-catalyzed C-H activation of simple arenes. *Angew. Chem. Int. Ed. Engl.* **2012,** *51* (41), 10236-10254.

22. Schneider, Y.; Chabert, P.; Stutzmann, J.; Coelho, D.; Fougerousse, A.; Gosse, F.; Launay, J. F.; Brouillard, R.; Raul, F., Resveratrol analog (Z)-3,5,4'-trimethoxystilbene

is a potent anti-mitotic drug inhibiting tubulin polymerization. *Int. J. Cancer* **2003,** *107* (2), 189-196.

23. Aggarwal, B. B.; Bhardwaj, A.; Aggarwal, R. S.; Seeram, N. P.; Shishodia, S.; Takada, Y., Role of resveratrol in prevention and therapy of cancer: preclinical and clinical studies. *Anticancer Res.* **2004,** *24* (5A), 2783-2840.
24. Andrus, M. B.; Liu, J.; Meredith, E. L.; Nartey, E., Synthesis of resveratrol using a direct decarbonylative Heck approach from resorcylic acid. *Tetrahedron Lett.* **2003,** *44* (26), 4819-4822.
25. Belleri, M.; Ribatti, D.; Nicoli, S.; Cotelli, F.; Forti, L.; Vannini, V.; Stivala, L. A.; Presta, M., Antiangiogenic and vascular-targeting activity of the microtubule-destabilizing trans-resveratrol derivative 3,5,4'-trimethoxystilbene. *Mol. Pharmacol.* **2005,** *67* (5), 1451-1459.
26. Botella, L.; Nájera, C., Synthesis of methylated resveratrol and analogues by Heck reactions in organic and aqueous solvents. *Tetrahedron* **2004,** *60* (26), 5563-5570.
27. Delmas, D.; Lançon, A.; Colin, D.; Jannin, B.; Latruffe, N., Resveratrol as a chemopreventive agent: a promising molecule for fighting cancer. *Curr. Durg Targets* **2006,** *7* (4), 423-442.
28. Fremont, L., Biological effects of resveratrol. *Life Sci.* **2000,** *66* (8), 663-673.
29. Han, G.; Xia, J.; Gao, J.; Inagaki, Y.; Tang, W.; Kokudo, N., Anti-tumor effects and cellular mechanisms of resveratrol. *Drug Discov Ther* **2015,** *9* (1), 1-12.

30. Kursvietiene, L.; Staneviciene, I.; Mongirdiene, A.; Bernatoniene, J., Multiplicity of effects and health benefits of resveratrol. *Medicina (Kaunas)* **2016,** *52* (3), 148-155.

31. Li, H.; Wang, A.; Huang, Y.; Liu, D.; Wei, C.; Williams, G. M.; Zhang, C.; Liu, G.; Liu, Y.; Hao, D.; Hui, R.; Lin, M.; Liang, C.-C., Isorhapontigenin, a new resveratrol analog, attenuates cardiac hypertrophy via blocking signaling transduction pathways. *Free Radical Biol. Med.* **2005,** *38* (2), 243-257.

32. Martínez, A. V.; García, J. I.; Mayoral, J. A., An expedient synthesis of resveratrol through a highly recoverable palladium catalyst. *Tetrahedron* **2017,** *73* (38), 5581-5584.

33. Mei, Y.; Liu, R.; Wang, D.; Wang, X.; Dai, C., Biocatalysis and biotransformation of resveratrol in microorganisms. *Biotechnol. Lett* **2015,** *37* (1), 9-18.

34. Mikula-Pietrasik, J.; Sosinska, P.; Wierzchowski, M.; Piwocka, K.; Ksiazek, K., Synthetic resveratrol analogue, 3,3',4,4',5,5'-hexahydroxy-trans-stilbene, accelerates senescence in peritoneal mesothelium and promotes senescence-dependent growth of gastrointestinal cancers. *Int J Mol Sci* **2013,** *14* (11), 22483-22498.

35. Moro, A. V.; Cardoso, F. S. P.; Correia, C. R. D., Heck arylation of styrenes with arenediazonium salts: short, efficient, and stereoselective synthesis of resveratrol, DMU-212, and analogues. *Tetrahedron Lett.* **2008,** *49* (39), 5668-5671.

36. Nam, K. A.; Kim, S.; Heo, Y. H.; Lee, S. K., Resveratrol analog, 3,5,2',4'-tetramethoxy-trans-stilbene, potentiates the inhibition of cell growth and induces apoptosis in human cancer cells. *Arch. Pharmacal Res.* **2001,** *24* (5), 441-445.

37. Nawaz, W.; Zhou, Z.; Deng, S.; Ma, X.; Ma, X.; Li, C.; Shu, X., Therapeutic Versatility of Resveratrol Derivatives. *Nutrients* **2017,** *9* (11), 1188.

38. Pervaiz, S.; Holme, A. L., Resveratrol: its biologic targets and functional activity. *Antioxid. Redox Sign.* **2009,** *11* (11), 2851-2897.

39. Pezzuto, J. M., Resveratrol as an inhibitor of carcinogenesis. *Pharm. Biol.* **2008,** *46* (7-8), 443-573.

40. Sale, S.; Tunstall, R. G.; Ruparelia, K. C.; Potter, G. A.; Steward, W. P.; Gescher, A. J., Comparison of the effects of the chemopreventive agent resveratrol and its synthetic analog trans 3,4,5,4'-tetramethoxystilbene (DMU-212) on adenoma development in the Apc(Min+) mouse and cyclooxygenase-2 in human-derived colon cancer cells. *Int. J. Cancer* **2005,** *115* (2), 194-201.

41. Ulrich, S.; Wolter, F.; Stein, J. M., Molecular mechanisms of the chemopreventive effects of resveratrol and its analogs in carcinogenesis. *Mol. Nutr. Food Res.* **2005,** *49* (5), 452-461.

42. Vang, O.; Ahmad, N.; Baile, C. A.; Baur, J. A.; Brown, K.; Csiszar, A.; Das, D. K.; Delmas, D.; Gottfried, C.; Lin, H.-Y.; Ma, Q.-Y.; Mukhopadhyay, P.; Nalini, N.; Pezzuto, J. M.; Richard, T.; Shukla, Y.; Surh, Y.-J.; Szekeres, T.; Szkudelski, T.; Walle, T.; Wu, J. M., What is new for an old molecule? Systematic review and recommendations on the use of resveratrol. *PLoS One* **2011,** *6* (6), e19881.

43. Yang, Y.; Weng, C.-J.; Ho, C.; Yen, G.-C., Resveratrol analog-3,5,4'-trimethoxy-trans-stilbene inhibits invasion of human lung adenocarcinoma cells by suppressing the MAPK pathway and decreasing matrix metalloproteinase-2 expression. *Mol. Nutr. Food Res.* **2009,** *53* (3), 407-416.

44. Frémont, L., Biological effects of resveratrol. *Life Sciences* **2000,** *66* (8), 663-673.

45. Nam, K. A.; Kim, S.; Heo, Y. H.; Lee, S. K., Resveratrol analog, 3, 5, 2′, 4′-tetramethoxy-trans-stilbene, potentiates the inhibition of cell growth and induces apoptosis in human cancer cells. *Archives of pharmacal research* **2001,** *24* (5), 441-445.

46. Belleri, M.; Ribatti, D.; Nicoli, S.; Cotelli, F.; Forti, L.; Vannini, V.; Stivala, L. A.; Presta, M., Antiangiogenic and vascular-targeting activity of the microtubule-destabilizing trans-resveratrol derivative 3, 5, 4′-trimethoxystilbene. *Molecular pharmacology* **2005,** *67* (5), 1451-1459.

47. Smidt, J.; Hafner, W.; Jira, R.; Sieber, R.; Sedlmeier, J.; Sabel, A., The Oxidation of Olefins with Palladium Chloride Catalysts. *Angew. Chem. Int. Ed.* **1962,** *1* (2), 80-88.

48. Fujiwara, Y.; Moritani, I.; Danno, S.; Asano, R.; Teranishi, S., Aromatic substitution of olefins. VI. Arylation of olefins with palladium(II) acetate. *J. Am. Chem. Soc.* **1969,** *91* (25), 7166-7169.

49. Jia, X.; Foley, A. M.; Liu, C.; Vaughan, B. A.; McKeown, B. A.; Zhang, S.; Gunnoe, T. B., Styrene Production from Benzene and Ethylene Catalyzed by Palladium(II):

Enhancement of Selectivity toward Styrene via Temperature-dependent Vinyl Ester Consumption. *Organometallics* **2019,** *38* (19), 3532-3541.

50. Zhang, X.; Fan, S.; He, C.; Wan, X.; Min, Q.; Yang, J.; Jiang, Z., Pd(OAc)(2) catalyzed olefination of highly electron-deficient perfluoroarenes. *Journal of the American Chemical Society* **2010,** *132* (13), 4506-4507.
51. Wang, P.; Verma, P.; Xia, G.; Shi, J.; Qiao, J. X.; Tao, S.; Cheng, P. T. W.; Poss, M. A.; Farmer, M. E.; Yeung, K.-S.; Yu, J.-Q., Ligand-accelerated non-directed C-H functionalization of arenes. *Nature* **2017,** *551* (7681), 489-493.
52. She, Z.; Shi, Y.; Huang, Y.; Cheng, Y.; Song, F.; You, J., Versatile palladium-catalyzed C-H olefination of (hetero)arenes at room temperature. *Chem. Commun.* **2014,** *50* (90), 13914-13916.
53. Ying, C.; Yan, S.; Duan, W., 2-Hydroxy-1,10-phenanthroline vs 1,10-phenanthroline: significant ligand acceleration effects in the palladium-catalyzed oxidative Heck reaction of arenes. *Org. Lett.* **2014,** *16* (2), 500-503.
54. Zhu, W.; Luo, Z.; Chen, J.; Liu, C.; Yang, L.; Dickie, D. A.; Liu, N.; Zhang, S.; Davis, R. J.; Gunnoe, T. B., Mechanistic Studies of Single-Step Styrene Production Catalyzed by Rh Complexes with Diimine Ligands: An Evaluation of the Role of Ligands and Induction Period. *ACS Catal.* **2019,** *9* (8), 7457-7475.
55. Chen, J.; Nielsen, R. J.; Goddard, W. A., 3rd; McKeown, B. A.; Dickie, D. A.; Gunnoe, T. B., Catalytic Synthesis of Superlinear Alkenyl Arenes Using a Rh(I) Catalyst

Supported by a "Capping Arene" Ligand: Access to Aerobic Catalysis. *J. Am. Chem. Soc.* **2018,** *140* (49), 17007-17018.

56. Vaughan, B. A.; Khani, S. K.; Gary, J. B.; Kammert, J. D.; Webster-Gardiner, M. S.; McKeown, B. A.; Davis, R. J.; Cundari, T. R.; Gunnoe, T. B., Mechanistic Studies of Single-Step Styrene Production Using a Rhodium(I) Catalyst. *J. Am. Chem. Soc.* **2017,** *139* (4), 1485-1498.
57. Webster-Gardiner, M. S.; Chen, J.; Vaughan, B. A.; McKeown, B. A.; Schinski, W.; Gunnoe, T. B., Catalytic Synthesis of "Super" Linear Alkenyl Arenes Using an Easily Prepared Rh(I) Catalyst. *J. Am. Chem. Soc.* **2017,** *139* (15), 5474-5480.
58. Vaughan, B. A.; Webster-Gardiner, M. S.; Cundari, T. R.; Gunnoe, T. B., Organic chemistry. A rhodium catalyst for single-step styrene production from benzene and ethylene. *Science* **2015,** *348* (6233), 421-424.
59. Liebov, N. S.; Zhu, W.; Chen, J.; Webster-Gardiner, M. S.; Schinski, W. L.; Gunnoe, T. B., Rhodium-Catalyzed Alkenylation of Toluene Using 1-Pentene: Regioselectivity To Generate Precursors for Bicyclic Compounds. *Organometallics* **2019,** *38* (19), 3860-3870.
60. Matsumoto, T.; Yoshida, H., Oxidative Arylation of Ethylene with Benzene to Produce Styrene. *Chem. Lett.* **2000,** *29* (9), 1064-1065.

61. Matsumoto, T.; Periana, R. A.; Taube, D. J.; Yoshida, H., Direct Synthesis of Styrene by Rhodium-Catalyzed Oxidative Arylation of Ethylene with Benzene. *J. Catal.* **2002,** *206* (2), 272-280.

62. Gorelsky, S. I.; Lapointe, D.; Fagnou, K., Analysis of the concerted metalation-deprotonation mechanism in palladium-catalyzed direct arylation across a broad range of aromatic substrates. *J. Am. Chem. Soc.* **2008,** *130* (33), 10848-10849.

63. Potavathri, S.; Pereira, K. C.; Gorelsky, S. I.; Pike, A.; LeBris, A. P.; DeBoef, B., Regioselective oxidative arylation of indoles bearing N-alkyl protecting groups: dual C-H functionalization via a concerted metalation-deprotonation mechanism. *J. Am. Chem. Soc.* **2010,** *132* (41), 14676-14681.

64. Sun, H. Y.; Gorelsky, S. I.; Stuart, D. R.; Campeau, L.-C.; Fagnou, K., Mechanistic analysis of azine N-oxide direct arylation: evidence for a critical role of acetate in the Pd(OAc)2 precatalyst. *J. Org. Chem.* **2010,** *75* (23), 8180-8189.

65. Walsh, A. P.; Jones, W. D., Mechanistic Insights of a Concerted Metalation–Deprotonation Reaction with [Cp*RhCl2]2. *Organometallics* **2015,** *34* (13), 3400-3407.

66. Ackermann, L., Carboxylate-assisted transition-metal-catalyzed C-H bond functionalizations: mechanism and scope. *Chem. Rev.* **2011,** *111* (3), 1315-1345.

67. McKeown, B. A.; Gonzalez, H. E.; Friedfeld, M. R.; Gunnoe, T. B.; Cundari, T. R.; Sabat, M., Mechanistic studies of ethylene hydrophenylation catalyzed by bipyridyl Pt(II) complexes. *J. Am. Chem. Soc.* **2011,** *133* (47), 19131-19152.

68. Jia, X.; Gary, J. B.; Gu, S.; Cundari, T. R.; Gunnoe, T. B., Oxidative Hydrophenylation of Ethylene Using a Cationic Ru(II) Catalyst: Styrene Production with Ethylene as the Oxidant. *Isr. J. Chem.* **2017,** *57* (10-11), 1037-1046.

69. Jia, X.; Frye, L. I.; Zhu, W.; Gu, S.; Gunnoe, T. B., Synthesis of Stilbenes by Rhodium-Catalyzed Aerobic Alkenylation of Arenes via C–H Activation. *Journal of the American Chemical Society* **2020,** *142* (23), 10534-10543.

70. Zhu, W.; Gunnoe, T. B., Advances in Rhodium-Catalyzed Oxidative Arene Alkenylation. *Acc. Chem. Res.* **2020,** *53* (4), 920-936.

71. Burgess, S. A.; Joslin, E. E.; Gunnoe, T. B.; Cundari, T. R.; Sabat, M.; Myers, W. H., Hydrophenylation of ethylene using a cationic Ru(ii) catalyst: comparison to a neutral Ru(ii) catalyst. *Chem. Sci.* **2014,** *5* (11), 4355-4366.

72. Joslin, E. E.; Quillian, B.; Gunnoe, T. B.; Cundari, T. R.; Sabat, M.; Myers, W. H., C-H activation of pyrazolyl ligands by Ru(II). *Inorg. Chem.* **2014,** *53* (12), 6270-6279.

73. McKeown, B. A.; Gonzalez, H. E.; Friedfeld, M. R.; Brosnahan, A. M.; Gunnoe, T. B.; Cundari, T. R.; Sabat, M., Platinum(II)-Catalyzed Ethylene Hydrophenylation: Switching Selectivity between Alkyl- and Vinylbenzene Production. *Organometallics* **2013,** *32* (9), 2857-2865.

74. Chen, J.; Yao, B.; Li, C.; Shi, G., An improved Hummers method for eco-friendly synthesis of graphene oxide. *Carbon* **2013,** *64*, 225-229.

75. Sinha, A. K.; Kumar, V.; Sharma, A.; Sharma, A.; Kumar, R., An unusual, mild and convenient one-pot two-step access to (E)-stilbenes from hydroxy-substituted benzaldehydes and phenylacetic acids under microwave activation: a new facet of the classical Perkin reaction. *Tetrahedron* **2007,** *63* (45), 11070-11077.

76. Kumar, V.; Sharma, A.; Sharma, A.; Sinha, A. K., Remarkable synergism in methylimidazole-promoted decarboxylation of substituted cinnamic acid derivatives in basic water medium under microwave irradiation: a clean synthesis of hydroxylated (E)-stilbenes. *Tetrahedron* **2007,** *63* (32), 7640-7646.

77. Yamada, Y. M.; Takeda, K.; Takahashi, H.; Ikegami, S., Assembled catalyst of palladium and non-cross-linked amphiphilic polymer ligand for the efficient heterogeneous Heck reaction. *Tetrahedron* **2004,** *60* (18), 4097-4105.

78. Wang, S. M.; Song, H. X.; Wang, X. Y.; Liu, N.; Qin, H. L.; Zhang, C. P., Palladium-catalyzed Mizoroki-Heck-type reactions of [Ph2SRfn][OTf] with alkenes at room temperature. *Chem Commun (Camb)* **2016,** *52* (80), 11893-11896.

79. Landge, V. G.; Yadav, V.; Subaramanian, M.; Dangarh, P.; Balaraman, E., Nickel(ii)-catalyzed direct olefination of benzyl alcohols with sulfones with the liberation of H2. *Chem Commun (Camb)* **2019,** *55* (43), 6130-6133.

80. Bhunia, A.; Studer, A., Synthesis of Highly Substituted Arenes via Cyclohexadiene–Alkene C–H Cross Coupling and Aromatization. *ACS Catal.* **2018,** *8* (2), 1213-1217.

81. Kothandaraman, P.; Foo, S. J.; Chan, P. W., Gold-catalyzed intramolecular allylic amination of 2-tosylaminophenylprop-1-en-3-ols. A concise synthesis of (+/-)-angustureine. *J. Org. Chem.* **2009,** *74* (16), 5947-5952.

82. Xiao, Q.; Ma, J.; Yang, Y.; Zhang, Y.; Wang, J., Pd-catalyzed C=C double-bond formation by coupling of N-tosylhydrazones with benzyl halides. *Org. Lett.* **2009,** *11* (20), 4732-4735.

83. Girase, T. R.; Kapdi, A. R., Novel Carbazole-Based N-Heterocyclic Carbene Ligands to Access Synthetically Relevant Stilbenes in Pd-Catalyzed Coupling Processes. *Chem Asian J* **2019,** *14* (15), 2611-2619.

84. Prasanna, R.; Guha, S.; Sekar, G., Proton-Coupled Electron Transfer: Transition-Metal-Free Selective Reduction of Chalcones and Alkynes Using Xanthate/Formic Acid. *Org. Lett.* **2019,** *21* (8), 2650-2653.

85. Zhou, Z.; Hou, Z.-L.; Yang, F.; Yao, B., Oxidative cross-coupling of allyl(trimethyl)silanes with aryl boronic acids by palladium catalysis. *Tetrahedron* **2018,** *74* (50), 7228-7236.

86. Ainembabazi, D.; Reid, C.; Chen, A.; An, N.; Kostal, J.; Voutchkova-Kostal, A., Decarbonylative Olefination of Aldehydes to Alkenes. *J. Am. Chem. Soc.* **2020,** *142* (2), 696-699.

87. Kumar, B. S.; Anbarasan, R.; Amali, A. J.; Pitchumani, K., Isolable C@Fe3O4 nanospheres supported cubical Pd nanoparticles as reusable catalysts for Stille and Mizoroki-Heck coupling reactions. *Tetrahedron Lett.* **2017,** *58* (33), 3276-3282.

88. Wang, Y.-P.; Lee, H. M., Catalytic application of zwitterionic palladium complexes in Mizoroki–Heck reactions using ionic liquid as solvent. *J. Organomet. Chem.* **2015,** *791*, 90-98.

89. Zhou, A.; Guo, R.-M.; Zhou, J.; Dou, Y.; Chen, Y.; Li, J.-R., Pd@ZIF-67 Derived Recyclable Pd-Based Catalysts with Hierarchical Pores for High-Performance Heck Reaction. *ACS Sustainable Chemistry & Engineering* **2018,** *6* (2), 2103-2111.

90. Baggi, N.; Garoni, E.; Colombo, A.; Dragonetti, C.; Righetto, S.; Roberto, D.; Boixel, J.; Guerchais, V.; Fantacci, S., Design of cyclometallated 5-π-delocalized donor-1,3-di(2-pyridyl)benzene platinum(II) complexes with second-order nonlinear optical properties. *Polyhedron* **2018,** *140*, 74-77.

6 Copper Catalyzed Oxygen Evolution Reaction and Alkane oxidation

6.1 Introduction

6.1.1 Fossil fuels and alternative energy sources

The world energy consumption is continuing to increase in the past few decades and the rate of growth is rising yearly. Based on a recent global energy report, more than 70% of the world's energy came from the combustion of fossil fuels, and the resultant CO_2 is a major source of greenhouse gas.[1] A sustainable economy based on clean and renewable energy could potentially be a replacement of fossil fuels. Harnessing energy from the sun could be an alternative to the use of fossil fuels as a report recently suggested approximately $1.74x10^5$ TWh of solar energy is delivered to each day.[2] However, electricity generated by solar power, through photovoltaics, cannot currently serve as a replacement of fossil fuel due to the following reasons: 1) the electricity has to be used at the time of generation since the large scale storage of electricity remains challenging; 2) the diurnal nature of sunlight means that electricity production can only occur during daylight hours. The production of carbon free fuels through photosynthesis is a promising alternative as it uses chemical bonds to store energy. Dihydrogen (H_2) in particular has attracted extensive attention as an environmentally friendly energy source with only water being produced after combustion.

Another way to decrease CO_2 production is to optimize the use of fossil fuels. Natural gas, which is primarily composed of methane, is burned for heating and electricity

generation. However, the use of methane for energy production is limited due to transportation costs.[3] In the absence of a gas pipeline, natural gas needs to be liquified which requires high pressure and expensive infrastructure. Because of transportation costs, the extraction of natural gas from deposits located far from industrial infrastructure is often impractical. For similar reasons, a significant amount of natural gas is flared during oil drilling, which releases large amounts of CO_2 into the atmosphere.[1]

6.1.2 Hydrogen production via catalytic water splitting

Water splitting into dihydrogen and dioxygen using electrochemical or photo-electrochemical methods provides a method to generate dihydrogen and converts electricity to a chemical fuel. However, water splitting to dihydrogen and dioxygen is a thermodynamically unfavored process. The oxidation half reaction (also call the oxygen evolving reaction or OER) is a bottleneck reaction due to the need for high overpotentials. At pH = 0, the standard potential difference requirement for water splitting is -1.23 V vs NHE (-0.82 at pH = 7).

In recent years, the development of transition metal catalysts for electrocatalytic water oxidation has been intensively investigated. Earth abundant first-row transition metal

complexes are promising because of their low cost and low toxicity. Examples of Cu containing catalysts are shown in Figure 6.1.

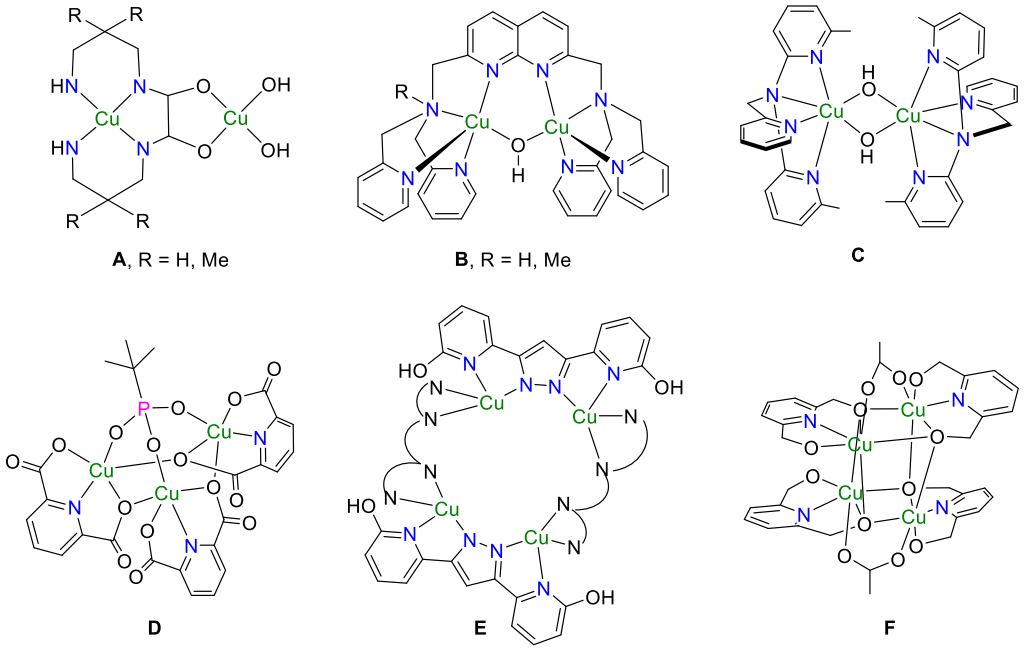

Figure 6.1. Examples of multi-nuclear Cu complexes for electrocatalytic water oxidation.

Zhan and co-workers reported a dinuclear copper complex $Cu(Me_2oxpn)Cu(OH)_2]$ (Me_2oxpn = N,N'-bis(2,2-dimethyl-3-aminopropyl)oxamido) for both electrolytic water oxidation and reduction. Water oxidation for this catalyst occurs at an overpotential of 636 mV vs SHE to give dioxygen with a turnover frequency (TOF) of ~2.14 s^{-1}, and water reduction occurs at an overpotential of 789 mV vs SHE (pH 7.0) with a TOF of 0.18 s^{-1}.[4] (Figure 6.1A). Liao, Zhang and co-workers studied water oxidation using the dinuclear copper complex $[Cu_2(BPMAN)(\mu\text{-}OH)]^{3+}$ (Figure 6.1B) supported by the ligand 2,7-[bis(2-pyridylmethyl)aminomethyl]-1,8-naphthyridine (BPMAN). This catalyst exhibits over 98 % Faraday efficiency toward oxygen evolution reaction and stable for at least 4

hours with no evidence of catalyst deactivation and decomposition. towards water oxidation in neutral aqueous solutions.[5] Kieber-Emmonsa and co-workers reported a dinuclear copper water oxidation catalyst supported by the Me_2TMPA ligand, $\{[(Me_2TMPA)Cu^{II}]_2(\mu\text{-}OH)_2\}(OTf)_2$ (Me_2TMPA = bis-((6-methyl-2-pyridyl)methyl)(2-pyridylmethyl)amine) that could mediate catalytic water oxidation with high Faradaic efficiency (> 90%) for dioxygen evolution and moderate rates (33 s^{-1} at ∼1 V overpotential, pH 12.5) (Figure 6.1C).[6] A trinuclear copper phosphonate complex, $[Cu_3(pda)_3(tBuPO_3)]\cdot_2(Et_3NH)$ (pda = pdaH2= 2, 6-pyri-dinedicarboxylate) (Figure 6.1D) has been synthesized and investigated by Fan, Wang and co-workers.[7] Its electrocatalytic activity for water oxidation was investigated in a neutral pH with a TOF of approximately 0.82 s^{-1} at the overpotential of about 800 mV vs. NHE. Masaoka and co-workers designed and synthesized a tetranuclear copper-based water oxidation catalysts supported by new multi-nucleating ligand containing two proton dissociation sites, 1,3-bis(6-hydroxy-2-pyridyl)-1H-pyrazole. This copper complex showed electrocatalytic activity for water oxidation reactions under aqueous basic conditions (pH 12.5) with an overpotential of approximately 500 mV.[7] Another example of tetranuclear copper catalyst for water oxidation is reported by Fan, Wang and coworkers. $[Cu_4(pdmH)_4(OAc)_2](NO_3)_2(H_2O)_3$ has been synthesized successfully with pyridine-2, 6-dimethanol as the ligand. Under aqueous alkaline conditions a relatively low overpotential of 400–665 mV vs. NHE is observed.[8]

6.1.3 Catalytic conversion of nature gas to liquid fuels

Catalytic conversion of natural gas, which is primarily methane, to partial oxidized liquid products (e.g., methanol, formaldehyde) under mild conditions that avoid the expensive syngas step have therefore been intensively researched.{Kerr, 2010 #804;, 2004 #684} Direct partial oxidation of methane to methanol is particularly promising since the reaction of methane with dioxygen to yield methanol is exothermic and thermodynamically favorable and there is also a large demand for methanol in chemical industry ~45 billion kilograms are manufactured annually.[3, 9] However, there are significant kinetic barriers for the reaction the C–H bonds of methane, and functionalized products often contain weaker C–H bonds and are frequently more reactive than the starting alkane. In terms of the bond dissociation energy (BDE), the C–H bonds of methane and methanol are 105 and 96 kcal/mol, respectively, which suggests that the C–H bonds in methanol and other oxidative products are often more reactive than methane. The heightened reactivity of oxidized products often results in unselective functionalization leading to over-oxidation as a chronic issue. [10]

In the 1970s, Shilov and co-workers investigated the H/D exchange between methane and water mediated by platinum complexes, which led to the development of a process using water soluble Pt^{II} salts to C–H activate and functionalize alkanes.[11-16] Notably, in this C–H activation reaction, stronger, more electron-rich bonds are preferentially activated over the C–H bonds of weaker, more electron-poor species that result from alkane

oxidation. This avoids the over-oxidation of substrate to thermodynamic sinks such as carbon dioxide. Therefore, the Shilov system can transform methane to methanol and chloromethane selectively under mild conditions. The catalytic cycle is shown in Scheme 6.1.

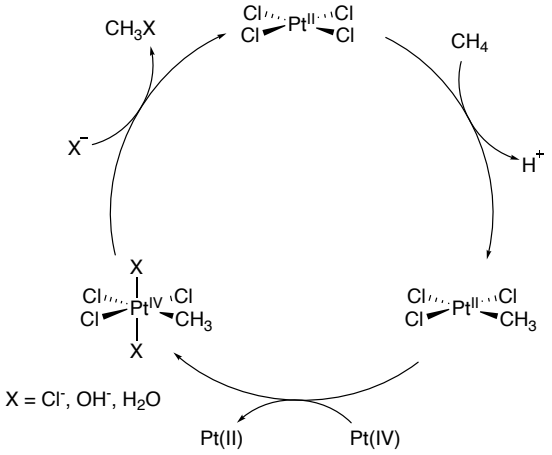

Scheme 6.1. Catalytic cycle of Shilov methane functionalization system.

The Shilov process starts with the coordination of methane to $[PtCl_4]^{2-}$ followed by C–H activation to result in the formation of Pt–Me bond. Then, the Pt(II) complex undergoes an oxidation to Pt(IV), after which X^- (OH^- or Cl^-) nucleophilic attack the complexes and result in the formation of functionalized product (MeOH or MeCl).[17] A major issue of the Shilov process is the use of Pt(IV) as a stoichiometric oxidant; the expense and lack of recyclability of the Pt(IV) oxidant ensures that the Shilov system is not industrially viable.

Periana and co-workers developed a process that uses Hg(II) salts in H_2SO_4 to convert methane to methyl bisulfate at 180 °C.[18] This process utilizes sulfuric acid as an oxidant. The electron-withdrawing nature of bisulfate deactivates the methyl bisulfate product

towards undesired overoxidation because there is less electron density at the methyl group of CH_3OSO_3H than that for methane, making electrophilic C–H activation of methane more favorable than for methyl bisulfate.[19, 20] Approximately 50% methane conversion with 85% of selectivity for CH_3OSO_3H was achieved with a catalytic turnover frequency of 10^{-3} s^{-1} at 180 °C. Later, Periana and co-workers designed the (bpym)$PtCl_2$ (bpym = 2,2'-bipyrimidine) system that catalyzes the conversion of methane to methyl bisulfate in oleum with and observed turnover frequency of 10^{-2} s^{-1} at 180-220 °C and ~500 psi CH_4 (Scheme 6.2).[21] However, drawbacks to both Hg(II) and Pt(II) systems are 1) TOFs too low to be economically competitive; 2) difficulty and expense of separating methanol from concentrated sulfuric acid; and 3) the corrosive nature of sulfuric acid.[21]

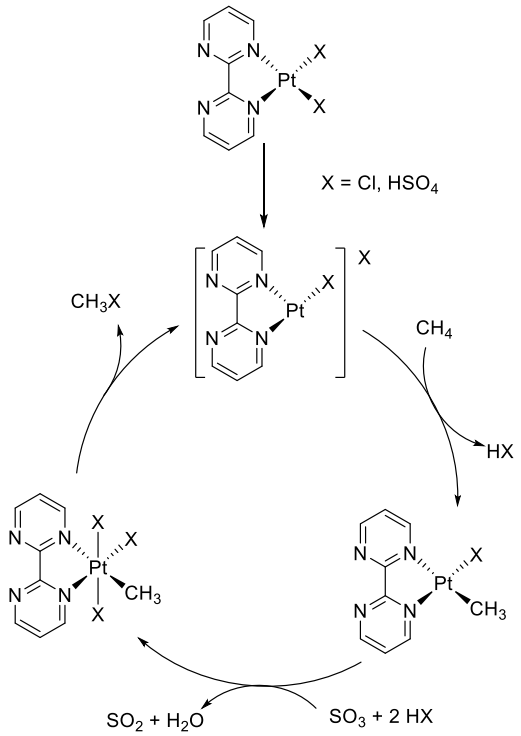

Scheme 6.2. Catalytic cycle of Periana's Pt system.

In biological systems, multi-nuclear copper cluster containing enzymes play a vital role in bioenergetics by facilitating multi-electron redox processes.[22] Particulate methane monooxygenase (pMMO), which is a copper containing enzyme found in methanotrophs, catalyzes the conversion from methane to methanol. Many recent structural studies discovered that the active site in this pMMO is likely a dinuclear Cu(II) cluster with a trinuclear copper cluster also be suggested as a possible active site.{Serrano-Plana, 2015 #779} Synthetic chemistry has played a pivotal role in highlighting the viability of proposed intermediates and expanding the library of known copper−oxygen cores and allow us the understand the role of the multi-copper complexes in catalysis.

6.2 Catalytic water oxidation using the copper complex [(DAM)$Cu_3(\mu^3$-O)][Cl]$_4$

The synthesis of the copper complex [(DAM)$Cu_3(\mu^3$-O)][Cl]$_4$ (**1**, DAM = dodecaaza macrotetracycle) was carried out under an atmosphere of N_2 inside the glovebox using a modification of a published procedure.[18] The molecular structure was confirmed by single-crystal X-ray crystallography and features a (μ_3-oxo)Cu_3 core which adopts a molecular bowl shaped structure with each Cu(II) in a distorted trigonal bipyramid geometry (Figure 6.2).

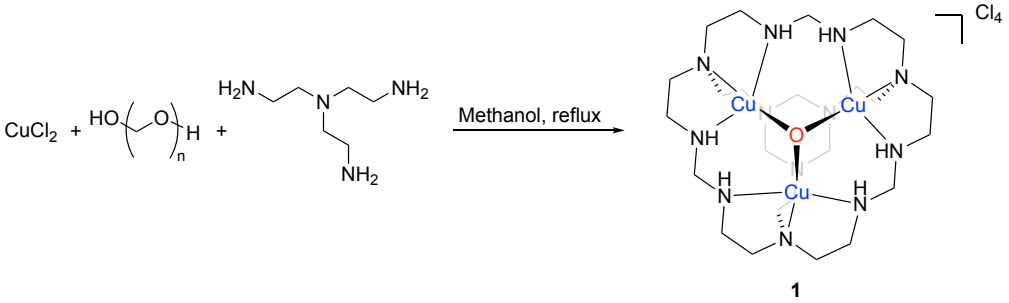

1

Scheme 6.3. One-pot synthesis of [DAM$Cu_3(\mu^3$-O)][Cl_4] (**1**)

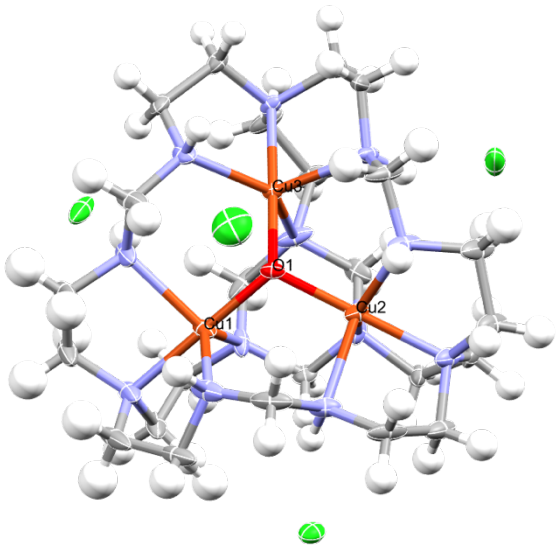

Figure 6.2. Molecular with anisotropic displacement ellipsoids set at 50% probability. and counterions have been omitted for clarity. Selected bond distances (Å) and angles (º): Cu1-O1 1.8987(18), Cu2-O1 1.8960(19), Cu3-O1 1.8915(18); Cu3-O1-Cu2 111.59(9), Cu2-O1-Cu1 111.60(9), Cu3-O1-Cu1 111.90(9).

Electrocatalytic water oxidation reaction using complex **1** as catalyst precursor was probed using a three-electrode system in a one compartment electrochemical cell. Glassy Carbon (GC) was used as working electrode, Ag/AgCl (3 M NaCl) as reference electrode and Pt wire as counter electrode.

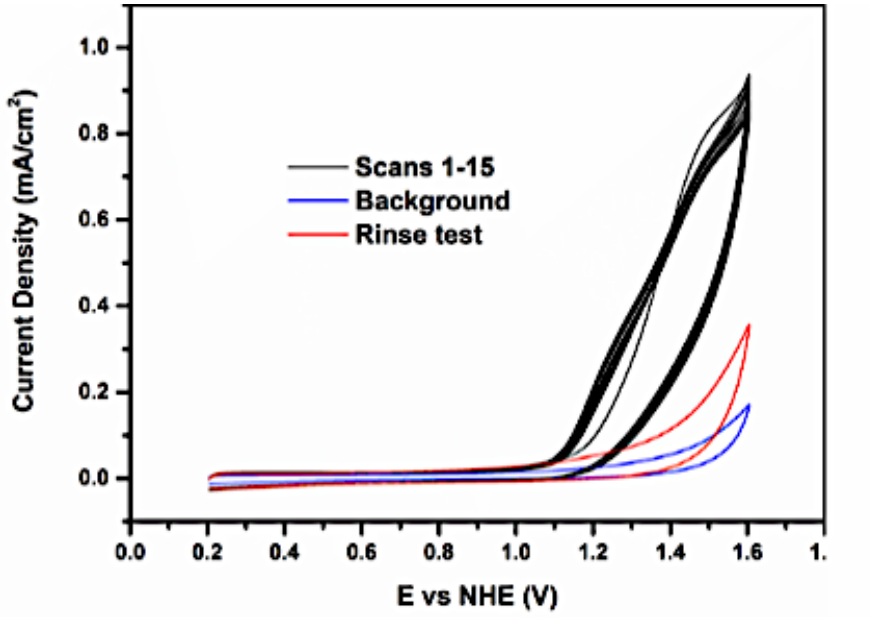

Figure 6.3. Consecutive CVs of 0.5 mM [DAMCu$_3$(μ^3-O)][Cl$_4$] at 20 mV/s (black) using a GC electrode at pH 7 0.1 M phosphate buffer solution. A rinse test after 15 scans is shown in red. The background CV in the absence of 1 is shown in blue.

An irreversible oxidation wave appears with E^{o}_{cat} of 1.33 V vs NHE (determined by half-peak method)[23] with an overpotential of 515 mV (Figure 6.3). After 15 consecutive scans at 20 mV/s, no deposited materials on the electrode can be seen. The electrode was rinsed with water to remove any water soluble homogeneous active species and placed in a fresh electrolyte solution, obtaining current densities similar to the background measurement. The performance of **1** electrocatalytic water oxidation was also examined under different pHs. As shown in Figure 6.4, catalyst is active for water oxidation reaction from pH 2 to 11.

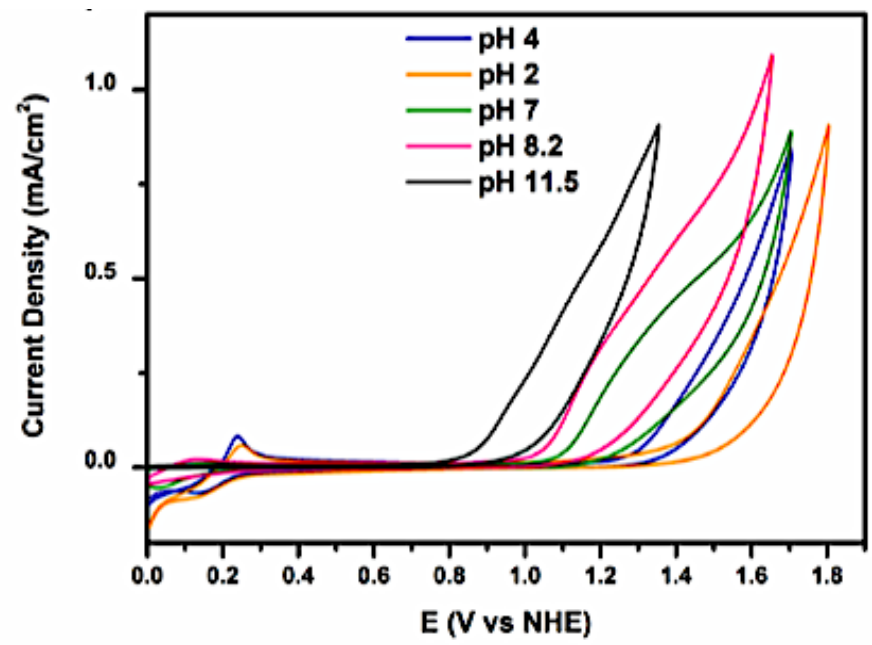

Figure 6.4. CVs of 0.5 mM [DAMCu$_3$(μ^3-O)][Cl$_4$] (**1**) at 20 mV/s (black) using a GC electrode at pH 7 0.1 M phosphate buffer solution at varying pHs.

At pH = 7, the catalysis was performed using different scan rates. A linear fit was obtained when plotting the catalytic peak current densities (i_{cat}) against the square root of the scan rate (Figure 6.5), which further supports a homogenous diffusion-controlled process.

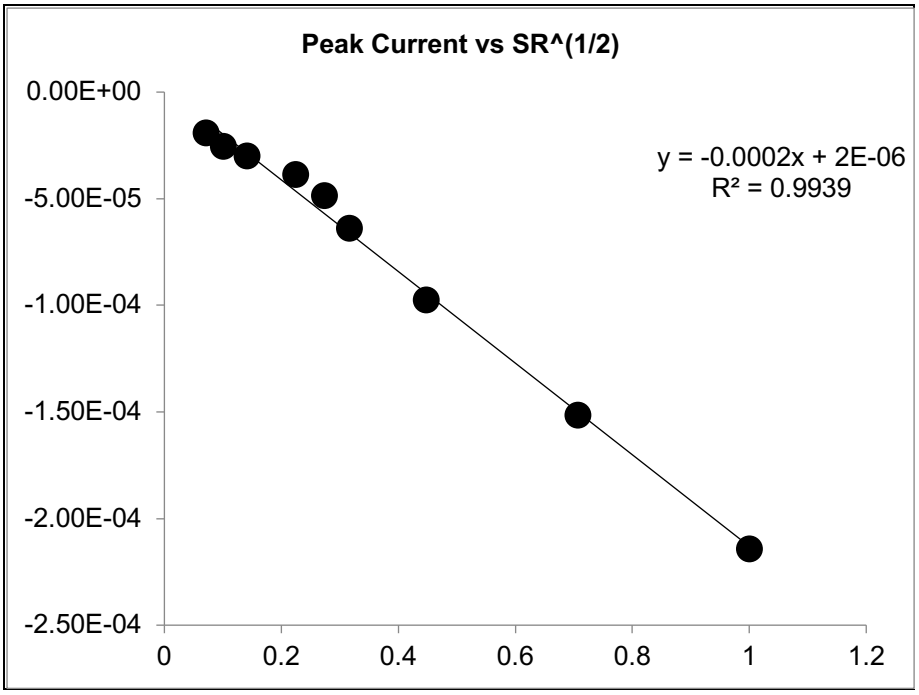

Figure 6.5. Peak current vs square root of san rate plot under pH = 7. Condition: 0.5 mM $[DAMCu_3(\mu^3\text{-}O)][Cl_4]$ (**1**) at different scan rates using a GC electrode at pH 7 0.1 M phosphate buffer solution .

To obtain kinetic information of the catalysis, the reaction was performed with different catalyst concentrations. Figure 6.6 shows current densities, i_{cat}, increase with increasing concentration of **1** at pH 7 displaying a linear relationship. This indicates that the rate law for water oxidation catalyzed by **1** can be expressed by using a pseudo first-order rate constant.

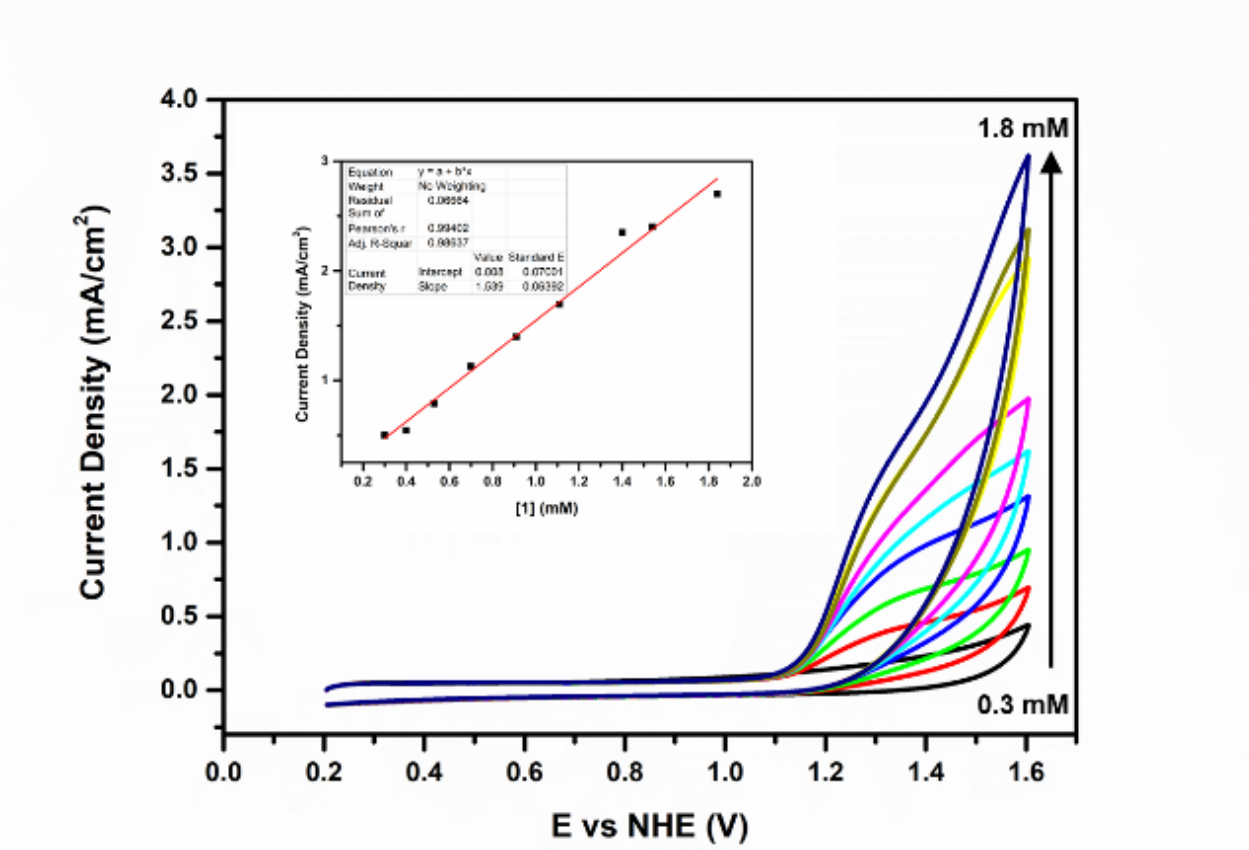

Figure 6.6. Concentration dependence by CVs at 20 mV/s from 0.3 to 1.8 mM of 1 using a GC electrode at pH 7 phosphate buffer solution. Inset: Concentration dependence of current density at 1.50 V.

The peak current for the $Cu^{II/I}$ redox couple is proportional to the square root of the scan rate in agreement with a diffusion-controlled process and the Randles-Sevcik equation (eq 1). Therefore, the first-order rate constant k_{obs} (or TOF) for the water oxidation reaction can be estimated from the catalytic current enhancement (i_{cat}/i_p) by applying eq 1 in which i_{cat} and i_p refer to the maximum catalytic current and the peak current of the $Cu^{II/I}$ redox couple, respectively, and n_p is the number of electrons transferred at $E_{p,a} = 302$ mV ($n_p = 1$) and $n_{cat} = 4$ for water oxidation to dioxygen. The plot of i_{cat}/i_p versus $\nu^{-1/2}$ shows a linear

relationship, consistent with a pure kinetic behavior in this scan rate range, yielding a TOF of 14.0 s^{-1} at pH 7 and of 17.7 s^{-1} at pH 8.2

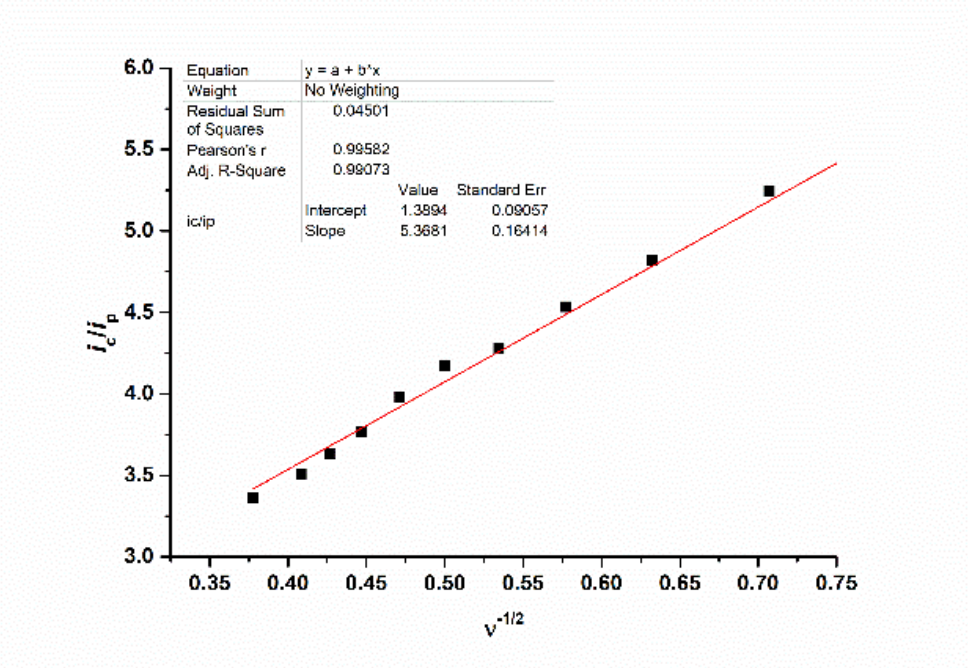

Figure 6.7. Plot of the ratio of the catalytic current at 1.6 V to the peak current for the Cu(II/I) couple vs. $v^{-1/2}$. Conditions: 0.5 mM of 1 in 0.1 M phosphate buffer solution at pH 7.

$$\frac{i_{cat}}{i_p} = 2.24 \frac{n_{cat}}{n_p^{3/2}} \sqrt{\frac{RTk_{cat}}{Fv}} \qquad (1)$$

6.3 Catalytic cyclohexane oxidation using copper complexes with hydrogen peroxide as oxidant

The Gunnoe lab has been developing multi-nuclear copper for the catalytic partial oxidation of hydrocarbons. Our group has prepared a series of multi-copper complexes that possess $Cu^{II}(\mu_2\text{-}O)Cu^{II}$ and $Cu^{II}_3(\mu_3\text{-}O)$ cores. The main aim of this project is to investigate

the catalytic activity of these complexes for alkane oxidation. The use of multinuclear copper catalysts is a promising strategy to achieve selective two-electron oxidation of organic molecules using one-electron redox steps.[4, 25-30]

Cyclohexane oxidation to cyclohexanol and cyclohexanone was used as a model reaction for catalyst screening due to the following reasons: 1) cyclohexane as a liquid substrate could reduce the complexity of the system; 2) the C–H bond dissociation energy of cyclohexane (100 kcal/mol) is similar to the C–H bond in light alkanes; and 3) the products of the reaction, cyclohexanol and cyclohexanone, can be readily quantified (Scheme 6.4).[27]

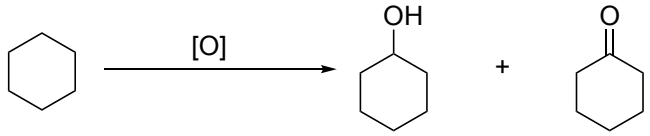

Scheme 6.4. Cyclohexane oxidation to cyclohexanol and cyclohexanone as a model reaction for alkane oxidation

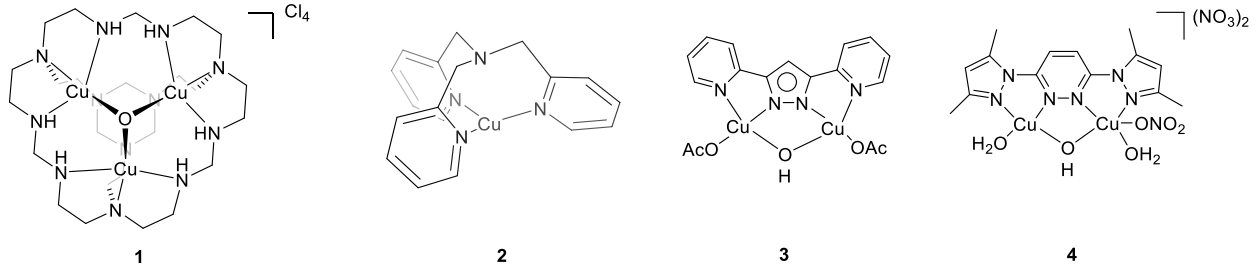

Figure 6.8. Candidate copper complexes for copper-mediated cyclohexane oxidation.

Figure 6.8 shows four copper complexes with mono-/multi copper cores that were used as candidates for catalytic cyclohexane oxidation. Copper complex **2** was made in situ by adding copper salt and ligand according to a published procedure.[27] The Cu complexes (3,5-bis(pyridin-2-yl)-pyrazole)$Cu_2(OAc)_2(\mu\text{-}OH)$ (**3**) and $[Cu_2(PPDMe)(\mu\text{-}OH)NO_3(H_2O)_2](NO_3)\cdot H_2O$ (**4**) (PPDMe = 3,6-bis(3,5-dimethyl-l-pyrazolyl)pyridazine) were synthesized based on modified procedures.[31] [29] [25]

The copper salt mediated cyclohexane oxidation was carried out under the following conditions: 1 mmol of cyclohexane, 1 mol % of copper catalyst relative to cyclohexane, 1000 equiv. of H_2O_2 (35% in water solution) relative to copper catalyst, 3 mL NCMe as solution, reactions performed in 20 mL vials and stirred at room temperature for 6 hours. The reaction mixtures were then quenched with triphenylphosphine to reduce the remaining hydrogen peroxide and cyclohexyl-peroxide species. The reaction mixture was analyzed by GC-FID, and turnovers were calculated based-on a calibration curve. All numbers were the average of two identical experiments.

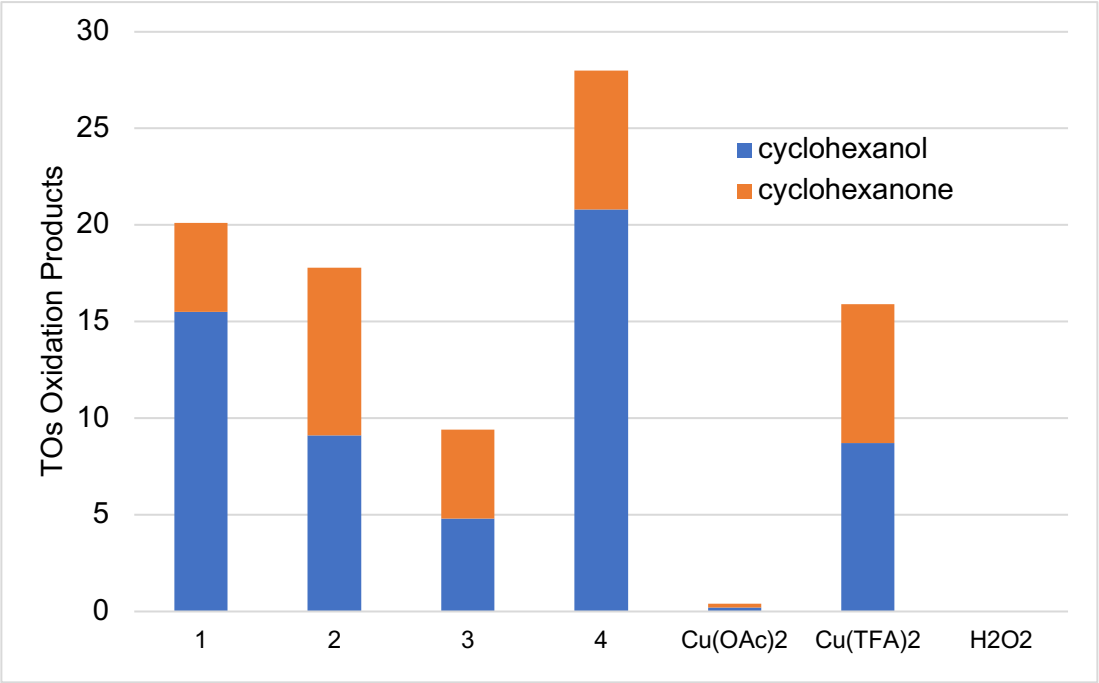

Figure 6.9. Copper mediated cyclohexane oxidation to cyclohexanol and cyclohexanone.

Figure 6.9 shows the results of the catalyst screening. All four copper complexes showed reactivity to some extent. The mono-nuclear complex **3** gave 9 total TOs of oxidation products. The dinuclear copper complexes **2** and **4** gave higher turnovers than complex **3** with 2 18 TOs and 28 TOs, respectively. The trinuclear complex **1** gave 20 total TOs of product. Control reactions using $Cu(TFA)_2$ showed 16 TOs. The reaction with no copper or $Cu(OAc)_2$ gave little or no product. The cyclohexane oxidation experiments suggested that complexes **1** and **4** might be good candidate for light alkane oxidation.

Methane oxidation was performed in high pressure reactors under follow conditions: 10 μmol of [Cu] complex (1 equiv. relative to copper complex) and 10 mmol of H_2O_2 (1000 equiv. relative to copper complex) were dissolved in 15 mL of DI water. The reactors were charged with 70 psig methane and vented 5 times and then pressurized with 30 bars of

methane. The reactor was stirred at room temperature for thirty minutes. The gas phase was collected in a 1L gas sampling bag and analyzed by GC-MS. and the liquid phase was transferred to a vial, combined with D_2O and analyzed by solvent suppression ^1H NMR spectroscopy. Table 6.1 shows the copper complexes 1 and 4 mediated methane oxidation. The result indicate that trinuclear copper complex 1 have better performance for this catalytic reaction.

Table 6.1. Methane oxidation mediated by complex 1 and 4

Copper catalyst	Methanol (μmol)	Yield
$[DAMCu_3(\mu^3\text{-}O)][Cl_4]$ (1)	7.7	77%
$[Cu_2(PPDMe)(\mu\text{-}OH)NO_3(H_2O)_2](NO_3)\cdot H_2O$ (4)	1.4	14%

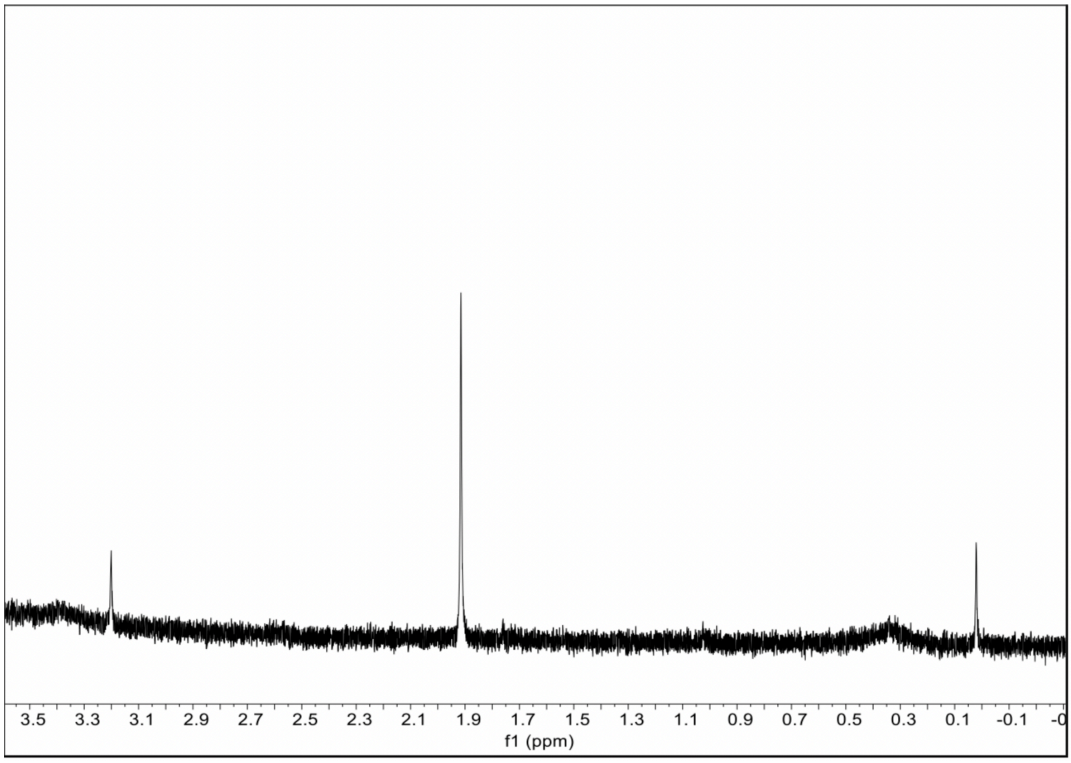

Figure 6.10. Representative ^{1}H NMR spectrum of the reaction mixture after catalysis. Methanol resonates at 3.18 ppm.

Figure 6.10 shows a representative solvent suppression ^{1}H NMR of a catalytic reaction mixture. The peak at 0.05 ppm is due to unreacted methane, the methanol peak resonates at 3.18 ppm. To confirm the methanol came from the catalysis, ethane oxidation was performed under identical conditions, and the ^{1}H NMR spectrum of a catalytic reaction mixture is shown in Figure 6.11. The peaks of ethanol were observed.

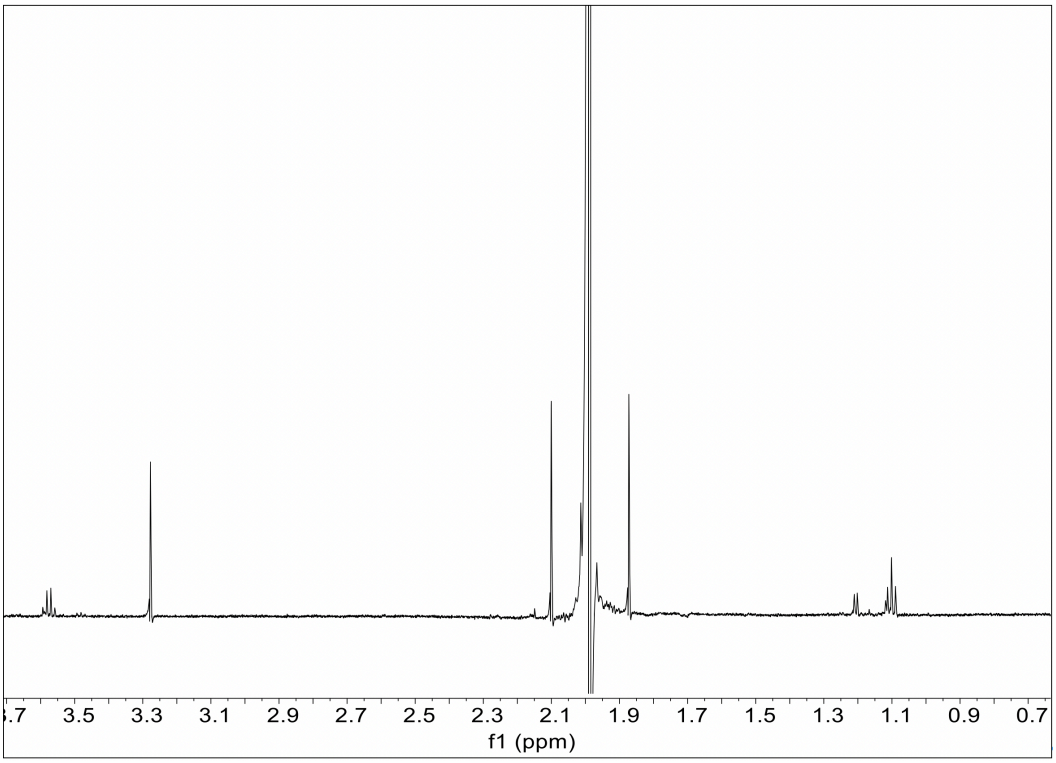

Figure 6.11. Representative ^{1}H NMR spectrum of the reaction mixture after ethane oxidation catalysis. Ethanol shows at 1.12 ppm and 3.58 ppm.

The reaction temperature effect was examined, as shown in Table 6.2. Reduced reaction rate is observed at 0 ºC with only 3.7 μmol methanol produced after 12 hours reaction. The reaction at 50 ºC also gave a low yield, which could be due to accelerated hydrogen peroxide deactivation at elevated temperature.

Table 6.2. The influence of temperature on the catalysis

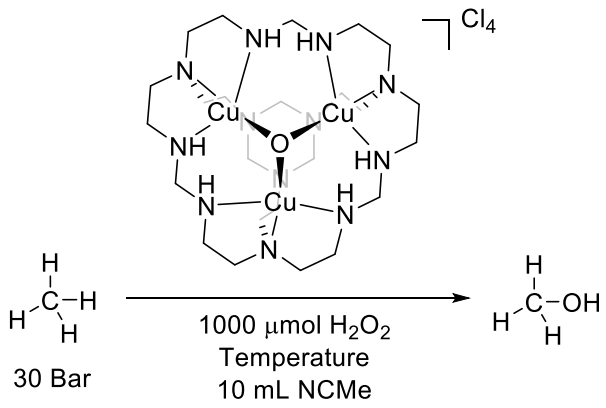

Temperature	Methanol (μmol)	Yield*
0	3.7(1)	37%
25	15.9(7)	159%
50	4.7(1)	47%

* Yield is calculated relative to Cu catalyst.

The influence of reaction solvent was examined, and the results are shown in Table 6.3. The organic solvent hexafluorobenzene was reported to be a good solvent for methane functionalization{Foster, 1985 #806}; however, due the poor solubility of the copper catalyst, the reaction performance does not compete with NCMe for our studies. The rection in THF results in a large amount of solvent oxidation. The catalysis performed in acetic acid and trifluoroacetic acid facilitate the deactivation of hydrogen peroxide and gave lower yield. The best catalytic performance was observed when using wet NCMe with 172% yield (1.72 TOs) of methanol produced when using 1:1 (v:v) of water to NCMe solvent mixture.

Table 6.3. The influence of reaction solvent on the catalysis

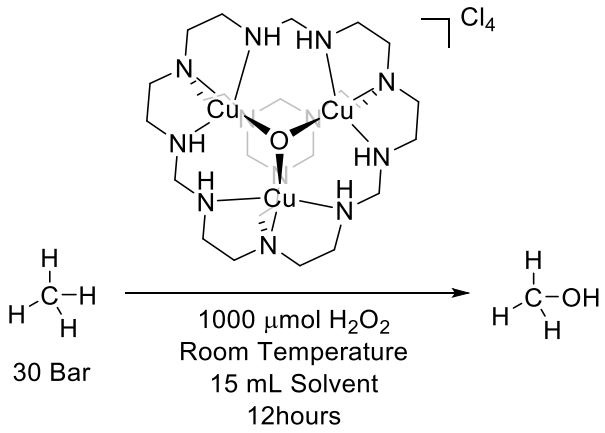

solvent	Methanol (μmol)	yield
NCMe	15.9(7)	159%
C_6F_6	4.4(9)	44%
THF	1.4(7)	14%
HOAc	7.7(4)	77%
HTFA	0	0
H_2O/NCMe 1:1	17.2(3)	172%
H_2O/NCMe 3:1	11.2(7)	112%

6.4 Experimental Section

Synthesis of the Complexes

[DAMCu$_3$(μ_3-O)][Cl$_4$] (1). The reaction was carried out under an atmosphere of N_2 inside the glovebox using a modification of a published procedure.[18] To the dry methanol solution (100 mL) of $CuCl_2$ anhydrate (1.38 g, 10.3 mmol) were added tris(2-aminoethyl)amine (3.14 g, 20.6 mmol) and paraformaldehyde (3.0 g, 100 mmol). The dark blue solution was heated at reflux for 20 hours until a green precipitate was observed. The reaction mixture was filtered, and the solid was washed with dry ethanol (20 mL) and dried in vacuo. The volume of filtrate was reduced by ~50% under vacuum, and the concentrated filtrate was heated back to reflux. After 10 hours, a green precipitate formed. The green sold was collected by filtration and washed with dry ethanol (20 mL) and dried in vacuo. Yield of two crops = 67%.

Single-crystal X-ray diffraction data were collected on a Bruker Kappa APEXII Duo diffractometer running the APEX3 software suite using the Mo Kα fine-focus sealed tube (λ = 0.71073 Å). The structure was solved and refined using the Bruker SHELXTL Software Package within APEX3 and OLEX2, using the space group P-1, with Z = 2 for the formula unit, $C_{24}H_{54}Cl_{3.56}Cu_3N_{12}O$.[21, 22] Non-hydrogen atoms were refined anisotropically. Hydrogen atoms were placed in geometrically calculated positions with $U_{iso} = 1.2U_{equiv}$ of the parent atom. The relative occupancies of the disordered atoms were freely refined, and no constraints or restraints were used on the bond lengths or anisotropic

displacement parameters of the disordered atoms. The solvent and one chloride anion were severely disordered and could not be successfully modeled with or without restraints. Thus, the structure factors were modified using the PLATON SQUEEZE technique, in order to produce a "solvate-free" structure factor set.[23] PLATON reported a total electron density of 135 e^- and total solvent accessible volume of 325 $Å^3$. The final anisotropic full-matrix least-squares refinement on F^2 with 571 variables converged at R1 = 4.06%, for the observed data and wR2 = 10.18% for all data. The goodness-of-fit was 1.024. The largest peak in the final difference electron density synthesis was 1.254 $e^-/Å^3$ and the largest hole was -1.811 $e^-/Å^3$ with an RMS deviation of 0.098 $e^-/Å^3$. On the basis of the final model, the calculated density was 1.430 g/cm^3 and F(000), 875 e^-.

(3,5-bis(pyridin-2-yl)pyrazole)$Cu_2(OAc)_2$(μ-OH) (3). Complex **3** was prepared based on a reported procedure.[25] To a solution of the 3,5-bis(pyridin-2-yl)pyrazole (0.1 g; 0.45 mmol) in ethanol (20 mL), copper(II) acetate hydrate (0.18 g; 0.9 mmol) was added. The solution turned green-blue and then was concentrated almost to dryness. The resulting green-blue crystalline solid was collected by filtration, washed with ethanol and diethylether and dried under vacuum with a yield of 66% (167 mg).

$[Cu_2$(PPDMe)(μ-OH)$NO_3(H_2O)_2](NO_3)\cdot H_2O$ (4). The pro-ligand PPDMe (3,6-bis(3,5-dimethyl-l-pyrazolyl)pyridazine) was synthesized based on a reported procedure.[25] PPDMe (0.50 g, 1.9 mmol) was dissolved in acetonitrile (50 mL) with warming, and the solution was filtered. A solution of $Cu(NO_3)_2\cdot 3H_2O$ (0.90 g, 3.7 mmol) dissolved in water

(10 mL) was filtered and then added to the NCMe solution of PPDMe, A blue crystalline product (880 mg, 71%) was obtained on standing overnight, which was collected by filtration and dried in air.

Cyclic voltammetry experiments (CVs) CVs were performed on a CH Instruments potentiostat. All electrochemical experiments were performed at room temperature. Glassy Carbon (GC) was used as working electrode, Ag/AgCl (3 M NaCl) as reference electrode and Pt wire as counter electrode. All experiments employed a platinum wire counter electrode. All potentials were reported versus the normal hydrogen electrode (NHE) by adding 0.205 V to the measured potential. GC working electrodes were polished with a 0.05 mm Al_2O_3 slurry, sonicated for 10 min in ultrapure water, and then rinsed prior to each sample. Solutions were purged with nitrogen for 10 min, and a stream of nitrogen was maintained over solutions for the duration of the experiments.

Catalytic cyclohexane oxidation using copper catalysts The copper salt mediated cyclohexane oxidation was carried out under following conditions: Adding cyclohexane (1 mmol), 1 mol % of copper catalyst (**1**-**4**) relative to cyclohexane, 1000 equiv. of H_2O_2 (35% in water solution) relative to copper catalyst to 3 mL of NCMe in a vial. The vial was sealed and stirred at room temperature on a stir plate. Reactions were performed in a 20 mL vial and stirred at room temperature for 6 hours. After the reaction, the reaction mixtures were quenched with 500 mg triphenylphosphine. Biphenyl was then added to the resulting solution as an internal standard and the mixture was then analyzed by GC-FID, turnovers

were calculated based-on a calibration curve. All numbers were the average of two identical experiments.

Catalytic light alkane oxidation using copper catalysts 10 μmol of catalyst, H_2O_2 (35% in water solution) and 15 mL of solvent were added to a par-reactor. The reactor was sealed and purged with 70 psig of light alkane (methane or ethane) 5 times and then pressurized with 30 bars of the light alkane. The reactor was then stirred at desired temperature for thirty minutes. After the reaction, the reactor was vented and collected in a 1L gas sampling bag using a venting valve and analyzed by GC-MS. The reaction solution phase was transferred to a vial, and liquid phase was combined with D_2O and analyzed by solvent suppression ^1H NMR.

6.5 References

1. Stringer, J.; Horton, L., Basic Research Needs to Assure a secure energy future. *Oak Ridge, Tenn.: Oak Ridge National Laboratory: pp. A-97-A-101* **2003**.
2. Kerr, R. A., Natural Gas From Shale Bursts Onto the Scene. *Science* **2010,** *328* (5986), 1624-1626.
3. Olah, G. A., Beyond Oil and Gas: The Methanol Economy. *Angew. Chem. Int. Ed.* **2005,** *44* (18), 2636-2639.
4. Zhou, L.-L.; Fang, T.; Cao, J.-P.; Zhu, Z.-H.; Su, X.-T.; Zhan, S.-Z., A dinuclear copper(II) electrocatalyst both water reduction and oxidation. *J. Power Sources* **2015,** *273*, 298-304.
5. Su, X.-J.; Gao, M.; Jiao, L.; Liao, R.-Z.; Siegbahn, P. E. M.; Cheng, J.-P.; Zhang, M.-T., Electrocatalytic Water Oxidation by a Dinuclear Copper Complex in a Neutral Aqueous Solution. *Angew. Chem. Int. Ed.* **2015,** *54* (16), 4909-4914.
6. Koepke, S. J.; Light, K. M.; VanNatta, P. E.; Wiley, K. M.; Kieber-Emmons, M. T., Electrocatalytic Water Oxidation by a Homogeneous Copper Catalyst Disfavors Single-Site Mechanisms. *Journal of the American Chemical Society* **2017,** *139* (25), 8586-8600.
7. Wang, J.-M.; Liu, Y.-R.; Mao, X.-Y.; Shi, N.-N.; Zhang, X.; Wang, H.-S.; Fan, Y.-H.; Wang, M., Two Trinuclear CuII Complexes: Effect of Phosphonate Ligand on the

Magnetic Property and Electrocatalytic Reactivity for Water Oxidation. *Chemistry – An Asian Journal* **2019,** *14* (15), 2685-2693.

8. Gao, W.-S.; Wang, J.-M.; Shi, N.-N.; Chen, C.-N.; Fan, Y.-H.; Wang, M., Electrocatalytic water oxidation studies of a tetranuclear Cu(ii) complex with cubane-like core Cu4(μ3-O)4. *New Journal of Chemistry* **2019,** *43* (11), 4640-4647.
9. Brown, M. J.; Parkyns, N. D., Progress in the partial oxidation of methane to methanol and formaldehyde. *Catal. Today* **1991,** *8* (3), 305-335.
10. Foster, N. R., Direct catalytic oxidation of methane to methanol — a review. *Applied Catalysis* **1985,** *19* (1), 1-11.
11. Shilov, A. E.; Shteinman, A. A., Activation of saturated hydrocarbons by metal complexes in solution. *Coord. Chem. Rev.* **1977,** *24* (2), 97-143.
12. Shilov, A. E.; Shul'pin, G. B., Activation of C−H Bonds by Metal Complexes. *Chem. Rev.* **1997,** *97* (8), 2879-2932.
13. Crabtree, R. H., *The organometallic chemistry of the transition metals*. John Wiley & Sons: 2009.
14. Labinger, J. A., Platinum-Catalyzed C–H Functionalization. *Chem. Rev.* **2017,** *117* (13), 8483-8496.
15. Hodges, R. J.; Webster, D. E.; Wells, P. B., The activation of saturated hydrocarbons by transition-metal complexes in solution. Part I. Hydrogen–deuterium exchange in

alkanes catalysed by potassium tetrachloroplatinate(II) in acetic acid. *Journal of the Chemical Society A: Inorganic, Physical, Theoretical* **1971,** (0), 3230-3238.

16. Luinstra, G. A.; Wang, L.; Stahl, S. S.; Labinger, J. A.; Bercaw, J. E., C H activation by aqueous platinum complexes: A mechanistic study. *J. Organomet. Chem.* **1995,** *504* (1), 75-91.
17. Webb, J. R.; Bolaño, T.; Gunnoe, T. B., Catalytic oxy-functionalization of methane and other hydrocarbons: fundamental advancements and new strategies. *ChemSusChem* **2011,** *4* (1), 37-49.
18. Periana, R. A.; Taube, D. J.; Evitt, E. R.; Löffler, D. G.; Wentrcek, P. R.; Voss, G.; Masuda, T., A Mercury-Catalyzed, High-Yield System for the Oxidation of Methane to Methanol. *Science* **1993,** *259* (5093), 340-343.
19. Sen, A., Catalytic Functionalization of Carbon−Hydrogen and Carbon−Carbon Bonds in Protic Media. *Acc. Chem. Res.* **1998,** *31* (9), 550-557.
20. Tijm, P. J. A.; Waller, F. J.; Brown, D. M., Methanol technology developments for the new millennium. *Applied Catalysis A: General* **2001,** *221* (1), 275-282.
21. Periana, R. A.; Taube, D. J.; Gamble, S.; Taube, H.; Satoh, T.; Fujii, H., Platinum catalysts for the high-yield oxidation of methane to a methanol derivative. *Science* **1998,** *280* (5363), 560-564.

22. Serrano-Plana, J.; Garcia-Bosch, I.; Company, A.; Costas, M., Structural and Reactivity Models for Copper Oxygenases: Cooperative Effects and Novel Reactivities. *Acc. Chem. Res.* **2015,** *48* (8), 2397-2406.

23. Appel, A. M.; Helm, M. L., Determining the Overpotential for a Molecular Electrocatalyst. *ACS Catalysis* **2014,** *4* (2), 630-633.

24. Liu, Y.; Han, Y.; Zhang, Z.; Zhang, W.; Lai, W.; Wang, Y.; Cao, R., Low overpotential water oxidation at neutral pH catalyzed by a copper(II) porphyrin. *Chem. Sci.* **2019,** *10* (9), 2613-2622.

25. Thompson, L. K.; Woon, T. C.; Murphy, D. B.; Gabe, E. J.; Lee, F. L.; Le Page, Y., Binuclear copper(II) complexes of a series of tetradentate pyrazolyldiazines. Crystal and molecular structures of [.mu.-3,6-bis(3,5-dimethyl-1-pyrazolyl)pyridazine-N,.mu.-N3,.mu.-N3',N](.mu.-hydroxo)dichlorodicopper(II) aquotrichlorocuprate hydrate, Cu3C14H21Cl5N6O3, and [.mu.-3,6-bis(3,5-dimethyl-1-pyrazolyl)pyridazine-N,.mu.-N6,.mu.-N7,N](.mu.-hydroxo)tris(nitrato)diaquodicopper(II) hydrate, Cu2C14H23N9O13. *Inorg. Chem.* **1985,** *24* (26), 4719-4725.

26. Iwamoto, M.; Yokoo, S.; Sakai, K.; Kagawa, S., Catalytic decomposition of nitric oxide over copper(II)-exchanged, Y-type zeolites. *Journal of the Chemical Society, Faraday Transactions 1: Physical Chemistry in Condensed Phases* **1981,** *77* (7), 1629-1638.

27. Garcia-Bosch, I.; Siegler, M. A., Copper-Catalyzed Oxidation of Alkanes with H2O2 under a Fenton-like Regime. *Angew. Chem. Int. Ed.* **2016,** *55* (41), 12873-12876.

28. Ozkal, E.; Llanes, P.; Bravo, F.; Ferrali, A.; Pericàs, M. A., Fine-Tunable Tris(triazolyl)methane Ligands for Copper(I)- Catalyzed Azide-Alkyne Cycloaddition Reactions. *Adv. Synth. Catal.* **2014,** *356* (4), 857-869.

29. Pons, J.; Sánchez, F. J.; Labarta, A.; Casabó, J.; Teixidor, F.; Caubet, A., Mixed bridged, dinuclear copper(II) complexes with dinucleating, pyrazole derived ligands. *Inorg. Chim. Acta* **1993,** *208* (2), 167-171.

30. Groothaert, M. H.; Smeets, P. J.; Sels, B. F.; Jacobs, P. A.; Schoonheydt, R. A., Selective Oxidation of Methane by the Bis(μ-oxo)dicopper Core Stabilized on ZSM-5 and Mordenite Zeolites. *Journal of the American Chemical Society* **2005,** *127* (5), 1394-1395.

31. Ball, P. W.; Blake, A. B., Magnetic properties of polynuclear complexes. Part I. Superexchange in some binuclear nickel(II) complexes. *Journal of the Chemical Society A: Inorganic, Physical, Theoretical* **1969,** (0), 1415-1422.